tanulmányok 39/1975

MTA Számitástechnikai és Automatizálási Kutató Intézet Budapest

A.Abd EL-Sattar

CONTROL OF INDUCTION MOTOR BY THREE PHASE THYRISTOR CONNECTIONS IN THE SECONDARY CIRCUIT

Supervisor

Prof. I.Rácz

Készült az
ORSZÁGOS MŰSZAKI KÖNYVTÁR ÉS DOKUMENTÁCIÓS KÖZPONT
Budapest, VIII., Reviczky u. 6.
Sokszorosító üzemében,
F. v.: Janoch Gyula

Eng. szám: 52911

ACKNOWLEDGEMENT

The author wishes to express his sincerest gratitude to Prof.Dr.I.Rácz for introducing him to the modern control techniques. He is greatly indebted also to Prof.Rácz for the keen supervision and fruitful guidance during the research work. Acknowledgement is made to the Computer and Automation Research Institute for the facilities offered for computations. The author wishes to thank the Dept. of Elec. Drives and Machines in Budapest Technical Univ. for the facilities used in the experimental work.

I should like to thank the Hungarian Academy of Sciences for the award of a grant in support of the research.

I am indebted to the Egyptian Culture office in Budapest for the help offered to me during my life in Hungary.

C o n t e n t s

CHABTER I.

INTRODUCTION

The venerable a.c. wound rotor induction motor long used mainly in fan, pump and hoisting applications, now offers still another choice, with characteristics in between d.c. and induction motors for adjustable speed drives. Using solid state controllers to vary the secondary resistance,the a.c. wound rotor motor can match d.c. motors in closed loop speed regulation while rivaling the induction motor for low maintenance and long life because of its unsegmented collector rings.

Although the induction motor is the most simple in construction and therefore the most widespread in use it does not lend itself easily to speed control and feed-back arrangements. Through the advent of complex automatically controlled drives a change took place in the required design and performance characteristics of induction motors. One of the objects of the design was a flat speed/torque characteristic.

With the development of the thyristor a variety of schemes have been evolved incorporating these devices for the purpose of controlling the speed of induction motors.

There is a number of "lossless" control methods which convert either the supply frequency to a variable frequency or the slip frequency to the supply frequency. These methods are expensive but may be used economically for the medium and high horse power drives. The low horse power induction motor can be controlled using simple, inexpensive but lossy control methods. Such methods use thyristors connection either in the stator or in the rotor circuits. There is a lot of publications

for the stator voltage control.

It is an advantage to connect the thyristors in the secondary side of the motor /see Fig. 1.1/. In this

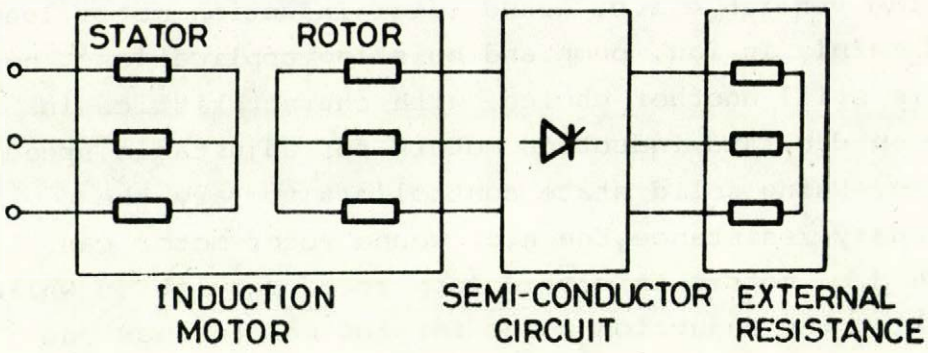

Fig. 1.1

scheme thyristor ratings are favourable, excess voltages and short-circuit currents are low and precise open-loop speed control is possible.

The basic principal of the controlled motor in that case is that of including thyristors in the secondary phases where they are used as a.c. phase-controlled switches, operating at slip-frequency. The control of the instant at which the current flow begins in each half cycle is obtained by controlling the phase of the firing pulses to each thyristor. Since the torque depends on the current flow through the secondary circuit, the control of the firing pulses controls the average torque developed by the machine. Thus at a constant speed, it becomes possible to control the motor torque between minimum value /decided by the value of the used external resistances/ and the value given by the normal torque/speed characteristic of the motor. The use of external resistances is necessary if higher torque

values are required at low speed.

An alternative possibility of controlling the motor is adapted from the changing of a d.c. resistance by firing angle control of a bridge or half controlled bridge rectifier connected to the slip rings.

The two alternatives were studied. It is convenient to refer to the first method of control by 3-ph resistance control, while the second one may be called d.c. resistance control. As it will be shown in chapter III, five different connections were investigated, three of them with the three phase resitance control and the other two with the d.c. resistance control. The steady-state solution for the mentioned connections was studied. Data for the working point, static characteristics, higher harmonics, R.M.S. and mean values for the currents, load limits of the motor and the requirements for the semi-conductors. A comparison was made, firstly among the connections of each part, afterwards between the two selected connections.

With the d.c. resistance control the torque can be reduced to zero value. Therefore this method of control is preferable when the operation with small torques is demandable. That method gives wider torque/speed range compared to the other solution of 3-ph resistance control.

The half controlled bridge connection was chosen for the detailed analysis. An analytical method for predicting the steady-state performance of such system is presented in chapter III. The analysis considers approximate solutions taking into considerations 2 or 4 energy-storages and a more exact solution using 6 energy-storages. Modern state variable techniques have been utilized throughout this analysis. The methods used are free from the maze of complex components which has

characterized similar problems in the past. Since matrix methods are exclusively employed, the analysis is well suited to a digital computer solution.

A comparison was made between that connection and the other solutions of stator voltage control and forced commutated d.c. chopper inserted in the rotor circuit of the motor.

In chapter IV the dynamic behaviour of the open-loop system is given. The analysis has been performed using the sampled-data theory. Despite the simplicity of the scheme, an analysis of even its steady-state performance is extremely complex owing to the difficulty of establishing a suitable set of boundary or initial conditions needed to generate a solution.

The closed-loop control system was studied and is presented in chapter V. Through this study the periodical steady-state solution was obtained using 8-energy storages. The dynamic behaviour and the system stability was also taken into consideration for that case.

The experimental work on the actual system is reported in chapter VI. It includes some performance characteristics for one connection of 3-phase resistance control. A detailed study for the performance of the drive in the case of half controlled bridge connection was made, steady-state characteristics, load limit, time functions, higher harmonics and so on. With that connection some oscillograms were made to compare the solutions obtained from the digital computer to the tested results of an actual system.

Also the experimental work contained the study of the dynamic behaviour of the controlled drive and the system stability with the mentioned connection. Step

functions for small and big changes were made to study the starting and braking processes. A review about some control methods concerned with the secondary circuit of the induction motor is given in chapter II, while in chapter VII the conclusions are reported.

It is well known that in the classical equivalent circuit of the induction motor, the stator leakage inductance is represented by L_s-L_m and that of the rotor by L_r-L_m where L_s, L_r and L_m are the stator, rotor and magnetizing inductances respectively. The flux equations have the following form:

$$\bar{\Psi}_s = L_s \bar{i}_s + L_m \bar{i}_r \qquad (1.1)$$

$$\bar{\Psi}_r = L_m \bar{i}_s + L_r \bar{i}_r \qquad (1.2)$$

The above equations can be rewritten as follows:

$$\bar{\Psi}_s = L_s \bar{i}_s + aL_m \frac{\bar{i}_r}{a} \qquad (1.3)$$

$$a\bar{\Psi}_r = aL_m \bar{i}_s + a^2 L_r \frac{\bar{i}_r}{a} \qquad (1.4)$$

By this modification the stator and the rotor leakage inductances become L_s-aL_m and $a^2L_r-aL_m$. If the value of a is chosen such that

$$a = \frac{L_s}{L_m}$$

the equivalent circuit of the induction motor is reduced to the simple form shown in fig. 1.2. In that figure

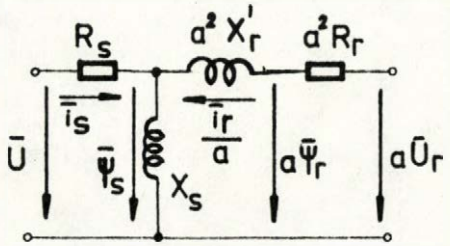

Fig.1.2

a=1.077. The figure gives the reduced equivalent circuit referred to the rotor side. The test measurements were made on 6.2 KWs, 4-pole, 50 Hz wound rotor induction motor. The machine has the following particulars:

stator: 220/380 volt Δ/λ

rotor : 110 volt star connected. The rated current is 36 A, no load speed 1410 r.p.m.

ALL the computations has been performed using the per-unit system. The required base values per phase are:

rotor base voltage = 96.72 V
rotor base current = 33.43 A
base impedance = 2.05 Ω
base torque = 43.6 Newton-meter
base speed = 314 rad./sec.
base flux = ·99 volt sec.

The motor parameters in the mentioned per-unit system are:

STATOR

resistance, R_s = 0.03
total reactance, X_s = 1.233
transient reactance, X'_s = 0.169
transient time contant, T'_s = 5.64

ROTOR

resistance, R_r = 0.068
transient reactance, X'_r = 0.197
transient time constant, T'_r = 2.895

The leakage factor $\sigma = 1 - \frac{L_m^2}{L_s L_r} = 0.138$

CHAPTER II.

REVIEW OF SOME CONTROL METHODS OF WOUND ROTOR INDUCTION MOTOR

Of the well known methods of controlling the speed of induction motors those based on the insertion of rotor resistance. The method also is most popular for starting processes. Normally stepped resistors are inserted in the rotor side result in a satisfactory saw tooth starting torque characteristic and reduced starting current [1,5]. The machine can also be operated as a variable speed motor. A variation on this connects the slip rings to electrodes in an electrolytic solution the opposite electrodes being shorted together and movable to form a liquid rheostat. Both of these methods require the movement of massive mechanical parts and are too slow for most closed-loop control applications.

In that case the method is not very easily adaptable to feed-back connections and inefficient, moreover it is relatively expensive due to its complicated control circuits and numerous components.

The other method based on pole changing gives only discrete synchronous speeds. Schemes which use rotary machines to change the supply frequency or recover slip-energy do give quite acceptable torque/speed characteristics and are quite efficient but they are quite expensive systems of control because of the cost of the additional control machines.

Within the broad category defined as "Control of wound rotor induction motor" there are several types. It is the task of this chapter to draw the attention to the most important techniques which were tried in the secondary side of the motor.

2.1 Speed Control of Induction Motors Using Saturable Reactors

With the progress in automation there was a growing need for precise and stepless control of motor speeds in driving fans, pumps, conveyors and all types of the machine. Usually, d.c. motors with field and/or voltage control, or induction motors driving the load through eddy-current clutches can be employed for this purpose. Another method of induction-motor speed control was considered. It uses feed-back controlled saturable reactors [2,3] in series with the motor winding. This method does not require a d.c. power supply, or any commutators or power tubes. The scheme only uses readily available reactors and control circuits. The direct current required for the control is only 1 or 2 percent of the motor rating and can readily be supplied from amplistats or equivalent devices just as in the case of the clutch. This method of speed control allows the speed of a wound rotor induction motor to be set at any desired value between 100% forward and 100% backward and to be held nearly constant at the set value. This method provides characteristics not attainable with eddy current clutch drive. The speed of the motor can be maintained precisely at any desired value by placing the saturable reactors in series with the motor windings and holding the direct current in the reactor at the appropriate value with feed-back control circuit. The reactor may be placed in either the primary or the secondary circuit. The latter case gives a good performance over wide speed range by employing a secondary reactor-resistor network. Also some advantages are attained in that case, namely, smaller size reactor and smaller iron losses. In the

described method a synthesis rather than analysis method is desirable.

For a given applied voltage constant torque and current circles can be constructed. These circles are drawn on an impedance plane.

It is a matter of engineering judgment to get the required values of the resistance and reactane which fulfil the required performance from the constant torque and current circles.

If the motor and reactor reactances are treated as linear impedances, then the arrangement is the same as that of the FISCHER-HINNEN motor. With the use of amplistats, feed back control circuits and saturable reactors a standard wound rotor motor can give adjustable constant speed performance similar to a WARD-LEONARD d.c. drive.

However, efficiency considerations limit the use of the reactor speed control to applications where the operation is intermittent, high torque is needed over only a moderate speed range, or where the power losses are not important.

No doubt the initial cost in that case is higher than conventional stepped resistor starting. However during the first use of saturable reactor for speed control processes the stage of technical development decided that its use was advantageous and economical.

2.2 Rotor Impedance Control

The extended possibilities of obtaining certain desirable torque/speed characteristics suitable for the control of speed of induction motors are achieved by means of rotor impedance control. A balanced 3-phase supply of constant frequency is used. Through the constraint

of rotor impedance it is shown that the shunt type torque/speed characteristics required of a stable variable speed drive may be synthesized. The system is applicable to counter-torque types of hoist control and with phase reversal of the supply, to the more general requirements of hoist and crane control. Also by the use of capacitive rotor [4] networks it is shown that much higher starting and braking torques are obtained than are otherwise available.

Some method of analysis can be used as in the previous case. Constant torque, current and power factor loci are constructed. By the use of loci the internal torque, stator and rotor currents and power factors may be determined directly or by interpolation for any point in the rotor impedance plane.

As an application to the method a constant torque can be developed over a speed range from full reversed speed (s=2) to near synchronous speed. It is clear that these characteristics can be obtained if the rotor impedance locus can be made to follow the circular constant torque locus. Operation at a fixed point in the rotor impedance plane would also result in constant torque but this is not achievable because of the variation with speed of all rotor resistance elements. These flat torque/speed characteristics were required in a closed-loop variable speed drive with variable voltage of reversible phase sequence applied to the stator.

Another example for the method is the realization of variable speed drive. In that case the speed of the shaft can be maintain constant at any set value regardless of load torque changes.

Since the change of resistance with slip is more or less at a fixed inverse rate, a rapid change of referred rotor reactance is sought. The referred reactance of a rotor capacitor varies inversely as slip squared if the

external rotor networks are calculated at the rotor frequency.

The required characteristics may be accomplished by using resistance-capacitance network. These characteristics are important for hoist control. The rating of the rotor capacitor is an important consideration in designing the rotor network for this type of characteristic. In practice capacitors having rated voltage equal to the rated voltage of the rotor have been used.

The advantage of the above method that it uses fixed external elements consisting of resistances and reactances combination instead of using saturable reactors or other feed-back devices.

Other further efforts were done for improving the method of synthesis. The effort was [14] directed to find some equations which are used straight forwardly in the determination of the value of external parameters at any applied voltage and any desired torque for any wound rotor induction motor. The published work in that situation gave equations for the determination of the parameters of the rotor circuit and the external network when the starting torque of the motor is constant during the starting period between s=1 and s=0.1.

The approach used in that case is the graphical "Trial and error method".

2.3 Wound-Rotor Motors Using Saturistors

The previous explained methods concerned with replacing the rotor resistors with "educated" secondary circuits. That in which the impedance will change automatically in the proper manner to produce the desired speed/torque characteristics.

The thinking was directed to the determination of the practicality of using the hysteresis loss in a hard magnetic material such as ALNICO V, to supplement the "I^2R" losses in the secondary circuit of a wound rotor motor as a mean of obtaining superior speed/torque/current characteristics. Alnico V has the properity of [8] high hysteresis loss. This loss is proportional to the frequency so that when it occurs in the secondary circuit at slip frequency and is devided by the slip to refer it to the primary, the corresponding effective resistance is constant at all speeds independent of the slip. The other properity of Alnico V is that its permeability remains at low value so long the magnetic intensity is below certain value then it jumps to about double its first value.

This means that the Alnico serves as a flux switch, which opens whenever the current rises above a certain value.

This properity suggests that an Alnico reactor may be so designed that at all currents up to perhaps 200% of full load the reactance is very low but whenever the current rises above that value, the reactance and resistance will reach high values thus limiting the motor current at low speed and providing additional torque.

The term saturistor has been adopted to designate any reactor with a hard magnetic material in its flux paths. The a.c. impedance of the saturistor has a large resistive component due to the hysteresis loss in the Alnico and its power factor is nearly constant over an appreciable frequency range.

Placing a saturistor in the secondary circuit of a wound rotor motor gives the motor a remarkably constant

torque and current over the speed range from rest-up to the breakdown torque point. The saturistors may be designed to go on the shaft [7] in the space normally taken by sliprings and brushes.

With the saturistor in the rotor circuit, the motor can be started directly across the line, drawing less than twice rated current, while producing more than rated torque. In addition to the starting characteristics the constant torque characteristic exhibited by the machine will provide smooth acceleration of loads.

It shows that the method improves the starting of wound rotor induction motor and gives torque/speed characteristic useful for certain application. The method is not familiar to speed control.

2.4 Modern Control Methods

1. Recent developments in semi-conductors leads to new possibilities of motor control in general and of induction motor in particular. The performance of the modern drive is judged more by its speed of response and the possibility and ease of applying feed-back than by the efficiency and power factor /though still important/ are not the main design considerations. The drive also should possess a wide and continuously controlled speed range. This type of control is based on switching currents by semi-conductors devices. It may applied to the stator or to the rotor side. The principle of switching may be accomplised by an electromagnetic switch. It has inherent disadvantages of very large inrush current at the start of each on period, too wide speed fluctuations between the on and off periods,the inapplicability for speed control due to the slow response of the switch and the extensive wear of the switch.

The other way of using magnetic amplifiers instead of switches improves the service life of the apparatus. Only the cost is increased and the other drawbacks remain, there is little advantage in it.

By employing semi-conductor devices [9] instead of electromagnetic switches a radical change in the drive performance can be achieved. The on and off periods are extremely short compared with the inertia of the drive, then the speed fluctuations will be negligable.

Before the adventure of the thyristors, the control is achieved using semiconductor elements of thyratron type.

2. With the advent of highly efficient solid-state thyristors, further attempts have been made to control the speed of induction motors more economically. The advantages of power control by thyristors [11] are: no mechanical power contacts, quite static operation, full electronic control, no collectors and very high control speed.

Present day variable speed electrical drives are almost exclusively built with thyristors control. In many respects the d.c. motor drives are the superior.

These drives are produced up to several hundred kilowatts and megawatts. Its initial and maintenance costs result in constant search for variable speed a.c. drives. Speed regulation of one-half percent or better can be achieved in closed-loop a.c. drives, thus rivaling d.c. adjustable speed drives. Poor efficiency will severely limit speed range in higher power if a lossy control methods are used. It is convenient for medium and large horse power drives to apply lossless control [26] methods. They are generally more expensive as compared

to d.c. motor drives but for special requirements the use of a.c. motor drives may be economical. These methods are applied in cases of limitation of the performance of d.c. machines for example very high speed or power or to avoid the use of the comutator. In the lossless control methods the speed control is accomplished by converting either supply frequency "f" to a variable frequency "f_1" or slip frequency "sf" to the supply frequency "f". The methods are particularly attractive and considerable amount of industrial development of these converters are progressed.

As these schemes involve a considerable amount of auxiliary equipment it is of interest to explore the possibility of using thyristors directly in the stator [20] or rotor [30] circuits of induction motors to achieve simpler and cheaper schemes of control. These methods are inexpensive but lossy control methods, therefore they are adaptable for low horse power drives.

In particular it is worth investigating the use of thyristors in the secondary circuits of an induction motor because then one can choose the operating voltage of the secondary circuit to suit the voltage rating of the thyristors which can be made available. However the two schemes of control which use the thyristors in the stator or in the rotor side have their merits depending on the type of applications.

A comparison between the two schemes will be given in the next chapter.

Another type of control is achieved by including three-phase bridge rectifier in the rotor circuit and a rotor resistance is controlled on the d.c. side of the bridge rectifier. Motor speed and torque are controlled by varying the secondary resistance in a time on, time off ratio. Time ratio [24] change of resistance permits variation of effective total resistance without actually

changing taps or moving electrodes. The resistor itself remains fixed. The variable is time and not metallic or liquid resistors. Such principle is used under various titles one of them being "chopper" other is "tirastat" controller for a.c. wound rotor motors. This solution could not come into general use partly because of the need of large chokes and forced commutated circuits with big capacitors, partly because of the large VA ratings of the thyristors that needed if the usual torque/speed range is required. Some detailed comparison between "chopper" and half controlled bridge connection inserted in the rotor side will be given in the next chapter.

Power lost inside the motor in any fashion except in-phase rotor I^2R has little effect on slip, and therefore contributes to motor heating.

Saturable reactor controllers and phase-controlled scr's in series with the three slip ring circuits cause wave-form distortions and lagging currents that produce motor heating and poor power-factors at reduced speeds and require selection of motors of large frame size than determined by load demands.

A simple, cheap and precise method is to use phase controlled thyristors in the secondary circuit of a normal a.c. wound rotor motor. Although this scheme of control has a fruitful role in the art of controlling the low horse-power drives a little number of publications has appeared, as yet, in the literature.

One of the methods was suggested by P.R.Basu [21]. The method use anti-parallel thyristor pairs connected to the slip-ring of wound rotor motor. He used two phase rotor winding but the method is applicable to the normal 3-phase wound rotor motor. In the described method no external rotor resistance is included.

It is advantageous to use external resistance in the rotor circuit if higher torques are required at low speeds.

As it will be shown in the next chapter that one of the studied connections /connection III YTT/ is exactly the same like the above described connection but the thyristor pairs are shunting the external resistance individually.

This method compared with the other studied schemes in our case is not the supperior because of the bad performance, the power factor is low. It is not the most economical method because a precise control and good performance drive is achieved for example by using only three thyristors in delta connections across the external resistance of the motor /connection II-ΔT, see the next chapter/. The method of firing the thyristors which was used by P.R.Basu is near to which was used in our studied connections in principle. The phase shift of the firing pulses in the former method is governed by the magnitude of a voltage proportional to the speed-error signal which is superimposed on constant modulus slip frequency reference signals. This can be obtained by using a small synchro similar in construction to the main motor. The two rotors must be properly aligned at the outset so that there is no mechanical phase difference between the synchro and the main motor secondary fluxes. The d.c. speed-error signal being derived by combining a speed-signal obtained by rectifying the synchro out-put with a desired speed-signal from potentiometer.

The constant modulus a.c. reference signals have been obtained by feeding the slip-frequency synchro E.M.F. through RC integrating circuit.

In our studied connections the firing delay is achieved by a voltage proportional to the speed-error signal which is superimposed on a signal proportional to the stator flux. The d.c. speed-error signal is obtained by combining a speed signal which is the output of a tachometer coupled with the main motor with a desired speed signal. The a.c. comparative signal is obtained according to the relation

$$\bar{\Psi}_s = \int(\bar{u}_r + R_r \bar{i}_r)dt + L'_r \bar{i}_r$$

using integrators and correction signals /see chapter VI/. The idea in the two methods is the same since constant modulus comparative signal in the case of BASU is near to the stator flux. The modern technique is to attain the control properities statically without the need to auxiliary rotating machines. The method suggested in our case is of advantageous if the speed-error signal can be obtained dispensing with the use of tachometers. It is possible to get the speed signal using digital-analog converters method. In that way the whole control circuitry can be made with static and passive elements.

The analytic methods for predicting the performance of the drive in our case use the most modern tool of analysis, that is the state-variable method based on Park-vector techniques.

The connections considered by A.BELLINI-A-DeCARL I [16,22,23] also use thyristors in the secondary side. The solutions considered have the drawback of excluding the external resistances. The analysis were based also on state variable methods. The method of control in the case of BELLINI is bad because the system is unstable. He used 6-thyristors and got only 3-strokes. Mr.BELLINI

had considered only the restricted case of assuming the motor speed constant. Our analysis consider both the approximate and the exact solutions using 2,4 and 6 energy-storages. In the controlled drive, the solution is implemented using "8" energy-storages. The study regards not only the steady-state performance but also the transient behaviour of the drive.

In the solution described by J.STRYCHARZ [27] the power factor is improved due to capacitor commutation of thyristors. The wave form of the current, however is not too favourable. That solution is little far from our work.

Different connections of thyristors in the secondary side of a wound rotor induction motor were studied in our case /see chapter III/. One solution was presented in which the resistors are short-circuited by thyristors beginning from a given firing angle. In spite of the importance of using external resistances parallel to the thyristors circuit, the published work had not employed these resistances.

The other was that a d.c. resistance is changed by firing angle control of semi-controlled bridge rectifier connected to the sliprings. This solution is a new one. The commutation of thyristors is provided by the rotor voltages.

The solutions are simple, precise and economic.

CHAPTER III

STEADY STATE CHARACTERISTICS

3.1 Introduction

In the solution of power control problems, thyristors and diodes are of rather increasing importance. In conduction they are equivalent to short-circuit, otherwise to open-circuit. In such systems, the steady-state condition is usually periodic, with a period τ. If the system, for example, involve only one thyristor, then τ may be cut up to $\tau = \tau_c + \tau_n$, in τ_c the thyristor is on and in τ_n it is off. It is assumed that the system may be described by constant coefficient linear differential equations.

Three-phase thyristor circuits are frequently used. The bridge circuit, for example, involves six thyristors and each period consists, generally, of 12 different conduction conditions. In most cases, however, it is quite sufficient to study two conditions since, knowing the data of a single one-sixth period, those of the other one-sixth periods may be obtained through phase and sign changes. In such cases τ indicates one-sixth of the whole period or sometimes its one third.

It is practical to fix the coordinate system to that part of the machine in which the semiconductors are connected. In that case we can obtain constant coefficients differential equations.

It is best to select the number of independent variables as much as the one of the independent energy-storages, because in that case the matrix dimension will not be unnecessarily large. In the operation of a controlled motor by thyristor circuits, different transient processes are brought out by the switchings of the semiconductor element, for example by its firing or extinguishing.

In most cases the exact calculation is not necessary as a simple approaching method gives good results for the steady-state characteristics.

However in the general solution it is necessary to know the exact calculation where the general equations without simplicity have to be taken into consideration.

3.2 Some Thyristor Connections in the Rotor Circuit

In this part the different studied connections of thyristors in the secondary side of the induction machine are given. These different connections belong to two main groups, three-phase resistance control and d.c. resistance control.

3.2.1 Three-Phase Resistance Control

The studied connections were as follows:

1. Inverse-parallel thyristor pairs connected in delta across the external resistances of the motor. /Connection I, Fig. 3.1/ [ΔTT]

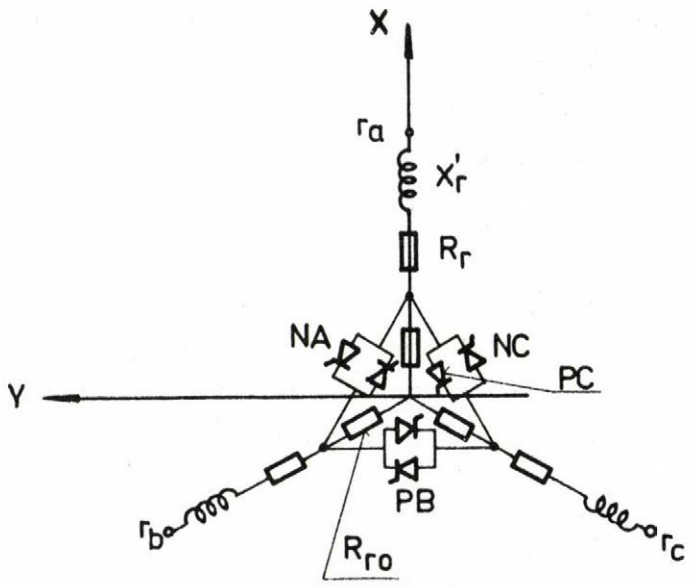

Connection I(Δ TT)

Fig.3.1

2. Three thyristors in delta-connection across the external resistances. /Connection II, Fig.3.2/ [ΔT]

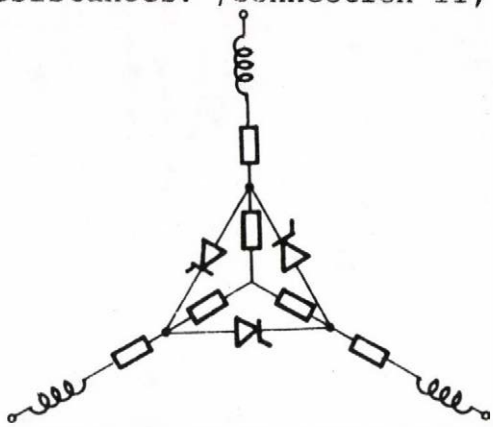

Connection Ⅱ(ΔT)

Fig. 3.2

3. Inverse-parallel thyristor pairs shunting the external resistance individually. /Connection III, Fig.3.3/ [YTT]

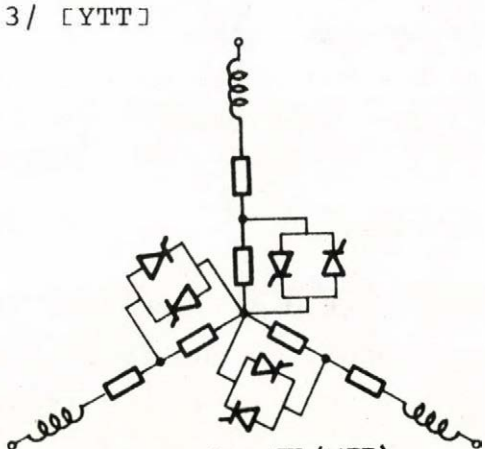

Connection Ⅲ (YTT)

Fig.3.3

For the purpose of understanding the general analyzing method of such circuits, the first connection will be considered as an example.

The equivalent circuit of the motor /neglecting the stator resistance as an approximation/ with connection I [ΔTT] is shown in Fig.3.4.

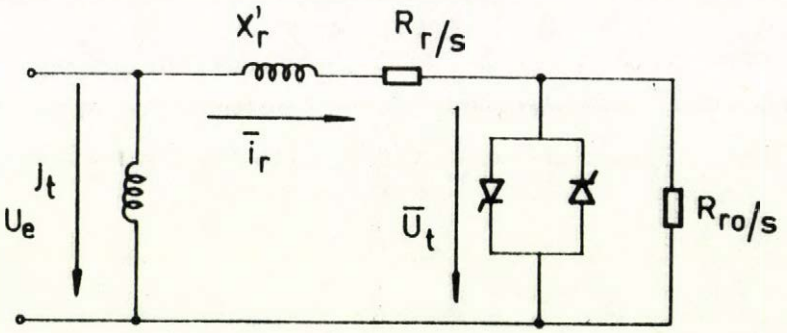

Fig.3.4

There are three different working conditions, 3-ph, 2-ph and o-ph condition. This means respectively that there are two thyristors in conduction which short-circuit the three phase external resistance /3-ph/, one thyristor is conducting which short-circuit two resistances of the external resistance /2-ph/ and no thyristor in conduction then the total three phase external resistance is in the rotor circuit /o-ph/.

In general the system is working in 3-ph - 2-ph or pure 2-ph or 2-ph - o-ph condition.

a/ 3-2 ph Condition

A coordinate system fixed to the rotor is chosen. In the three phase condition the equivalent circuit, on the base of Park-vector analysis, is given in Fig.3.5.

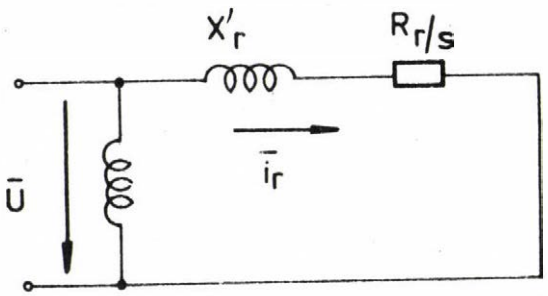

3- Ph condition

Fig.3.5

Because of symmetry, this equivalent circuit is valid in both x and y coordinate system.

The three phase conduction interval is denoted by τ_c. At the end of that interval one thyristor is turned off, the other thyristor short-circuit two resistances of the external resistance and the equivalent circuits in the x and in the y-directions are shown in Fig.3.6 and 3.7 respectively.

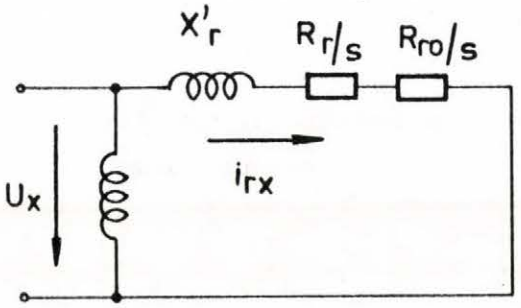

X - direction

Fig.3.6

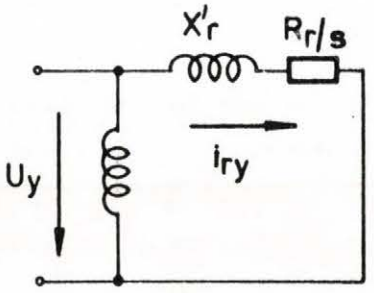

Y - direction

Fig.3.7

2-Ph condition

This 2-ph condition has a conduction interval τ_n so that $\tau_n+\tau_c = \tau$, where τ is the interval of the stroke which equals one six of the whole period.

In the following analysis some assumptions are made:

1. The power source may be considered as a set of balanced sinusoidal three-phase voltages having zero source impedance.

2. The six thyristors have identical characteristics, are symmetrically triggered and can be considered as a device which presents an infinite impedance in the blocking mode when the forward or anode-to-cathode voltage changes from positive to negative. The impedance changes to zero whenever a trigger pulse is applied, provided the forward voltage is positive.

3. The stator resistance is neglected.

4. The motor speed /or the slip s/ is constant.

5. All parameters of the machine are assumed to be constant and saturation of the magnetic circuit is neglected.

With the coordinate system fixed to the rotor and utilizing the above assumptions the equivalent circuits in Fig.3.5, 3.6, and 3.7 may be used. The analysis of the motor can be reduced to that of the static three-phase R-L circuits [28].

The fundamental equations of the system in the two phase condition can be written in the following form:

$$u_x = s\ U\ \cos(s\omega_1 t) = (R_r+R_{ro})i_{rx} + L'_r \frac{di_{rx}}{dt} \qquad (3.1)$$

$$u_y = s\ U\ \sin(s\omega_1 t) = R_r\ i_{ry} + L'_r \frac{di_{ry}}{dt} \qquad (3.2)$$

where s is the slip and ω_1 is the electric angular velocity of the source voltages /the synchronous angular velocity/, R_r is the resistance of the rotor phase, R_{ro} is the phase value of the external resistance and L'_r is the transient inductance of the rotor circuit. i_{rx} and i_{ry} are the x and y components of the rotor current.

In per-unit system U=1 and ω_1=1.

Let us assume:

$$t' = s\omega_1 t$$

$$r = \frac{R_r}{sX'_r} \qquad (3.3)$$

$$r_2 = \frac{R_r+R_{ro}}{sX'_r} = (1+RR)r$$

where t' is the reduced time and RR is the resistance ratio which is equal to $\frac{R_{ro}}{R_r}$. For the purpose of

abbreviations in writing the following equations t is written instead of t′ and i_{rx}, i_{ry} are written in the place of $i_{rx}\ X'_r$, $i_{ry}\ X'_r$ respectively.

Utilizing equation (3.3) equations (3.1) and (3.2) can be transformed to:

$$\cos t = r_2\ i_{rx} + \frac{di_{rx}}{dt} \tag{3.4a}$$

$$\sin t = r\ \ i_{ry} + \frac{di_{ry}}{dt} \tag{3.5a}$$

In the three phase condition the fundamental equations of the system are the same as in the two phase condition but the coefficient of both i_{rx} and i_{ry} is "r". At "t_e" instant /see Fig.3.8/, the thyristor PC is turned off and only thyristor NB is conducting. At $t_c=t_e+\tau_n$ the thyristor PA is switched on then PA and NB thyristors are in conducting state during τ_c. At $t_1=t_c+\tau_c$ the thyristor NB is turned off and the total process is repeated with changing the thyristors.

The solution of the above differential equations is:

$$i_{rx}(t) = \mathrm{Re}\{\bar{Y}_2(e^{jt} - e^{-r_2(t-t_e)}e^{jt_e})\} \tag{3.4b}$$

$$i_{ry}(t) = \mathrm{Re}\{-j\bar{Y}(e^{jt} - e^{-r(t-t_e)}e^{jt_e}) + i_{ryo}\ e^{-r(t-t_e)}\} \tag{3.5b}$$

where

$$\bar{Y} = \frac{1}{r+j} \tag{3.6}$$

$$\bar{Y}_2 = \frac{1}{r_2+j} \tag{3.7}$$

and i_{ryo} is the value of the y-component of the rotor current at the extinction instant "t_e".

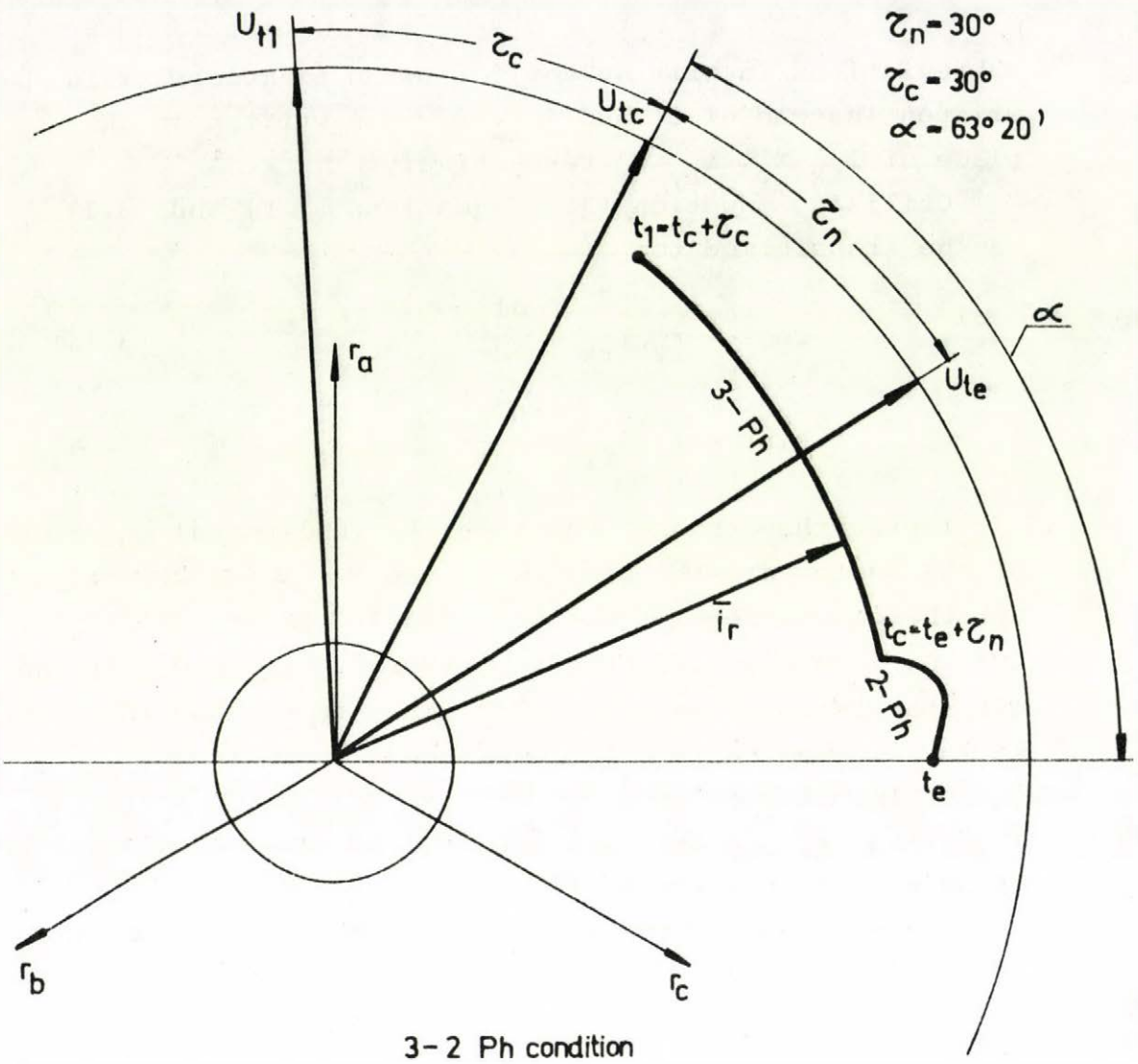

Fig.3.8

The extinction condition is:

$$\mathrm{Re}\{\bar{i}_r(t_1)\bar{e}^{j\tau}\} = 0 \qquad (3.8)$$

A closed form of solution for a set of initial conditions can be found when τ_n or τ_c is selected as the basic parameter.

In that case the instant "t_e" can be calculated from

the following equation:

$$\mathrm{Re}\{[\bar{Y}(e^{j\tau} - e^{j\tau_n} e^{-r\tau_c} - j\,\frac{e^{j\tau} - e^{-r\tau}}{\cos\tau - e^{-r\tau}}\sin\tau) + \bar{Y}_2(e^{j\tau_n} - e^{r_2\tau_n})\, e^{-r\tau_c}]\, e^{j\tau}\} = 0 \qquad (3.9)$$

Equation (3.9) may be deduced from equations (3.4b), (3.5b) together with equations (3.6)-(3.8).

The firing angle α, measured from the positive zero point of the voltage u_a is given by the equation:

$$\alpha = t_c + \frac{\Pi}{2} \qquad (3.10)$$

b/ Pure 2-ph Condition

If the firing angle of the thyristor is delayed such that at the instant of firing the thyristor, the other thyristor is turned off, then the 2-ph conduction period τ_n equals τ. In that case a pure 2-ph condition is obtained. This 2-ph condition is found for a small region. If the motor reactances are neglected, this region is 30° as shown in Fig.3.9.

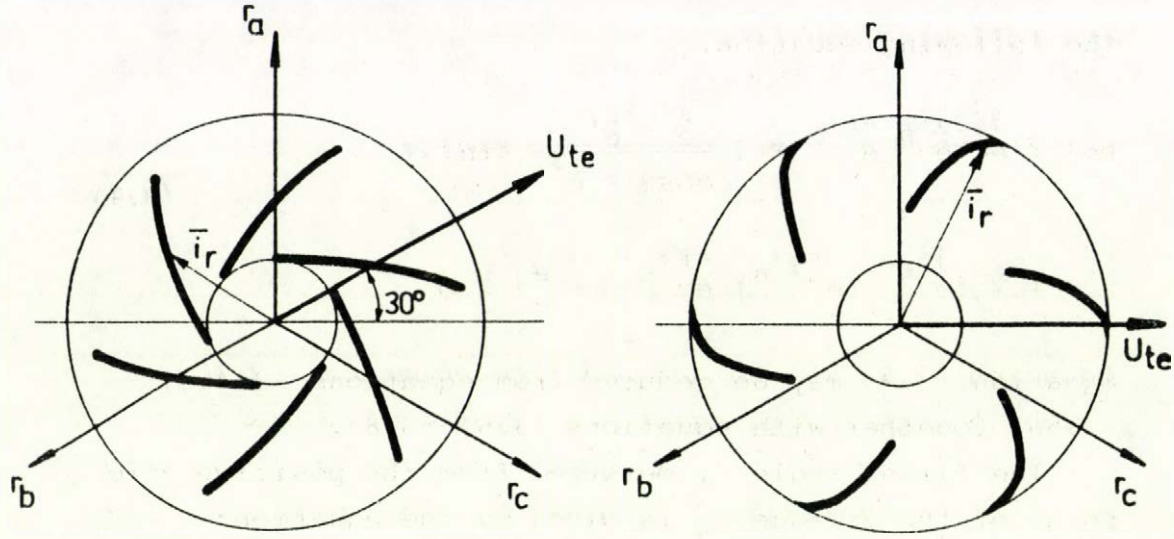

pure 2-Ph condition
pure resistive case

Fig.3.9

c/ 2-O_ph_Condition

For further delaying of the firing angle, the fired thyristor is conducting alone which gives 2-ph condition with a conduction interval of τ_n. In the remaining interval of the stroke all the thyristors are in the forward-biased blocking mode. This gives the O-ph condition.

That remaining interval is denoted by τ_o.

In a similar way as in the 3-2 phase condition, the firing instant "t_c" in that case may be obtained from the following equation:

$$\mathrm{Re}\{[-j\bar{Y}(e^{j\tau_n} - e^{-r\tau_n}) + \frac{e^{-r\tau_n}}{1 - e^{-r_2\tau}\cos\tau}(-\bar{Y}_2)((e^{j\tau} - e^{-r_2\tau})\sin\tau +$$

$$+ j(e^{j\tau} - e^{-r_2\tau_o}e^{j\tau_n})(\cos\tau - e^{-r_2\tau}))]e^{jt_c}\} = 0 \qquad (3.11)$$

In equation (3.11) τ_n or τ_o may be selected to be the basic parameter.

The firing angle in that case is given by the equation:

$$\alpha = t_c + \frac{\Pi}{2} + \tau \qquad (3.12)$$

The addition of τ in equation (3.12) comes from the fact that:

In the 3-2 ph and pure 2 ph conditions the calculation of the firing angle is concerned with thyristor PA. In the 2-O ph condition the calculation have to be made considering the same thyristor to get the value of α in succession with that in the 3-2 ph and pure 2 ph conditions. Equation (3.11) is written when thyristor NB is taken into consideration. Since thyristor NB preceeds PA in triggering by an interval of τ, therefore the addition of τ in equation (3.12) is necessary.

Harmonic Analysis

If the course of the vectors has symmetry with side "g", then the following order of the upper harmonics is possible:

$$\nu = 1 + gk \qquad (3.13)$$

where k = O, $\pm$1, $\pm$2 ... .
For the connections in the example

ν = ... -11, -5, 1, 7, 13, 19 ...

a/ 3-2 ph Conduction

It is convenient in the following analysis to use i_{rx} and i_{ry} as the x and y components of the rotor current.

In 3-ph conduction state the thyristor voltage is zero. The value of the upper harmonics of the thyristor voltage is given by the equation:

$$\bar{U}_{t\nu} = \frac{1}{\tau} \int_{\tau_n} u_{tx}\, \bar{e}^{j\nu t}\, dt \qquad (3.14)$$

the value of u_{tx} as seen from Fig. 3.10 is given by

$$u_{tx} = i_{rx}\, R_{ro} \qquad (3.15)$$

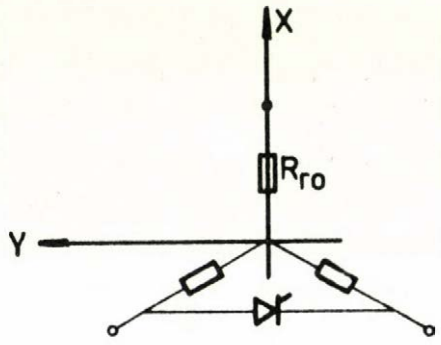

Fig.3.10

Equation (3.15) is deduced for the equivalent star connection of the thyristors. The real thyristor voltage equals $\frac{3}{2}$ of the obtained value

$$\bar{U}_{t\nu} = \frac{R_{ro}}{\tau} \int_{\tau_n} i_{rx}\, \bar{e}^{j\nu t}\, dt \qquad (3.16)$$

From equations (3.4a) and (3.16)

$$\bar{U}_{t\nu} = \frac{R_{ro}\, e^{-j\nu t_e}}{\tau(1-j\frac{r_2}{\nu})} \left[j \frac{i_{rx}(t_c)}{\nu} e^{-j\nu\tau_n} + \right.$$

$$+ \frac{1}{2\nu X'_r} \left\{ \frac{1}{\nu-1} e^{jt_e} \left(e^{-j(\nu-1)\tau_n} - 1\right) + \right.$$

$$\left. \left. + \frac{1}{\nu+1} e^{-jt_e} \left(e^{-j(\nu+1)\tau_n} - 1\right) \right\} \right] \qquad (3.17)$$

The curves of $U_{t(-5)}$, $U_{t(7)}$, $U_{t(-11)}$ and $U_{t(13)}$ for the different values of the 2-phase conduction interval τ_n are given in Fig.3.11 at speed of 0.47 p.u. and resistance ratio 5.9. It is clear that the minus fifth

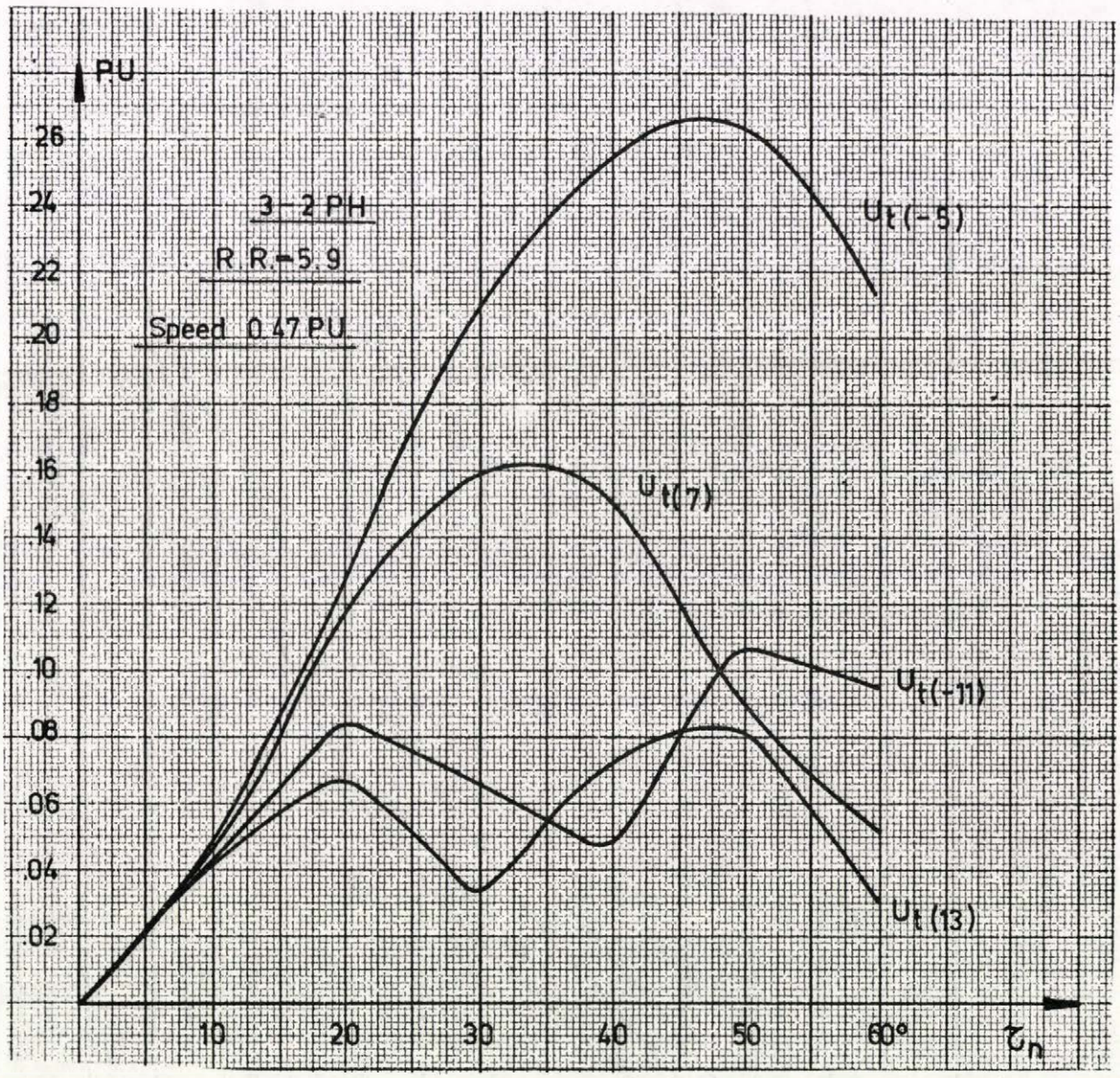

Fig.3.11

and seventh harmonic components of the thyristor voltage are dominant. For $\nu=1$, the fundamental component of the thyristor voltage is given by the equation:

$$\bar{U}_{t1} = \frac{R_{ro}}{\tau(1-jr_2)} \left[-j \frac{\tau_n}{2X'_r} + j\, i_{rx}(t_c)\, e^{-jt_c} + \right.$$

$$\left. + \frac{1}{4X'_r} \left(e^{-j2t_c} - e^{-j2t_e}\right)\right] \qquad (3.18)$$

In Fig.3.12 the amplitude of $\bar{U}_{t1}$ is drawn for different τ_n values at three different speeds.

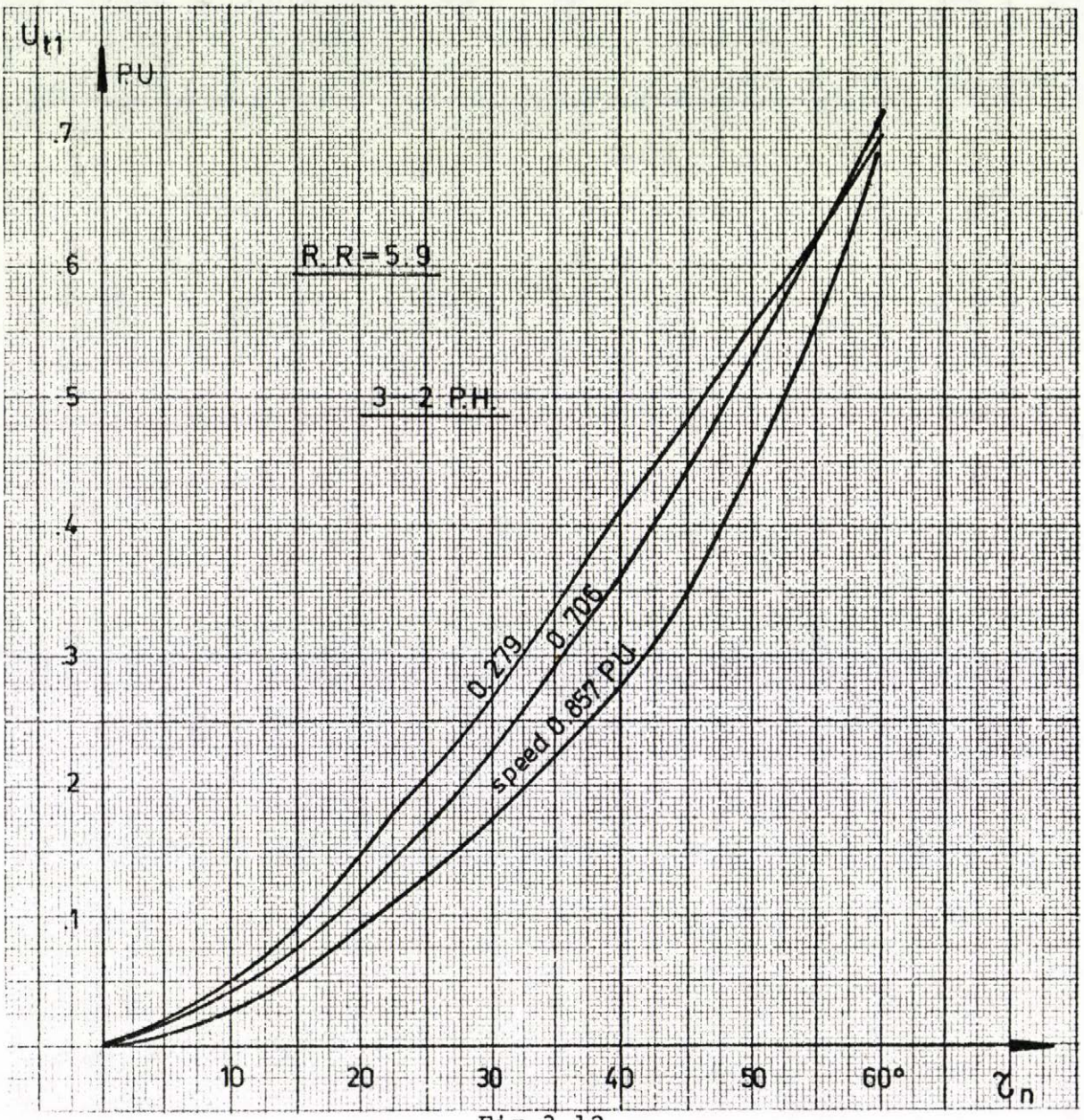

Fig.3.12

The value of the upper harmonics of the rotor current is given by the following equation /see Fig.3.4/

$$\bar{I}_{r\nu} = \frac{1}{X'_r} \frac{\bar{U}_\nu - \bar{U}_{t\nu/s}}{r+j\nu} \qquad (3.19)$$

where $\bar{U} = 0$, if $\nu \neq 1$.

Similarly the curves of the upper harmonics of the rotor currents versus τ_n are shown in Fig.3.13.

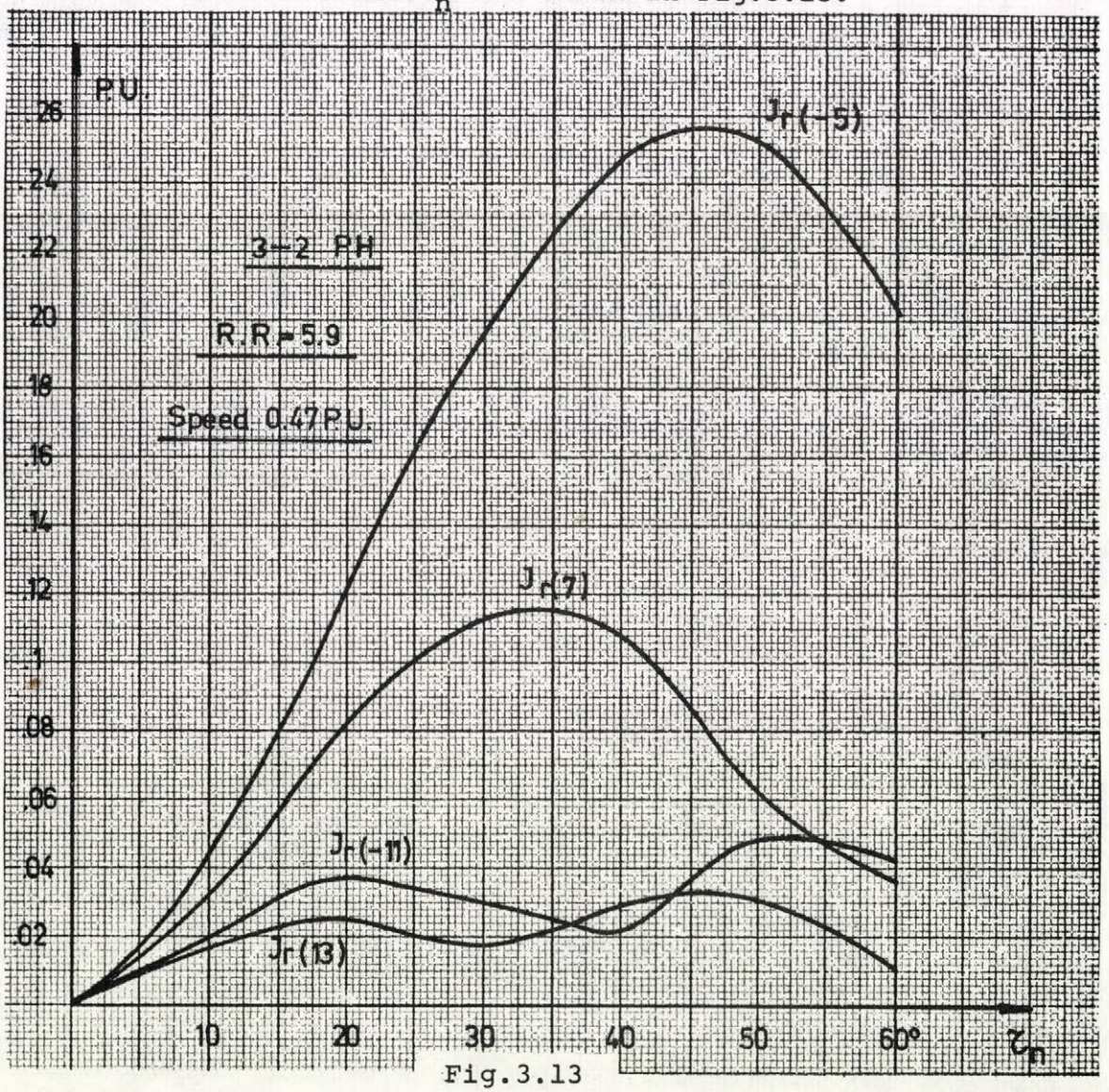

Fig.3.13

The amplitude of the fundamental component of the rotor current $\bar{I}_{r1}$ against τ_n is given in Fig.3.14 for three different speeds.

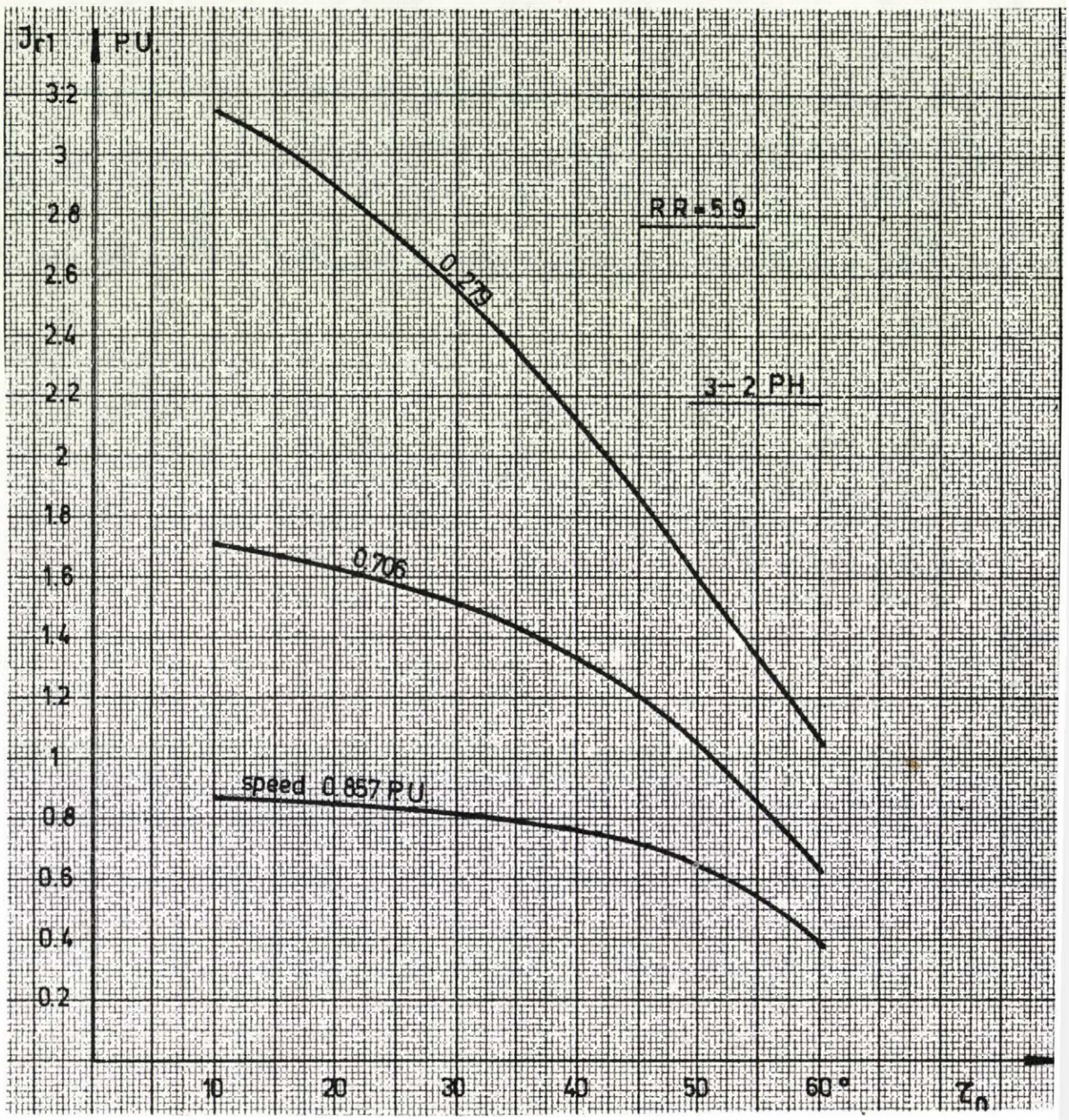

3.14

Knowing $\bar{U}_{t1}$, the fundamental component of the thyristor current can be calculated from /see Fig.3.4/:

$$\bar{I}_{t1} = \bar{I}_{r1} - \bar{I}_{ro1} \tag{3.20}$$

where

$$\bar{I}_{ro1} = \frac{\bar{U}_{t1}}{R_{ro}} \tag{3.21}$$

and the equivalent thyristor impedance is

$$\bar{Z}_{t1} = \frac{\bar{U}_{t1}}{\bar{I}_{t1}} \tag{3.22}$$

The curves of the amplitude of $\bar{I}_{t1}$ against τ_n for three different speed values are shown in /Fig.3.15/.

In /Fig.3.16/ the equivalent thyristor impedance $\bar{Z}_{t1}$ is drawn /in an impedance plane/ for different τ_n values and at two different speeds, while Fig.3.17 shows the reactive part of the impedance versus τ_n. From the two figures /3.16, 3.17/ it is shown that the inductive part of the equivalent impedance is high w.r.t. the resistive part and the inductive part increases rapidly for higher values of τ_n and at high speed. The inductive part is about 10 times as big as the resistive part at pure two phase conduction state and high speed of 0.87 of the synchronous speed.

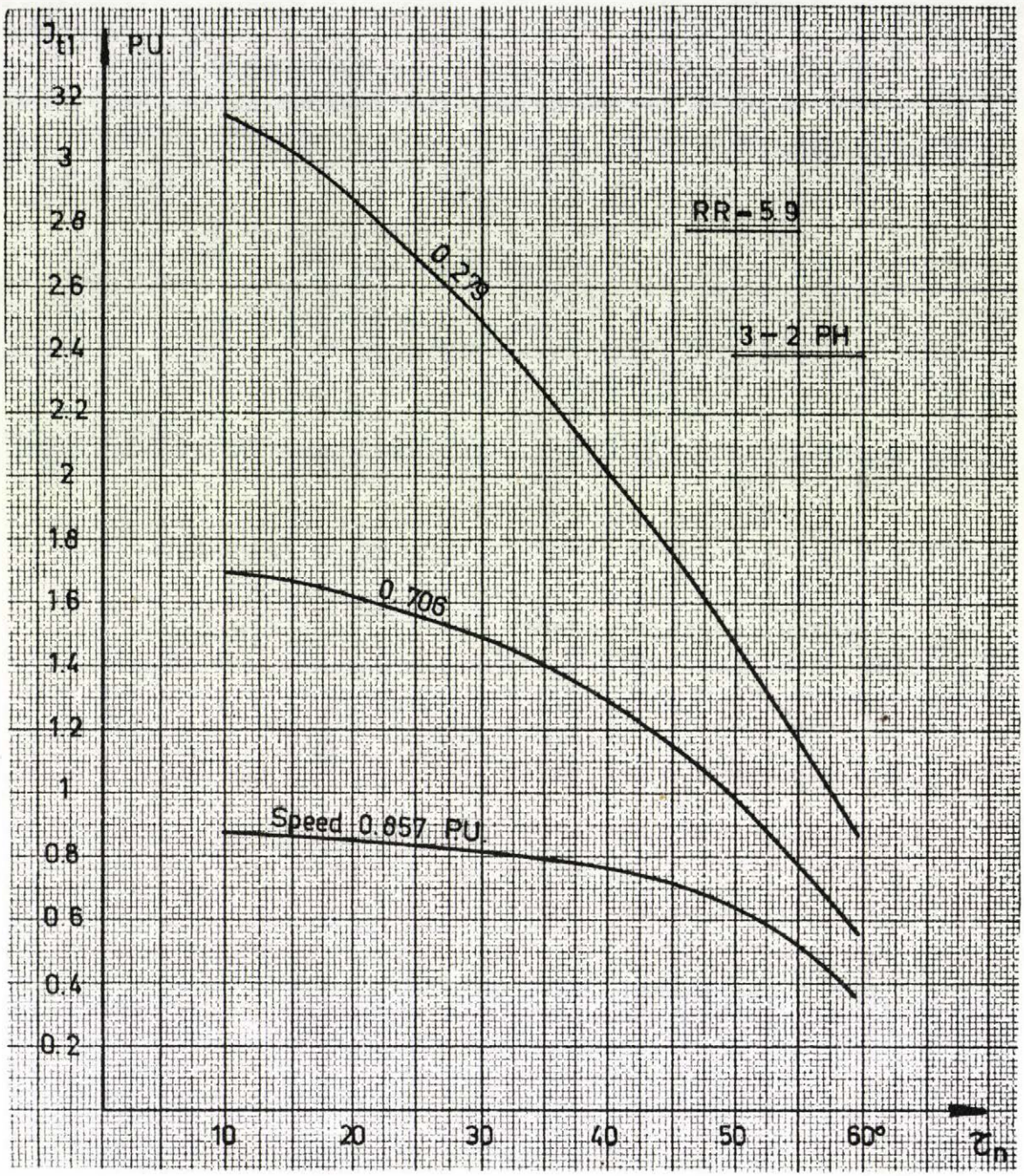
T_{t1} PU
3.2
3
2.8
2.6
2.4
2.2
2
1.8
1.6
1.4
1.2
1
0.8
0.6
0.4
0.2
RR-5.9
3-2 PH
0.729
0.706
Speed 0.857 PU
10
20
30
40
50
60°
γ_n

Fig.3.15

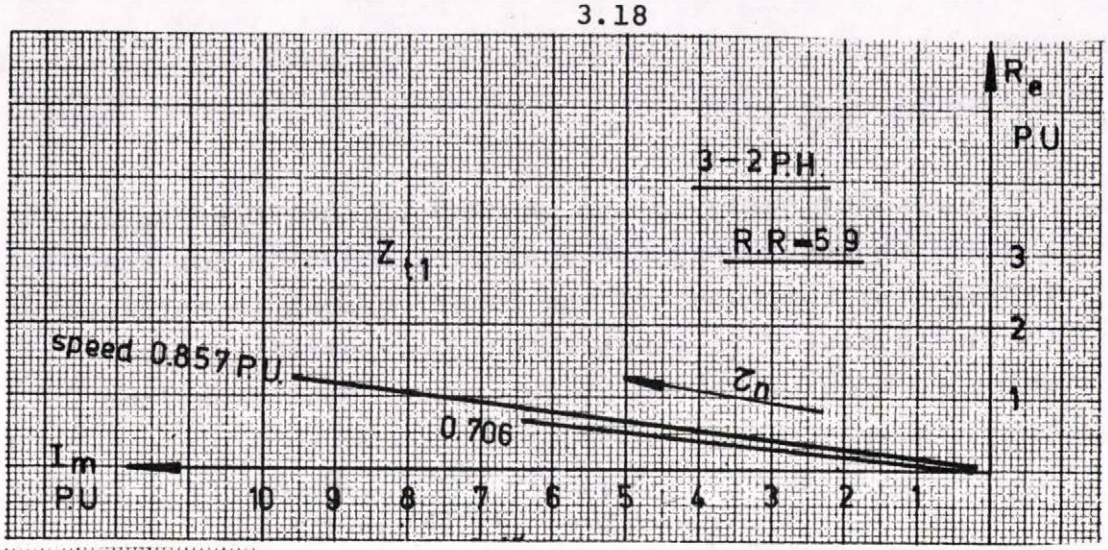

Fig.3.16

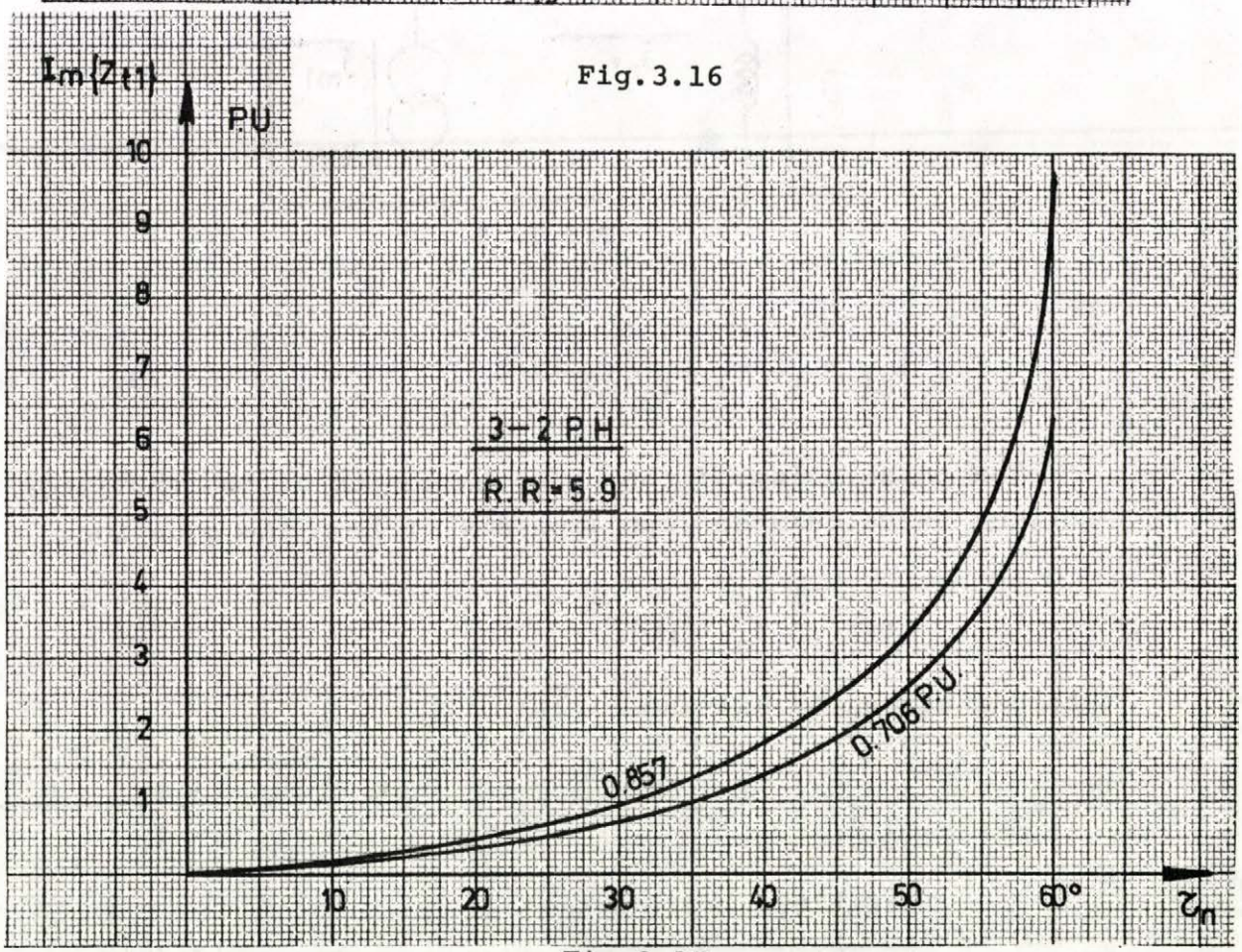

Fig.3.17

b/ 2-0 ph Condition

A similar analysis can be used in that case as in the 3-2 ph condition, but a simpler solution for the fundamental component of the rotor current is obtained if the thyristor is substituted by a current source which is open circuited at zero-phase condition /see Fig.3.18./.

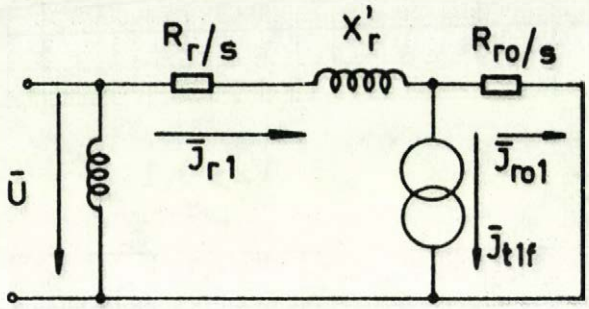

Fig.3.18

$$\bar{I}_{r1} = \frac{1}{X'_r} \frac{\bar{U} + \bar{I}_{t1f} R_{ro/s}}{r_2 + j} \qquad (3.23)$$

The phase value of the upper harmonics of the thyristor current is calculated /see appendix I/ from the equation:

$$\bar{I}_{t\nu f} = \frac{1}{\tau} \int_{\tau_n} j i_{ry} \bar{e}^{j\nu t} dt \qquad (3.24)$$

From equations (3.5a) and (3.24):

$$\bar{I}_{t\nu f} = \frac{1}{\tau(1-j\frac{r}{\nu})} \left[i_{ryo} \frac{\bar{e}^{j\nu t_c}}{\nu} + \frac{1}{2\nu X'_r} \left(\frac{e^{-j(\nu-1)t_e} - e^{-j(\nu-1)t_c}}{\nu - 1} - \right.\right.$$

$$\left.\left. - \frac{e^{-j(\nu+1)t_e} - e^{-j(\nu+1)t_c}}{\nu + 1} \right) \right] \qquad (3.25)$$

and for $\nu=1$

$$\bar{I}_{t1f} = \frac{1}{\tau(1-jr)} \left[i_{ryo} e^{-jt_c} - \frac{j\tau_n}{2X'_r} - \frac{1}{4X'_r} (e^{-j2t_e} - e^{-j2t_c}) \right] \quad (3.26)$$

In equations (3.25) and (3.26) "t_e" is the instant at which the thyristor turns off, i.e. $t_e = t_c + \tau_n$.

The R.M.S. Value of the Rotor Current

In general the R.M.S. value for the rotor current is calculated from the equation:

$$I^2_{r\ R.M.S.} = \frac{1}{\tau} \int_{\tau} I^2_r \, dt \quad (3.27)$$

In that case, the time function of the rotor current in the different modes of operation must be known and usually a numerical methods of integration are used to calculate that R.M.S. value. But in the considered example a simpler method was used for the calculation of that value.

1. 3-2 ph Condition

On the base of the power balance the following equation is written:

$$\frac{3}{2} U_1 |I_{r1}| \cos\phi = 3 I^2_{r\ R.M.S.} R_r/s + P_o/s \quad (3.28)$$

where

$$P_o = \frac{3}{2\tau} \int_{\tau_n} i^2_{rx\ R.M.S.} R_{ro} \quad (3.29)$$

is the power dissipated in the external resistance in the 2-ph conduction state.

From equations (3.29) and (3.4a)

$$P_o = \frac{3}{2}\frac{R_{ro}}{\tau}\left[\frac{-i_{rx}^2(t_c)}{2r_2} + \frac{1}{r_2 X'_r}\,\frac{1}{1+r_2^2}\left\{i_{rx}(t_c)(\sin t_c - r_2\cos t_c) + \right.\right.$$

$$+ \frac{1}{4X'_r}(\cos 2t_c + r_2 \sin 2t_c) - \frac{1}{4X'_r}(\cos 2t_e + r_2 \sin 2t_e) +$$

$$\left.\left. + \frac{1}{2}\frac{r_2}{X'_r}\tau_n\right\}\right] \qquad (3.30)$$

and from equation (3.30) and (3.28) the R.M.S. value of the rotor current can be calculated.

The R.M.S. value of the rotor current for different τ_n values are shown in Fig.3.19 at three different speeds. It is shown from Fig.3.14 and 3.19 that the difference between $|I_{r1}|$ and $I_{r\ R.M.S.}$ is very small, this indicates that the summation of the harmonic components of the rotor current is very small in such case but that difference will be increased in the 2-0 ph condition.

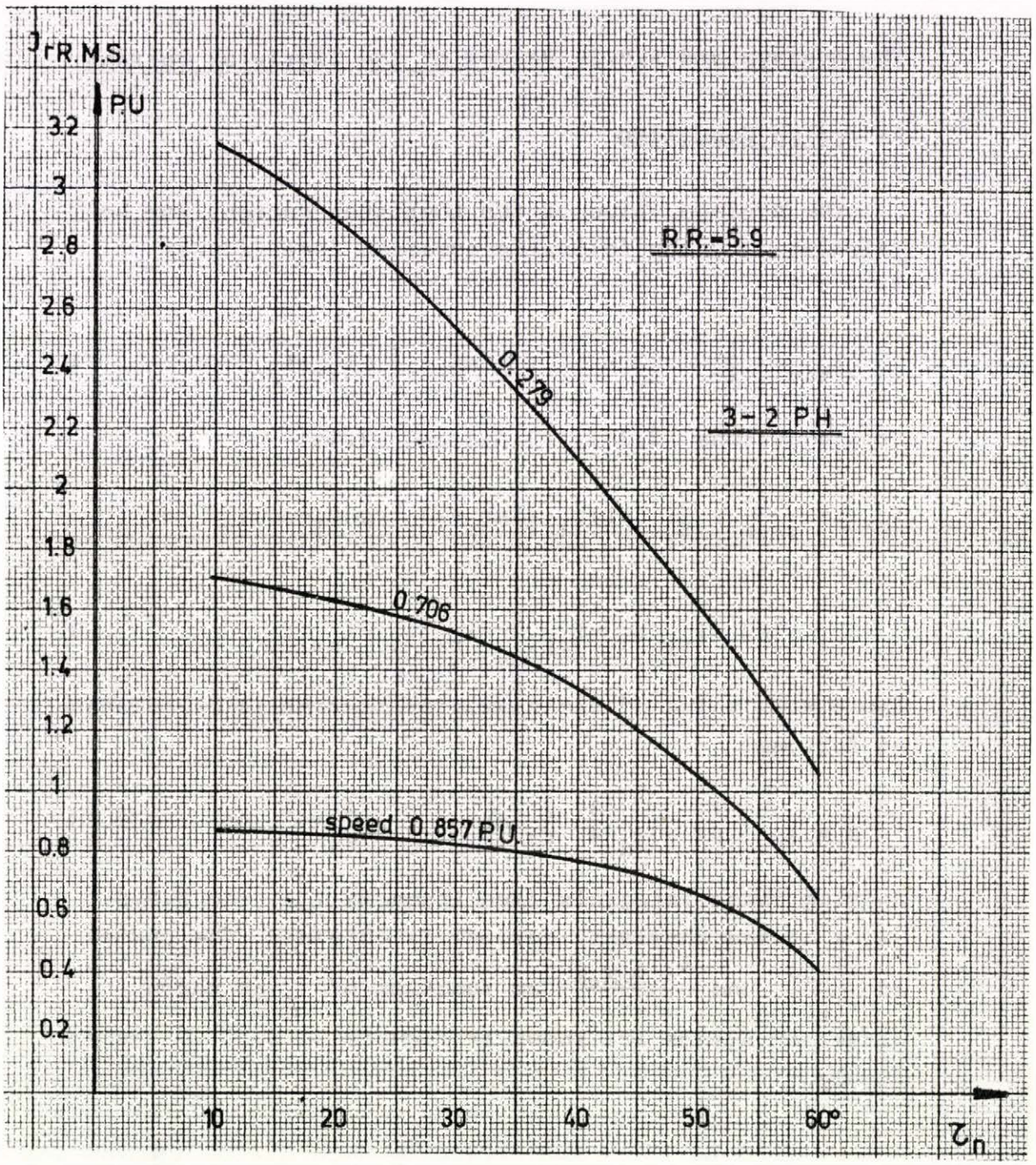
Ir R.M.S.
P.U
3.2
3
2.8
2.6
2.4
2.2
2
1.8
1.6
1.4
1.2
1
0.8
0.6
0.4
0.2
R.R.-5.9
3-2 P H
0.279
0.706
speed 0.857 P.U.
10
20
30
40
50
60°
τ_n

Fig.3.19

The Average and R.M.S. Values of the Thyristor Current

1/ 3-2 ph Condition

The average value of the thyristor current can be calculated by the following equation /see figures 3.1, 3.8/

$$I_{tav} = \frac{1}{6\tau} \left[\int_{\tau_n} - \frac{\sqrt{3}}{2} i_{ry} \, dt + \int_{\tau_c} (i_{ra}+i_{rc}) \right] dt \qquad (3.34)$$

From equations (3.34), (3.4a) and (3.5a)

$$I_{tav} = \frac{1}{12\tau r} \left[\frac{1}{X'_r} (\sin t_1 - \sin t_c + \sqrt{3} (\cos t_1 - \cos t_e)) + \right.$$

$$\left. + \sqrt{3} (i_{ry}(t_1) - i_{ryo}) - (i_{rx}(t_1) - i_{rx}(t_c)) \right] \qquad (3.35)$$

The R.M.S. value of the thyristor current is calculated as follows:

$$I^2_{t\ R.M.S.} = \frac{1}{6\tau} \left[\int_{\tau_n} \frac{3}{4} i^2_{ry} \, dt + \int_{\tau_c} (i^2_{ra}+i^2_{rc}) dt \right] \qquad (3.36)$$

Solving these integrals /see Appendix II/, the R.M.S. value of the thyristor current is obtained. The curves of $\frac{I_{tav}}{|I_{t1}|}$ and $\frac{I_{t\ R.M.S.}}{|I_{t1}|}$ as function of τ_n at three different speeds are shown in figures 3.20, 3.21 respectively.

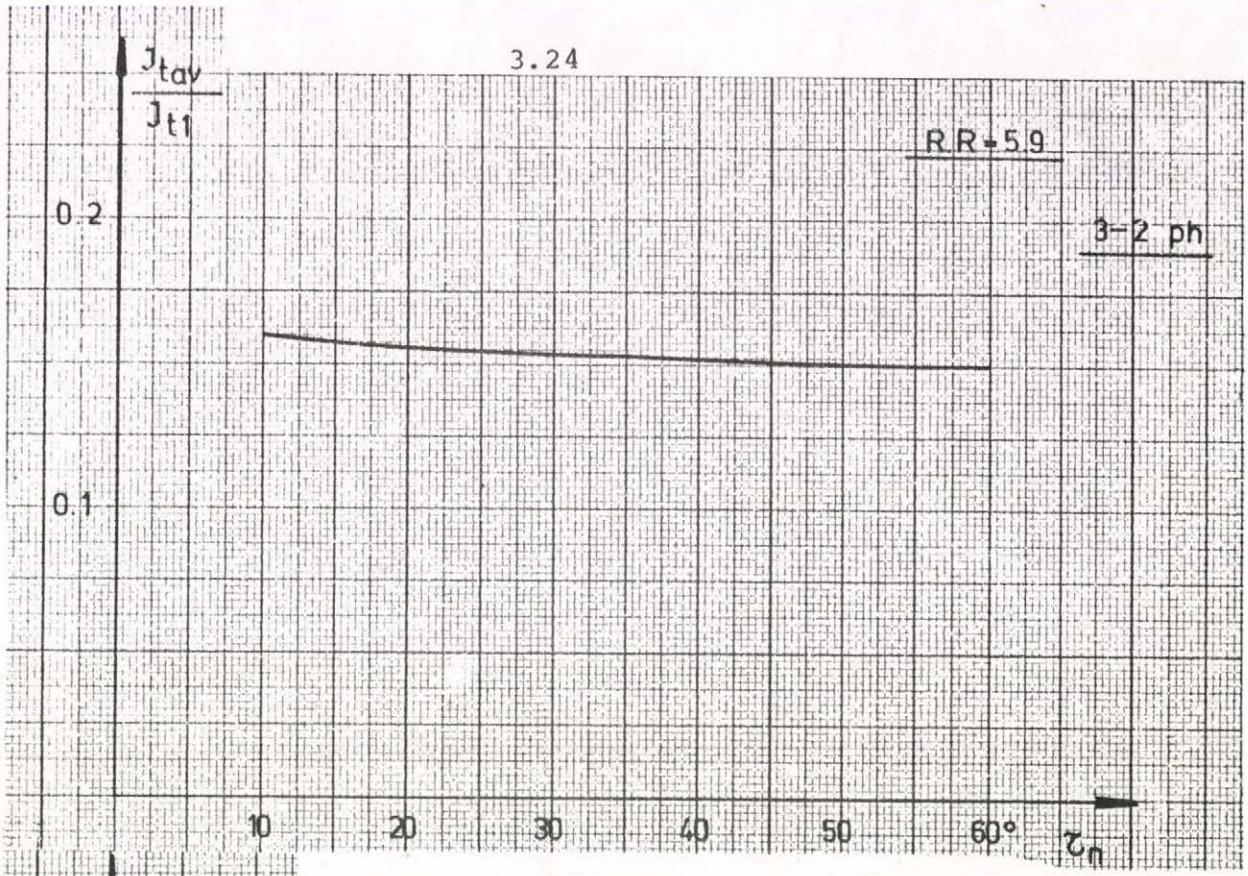

Fig.3.20

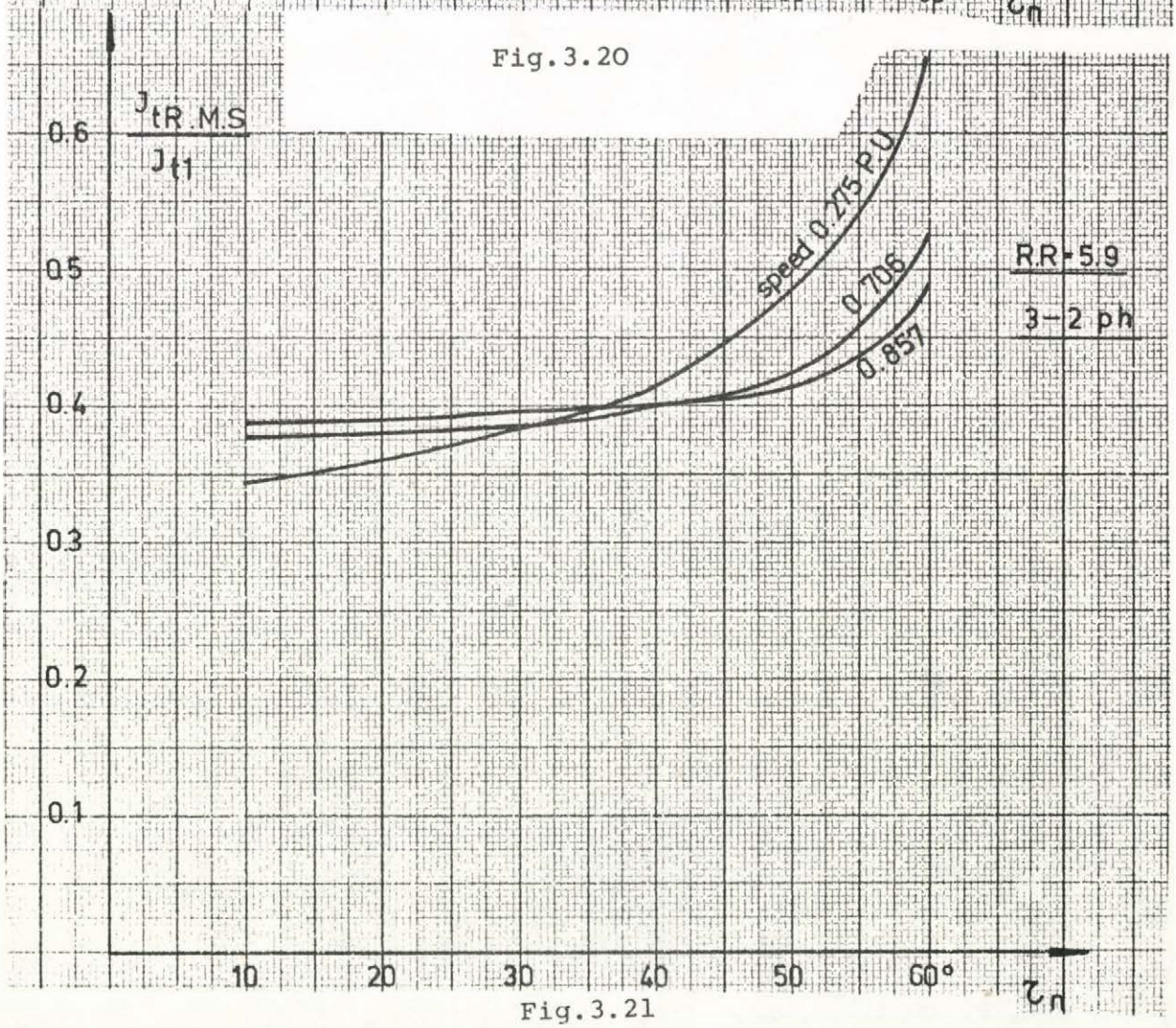

Fig.3.21

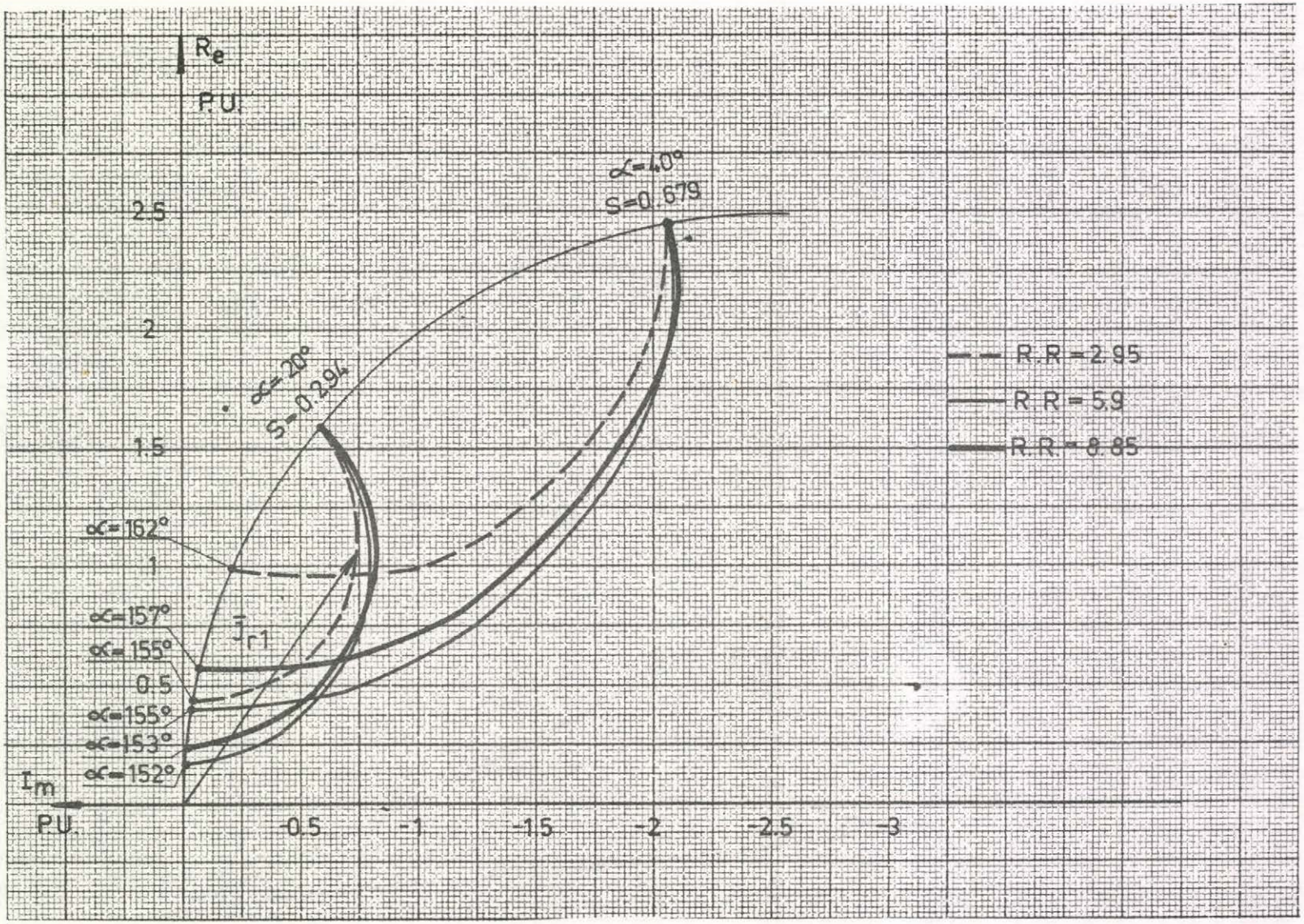
Re
P.U.
2.5
2
1.5
1
0.5
Im
P.U.
-0.5
-1
-1.5
-2
-2.5
-3
α=40°
S=0.679
α=20°
S=0.294
α=162°
α=157°
α=155°
α=155°
α=153°
α=152°
$\bar{I}_{r1}$
R.R=2.95
R.R=5.9
R.R=8.85

Fig.3.22

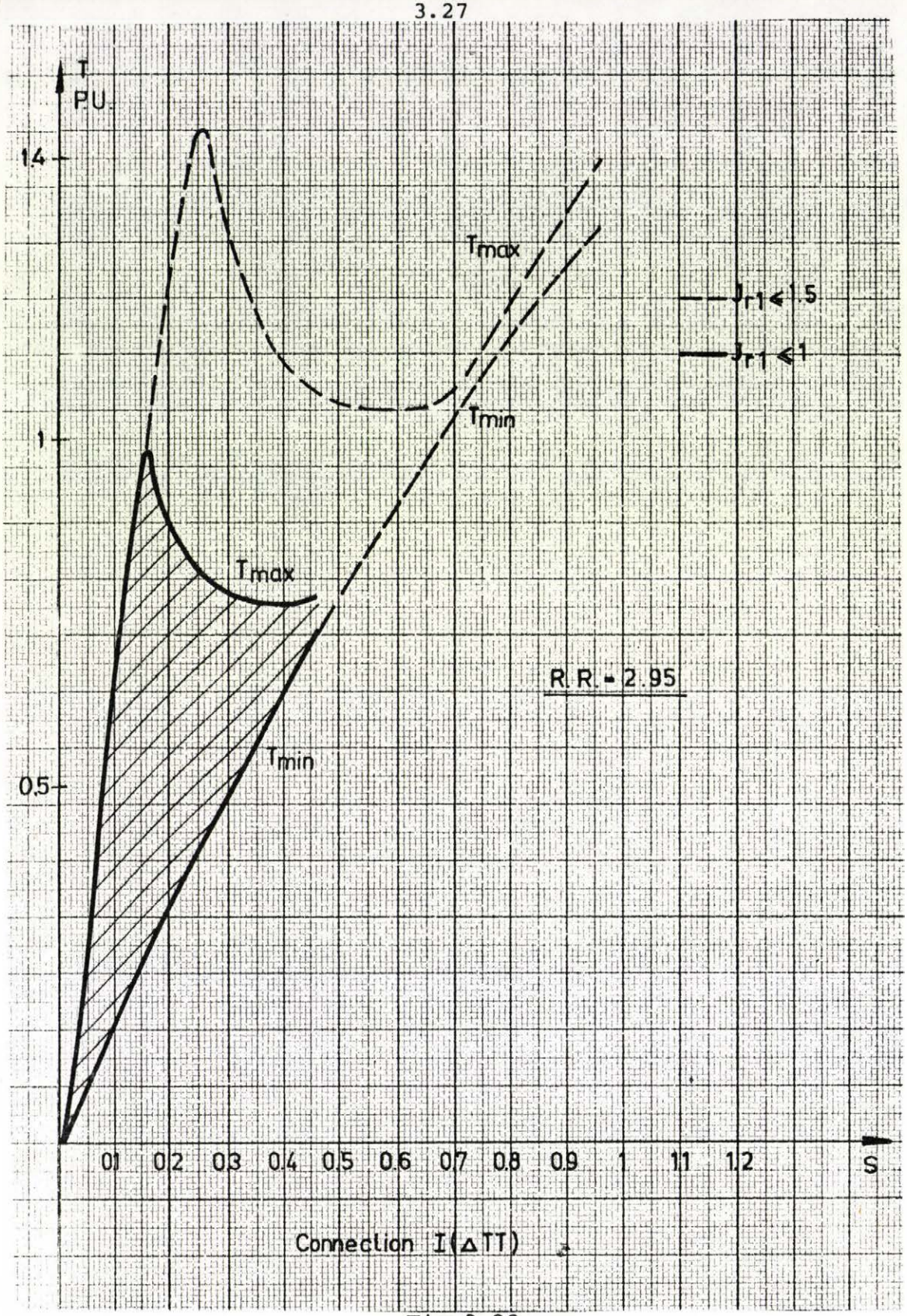
T
P.U.
1.4
1
0.5
Tmax
Tmin
Tmax
Tmin
Jr1 < 1.5
Jr1 < 1
R.R. = 2.95
0.1 0.2 0.3 0.4 0.5 0.6 0.7 0.8 0.9 1 1.1 1.2
S
Connection I(ΔTT)

Fig.3.23

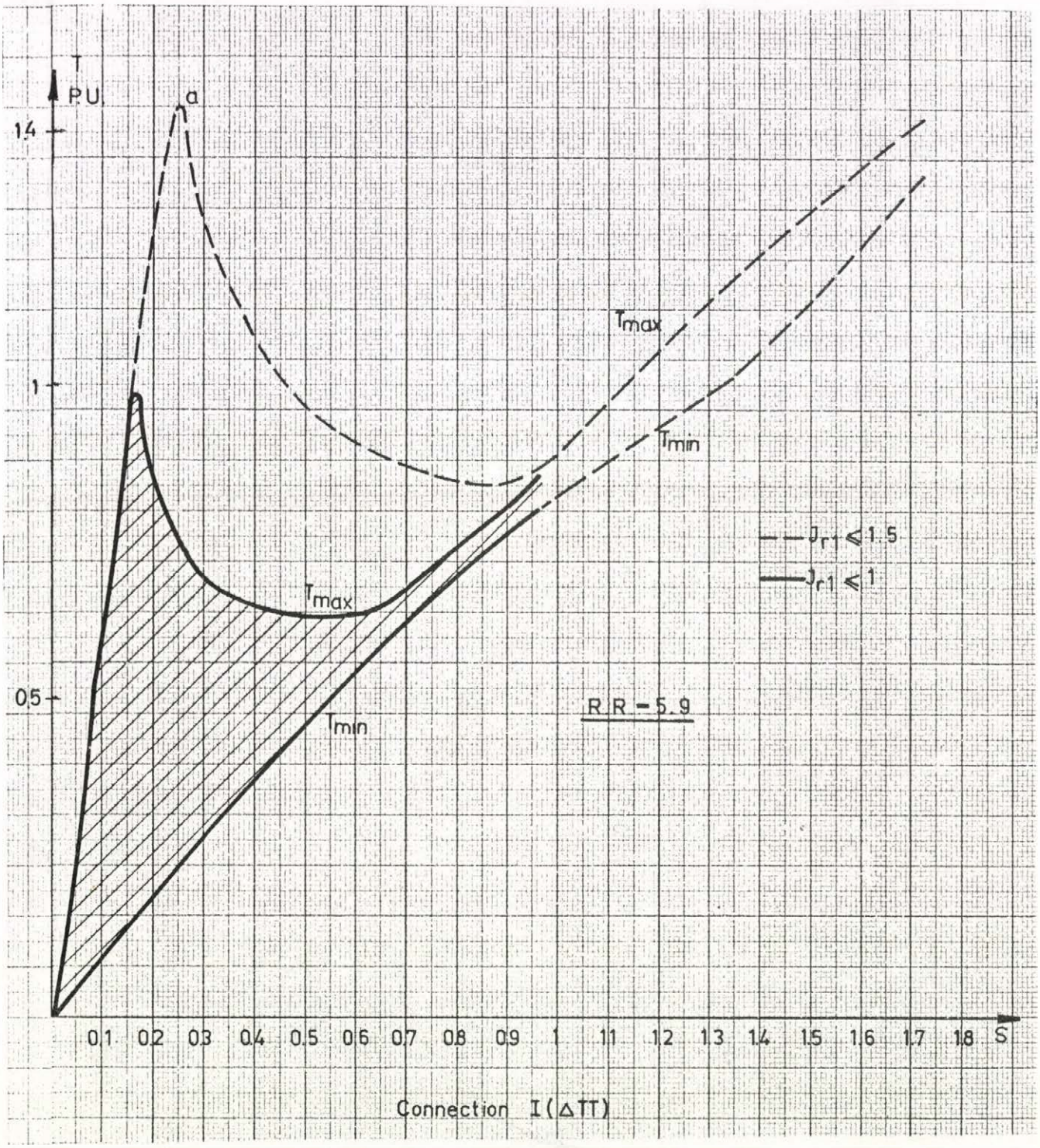
T
P.U.
a
1.4
1
0.5
T_{max}
T_{min}
T_{max}
T_{min}
$J_{r1} \leq 1.5$
$J_{r1} \leq 1$
R.R - 5.9
0.1 0.2 0.3 0.4 0.5 0.6 0.7 0.8 0.9 1 1.1 1.2 1.3 1.4 1.5 1.6 1.7 1.8 S
Connection I(ΔTT)

Fig.3.24

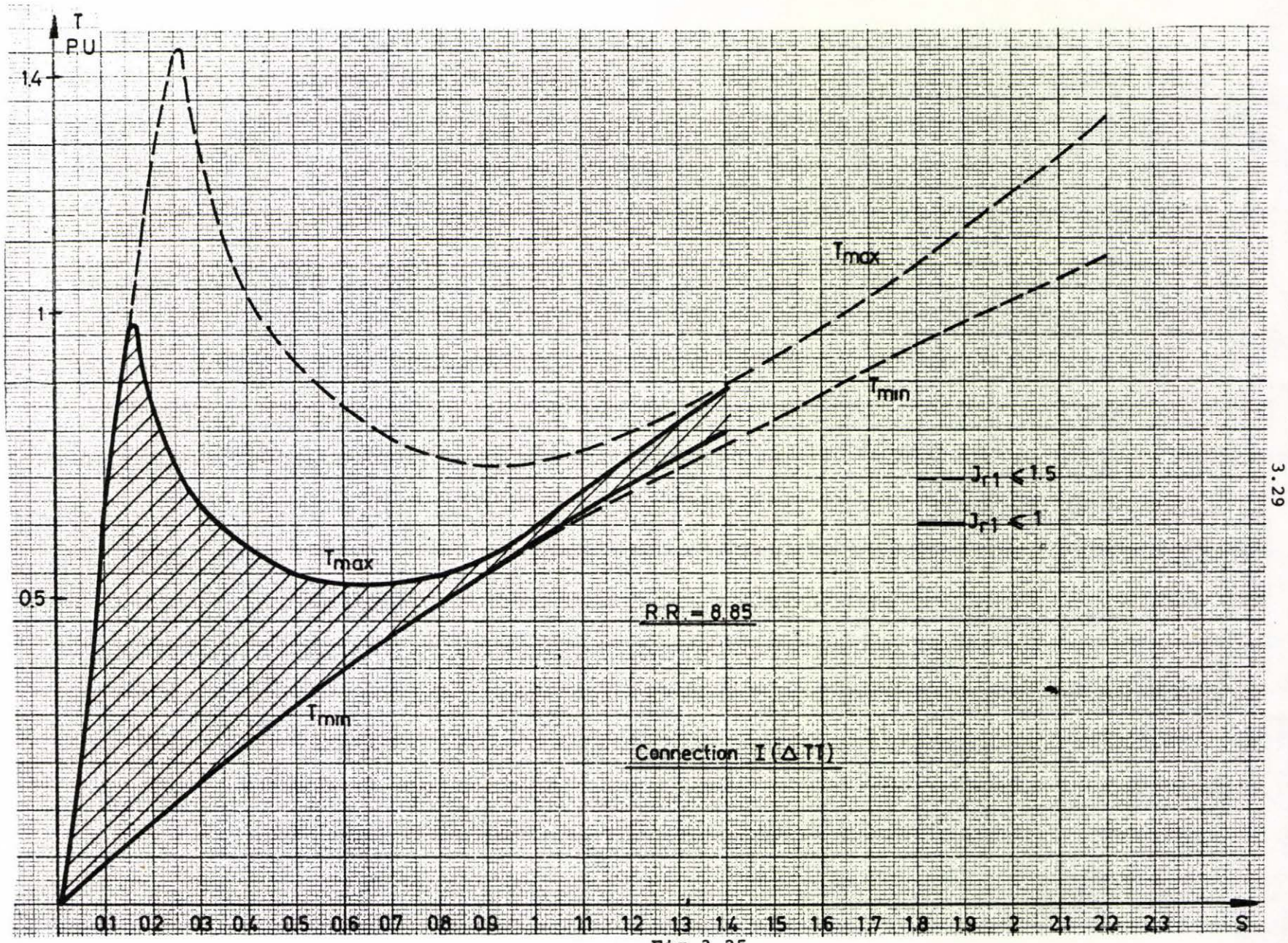
T
P.U
1.4
1
0.5
T_{max}
T_{min}
T_{max}
T_{min}
$J_{r1} \leq 1.5$
$J_{r1} \leq 1$
R.R. = 8.85
Connection I (ΔT1)
0.1 0.2 0.3 0.4 0.5 0.6 0.7 0.8 0.9 1 1.1 1.2 1.3 1.4 1.5 1.6 1.7 1.8 1.9 2 2.1 2.2 2.3
S

Fig.3.25

It has been confirmed from fig. 3.22 - 3.25 that for small resistance ratio:

1. The first harmonic component of the rotor current is increased for the same torque and the drive power-factor is better.
2. The minimum torque values are relatively high which decrease the operating region of the drive and make the range of the control narrow.
3. The range of variation of the firing angle "α" is larger for the same speed.

The small resistance ratio is needed at small slips because of the better performance. At high slips the high resistance ratio is required to get a wide control range. As a conclusion two values of the external resistance are needed to cover the whole region for the drive in driving and braking quadrants maintaining the good characteristic performance.

3.2.2 D.C. Resistance Control

The studied connections in that part were:

1. 6-thyristors in bridge connection /see Fig.3.26/; the bridge is connected to the slip-rings of the motor while a d.c. Resistance "$R_{d.c.}$" loads the bridge.
2. Half controlled bridge /see Fig.3.27/; the arrangement is the same like the above connection, only three diodes replace three thyristors of the bridge.

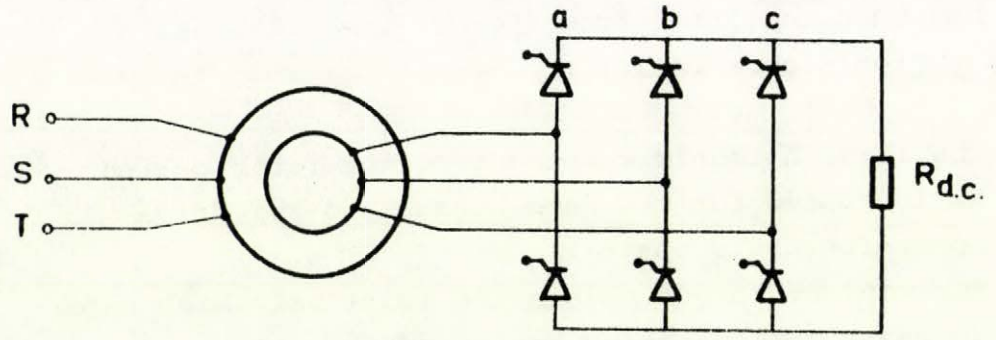

Bridge connection

Fig.3.26

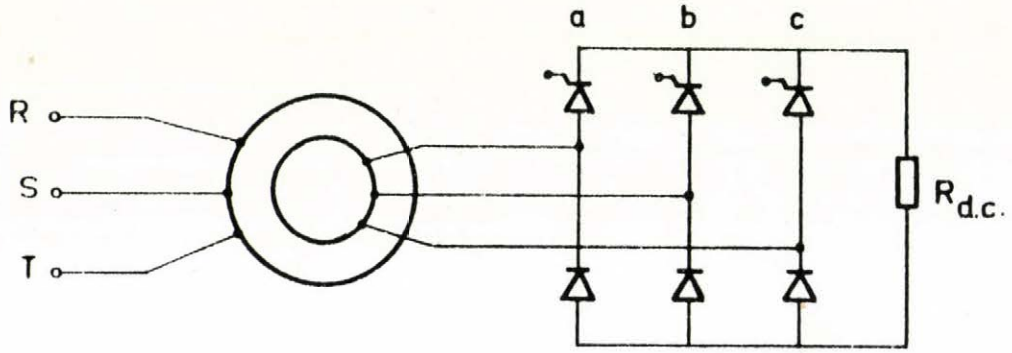

Half Controlled Bridge

Fig.3.27

3.3 Comparison Between the Studied Connections

A comparison was made between the investigated connections of the 3-ph resistance control part and then between connections of the d.c. resistance control and an over all comparison was made between all these connections.

The comparison has regarded the following aspects:

1. The fundamental component of the rotor current and machine power factor.
2. The torque/slip curves and the possible working region of the drive.
3. The thyristor ratings.
4. Harmonics content and the anomalistic characteristics at certain slips.

3.3.1 The Fundamental Component of the Rotor Current

At high speeds the slip is small and the rotor reactances are relatively small. As a preliminary study of the problem, an approximation was made that the motor leakage reactances were neglected compared to the resistances. In that case, the equation for the fundamental component of the rotor current was derived for the different connections. Subsequently the study of the real case was considered. The method of calculation is written only for one connection, since the other connections are treated in similar way. Let us, for example, consider connection II (ΔT). As in a 3-ph conduction state the rotor voltage is zero, then the fundamental component of the rotor voltage is calculated as follows /see Fig. 3.28 and 3.29/:

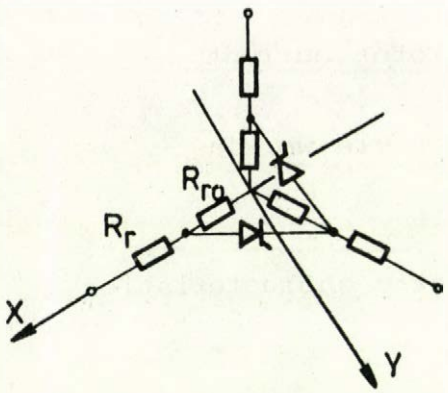

Connection II

pure resistive case

Fig.3.28

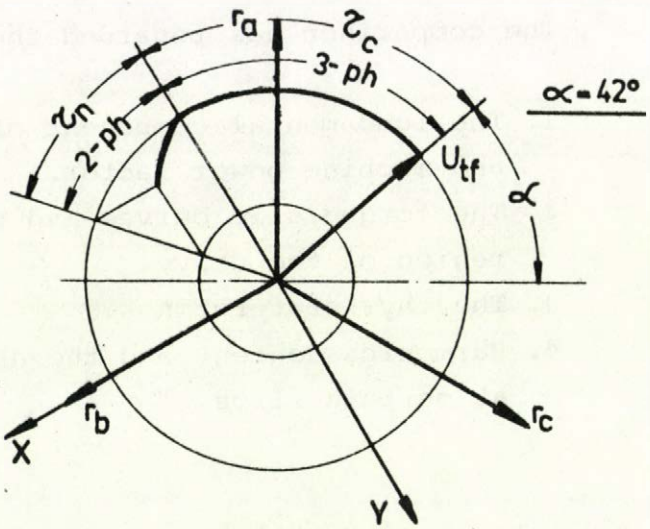

3-2 ph condition pure

resistive case

Fig.3.29

$$\bar{U}_{rl} = \frac{1}{\tau} \int_{-\frac{\Pi}{2}+\alpha+\tau_c}^{-\frac{\Pi}{2}+\alpha+\tau} U \frac{RR}{1+RR} \cos(t - \frac{2\Pi}{3})\, e^{j\frac{2\Pi}{3}} \bar{e}^{jt}\, dt \quad (3.39)$$

Since $\tau_c+\tau_n = \tau = \frac{2\Pi}{3}$

and $\alpha + \tau_c = \frac{2\Pi}{3}$

then $\alpha=\tau_n$ and the solution of the above integral gives:

$$\frac{\bar{U}_{rl}}{U} = \frac{RR}{1+RR} \quad \frac{1}{2\Pi} \left[\alpha - \sin\alpha\, \bar{e}^{j\alpha} \right] \quad (3.40)$$

Equation (3.40) is valid for $0 \leqslant \alpha \leqslant \frac{\Pi}{2}$, in which the drive is working in 3-2 ph condition.

There are two other working conditions namely 3-2-0 ph and 2-0 ph.

For 3-2-0 ph condition:

$$\frac{\bar{U}_{r1}}{U} = \frac{1}{2\tau}\,\frac{RR}{1+RR}\,\left(\frac{\Pi}{2}+j\right) + \frac{1}{\tau}\,\frac{RR}{1+RR}\,\left(\alpha-\frac{\Pi}{2}\right) \qquad (3.41)$$

for the range $\frac{\Pi}{2}\leq\alpha\leq\frac{2\Pi}{3}$ and in the 2-O ph condition:

$$\frac{\bar{U}_{r1}}{U} = \frac{1}{2\tau}\,\frac{RR}{1+RR}\,\left[\frac{7\Pi}{6} - \alpha + \cos\left(\alpha-\frac{2\Pi}{3}\right)\,e^{-j\left(\alpha-\frac{7\Pi}{6}\right)}\right] +$$

$$+ \frac{1}{\tau}\,\frac{RR}{1+RR}\,\left(\alpha-\frac{\Pi}{2}\right) \qquad (3.42)$$

It is applied for the range $\frac{2\Pi}{3} \leq \alpha \leq \frac{7\Pi}{6}$. From Fig.3.30 the following equation may be written

$$\frac{\bar{I}_{r1}}{U/R_r} = 1 - \frac{\bar{U}_{r1}}{U} \qquad (3.43)$$

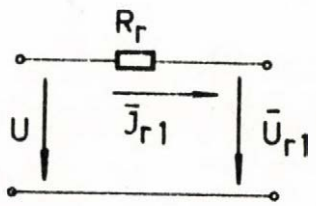

Fig.3.30

Equations (3.40) - (3.43) are used in drawing the value $\frac{\bar{I}_{r1}}{U/R_r}$ at different α values. For connection I(ΔTT), connection II(ΔT) and connection III(YTT) the value $\frac{\bar{I}_{r1}}{U/R_r}$ at different α values are given in figures 3.31, 3.32 and 3.33 respectively. These figures confirm the following:

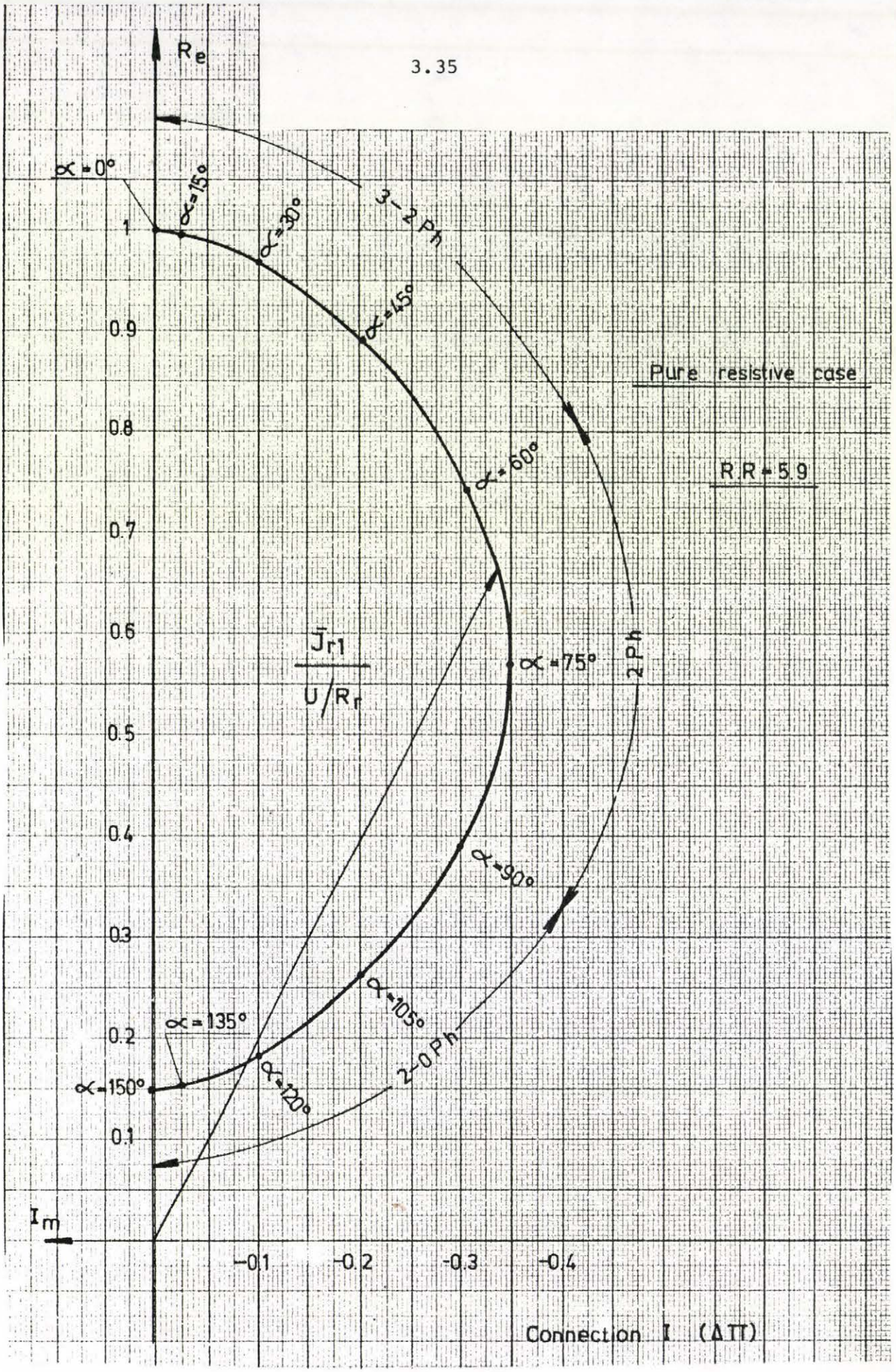
Re
Im
α = 0°
α = 15°
α = 30°
α = 45°
α = 60°
α = 75°
α = 90°
α = 105°
α = 120°
α = 135°
α = 150°
3-2 Ph
2 Ph
2-0 Ph
Pure resistive case
R.R = 5.9
J r1 / U/Rr
1
0.9
0.8
0.7
0.6
0.5
0.4
0.3
0.2
0.1
-0.1
-0.2
-0.3
-0.4
Connection I (ΔTT)

Fig.3.31

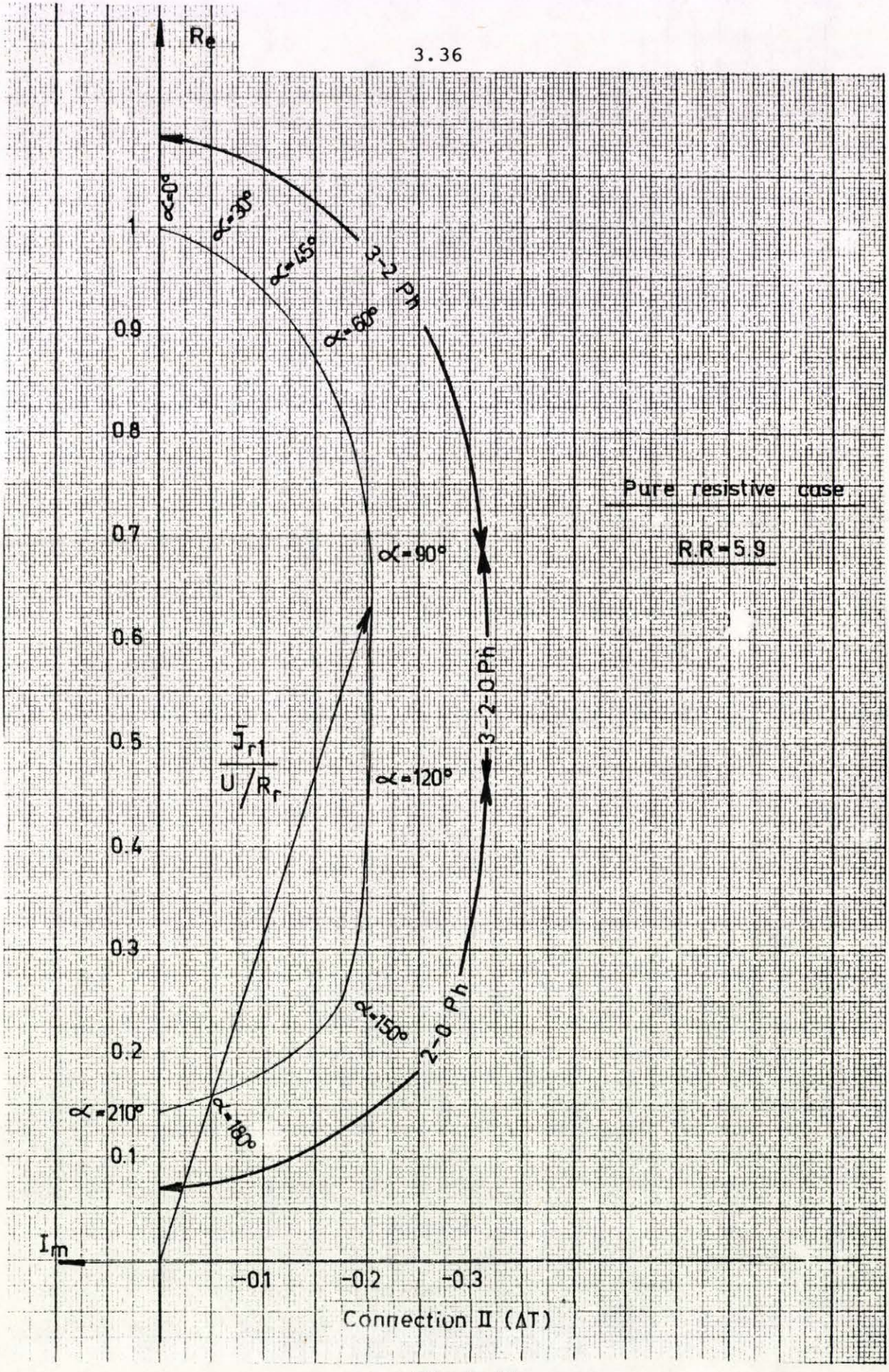
Re
1
0.9
0.8
0.7
0.6
0.5
0.4
0.3
0.2
0.1
α=0°
α=30°
α=45°
α=60°
α=90°
α=120°
α=150°
α=180°
α=210°
3-2 Ph
3-2-0 Ph
2-0 Ph
Pure resistive case
R.R=5.9
$\frac{I_{r1}}{U/R_f}$
Im
-0.1
-0.2
-0.3
Connection II (ΔT)

Fig.3.32

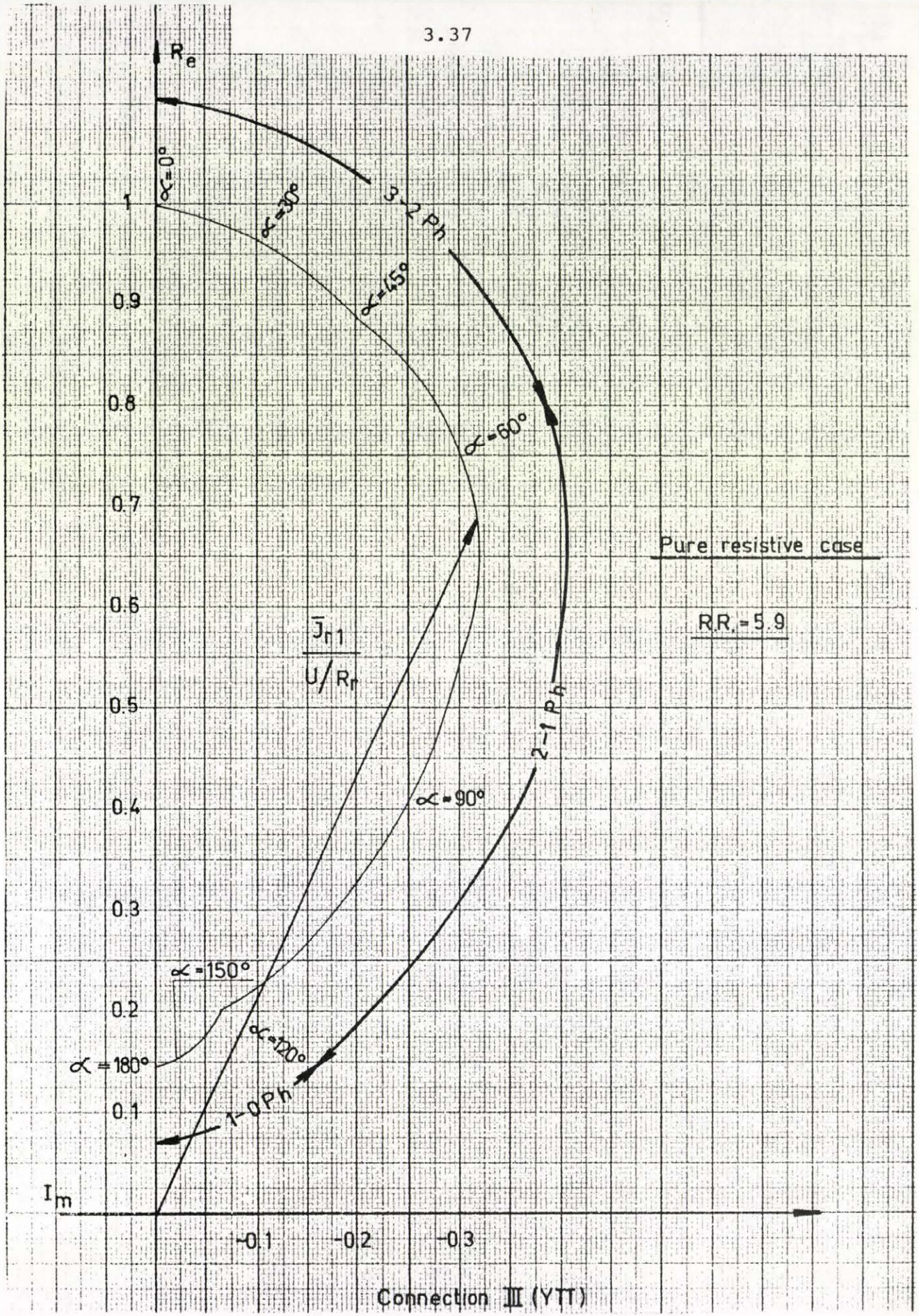
R_e
I_m
$\alpha=0°$
$\alpha=30°$
$\alpha=45°$
$\alpha=60°$
$\alpha=90°$
$\alpha=120°$
$\alpha=150°$
$\alpha=180°$
3-2 Ph
2-1 Ph
1-0 Ph
$\frac{\bar{I}_{r1}}{U/R_r}$
1
0.9
0.8
0.7
0.6
0.5
0.4
0.3
0.2
0.1
-0.1
-0.2
-0.3
Pure resistive case
RR = 5.9
Connection III (YTT)

Fig.3.33

it will be shown later, it is unnecessary to use any additional resistances in series with the internal rotor resistances. During the above range of α, the drive is operating in 3-2 ph condition. The other working conditions are 2ph and 2-O ph.

For 2ph condition:

$$\frac{\bar{I}_{rl}}{U/R_r} = \frac{1}{1 + \frac{3}{4} RR} \left[\frac{1}{2} + \frac{1}{2} \frac{\sin\tau}{\tau} e^{-j2\alpha}\right] \qquad (3.45)$$

and

$$\alpha_e < \alpha < 60^o .$$

For 2-O ph condition:

$$\frac{\bar{I}_{rl}}{U/R_r} = \frac{1}{1 + \frac{3}{4} RR} \frac{\frac{2\Pi}{3} - \alpha}{2\tau} +$$

$$+ \frac{1}{1 + \frac{3}{4} RR} \frac{1}{2\tau} \sin\left(\frac{2\Pi}{3} - \alpha\right) e^{-j\left(\alpha + \frac{\Pi}{3}\right)} \qquad (3.46)$$

for $60^o < \alpha < 120^o$.

In fig.3.34 the value $\frac{\bar{I}_{rl}}{U/R_r}$ is drawn at different α values using equations (3.44) - (3.46). In a similar way $\frac{\bar{I}_{rl}}{U/R_r}$ is drawn at different α values for half controlled bridge in Fig.3.35.

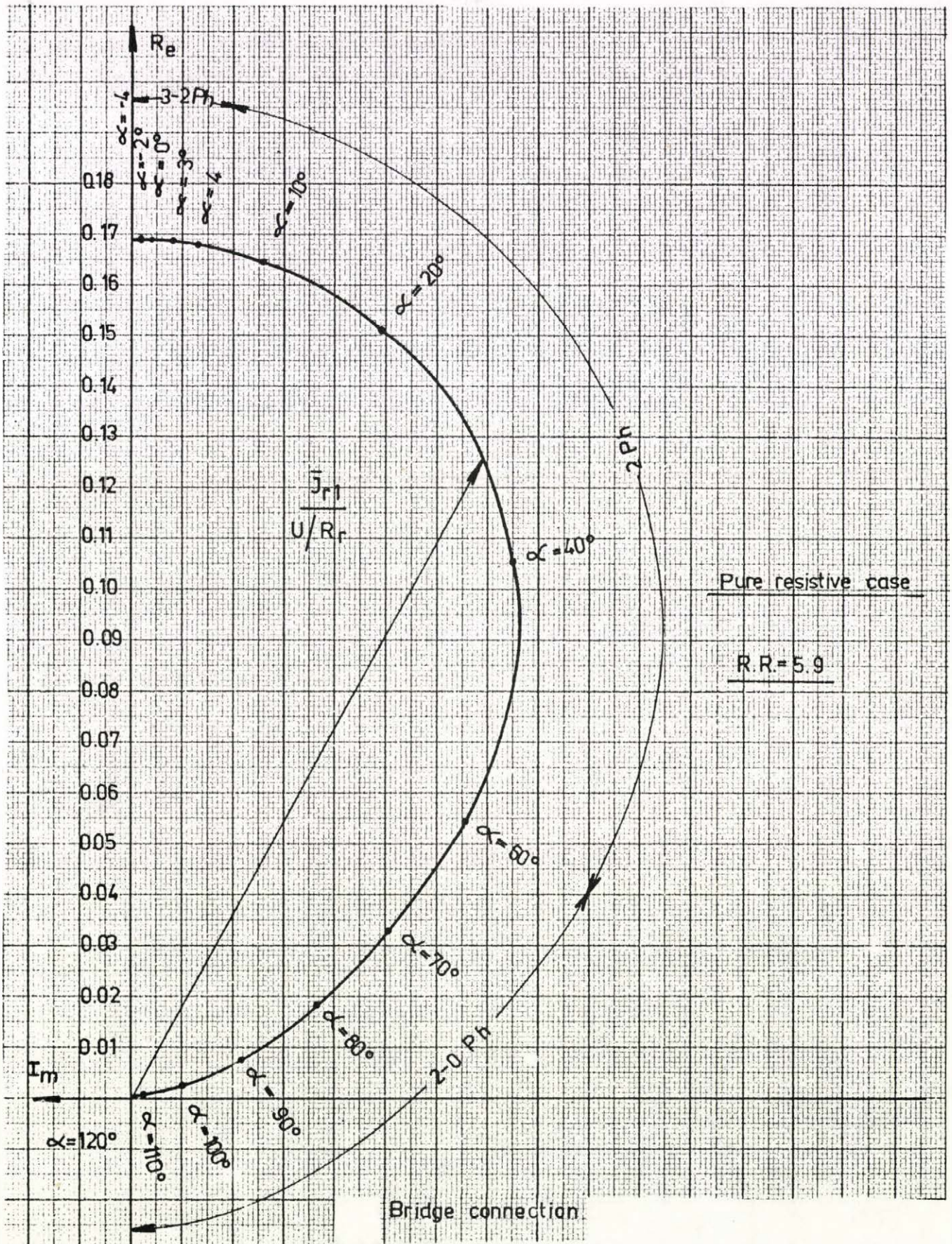
Re
3-2Ph
γ=-4°
γ=-2°
γ=0°
γ=3°
γ=4°
α=10°
α=20°
α=40°
α=60°
α=70°
α=80°
α=90°
α=100°
α=110°
α=120°
2Ph
2-0 Ph
Im
0.18
0.17
0.16
0.15
0.14
0.13
0.12
0.11
0.10
0.09
0.08
0.07
0.06
005
0.04
0.03
0.02
0.01
Jr1 / U/Rr
Pure resistive case
R.R.= 5.9
Bridge connection

Fig. 3.34

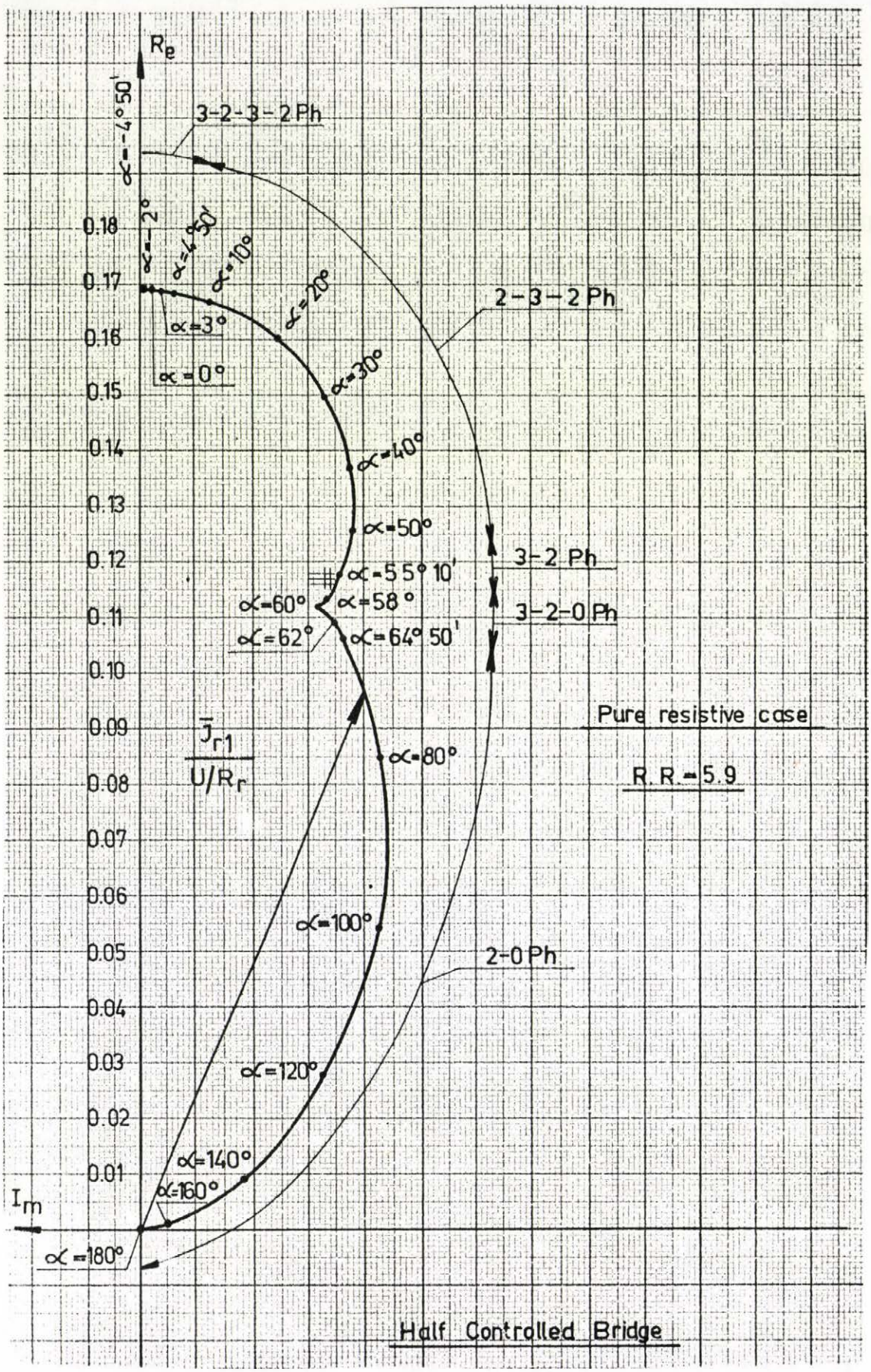
R_e
I_m
$\frac{\bar{I}_{r1}}{U/R_r}$
0.18
0.17
0.16
0.15
0.14
0.13
0.12
0.11
0.10
0.09
0.08
0.07
0.06
0.05
0.04
0.03
0.02
0.01
$\alpha = -4° 50'$
$\alpha = -2°$
$\alpha = 4° 50'$
$\alpha = 10°$
$\alpha = 20°$
$\alpha = 30°$
$\alpha = 40°$
$\alpha = 50°$
$\alpha = 55° 10'$
$\alpha = 58°$
$\alpha = 60°$
$\alpha = 62°$
$\alpha = 64° 50'$
$\alpha = 80°$
$\alpha = 100°$
$\alpha = 120°$
$\alpha = 140°$
$\alpha = 160°$
$\alpha = 180°$
$\alpha = 3°$
$\alpha = 0°$
3-2-3-2 Ph
2-3-2 Ph
3-2 Ph
3-2-0 Ph
2-0 Ph
Pure resistive case
R. R. = 5.9
Half Controlled Bridge

Fig. 3.35

The figures 3.34 and 3.35 confirm the following:

1. The power factor is better for the half controlled bridge.
2. The zero value of the torque is possible in both connections.
3. The range of α variation is:
   a. $0<\alpha<120^{o}$ for bridge connection
   b. $0<\alpha<180^{o}$ for half controlled bridge.

The magnitude of the current $\bar{I}_{rl}$ is small in the case of the bridge or half controlled bridge connections if the same resistance ratio is taken as in connections I(ΔTT), II(ΔT) or III(YTT). In such a way suitable values of $R_{d.c.}$ must be chosen to get proper values of the currents.

The above results show that the p.f. in the case of the bridge connection is the worst. The number of thyristors needed in that case is double that in connection II(ΔT) or in half controlled bridge. However the bridge connection, besides its bad performance, it is also not economic. Therefore this connection is excluded in the next comparison.

The real case was considered for the different connections and the fundamental component of the rotor current $\bar{I}_{rl}$ was calculated using digital computer and for some connections a numerical method for solving the integration like Runge-Kutta method was used.

The curves of $\bar{I}_{rl}$ /at different α values/ for the different connections at s=0.465 is shown in Fig.3.36. The results agree with the approximate method of pure resistive case.

Connection II(ΔT) gives better performance characteristics since the power factor is high. It has a drawback that the

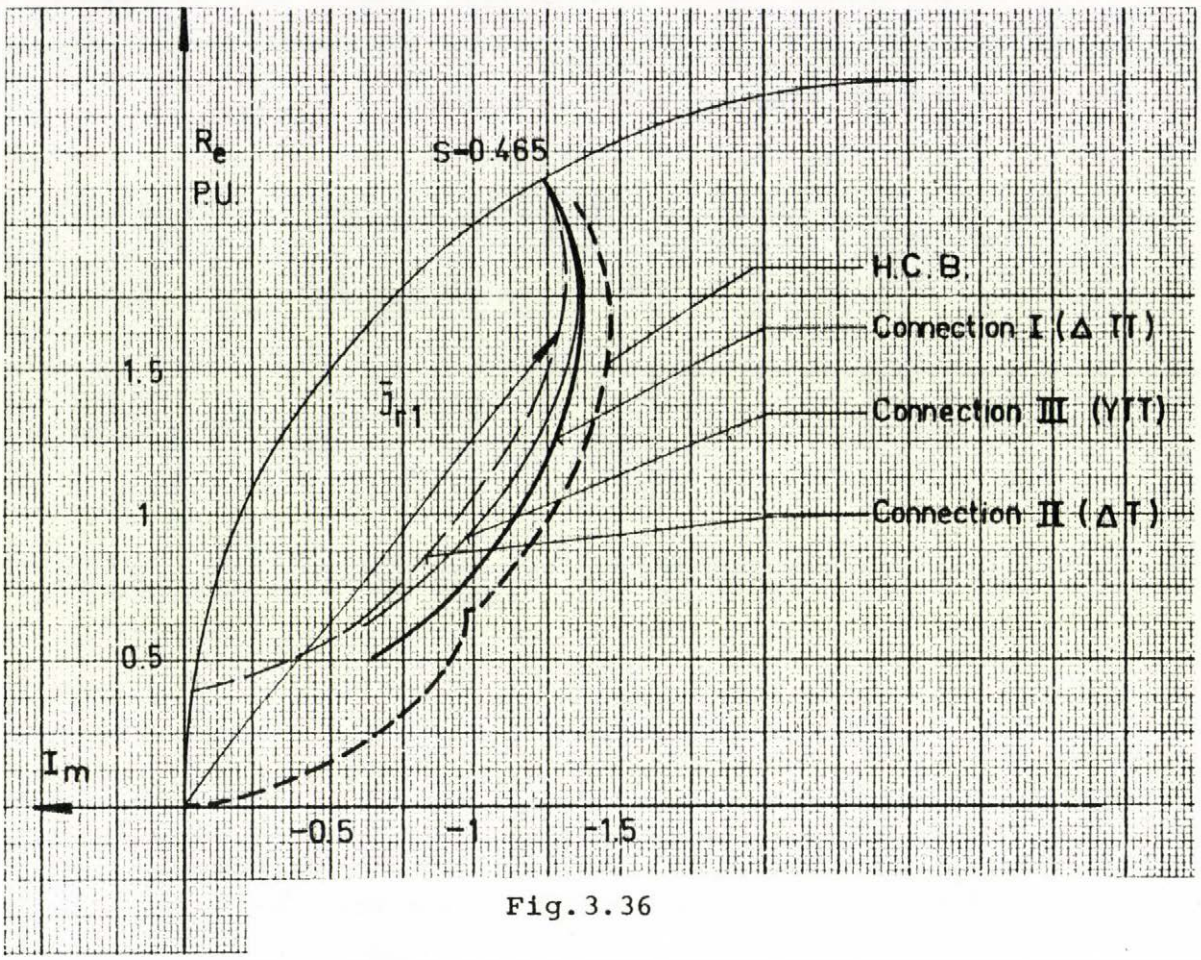

Fig.3.36

torque has a minimum value. In the case of the half controlled bridge it is possible to get zero value of the torque which makes the drive suitable for further applications such as crane drives.

3.3.2 Torque/Slip Curves and the Possible Working Region of the Drive

The possible working region of the drive is shown for connection I(ΔTT) and II(ΔT), if the rotor current is less than or equal to the rated value, in Fig.3.24 and Fig.3.37 respectively. The regions if the rotor current is equal one and half times the rated value are also given in the figures. Comparing the two figures, the possible working region of the drive with connection II(ΔT) is wider for the same resistance ratio.

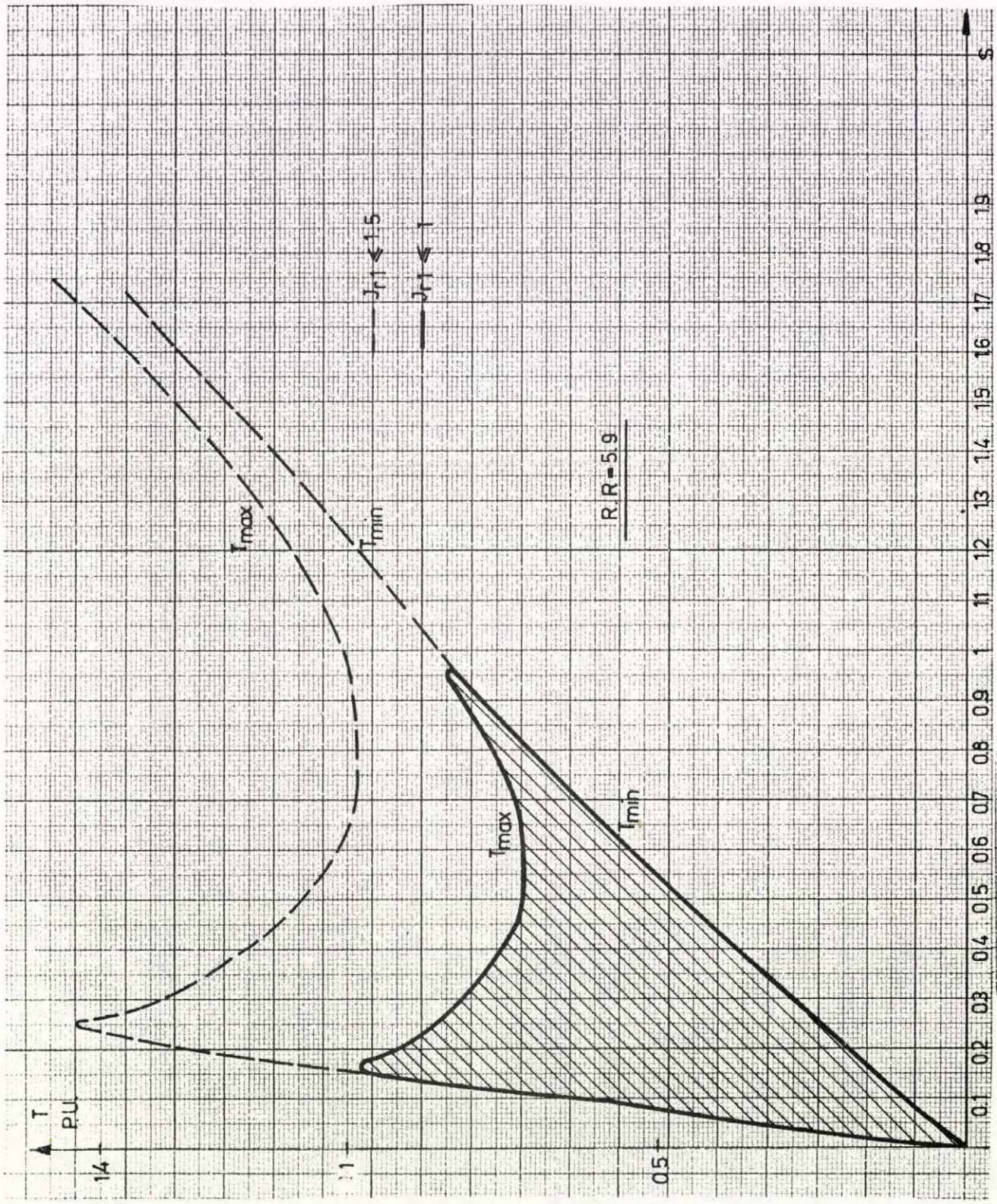
T
PU
1.4
1
0.5
0.1 0.2 0.3 0.4 0.5 0.6 0.7 0.8 0.9 1 1.1 1.2 1.3 1.4 1.5 1.6 1.7 1.8 1.9
S
T_{max}
T_{min}
$J_{r1} = 1.5$
$J_{r1} = 1$
R.R=5.9
T_{max}
T_{min}
Connection II (Δ Γ)

Fig.3.37

For the half controlled bridge two different values of $R_{d.c.}$ are used. The corresponding T/s curves and the possible regions are shown in Fig.3.38. In the figure, it is clear that the torque can be reduced to zero value which is the advantage of this connection.

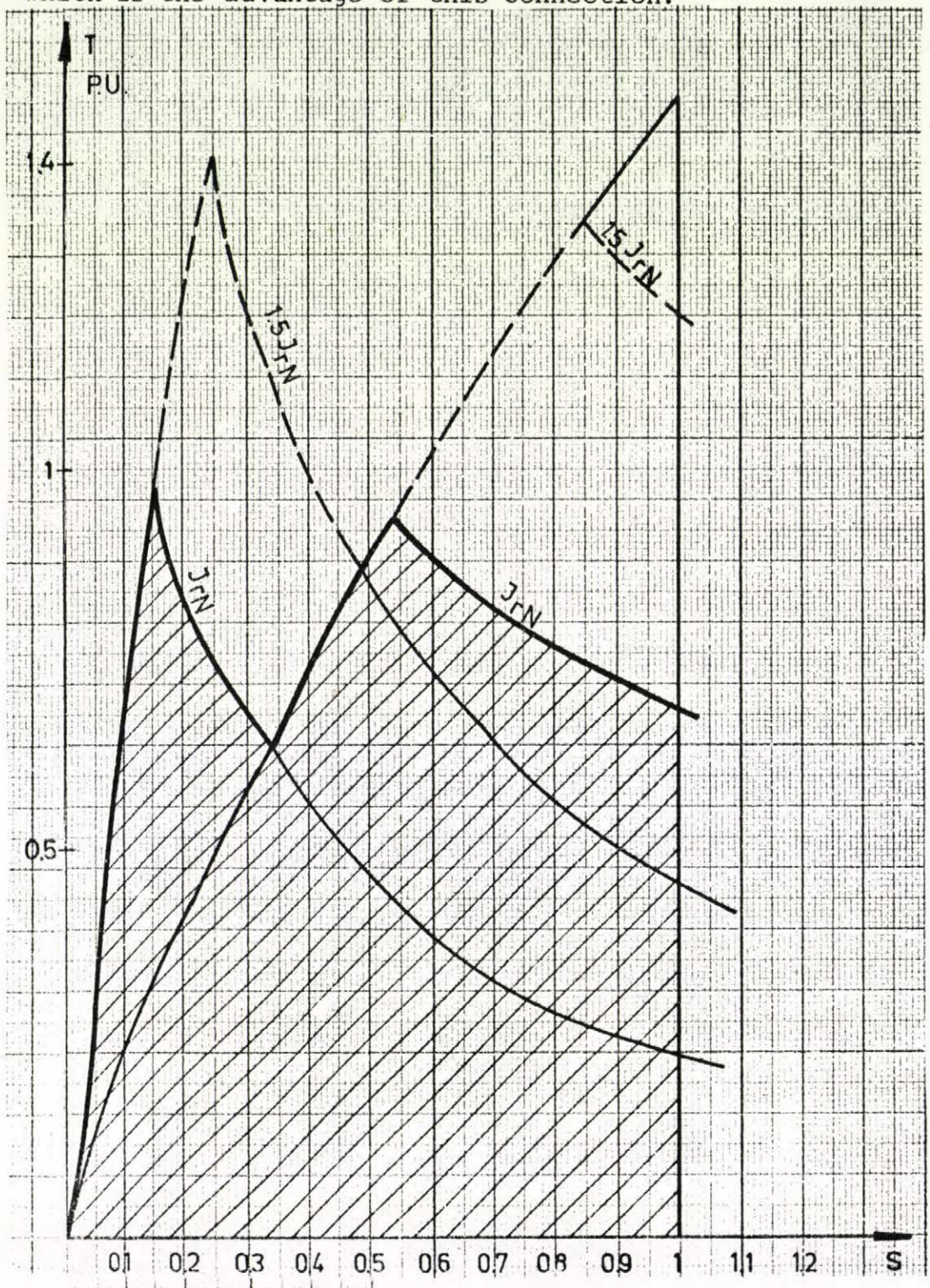

Half Controlled Bridge

Fig.3.38

It is also possible to use two different resistance ratios for connections I(ΔTT), II(ΔT) and III(YTT) to use the drive in the both quadrants.

3.3.3 The Thyristor Ratings

The maximum value of the thyristor voltage and the mean and R.M.S. values of the thyristor current are needed to decide the rating of the thyristor. These values can be calculated exactly using digital computations for some connections. For the purpose of comparison it is useful to get approximate equations to calculate such values directly. As an example, the equations are derived for connection III(YTT) while the results for the other connections are given.

1. Maximum Thyristor Voltage

With connection III(YTT), there are four conduction states, namely 3-ph, 2-ph, 1-ph and O-ph. At 3-ph condition the thyristor voltage equals zero. At 2-ph conduction state, the thyristor voltage equals $i_{rx}R_{ro}/s$ /see Fig.3.39/. At 1-ph conduction state, see Fig.3.40, the thyristor voltage is:

$$u_{ta} = \left(\frac{1}{2} i_{rx} + \frac{\sqrt{3}}{2} i_{ry} \right) R_{ro}/s \qquad (3.47)$$

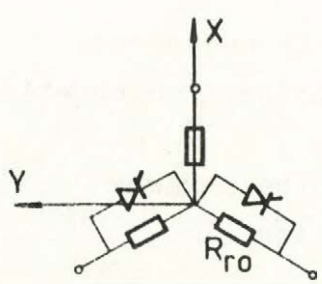

2-Ph conduction
Connection III.(YTT)

Fig.3.39

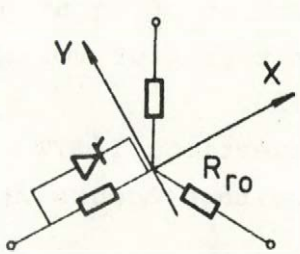

1-Ph conduction
Connection III.(YTT)

Fig.3.40

The maximum thyristor voltage for connection III(YTT) occurs during the 1-ph conduction state. From equation (3.47):

$$u_{ta} = \frac{1}{2}\frac{u_x R_{ro}/s}{\sqrt{\left(\frac{R_r + \frac{1}{3}R_{ro}}{s}\right)^2 + X_r'^2}} + \frac{\sqrt{3}}{2}\frac{u_y R_{ro}/s}{\sqrt{\left(\frac{R_r+R_{ro}}{s}\right)^2 + X_r'^2}} \quad (3.48)$$

The voltage equation in the coordinate system shown in Fig.3.40 is:

$$\bar{u} = U\, e^{jt}\, e^{j\frac{\Pi}{3}} \quad (3.49)$$

$$U = 1$$

$$u_x = \frac{1}{2}\cos t - \frac{\sqrt{3}}{2}\sin t \quad (3.50)$$

$$u_y = \frac{1}{2}\sin t + \frac{\sqrt{3}}{2}\cos t \quad 3.51$$

t is the reduced time measured from the instant when the voltage in phase a is maximum. From equations (3.48)-(3.51) the thyristor voltage at any instant can be obtained. For motoring region the thyristor voltage is calculated at s=1. The instant at which the maximum thyristor voltage occurs can be calculated by differentiating u_{ta} w.r.t. the reduced time "t" and equating the result to zero. This time is given by the following equation:

$$t = \arctan \sqrt{3}\,\frac{2+RR}{RR} \quad (3.52)$$

In the deduction of equation (3.52) X_r' is neglected. The maximum thyristor voltage is calculated from equations (3.48)-(3.52).

For connections I(ΔTT) and II(ΔT); the maximum thyristor voltage occurs at O-ph condition

$$U_{t\ max} = \frac{\sqrt{3}\ R_{ro}}{\sqrt{(R_r+R_{ro})^2+X_r'^2}} \qquad (3.53)$$

For the half controlled bridge connection the maximum thyristor voltage occurs at the O-ph condition. In P.U. system, it is equal to $\sqrt{3}$.

2. Mean and R.M.S. Values of Thyristor Current

Connection I(ΔTT) is considered as an example and the results for the other connections are given:

For the connections of the first part /3-phase resistance control/, the mean and R.M.S. values of the thyristor current are calculated for the pure 3-ph conduction state.

As shown from Fig.3.1

$$i_{t\ PA} = i_{ra} \quad \text{in the first stroke}$$

$$i_{t\ PA} = -i_{rb} \quad \text{in the second stroke}$$

and afterwards the thyristor turns off and remains in the blocking mode till the end of the period.

$$I_{tav} = \frac{1}{2\Pi}\left[\int_{o}^{\Pi/3} I_m \sin t\ dt + \int_{\Pi/3}^{2\Pi/3} I_m \sin\left(t+\frac{\Pi}{3}\right) dt\right]$$

$$I_{tav} = \frac{1}{2\Pi}\ \frac{1}{\sqrt{\left(\frac{R_r}{s}\right)^2+X_r'^2}} \qquad (3.54)$$

$$I_{t\ R.M.S.} = \frac{1}{\sqrt{\left(\frac{R_r}{s}\right)^2+X_r'^2}}\ \sqrt{\frac{1}{6}-\frac{\sqrt{3}}{8\Pi}} \qquad (3.55)$$

Similarly for the other connections:

Connection II(ΔT):

$$I_{tav} = \frac{3}{2\Pi} \frac{1}{\sqrt{\left(\frac{R_r}{s}\right)^2 + X_r'^2}} \tag{3.56}$$

$$I_{t\ R.M.S.} = \frac{1}{\sqrt{\left(\frac{R_r}{s}\right)^2 + X_r'^2}} \sqrt{\frac{1}{3} + \frac{\sqrt{3}}{8\Pi}} \tag{3.57}$$

Connection III(YTT):

$$I_{tav} = \frac{1}{\Pi} \frac{1}{\sqrt{\left(\frac{R_r}{s}\right)^2 + X_r'^2}} \tag{3.58}$$

$$I_{t\ R.M.S.} = \frac{1}{2} \frac{1}{\sqrt{\left(\frac{R_r}{s}\right)^2 + X_r'^2}} \tag{3.59}$$

The calculation in the case of the half controlled bridge is relatively complicated. The required values may be obtained using the approximate method of 2-energy storages as it will be explained later.

The comparison between the thyristor ratings for the different connections with the 3-ph resistance control part is given in table 1. In that table the maximum thyristor voltage is calculated at s=1. The average and R.M.S. values of the thyristor current are calculated for the working point of 1.5 times the rated current and maximum available torque /point "a" in Fig.3.24/. In all

the connections the resistance ratio is the same and equals 5.9. The working point at which I_{tav} and $I_{t\ R.M.S.}$ are calculated has a slip of 0.25. In the calculation the peak value of the rotor phase voltage is taken as a base value.

For the purpose of comparison the rated value of the thyristor current is considered as the arithmetic mean of I_{tav} and $I_{t\ R.M.S.}/\frac{\Pi}{2}$

	ΔTT	ΔT	YTT
$U_{t\ max}$	1.46	1.46	1.17
I_{tav}	0.24	0.72	0.48
$I_{t\ R.M.S.}$	0.47	0.95	0.75
$I_{t\ rated}$	0.27	0.66	0.48
$U_{t\ max}\ I_{t\ rated}$	0.39	0.96	0.56
№ of thyristors	6	3	6

Table 1

Table 1 shows that connection I(ΔTT) needs lower rating thyristors. But for connection II(ΔT) the number of thyristors is only three, then the drive with connection II(ΔT) may give the economic solution if the price of the firing circuits are relatively high.

The comparison between connection II(ΔT) and half controlled bridge is given in table 2. Connection ΔT has R_{ro} equals 94% and with the half controlled bridge $R_{d.c.}$ equals 75.96%. These values correspond to the

used drive in the laboratory. For connection ΔT a resistance of 9.13% is added to the internal rotor resistance. The method of the comparison is the same as in table 1.

	$U_{t\ max}$	I_{tav}	$I_{t\ RMS}$	$I_{t\ rated}$	$U_{t\ max} I_{t\ rated}$	N° of elements
ΔT	1.46	.72	.95	.66	.96	3T
H.C.B.	1.73	.452	.784	.48	0.83	3T+3D

Table 2

H.C.B. = half controlled bridge connection
T = thyristor
D = diode

3.3.4 Harmonic Contents

Regarding equation (3.13) the order of the upper harmonics for the different connections is:

1. Connection I(ΔTT) : ....-11, -5, 1, 7, 13, ...
2. Connection II(ΔT) : .... -5, -2, 1, 4, 7, ...
3. Connection III(YTT) : ....-11, -5, 1, 7, 13, ...
4. Half controlled bridge : .... -5, -2, 1, 4, 7, ...

These upper harmonics cause additional losses. As it will be discussed later, the stator frequency related to some harmonic components at certain speeds, for example $\frac{2}{3}$ of the synchronous speed, is zero. This cause some anomalies in the characteristics of the system. At these points there are some oscillations and irregularities in the torque/speed characteristic for constant rotor current.

In the motoring region connection II(ΔT) and half controlled bridge connection have more of such special points than connection I(ΔTT) and connection III(YTT).

The comparison of the different connections confirms the following:

1. Among the studied connections of the 3-ph resistance control, connection II(ΔT) has the best characteristic performance, the range of operation of the drive is wider and the drive with this connection is economic.
2. Between the connections of the d.c. resistance control part, the bridge connection gives bad performance and it is not economic.
3. Comparing connection II and the half controlled bridge connection, the latter has an advantage that the torque can be reduced to zero value. Therefore the drive is suitable for the applications which need low torque values. The power-factor may be relatively better with connection II(ΔT). The cost of the drive with the two connections is nearly the same.

3.4 Modes of Operation

There are four different conduction states, namely, 3 ph, 2ph, 1ph and 0ph. For connections of the three phase resistance control part the three phase conduction state means that the thyristors short-circuit the external resistance. In the 2-ph conduction state two resistances of the external resistance are short-circuited by the thyristors and so on. For the connections of the D.C. resistance control part, the three phase conduction state occurs due to the commutation between two thyristors in

two phases and the diode in the third phase is in conducting state, or when commutation between two diodes happens and the thyristor in the third phase is fired. The two phase conduction state is obtained from the firing of a thyristor in one phase of the motor and the diode in the other phase is conducting, the third phase of the motor in that case is open. It is shown from figures 3.31 - 3.35 that the following modes of operations are possible:

1. For connection I(ΔTT) there are 3-2 ph, 2ph and 2-Oph
2. For connection II(ΔT) there are 3-2 ph, 3-2-O ph and 2-Oph
3. For connection III(YTT)there are 3-2 ph, 2-1ph and 1-Oph
4. For half controlled bridge connection there are 3-2-3-2ph, 2-3-2ph, 3-2ph, 3-2-Oph and 2-Oph.

Normally for the half controlled bridge connection the system is operated in 3-2-3-2ph, 3-3-2ph and 2-Oph.

In the case of 3-3-2ph the diodes begin to commutate at the end of the thyristors commutation, so there are two successive 3-ph conduction states.

In the further studies not only here but also for the dynamic behaviour and control properities the half controlled bridge was selected to be the chosen connection.

3.5 Half Controlled Bridge Connection

For the general solution the speed variation is considered, then the torque equation and equations of motion are needed. The differential equations of the system are non linear. This solution is very complicated for practical purposes since it needs some numerical integration and iteration procedures.

In general it is unnecessary to solve the above set of equations. Simpler solutions can be developed that

give results of good accuracy for practical steady-state characteristics of the system such as additional losses, the loading limits, the different upper harmonics of the voltage and current and so on.

The exact method is to be used if the transient performance and/or the control properties are studied.

3.5.1 Approximate Solutions

If some proper approximations are made the solution of the equations of the system is greatly simplified while the results maintain the required good accuracy.

a/ 2-Energy Storages

A coordinate system fixed to the rotor is chosen. If the motor speed is considered constant and the stator resistance is neglected, the analysis is reduced to simple R-L circuit. Utilizing the symmetry of the circuits, the coordinate system is fixed to the symmetry axes. As stated before, there are four different conduction states, 3-phase conduction due to thyristors commutation, 3 phase conduction due to diodes commutation, 2-ph and 0-ph conduction states. Then different reference frames are used for the different conduction states /see Fig.3.41/. The equivalent circuits in the 3-ph and 2-ph conduction states are shown in figures 3.42 and 3.43 respectively.

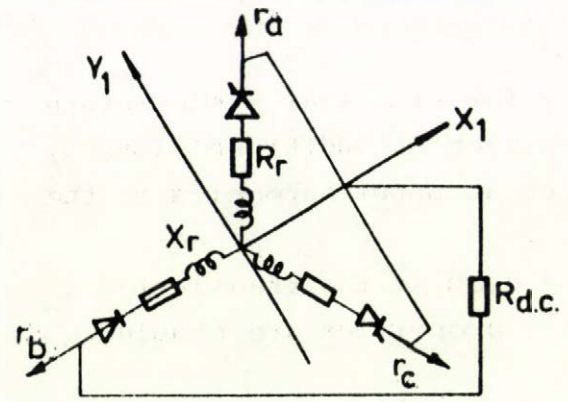

3-Ph conduction: thyristorscommutation

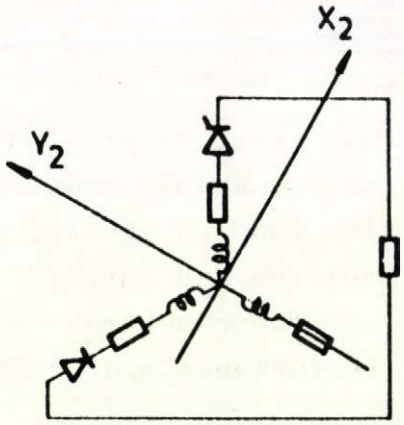

2-Ph conduction

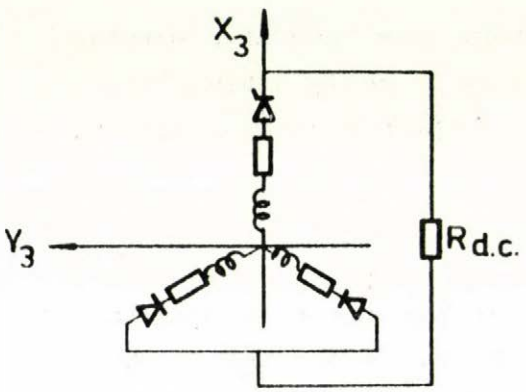

3-Ph conduction: diodes commutation

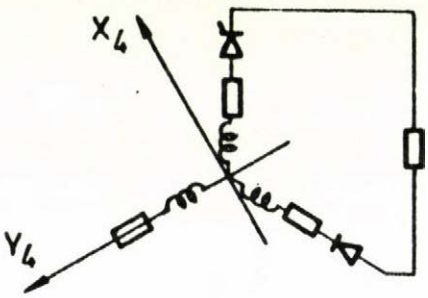

2-Ph conduction

Fig.3.41

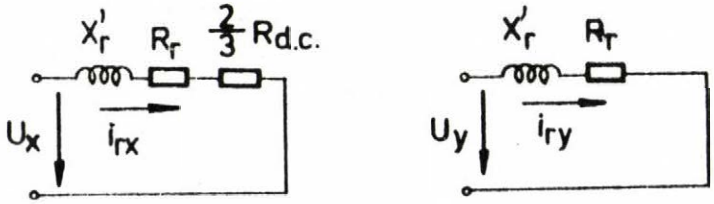

3-Ph conduction

Fig.3.42

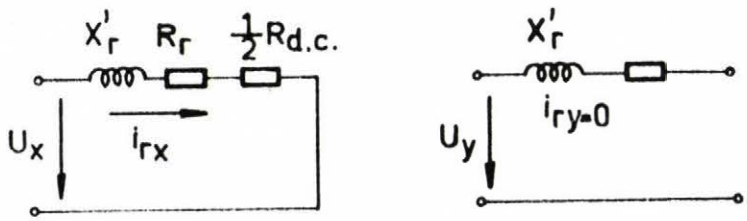

2-Ph conduction

Fig.3.43

The principal equation to be solved is:

$$\frac{d\underline{X}}{dt} = \underline{A}_c \underline{X} + \underline{B}\,\underline{u} \tag{3.60}$$

$$\underline{X} = \begin{bmatrix} i_{rx} \\ i_{ry} \end{bmatrix} \tag{3.61}$$

The matrices $\underline{A}_c$ and $\underline{B}$ depend on the conduction state.
At 3-ph condition

$$\underline{A}_{c3} = \begin{bmatrix} R_r + \frac{2}{3} R_{d.c.} & 0 \\ 0 & R_r \end{bmatrix}, \quad \underline{B}_3 = \begin{bmatrix} 1 & 0 \\ 0 & 1 \end{bmatrix} \tag{3.62}$$

At 2-ph condition:

$$\underline{A}_{c2} = \begin{bmatrix} R_r + \frac{1}{2} R_{d.c.} & 0 \\ 0 & 0 \end{bmatrix}, \quad \underline{B}_2 = \begin{bmatrix} 1 & 0 \\ 0 & 0 \end{bmatrix} \tag{3.63}$$

$$\underline{u} = \begin{bmatrix} U\ \cos(st+\beta) \\ U\ \sin(st+\beta) \end{bmatrix} \tag{3.64}$$

β equals $\frac{\Pi}{3}$ in the first 3-phase conduction state /see Fig.3.41/ and for each sequent state the coordinate axes are rotated by $\Pi/6$ in the forward direction.

The 3-ph conducting state due to thyristors commutation or diodes commutation exsists so long the condition $\sqrt{3}\, i_{ry} \leqslant i_{rx}$ is realizing. It is so because, for example, during the three phase conduction state due to thyristors commutation, /see Fig.3.41/ the current in phase "r_c" tends to zero when $\sqrt{3}\, i_{ry} = i_{rx}$. Then the thyristor in that phase turns off and 2-ph conduction

state occurs. This two phase condition continues until $u_{rc} > u_{rb}$, afterwards the diode in the rotor phase "c" begins to commutate with the other diode and the other 3-ph conduction state occurs.

Therefore the condition for that 2-ph conduction state is:

$$u_{rbc} < 0 \quad \text{or} \quad \frac{\sqrt{3}}{2} i_{rx} \frac{R_{d.c.}}{2} > \frac{3}{2} u_{ry}$$

The interval of the last conduction state is determined such that the length of the stroke is $\frac{2\Pi}{3}$.

The solution of the system's equations is simple and the steady-state characteristics can be calculated. Because that the number of the conduction states is more than two, it is impossible to get a closed form solution in that case and an iteration method is necessary. The steady-state characteristic performances of the drive are shown in figures 3.44 - 3.49.

The operating region of the drive with the two values of $R_{d.c.}$ is shown from the T-S curves in Fig.3.38.

It is seen in Fig.3.50 that it does not make any difference in the result if the added rotor resistance is transformed to the right hand side of the bridge. Therefore in half controlled bridge connection, only suitable values of $R_{d.c.}$ are chosen and it is unnecessary to use any additional resistances to the internal rotor resistances as in connections I, II or III.

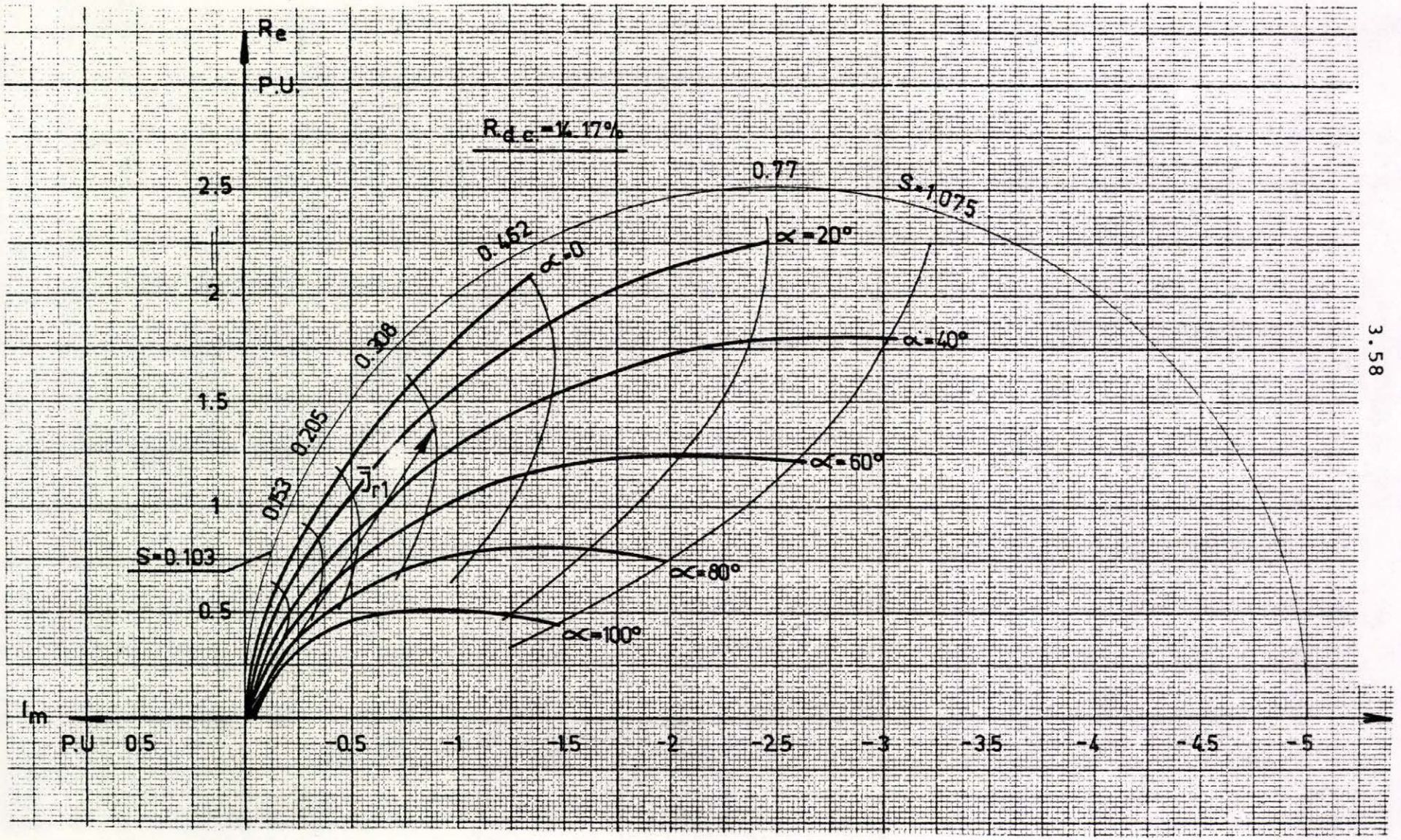
Re
P.U.
Rd.c.=1.17%
2.5
2
1.5
1
0.5
0.77
S=1.075
0.462
0.308
0.205
0.153
S=0.103
∝=0
∝=20°
∝=40°
∝=60°
∝=80°
∝=100°
Im
P.U
0.5
-0.5
-1
-1.5
-2
-2.5
-3
-3.5
-4
-4.5
-5

Fig.3.44

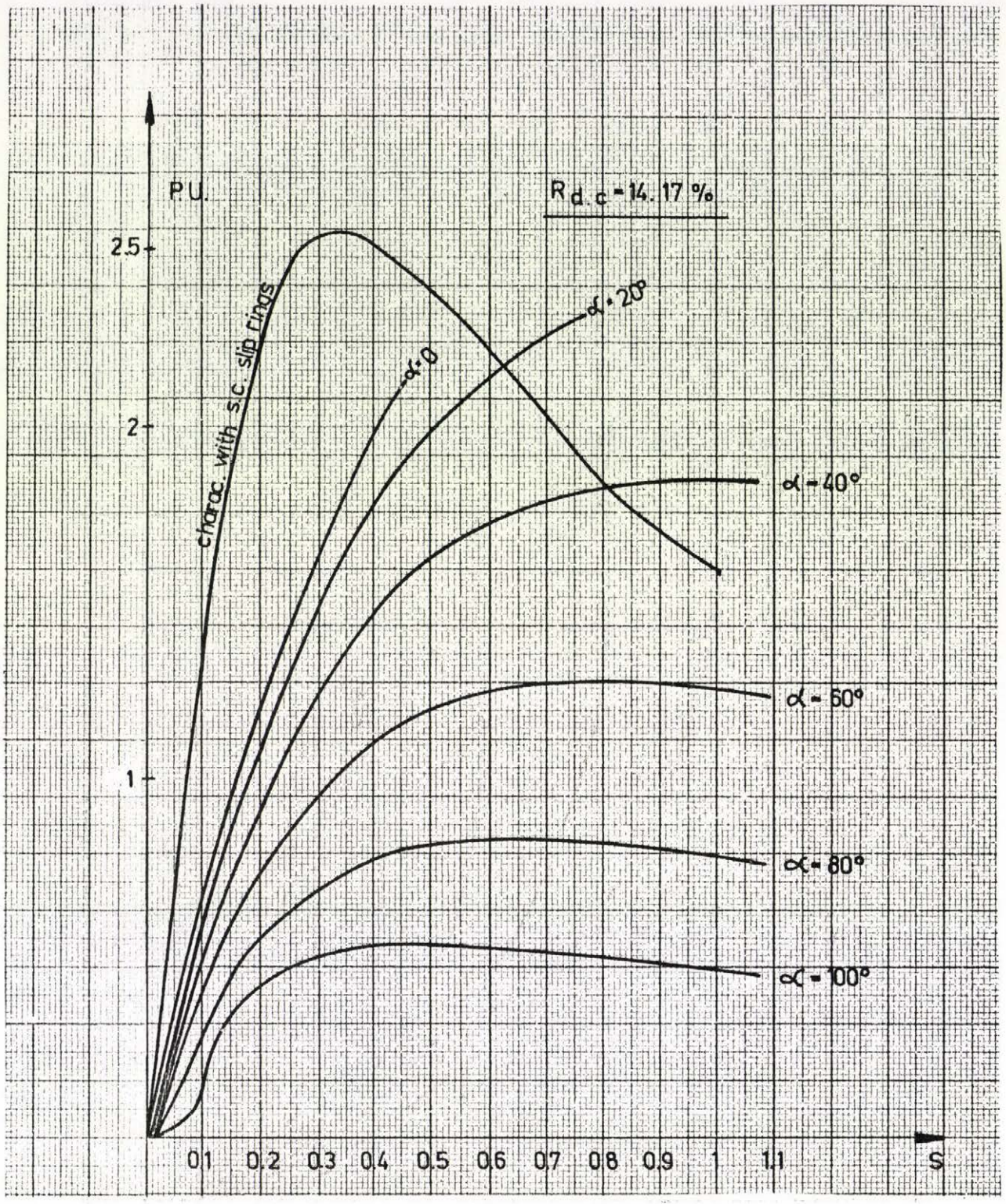
P.U.
$R_{d.c}$ = 14.17 %
2.5
2
1
charac. with s.c. slip rings
α = 0
α = 20°
α = 40°
α = 60°
α = 80°
α = 100°
0.1
0.2
0.3
0.4
0.5
0.6
0.7
0.8
0.9
1
1.1
S

Fig.3.45

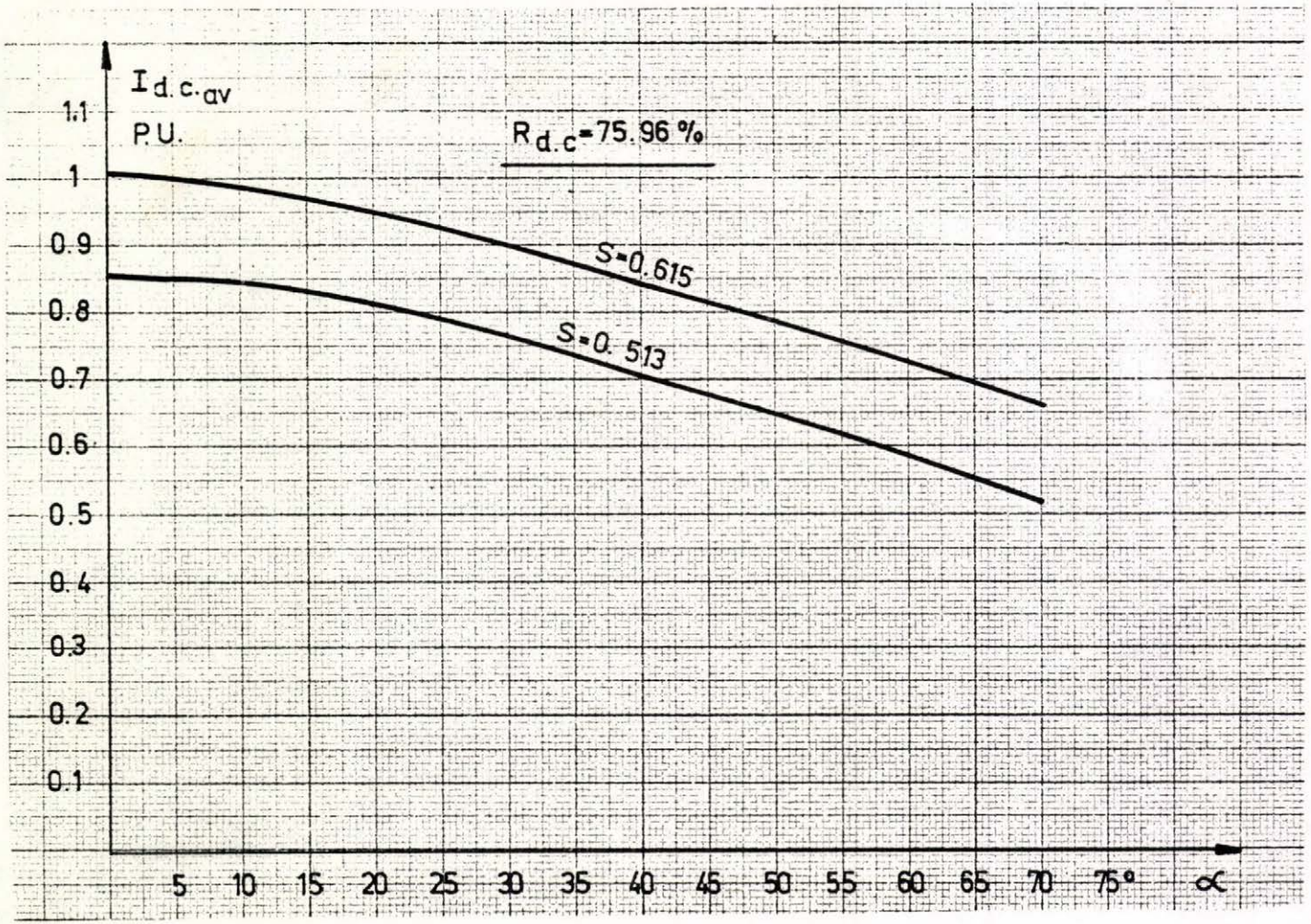
$I_{d.c.av}$
P.U.
$R_{d.c}$=75.96 %
S=0.615
S=0.513
1.1
1
0.9
0.8
0.7
0.6
0.5
0.4
0.3
0.2
0.1
5 10 15 20 25 30 35 40 45 50 55 60 65 70 75° ∝

Fig.3.46

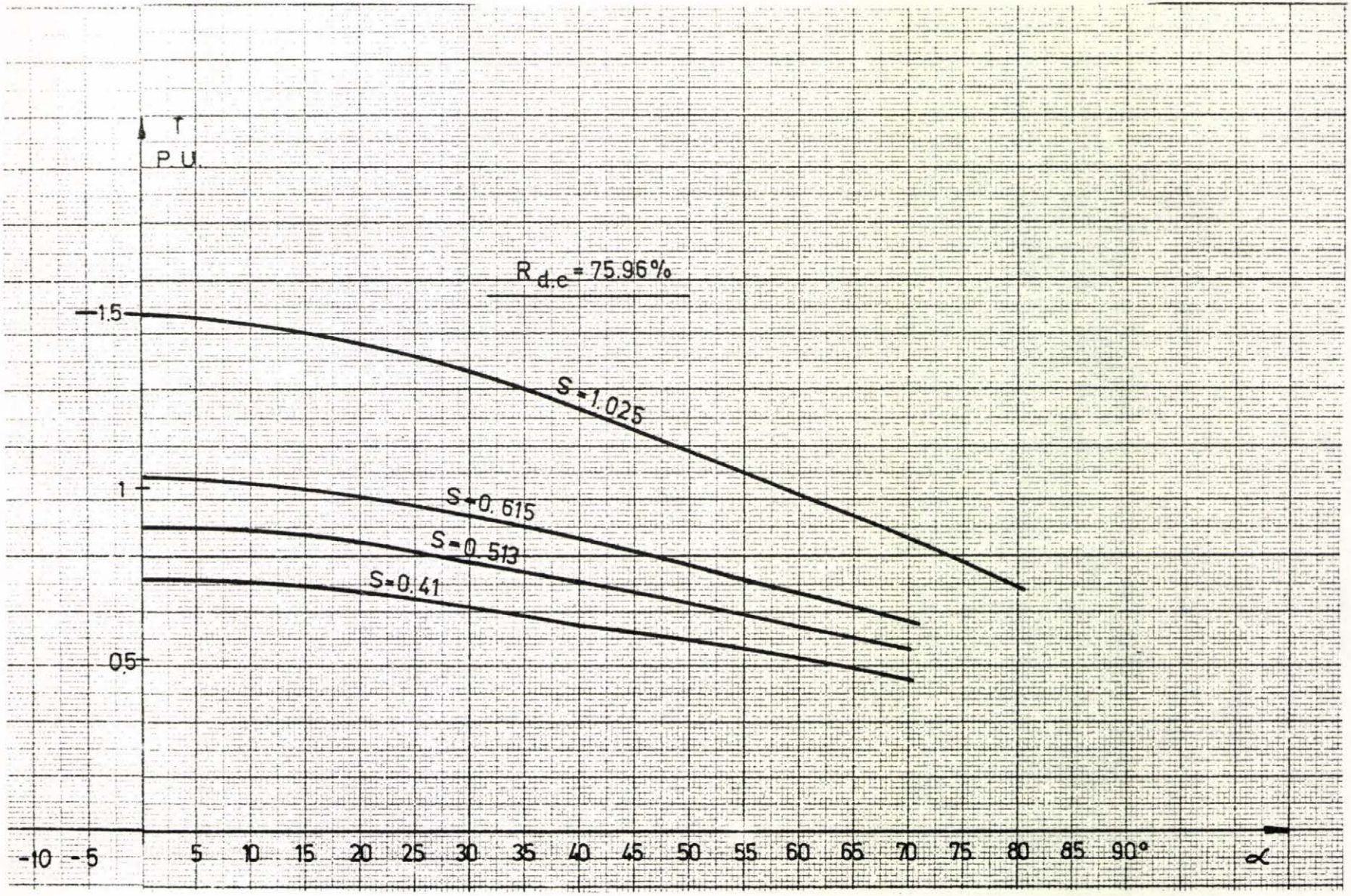
T
P.U.
$R_{d.c}$ = 75.96%
1.5
1
0.5
S=1.025
S=0.615
S=0.513
S=0.41
-10 -5 5 10 15 20 25 30 35 40 45 50 55 60 65 70 75 80 85 90° α

Fig.3.47

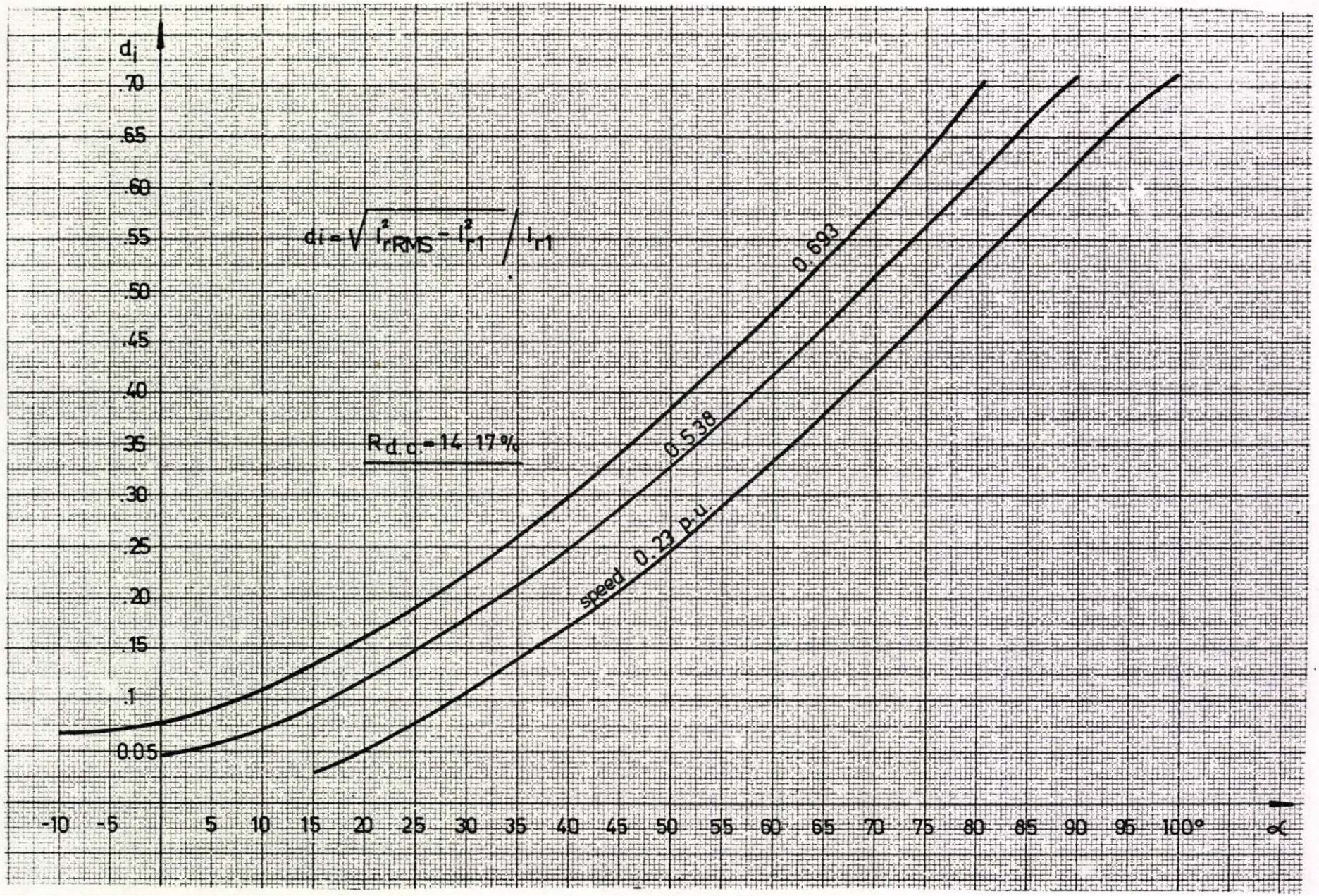
d_i
.70
.65
.60
.55
.50
.45
.40
.35
.30
.25
.20
.15
.1
0.05
$d_i = \sqrt{I^2_{rRMS} - I^2_{r1}} \,/\, I_{r1}$
$R_{d.c.} = 14.17\,\%$
0.693
0.538
speed 0.23 P.u.
-10 -5 5 10 15 20 25 30 35 40 45 50 55 60 65 70 75 80 85 90 95 100°
α

Fig.3.48

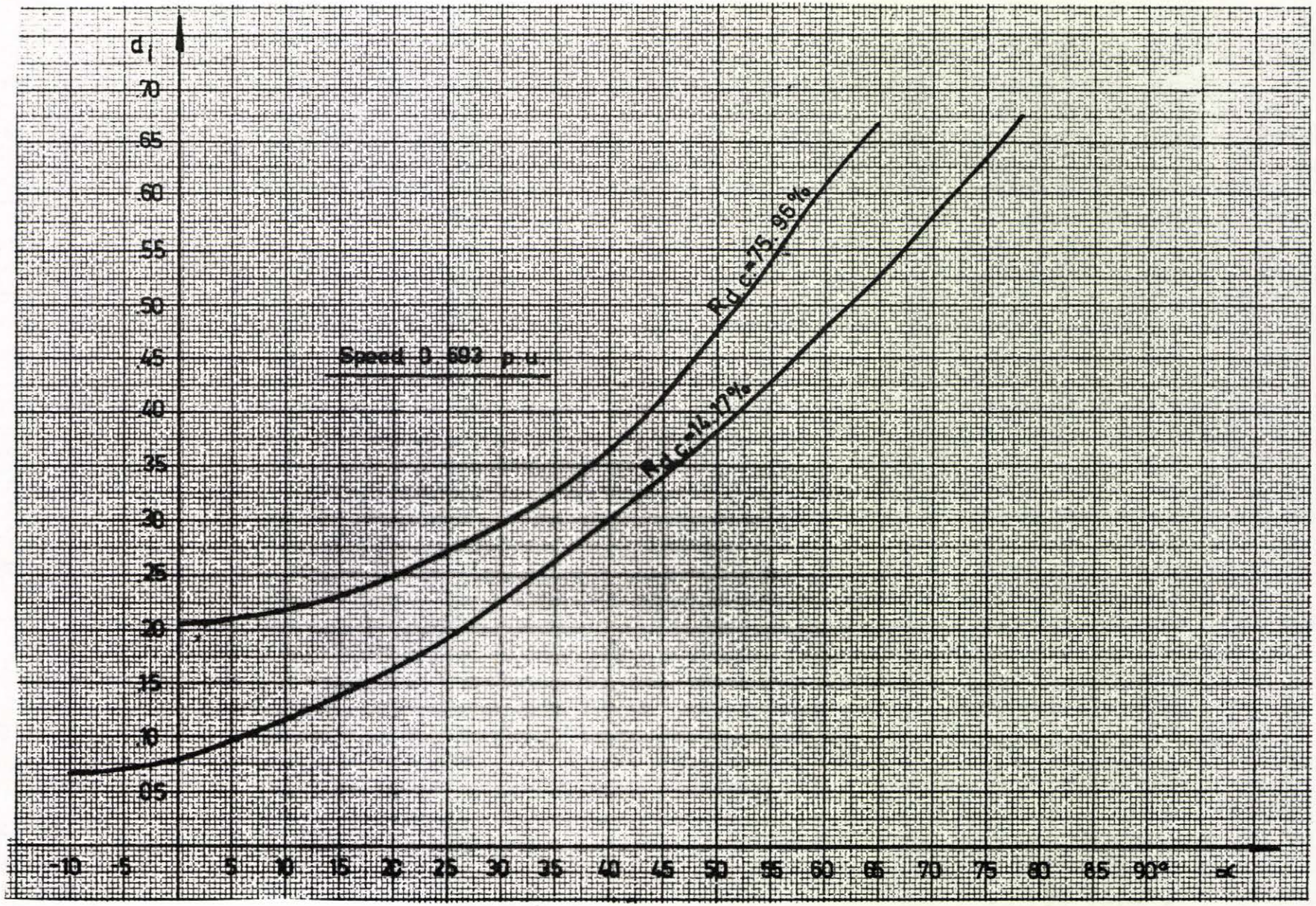
Cd
.70
.65
.60
.55
.50
.45
.40
.35
.30
.25
.20
.15
.10
.05
Speed 0.693 p.u
Rdc=75.96%
Rdc=14.17%
-10 -5 5 10 15 20 25 30 35 40 45 50 55 60 65 70 75 80 85 90° α

Fig.3.49

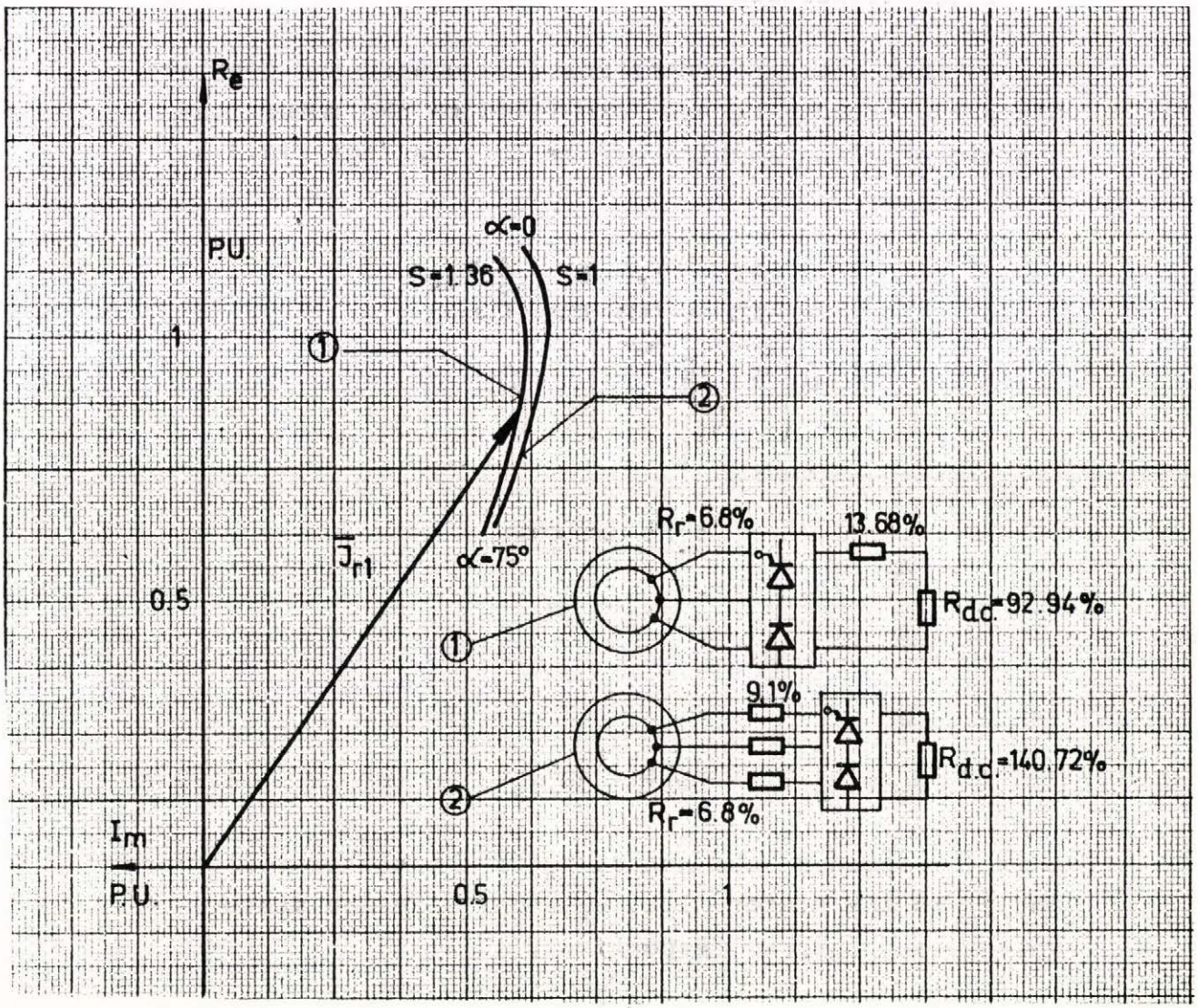
Re
P.U.
1
0.5
∝=0
S=1.36
S=1
∝=75°
$\bar{J}_{n1}$
Rr=6.8%
13.68%
Rd.c=92.94%
9.1%
Rd.c=140.72%
Rr=6.8%
Im
P.U.
0.5
1

Fig.3.50

b/ 4-Energy-Storages

In that case the motor speed is considered constant. Since the coordinate axes are fixed to the rotor, the equations of the machine are as follows /see Fig.3.51/

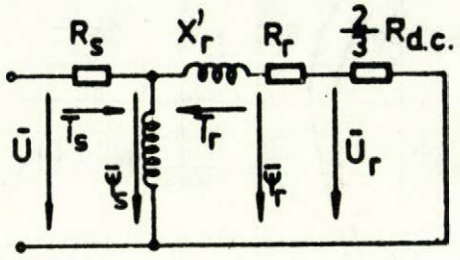

3-Ph conduction

Fig.3.51

$$\bar{u}_s = R_s \bar{i}_s + \frac{d\bar{\Psi}_s}{dt} + j\omega \bar{\Psi}_s \qquad 3.65$$

ω is the speed of the rotor, R_s is the stator resistance and $\bar{\Psi}_s$ is the stator flux. $\bar{u}_s$ and $\bar{i}_s$ are the stator voltage and current respectively.

$$0 = (R_r + R)\,\bar{i}_r + \frac{d\bar{\Psi}_r}{dt} \qquad (3.66)$$

In equation (3.66) R depends on the conduction state; at 3-ph conduction $R = \frac{2}{3} R_{d.c.}$ and at 2-ph conduction $R = \frac{1}{2} R_{d.c.}$. $\bar{\Psi}_r$ is the rotor flux

$$\bar{\Psi}_s = L_s \bar{i}_s + L_m \bar{i}_r \qquad (3.67)$$

$$\bar{\Psi}_r = L_m \bar{i}_s + L_r \bar{i}_r \qquad (3.68)$$

L_s, L_m and L_r are the stator, magnetizing and rotor inductances respectively. Then:

$$\bar{i}_s = \frac{\bar{\Psi}_s - (1-\sigma)\,\bar{\Psi}_r}{L'_s} \qquad (3.69)$$

σ is the leakage factor

$$\sigma = 1 - \frac{L_m^2}{L_s\,L_r} \qquad (3.70)$$

$$\bar{i}_r = \frac{\bar{\Psi}_r - \bar{\Psi}_s}{L'_r} \qquad (3.71)$$

The state equation of the system has the same form as equation (3.60). If the machine fluxes are chosen as state variables, then:

$$\underline{X} = \begin{bmatrix} \Psi_{sx} \\ \Psi_{sy} \\ \Psi_{rx} \\ \Psi_{ry} \end{bmatrix} \qquad (3.72)$$

Similarly, as in the 2-energy storages, the matrix $\underline{A}_c$ depends on the conduction states; at 3-ph conduction; it equals to:

$$\underline{A}_{c3} = \begin{bmatrix} \frac{-1}{T'_s} & \omega & \frac{1-\sigma}{T'_s} & 0 \\ -\omega & \frac{-1}{T'_s} & 0 & \frac{1-\sigma}{T'_s} \\ \frac{1}{T_1} & 0 & \frac{-1}{T_1} & 0 \\ 0 & \frac{1}{T'_r} & 0 & \frac{-1}{T'_r} \end{bmatrix} \qquad (3.73)$$

T'_s and T'_r are the transient time constants of the stator and rotor respectively.

$$T_1 = \frac{L'_r}{R_r + \frac{2}{3} R_{d.c.}}$$

at 2-ph conduction:

$$\underline{A}_{c2} = \begin{bmatrix} \frac{-1}{T'_s} & \omega & \frac{1-\sigma}{T'_s} & 0 \\ -\omega & \frac{-1}{T'_s} & 0 & \frac{1-\sigma}{T'_s} \\ \frac{1}{T_2} & 0 & \frac{-1}{T_2} & 0 \\ 0 & 1 & 0 & 0 \end{bmatrix} \tag{3.74}$$

$$T_2 = \frac{L'_r}{R_r + \frac{1}{2} R_{d.c.}}$$

The matrix $\underline{B}$ for 3-ph and 2-ph conduction conditions is:

$$\underline{B} = \begin{bmatrix} 1 & 0 \\ 0 & 1 \\ 0 & 0 \\ 0 & 0 \end{bmatrix} \tag{3.75}$$

$\underline{u}$ is the same as in equation (3.64).

The extinction conditions are the same as explained in the 2-energy storages. The solution now is relatively complicated.

3.5.2 The Exact Method
6-Energy Storages

The speed variation is considered. In that case the torque equation and the equations of motion are required. Therefore the equations of the system are as in (3.65), (3.66) and

$$T - T_\ell = T_{sn} \frac{d\omega}{dt} \tag{3.76}$$

$$\frac{d\theta}{dt} = \omega - W \tag{3.77}$$

where

$$W = 1 - s = \frac{1}{\tau} \int_\tau \omega \, dt \tag{3.78}$$

$$T = \frac{1}{L'_r} (\bar{\psi}_s \times \bar{\psi}_r) \tag{3.79}$$

T_ℓ is the load torque and T_{sn} is the nominal starting time of the motor. ω is the actual speed of the motor, W is the average speed of the shaft and θ is the angle between an axis fixed to the rotor and a virtual axis rotating with the average speed W.

In that case the state equation of the system is:

$$\frac{d\underline{X}}{dt} = \underline{A}_c \underline{X} + \underline{B} \underline{u} + \underline{k}_{T_\ell} T_\ell \tag{3.80}$$

In equation (3.80) $\underline{A}_c$ is function of the state vector $\underline{X}$

$$\underline{X} = \begin{bmatrix} \psi_{sx} \\ \psi_{sy} \\ \psi_{rx} \\ \psi_{ry} \\ \omega - W \\ \theta \end{bmatrix} = \begin{bmatrix} x(1) \\ x(2) \\ x(3) \\ x(4) \\ x(5) \\ x(6) \end{bmatrix} \tag{3.81}$$

At 3-ph conduction state the matrix $\underline{A}_c$ equals:

$$\underline{A}_{c3}=\begin{bmatrix} -\frac{1}{T_s} & \omega & \frac{1-\sigma}{T'_s} & 0 & 0 & 0 \\ -\omega & -\frac{1}{T'_s} & 0 & \frac{1-\sigma}{T'_s} & 0 & 0 \\ \frac{1}{T_1} & 0 & -\frac{1}{T_1} & 0 & 0 & 0 \\ 0 & \frac{1}{T'_1} & 0 & -\frac{1}{T'_r} & 0 & 0 \\ \frac{\Psi_{ry}}{T_{sn}L'_r} & -\frac{\Psi_{rx}}{T_{sn}L'_r} & 0 & 0 & 0 & 0 \\ 0 & 0 & 0 & 0 & 1 & 0 \end{bmatrix} \qquad (3.82)$$

At 2-ph conduction state:

$$\underline{A}_{c2}=\begin{bmatrix} -\frac{1}{T'_s} & \omega & \frac{1-\sigma}{T'_s} & 0 & 0 & 0 \\ -\omega & -\frac{1}{T'_s} & 0 & \frac{1-\sigma}{T'_s} & 0 & 0 \\ \frac{1}{T_2} & 0 & -\frac{1}{T_2} & 0 & 0 & 0 \\ 0 & 1 & 0 & 0 & 0 & 0 \\ \frac{\Psi_{ry}}{T_{sn}L'_r} & -\frac{\Psi_{rx}}{T_{sn}L'_r} & 0 & 0 & 0 & 0 \\ 0 & 0 & 0 & 0 & 1 & 0 \end{bmatrix} \qquad (3.83)$$

$\underline{B}$ and $\underline{k}_{T\ell}$ are the same both in 3-ph and 2-ph conditions.

$$\underline{B} = \begin{bmatrix} 1 & 0 \\ 0 & 1 \\ 0 & 0 \\ 0 & 0 \\ 0 & 0 \\ 0 & 0 \end{bmatrix} \quad (3.84) \quad , \quad \underline{k}_{T\ell} = \begin{bmatrix} 0 \\ 0 \\ 0 \\ 0 \\ \frac{-1}{T_{sn}} \\ 0 \end{bmatrix} \quad (3.85)$$

$$\underline{u} = \begin{bmatrix} \cos \{t_o + s(t-t_o) - x(6) + \beta \} \\ \\ \sin \{t_o + s(t-t_o) - x(6) + \beta \} \end{bmatrix} \quad (3.86)$$

where t_o is the instant at which the thyristor is fired. In equation (3.86) the stator voltage is written w.r.t. a coordinate system fixed to the rotor. Since the rotor position equals $W(t-t_o)+ x(6)$ therefore:

$$\bar{u} = U\, e^{j\omega_1 t}\; e^{-jW(t-t_o)}\; e^{-j\, x(6)} \quad (3.87)$$

Since U=1 and ω_1=1, then writing $\bar{u}$ in the above equation in the form $u_x + j\, u_y$, equation (3.86) is obtained.

The extinction conditions are the same as in the 2-energy or 4-energy storages. In the solution of the equations of the system "t_o" and "T_ℓ" are given. The steady-state working point can be determined by an iteration method using the periodicity condition. That condition may be written, if the coordinate system (x_4-y_4) in Fig.3.41 is rotated forwardly by $\frac{\Pi}{6}$, as follows:

$$\underline{X}_{end} + \underline{\Delta X}_{end} = \underline{X}_{st} + \underline{\Delta X}_{st} \quad (3.88)$$

$\underline{X}_{st}$ is the initial state vector for the operating point which is determined from an approximate method, for example, 4 energy-storages method. $\underline{X}_{end}$ is determined by

the solution of the differential equations of the system taking into consideration the limit conditions. $\underline{\Delta X}_{st}$ is the small variation of the starting vector while $\underline{\Delta X}_{end}$ is that at the end of the stroke.

The solution may be achieved using the method of Runge-Kutta /fourth order/.

In general some steps of iteration procedures are necessary to find the limit point.

Let us consider:

$$\underline{dev} = \underline{X}_{end} - \underline{X}_{st} \tag{3.89}$$

where $\underline{dev}$ is the difference vector, showing the deviation between the vectors $\underline{X}_{end}$ and $\underline{X}_{st}$.

$\underline{\Delta X}_{end}$ may be obtained from $\underline{\Delta X}_{st}$ knowing the transfer matrix for small variations. Calling that matrix by $\underline{A}$ then:

$$\underline{\Delta X}_{end} = \underline{A}\ \underline{\Delta X}_{st} \tag{3.90}$$

From equations (3.88) - (3.90)

$$\underline{\Delta X}_{st} = [\underline{I} - \underline{A}]^{-1}\ \underline{dev} \tag{3.91}$$

$\underline{I}$ is the identity matrix and $[\underline{I} - \underline{A}]^{-1}$ is the inverse of $[\underline{I} - \underline{A}]$. Knowing $\underline{\Delta X}_{st}$ the new starting values are determined from:

$$\underline{X}_{st\ new} = \underline{X}_{st} + \underline{\Delta X}_{st} \tag{3.92}$$

The procedure is repeated until the deviation is less than the prescribed value. The problem is solved using digital computer. The flow-chart is given in appendix IV. The

method of calculating the transfer matrix $\underline{A}$ is explained in the appendix.

If the proper values of $\underline{X}_{st}$ and $\underline{A}$ are known, then the calculations of both the steady-state and dynamic behaviours are achieved easily. Figures 3.52, 3.53 give the Park-vector path of the rotor current in a coordinate system fixed to the rotor and synchronously rotating coordinate system respectively.

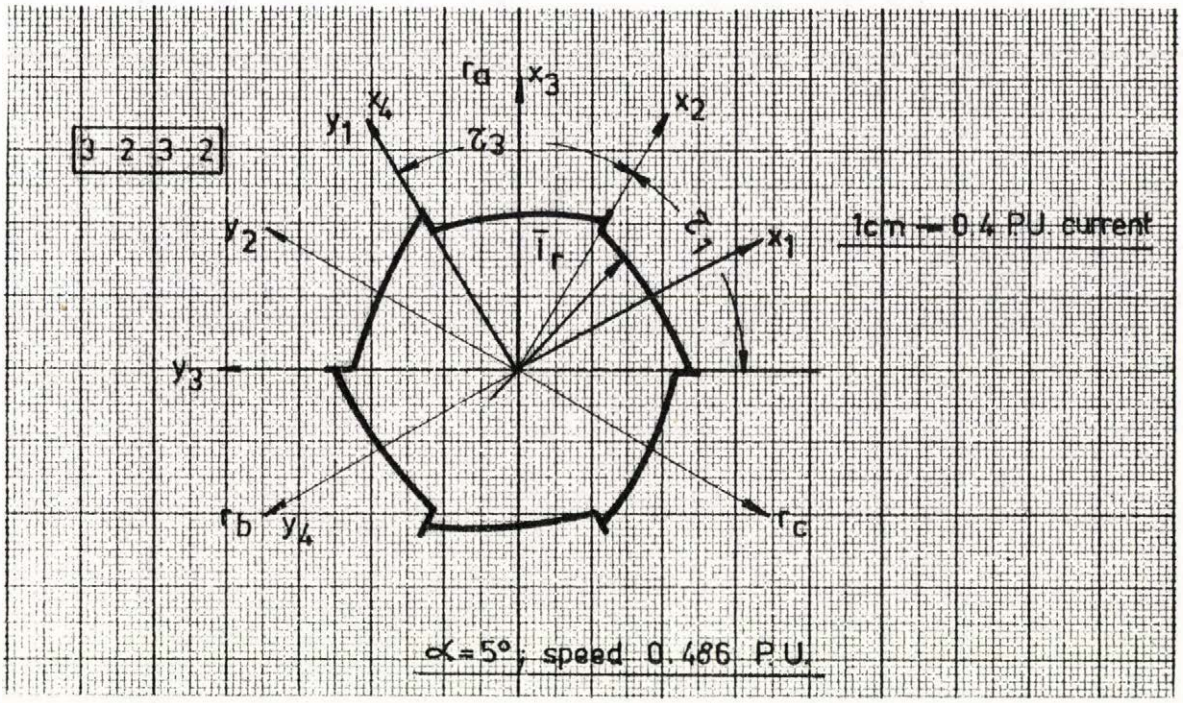

Fig.3.52

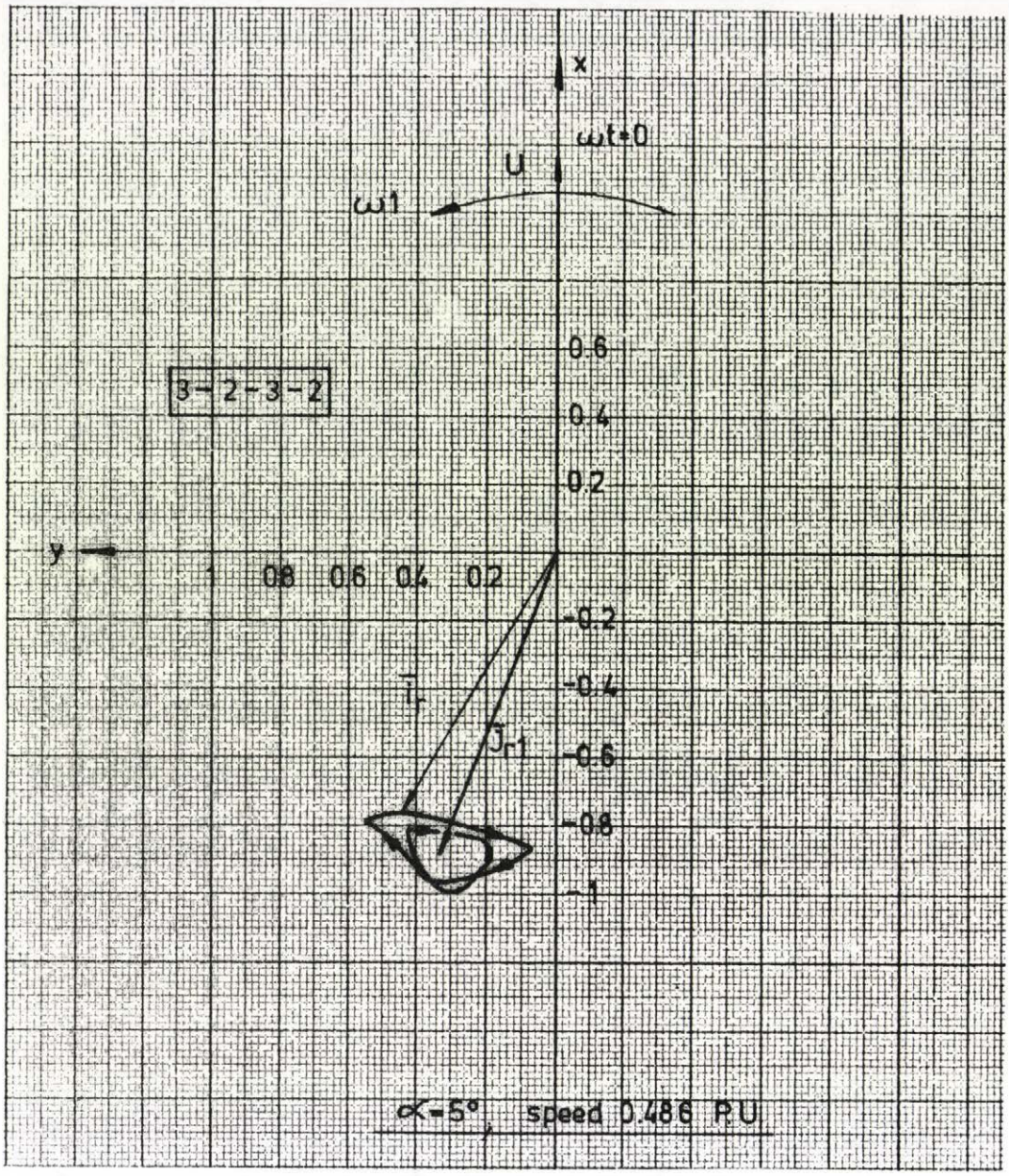

Fig.3.53

The Park-vector pathes of the stator and rotor fluxes in coordinate system fixed to the rotor are shown in Fig.3.54. In Fig.3.55 the vector diagram for the fundamental component of the current, fluxes and voltages is given.

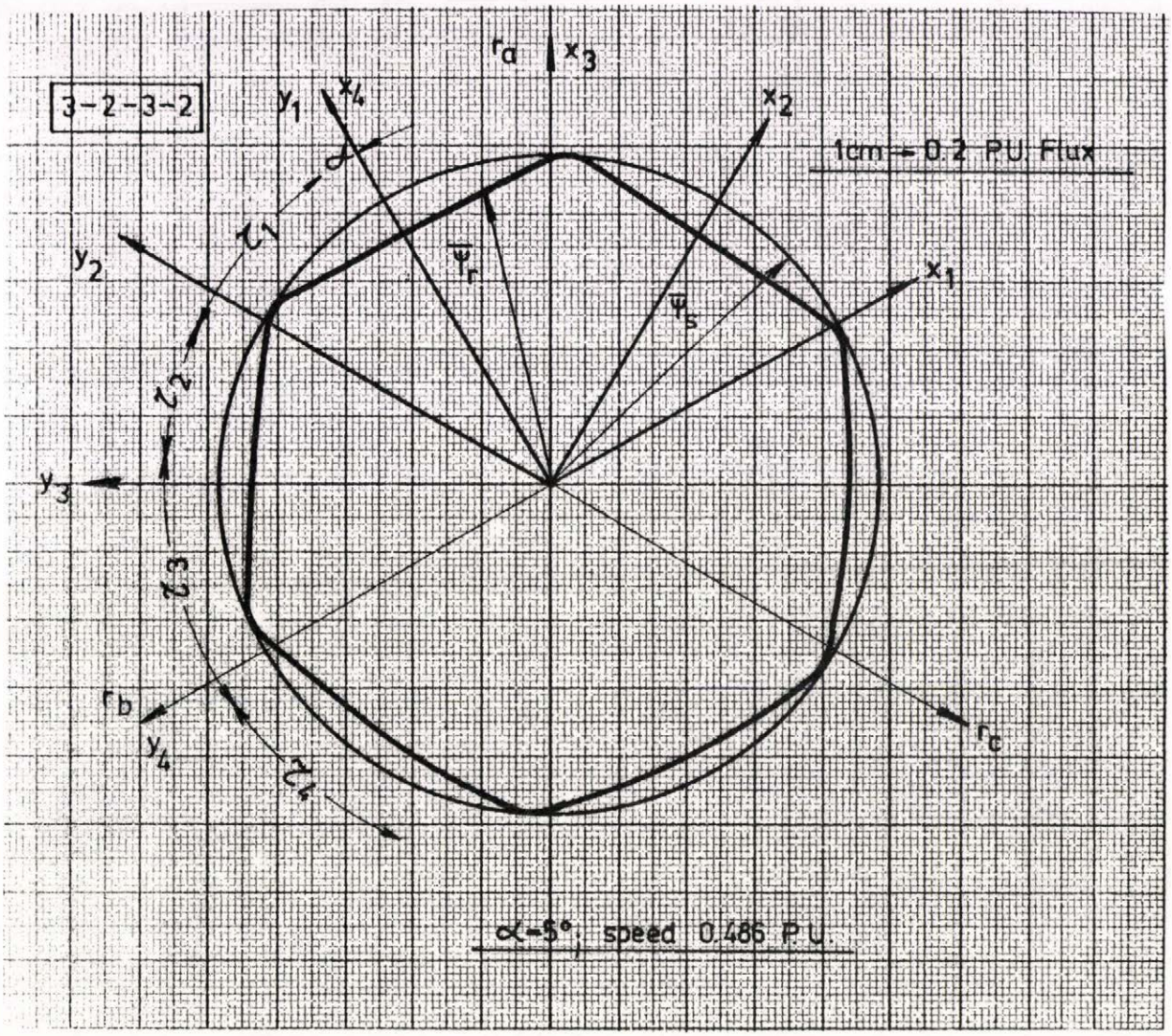
3-2-3-2
r_a
x_3
y_1
x_4
x_2
1cm → 0.2 PU Flux
y_2
τ_1
$\bar{\psi}_r$
$\bar{\psi}_s$
x_1
τ_2
y_3
τ_3
r_b
y_4
r_c
τ_4
α=5°, speed 0.486 P.U.

Fig. 3.54

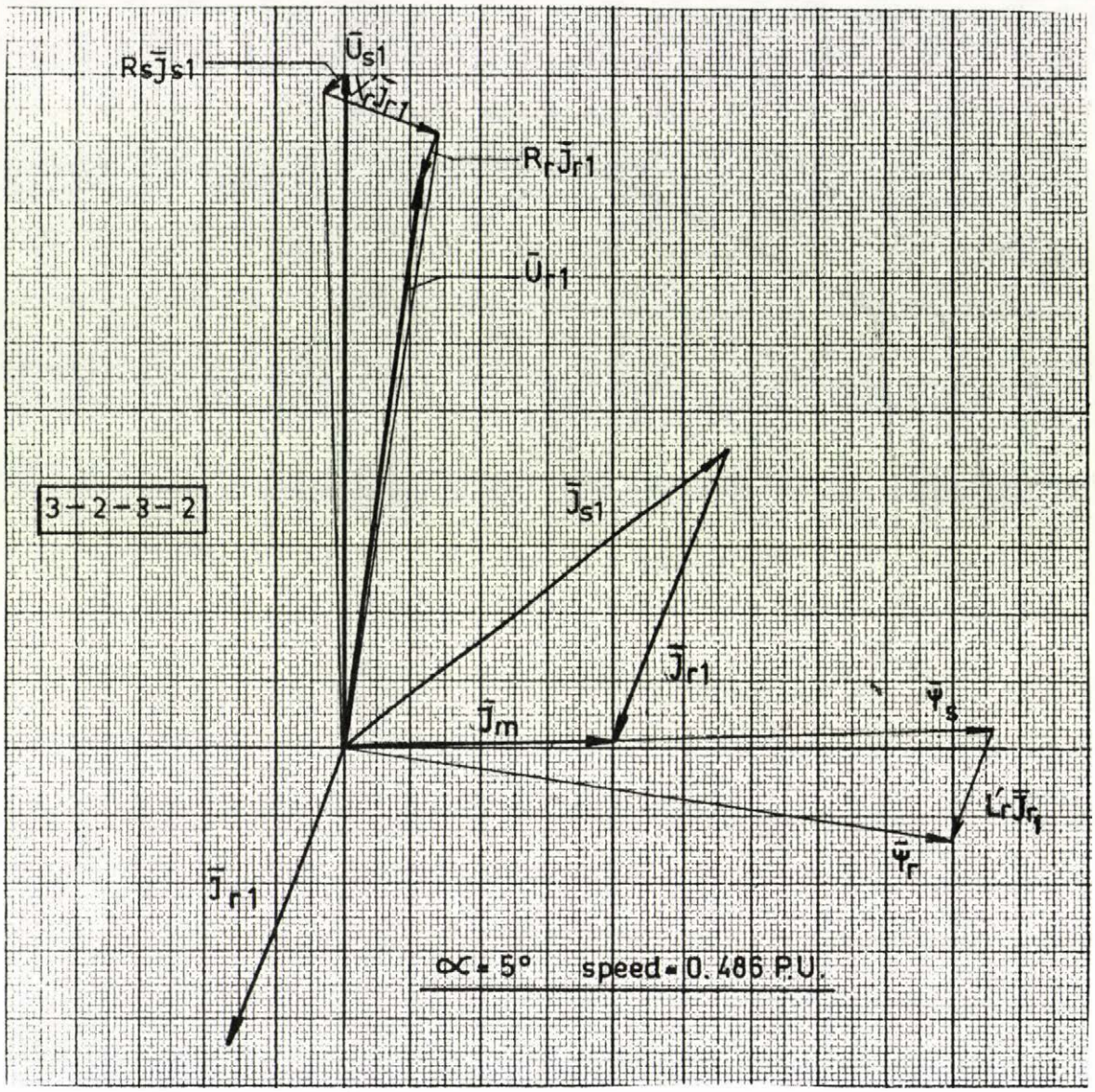

Fig.3.55

It is clear from the fig. that $\bar{U}_{r1}$ is out of phase of $\bar{I}_{r1}$ due to the semiconductors impedance.

The results of the three methods are tabulated for an operating point, slip=0.205, firing angle=50° and $R_{d.c.}$=14.17% in table 3.

	2-Energy Storages	4-Energy Storages	6-Energy Storages
$I_{r\ R.M.S.}$	1.0924	1.0939	1.1032
$\bar{I}_{rl}$	-.8402 +j0.5496	-0.8487 +j0.5238	-0.8494 +j0.5213
$I_{rl\ R.M.S.}$	1.0040	0.9973	0.9966
$I_{s\ R.M.S.}$	-	1.2186	1.2274
$I_{d.c.R.M.S.}$	-	0.9795	0.9774
d_i	0.4288	0.4505	0.4746

Table 3.

$d_i = \sqrt{\Sigma I_{r\nu}^2}/I_{rl\ R.M.S.}$; the current distortion factor.

It is clearly shown from the table that for steady-state characteristics the approximate methods are quite satisfactory. The exact method is only required for the study of dynamic behaviour and control properities.

3.6 Harmonic Analysis

For the half controlled bridge connection g=3 in equation (3.13), therefore the possible upper harmonics are:

$$\nu = \ldots -5, -2, 1, 4, 7, \ldots$$

These upper harmonics can drive or brake, but they cause additional losses in all cases. The equivalent circuit of the induction motor for the upper harmonics is shown in fig.3.56.

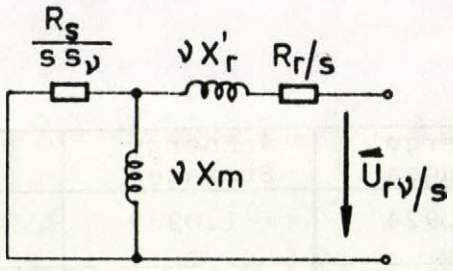

Fig.3.56

The slip for the upper harmonics is:

$$s_\nu = 1 + \frac{1-s}{s\ \nu} \qquad (3.93)$$

Substituting $s=\frac{1}{3}$ and $\nu= -2$ in equation (3.93) the value of $s_{(-2)}$ is zero. This means that the stator frequency corresponding to the minus two upper harmonic component is zero when the motor speed is $\frac{2}{3}$. In that case the equivalent stator resistance, see Fig.3.56, is very high. That result shows that the neglection of the stator resistance in the approximate method of 2-energy-storages is unsuitable. Therefore it is necessary to use the 4-energy-storages method for the approximate method of analysis. Similar phenomena occurs at the speed of $\frac{5}{6}$ for minus five harmonic component.

As a result of these upper harmonics, there are some oscillations in the operation of the drive at $s = \frac{2}{3}$. Also the shape of the torque/speed curve /if the rotor current or the current through $R_{d.c.}$ is constant/ has some irregularities at $s = \frac{1}{3}$. This will be shown in chapter VI.

3.7 Comparison Between Different Techniques of Thyristor Controlled Induction Motor /Lossy and Cheap Methods/

The comparison is made, here, between the half controlled bridge connection and both the stator voltage control and forced commutated D.C. chopper connection inserted in the rotor circuit.

3.7.1 Stator Voltage Control

In that case, thyristor or thyristor-diode pairs or incidentally triacs, connected in series with the stator winding, block the supply voltage in a part of the cycle, thus the fundamental component of the motor voltage can be varied from 0 to 100% and speed control is possible in this way [15].

Connecting the thyristors in the rotor side, lower rating thyristors are resulted in as compared to the stator voltage control and the excess voltages and short circuit currents are low. In table 4. a comparison is given between stator voltage control and the half controlled bridge connection. The ratios of the R.M.S. and average values of the thyristor current and the peak value of the fundamental component of the stator current are given. This comparison is made for the same value of slip and torque in both cases. The chosen points are /s=0.31, T=.69 and s=0.62, T=0.84/. It is convenient to compare the maximum thyristor voltage in both cases at unity slip for the motoring operation. The base voltage is the peak value of the rotor phase voltage.

	Stator Voltage Control		Half Controlled Bridge	
N° of elements	3T + 3D		3T + 3D	
$I_{t\ R.M.S.}/I_{sl}$	s=0.31	s=0.62	s=0.31	s=0.62
	.82	0.74	0.36	0.34
I_{tav}/I_{sl}	0.32	0.32	0.19	.20
$U_{t\ max}$	1.73		1.73	

Table 4.

T: thyristor

D: Diode

Stator voltage control: T-D connection

It may be confirmed from the above results that in motoring quadrant the half controlled bridge gives better solution compared to the stator voltage control while in braking quadrant for slip higher than unity the stator voltage control is better because in such cases higher rated thyristors are needed for the connections in the rotor.

3.7.2 D.C. Chopper in the Rotor Circuit

As it is well known from the literature the connection for the d.c. chopper is as shown in Fig.3.57. The value of

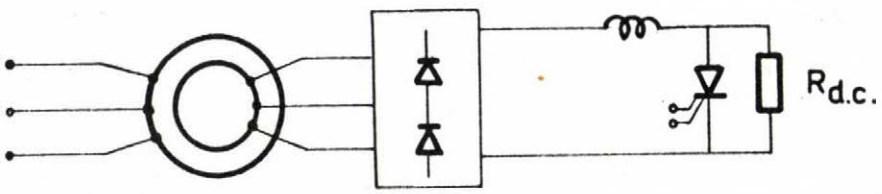

Fig.3.57

the d.c. resistance changes due to the turnning on and off of the thyristor. The relation between the effective and actual values of $R_{d.c.}$ depends on the ratio between the

turnning on interval of the thyristor and the total period. This ratio is denoted by "b". By this method a speed control of the motor can be achieved. The average and R.M.S. values of the thyristor current in the case of d.c. choppers connections depend on the ratio "b" for constant slip. The maximum thyristor voltage depends on the value of the resistance $R_{d.c.}$ for constant d.c. current. The torque/speed characteristics for the half controlled bridge and d.c. chopper are shown in Fig.3.58. It is shown that the zero value of the torque cannot be obtained with the d.c. chopper connection. It is possible to have a wider torque/speed range but in the dispense of the maximum thyristor voltage. The wider the torque/speed range the higher the thyristor rating. Fig. 3.59 shows the locus of the ratio of the fundamental component of the rotor current to the maximum short-circuit current of the motor [19] at constant speed of 0.308 in both cases. From the figure it is clear that the p.f. in the case of d.c. choppers is better.

It may be concluded from the comparison between the d.c. choppers and the half controlled bridge connection that [18]:

1. Large choke coils and capacitors are needed in the case of d.c. choppers.
2. The zero value of the torque is impossible with the d.c. chopper connection. Therefore it is not applicable for crane drives.
3. The torque/speed characteristic with the half controlled bridge diverges slightly from the normal torque/speed characteristic of the motor at very small slips. A small operating range is missing in the half controlled bridge at these slips.
4. The d.c. choppers are not a good solution if small torque values are required. It is so because the thyristor rating is high and the cost is high.

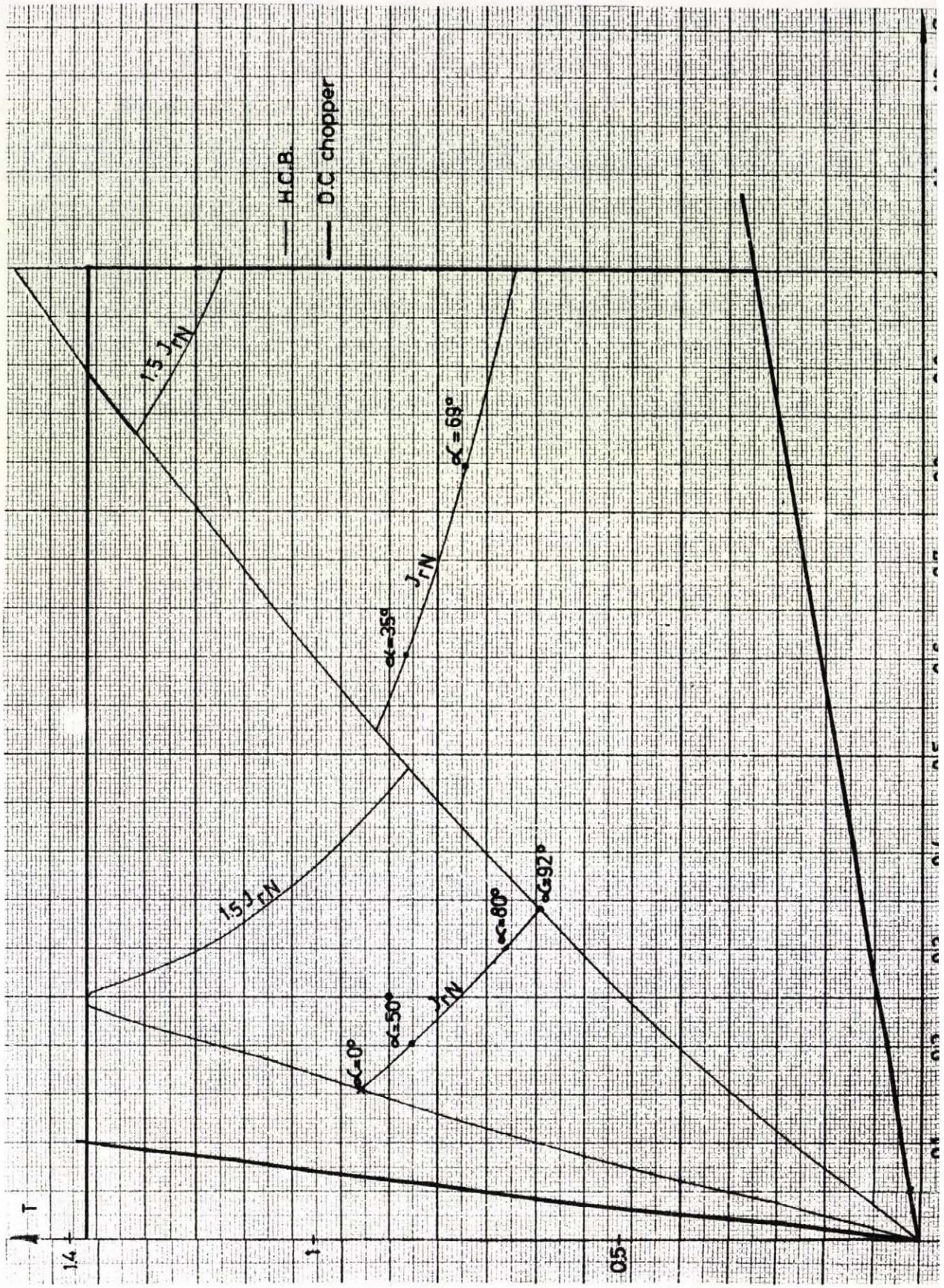
H.C.B.
D.C chopper
1.5 J_{rN}
J_{rN}
α=69°
α=35°
1.5 J_{rN}
J_{rN}
α=92°
α=80°
α=50°
α=0°
T
1.4
1
0.5

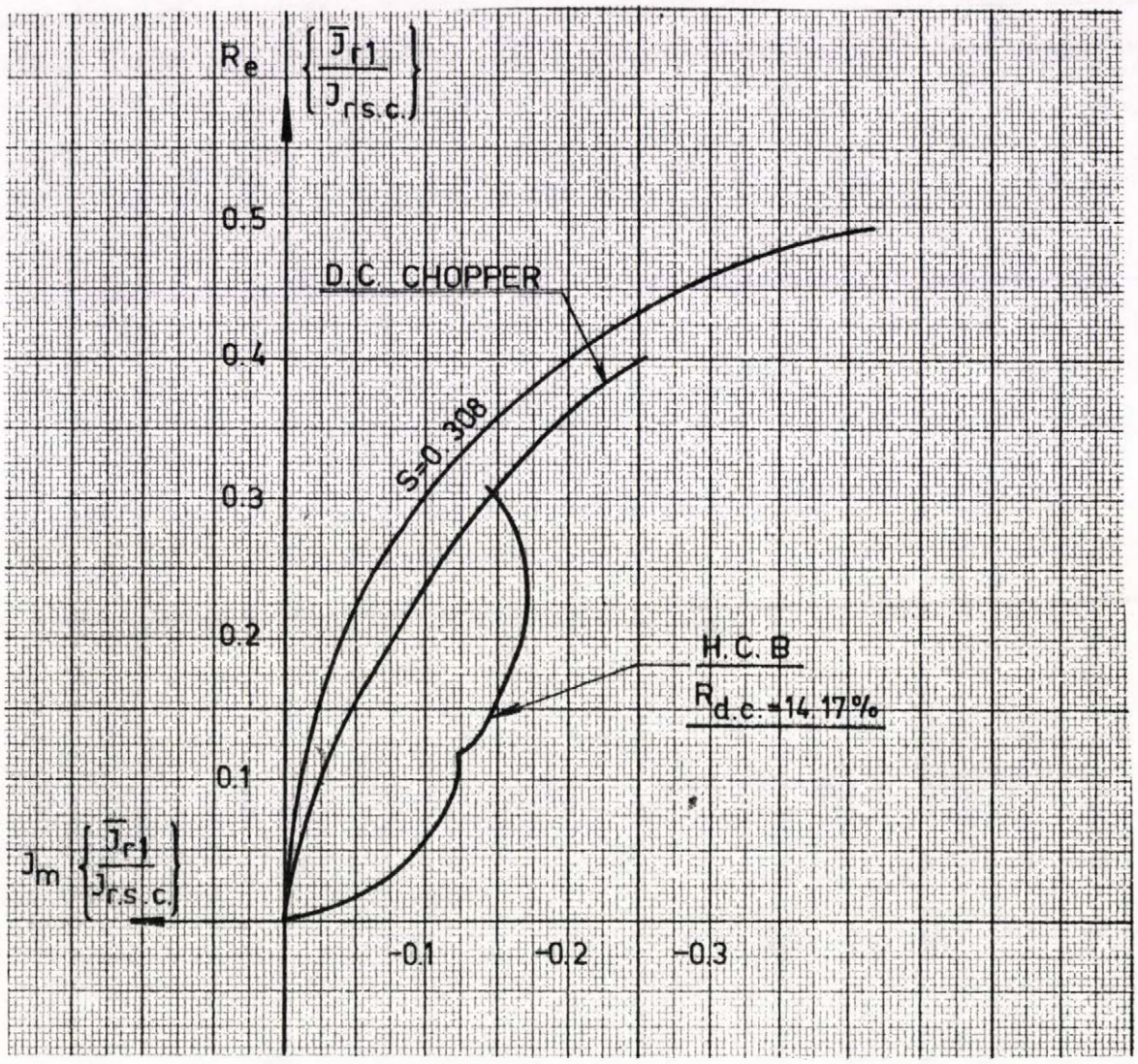
Re {Ī_r1 / I_r.s.c.}
0.5
0.4
0.3
0.2
0.1
D.C. CHOPPER
S=0.308
H.C.B
R_d.c.=14.17%
Im {Ī_r1 / I_r.s.c.}
-0.1
-0.2
-0.3

Fig.3.59

CHAPTER IV

THE DYNAMIC BEHAVIOUR OF THE SYSTEM

4.1 General

In the operation of the controlled induction motor transient phenomena are occuring. The study of the dynamic behaviour of the drive requires the determination of the transfer functions, oscillation properities, stability limit, ... etc.

If the control of the motor is performed by thyristor techniques, then during the operation of the motor, transients are caused by the switchings of the semi-conductors even in the steady-state.

As stated in the previous chapter it is unnecessary to carry out the exact method of calculation for such steady-state transient, since the approximate methods give results with good accuracy. The exact solution is necessary for the analysis of the real transient condition and control properties. In the case of motor with thyristor circuits inserted in the secondary side, the system equations are only piece-wise linear differential equation if the motor speed is considered constant. The coefficients of these equations depend on the conduction state.

The most general case if the speed variation is taken into consideration, then the differential equations of the system are non-linear.

In synchronous rotating coordinate system the periodical trajectory vectors coincide in the instants of firing the thyristor t_o, t_1,...,$t_k=t_o+k\tau$ and the values of the vector [25] $\underline{X}_k(t)$ may be considered the sampled one in the sampling instant "t_k".

These instants are of rather importance, since the operation of the control circuits and the firing of the

thyristors depend on the value of the state variables at this moment.

4.2 Small Variation from the Periodic Steady-State Condition

The deviation from the steady-state operating point may be caused, for example, by input signal Δu, by changing the firing instant t_o or by deviation ΔX_o from the steady-state value, i.e. change in the initial conditions. The latter case is given in Fig.4.1.

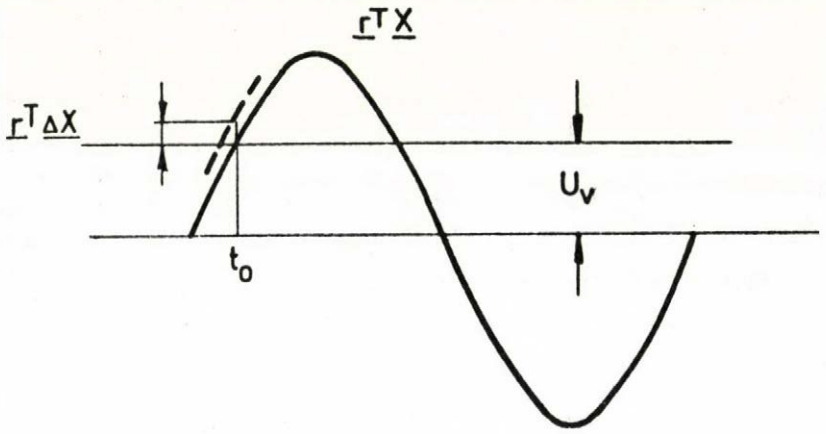

Fig.4.1

In the figure the instant of firing the thyristors is determined by combining a d.c. reference signal with an a.c. comparative signal. The latter is obtained so that it is proportional to the stator flux because in that case the signal will has a constant modulus. Practically that signal can be obtained as it will be explained in chapter VI. For firing the thyristor in the phase r_a, for example, a signal proportional to the stator line flux Ψ_{ac} is required. The mentioned comparative signal is obtained analytically from the projection of the state vector $\underline{X}$.

It may be represented by $\underline{r}^T\underline{X}$. In that case $\underline{r}^T$ is equal to [O 1 O,...O]. If a change occurs in the initial conditions it results in a change in the comparative signal. That is represented in the figure by $\underline{r}^T\ \underline{\Delta X}$.

Considering the state vector $\underline{X}=\underline{X}_{st}+\underline{\Delta X}$, where $\underline{X}_{st}$ is the solution of steady-state condition, the small variation $\underline{\Delta X}$ may be written in the following form with usual approximation of first order:

$$\frac{d\ \underline{\Delta X}}{dt} = \underline{A}_c\ \underline{\Delta X} + \underline{B}\ \underline{\Delta u} \qquad (4.1)$$

Equation (4.1) is applied only if $\underline{A}_c$ is constant and if the differential equations of the system are considered piece-wise linear. Therefore this method is suitable only for the approximate solutions /4 energy-storages/

The above equation can be solved in the same manner as described in the previous chapter. Considering only the homogenous part of the general solution, the following equations hold true [29]:

$$\underline{\Delta X}'_k = \underline{A}^k\ \underline{\Delta X}'_o \qquad (4.2)$$

where

$\underline{\Delta X}'_o$: small deviation around the steady-state vector $\underline{X}_o$, in a coordinate system fixed to the rotor and the values at the end of the stroke are rotated forwardly by $\frac{\Pi}{6}$ as explained in the previous chapter

$\underline{\Delta X}'_k$: the value of $\underline{\Delta X}'_o$ at the end of the $K^{\underline{th}}$ stroke

$\underline{A}$: transfer matrix

Different functions of a quadratic matrix can be expressed by a power series. It is more convenient to use

the diagonalised form:

$$\underline{A} = \underline{T}\ \underline{\Lambda}\ \underline{T}^{-1} \tag{4.3}$$

$$\underline{T} = [s_1, s_2, \ldots, s_n] \tag{4.4}$$

$$\underline{\Lambda} = \begin{bmatrix} \lambda_1 & 0 & 0 \\ 0 & \lambda_2 & \\ 0 & & \lambda_n \end{bmatrix} \tag{4.5}$$

where λ_i is an eigen-value of matrix $\underline{A}$ and $\underline{s}_i$ is a post eigen vector. The powers of the matrix $\underline{A}$ can be calculated using the eigen-values of $\underline{A}$. The eigen-values determine the transition speed among differed steady-state conditions. They determine the dynamic performance of the open-loop system.

If the absolute value of each eigen-value is smaller than 1, then the system is stable, $\underline{A}^k \to 0$. If only one $|\lambda_i|>1$, then the system is unstable. The components of the vector $\underline{\Delta X}$ vary proportionally with λ_i^k, thus an equivalent time constant T_i and an oscillation frequency ω_i can be defined by the following expressions:

$$\lambda_i = \mathrm{EXP}\left(\frac{-1}{T_i} + j\omega_i\right)\tau \tag{4.6}$$

$$T_i = -\tau\,\frac{1}{\mathrm{Ln}|\lambda_i|} \tag{4.7}$$

$$\omega_i = \frac{\mathrm{arc}\ \lambda_i}{\tau} \tag{4.8}$$

τ is the length of the stroke.

The calculation with the values of the deviations at the firing instants is compatible to the theory of sampling system, the sampling time is $\tau=T/g$ where T is the time of one period and g is the number of strokes in one period. It must be noted that the time of one period in our case

equals $\frac{2\Pi}{s}$, where s is the slip.

4.3 Analysis for Small Variations Using Sampled Data Theory

The time function for one stroke is shown in Fig.4.2.

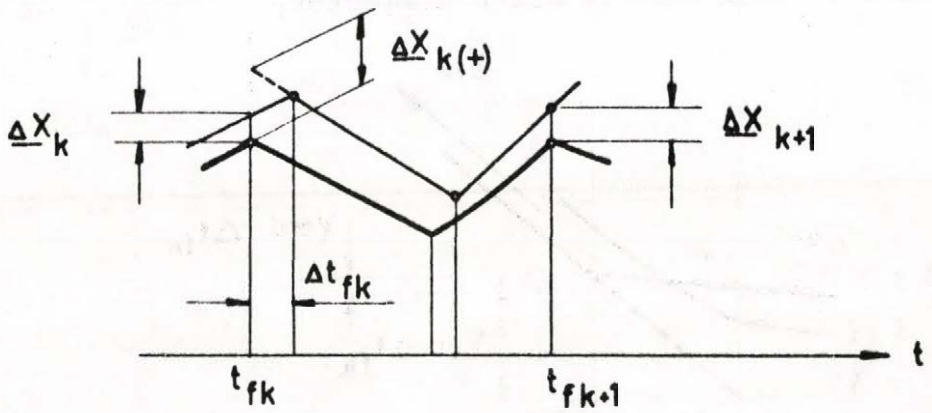

Fig.4.2

The curve with thick line is refering to the periodical working point. The variation from that is denoted with $\underline{\Delta X}$ /the thinner line/. In general if the firing angle of the thyristors is changed from t_{fk} to $t_{fk}+\Delta t_{fk}$, the deviatives are extrapolated to the instant t_{fk}. Therefore the deviation $\underline{\Delta X}(t_{fk})= \underline{\Delta X}_k$ is applied before the changing while the vector $\underline{\Delta X}_{k+}(t_{fk})$ is valid after changing by Δt_{fk}. Therefore the signals of small variations extrapolated in the mentioned way are jumping in the instant of changing the firing angle. The relation between $\underline{\Delta X}_k$ and $\underline{\Delta X}_{k(+)}$ is given by:

$$\underline{\Delta X}_{k(+)} = \underline{\Delta X}_k + \underline{b}_f \, \Delta t_{fk} \qquad (4.9)$$

$$\underline{b}_f = \underline{V}_{end} - \underline{V}_{st} \qquad (4.10)$$

$\underline{V}_{end}$ is the velocity of the state vector at the end of the stroke before the instant of the following firing, while $\underline{V}_{st}$ is the velocity at the beginning of the new stroke. i.e. $\underline{V}_{end}$ is, for example, the velocity of the state vector at the end of the $k^{\underline{th}}$ stroke, then $\underline{V}_{st}$ is the velocity at the beginning of k+1 stroke. Equation (4.9) can be understood by regarding Figures 4.3 and 4.4. Figure 4.3 gives the time function of one coordinate. Figure 4.4 represents the state trajectory.

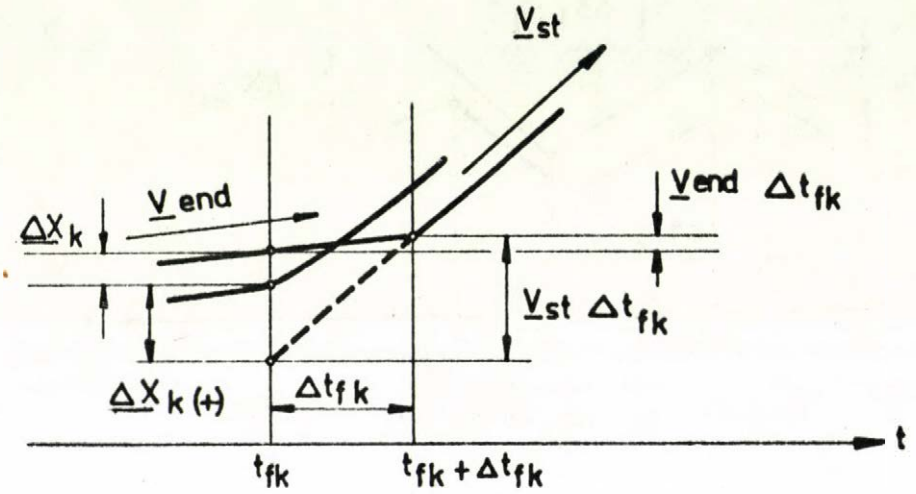

Fig.4.3

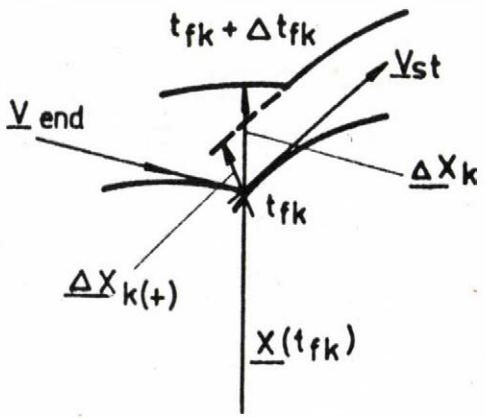

Fig.4.4

The relation between the small variations of the state vector through two successive strokes can be obtained knowing the transfer matrix $\underline{A}$ of the system. If the driving function $\underline{u}$ is not changed, then the following recursive difference equation is obtained:

$$\underline{\Delta X}_{k+1} = \underline{A} \ (\underline{\Delta X}_k + \underline{b}_f \ \Delta t_{fk}) \qquad (4.11)$$

This equation can be represented by the block-diagram as shown in Fig.4.5. In equation (4.11) the matrix $\underline{A}$ can be calculated explicitly if the system is piece-wise linear. However in the general case the differential equations are non linear. The matrix $\underline{A}$ is computed in that case by numerical method.

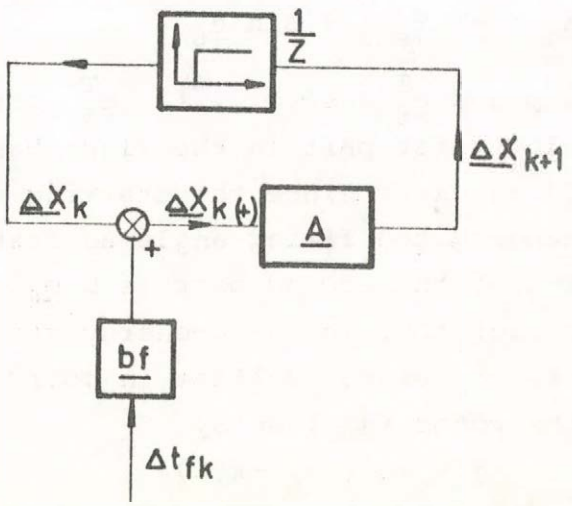

Fig.4.5

In the following analysis the exact method /6-energy storages/ is used. Having studied the dynamic behaviour of the open loop system /no feed-back from the speed or the currents/ a special properity has been appeared that the characteristic equation of the system possesses one

root equals unity. This nature is explained and proved as follows:

If an incremental change in the firing angle is presented and denoted by:

$$\Delta t_o = h \qquad (4.12)$$

It is required that the values of the state variables at the beginning of the stroke in both cases before and after the changing of the firing instant by "h" remain the same.

That condition can be verified if a small variation in the starting state vector has occured. That small variation vector may be expressed by:

$$\underline{\Delta X}_o = -h\ \underline{V}_{end} + s\ h\ \underline{e}_6 \qquad (4.13)$$

where s is the slip and $\underline{e}_6^T = [0,0....1]$, $\underline{e}_6^T$ is the transpose of $\underline{e}_6$. The first part in the right hand side of equation (4.13) is clear since the starting vector is the same after changing the firing angle as stated above. The addition of the second part ($s\ h\ \underline{e}_6$) is obtained from the fact that in the 6-energy storage method of analysis, the stator voltage in coordinate system fixed to the rotor is given by

$$\underline{\dot{u}} = U\ e^{j(t_o+s(t-t_o)-x(6))}$$

as stated in chapter III. t_o is the firing instant. Therefore, if Δt_o occurs and the starting vector remains constant, $\Delta x(6)$ must equal $s\ \Delta t_o$.

Using equation (4.11) with k=0

$$\underline{\Delta X}_1 = \underline{A}\ \underline{\Delta X}_o + \underline{b}\ \Delta t_o \qquad (4.14)$$

The vector $\underline{b}$ is obtained from $\underline{b}_f$, that:

$$\underline{b} = \underline{A}\ \underline{b}_f \qquad 4.15$$

In periodical operation the small variation vectors at the end and the beginning of the stroke are equal if the state variables at the end of the stroke are rotated forwardly by $\frac{\Pi}{6}$.

To satisfy the periodicity condition, $\underline{\Delta X}_1$ equal $\underline{\Delta X}_o$ therefore:

$$\underline{A}\ \underline{\Delta X}_o + \underline{b}\ \Delta t_o = \underline{\Delta X}_o \qquad (4.16)$$

If modified forms for the velocities at the end and the beginning of the stroke are introduced, that:

$$\underline{V}'_{end} = \underline{V}_{end} - s\ \underline{e}_6 \qquad (4.17)$$

$$\underline{V}'_{st} = \underline{V}_{st} - s\ \underline{e}_6 \qquad (4.18)$$

Then from equations (4.16), (4.15) and (4.13)

$$\underline{V}'_{end} = \underline{A}\ \underline{V}'_{st} \qquad (4.19)$$

In the general case the transfer matrix $\underline{A}$ is computed by numerical methods. Therefore equation (4.19) can be utilized as a good tool to check the accuracy of the calculations of $\underline{A}$. As an example, the results of an operating point, $\alpha=5^o$, s=0.514 and $R_{d.c.} = 75.96\%$ are given:

$$\underline{V}'_{end} = \begin{bmatrix} -0.49817264E+00 \\ -0.69112668E-01 \\ -0.53121929E+00 \\ -0.50033177E-01 \\ -0.21650419E-03 \\ -0.51389197E+00 \end{bmatrix} \qquad \underline{A}\ \underline{V}'_{st} = \begin{bmatrix} -0.49817900E+00 \\ -0.69152784E-01 \\ -0.53122737E+00 \\ -0.50072049E-01 \\ -0.21573939E-03 \\ -0.51389013E+00 \end{bmatrix}$$

Now it is required to get the characteristic equation of the system for the working point where the firing instant is t_o. The procedure is to assume that a small change Δt_o occurs in the firing angle. Since the modified velocity at the end of the stroke is $\underline{V}'_{end}$, then a small change vector $\underline{V}'_{end}\ \Delta t_o$ will result. The comparative signal for firing the thyristor is obtained from the state vector $\underline{X}$, as stated before, from the relation $\underline{r}^T\underline{X}$.

$$\underline{r}^T = [0,1,0,\ldots 0] \qquad (4.20)$$

Therefore a small change vector $\underline{r}^T\ \underline{V}'_{end}\ \Delta t_o$ will arise due to the small change Δt_o. If the comparative signal is changed by $\underline{r}^T\ \underline{\Delta X}_o$ and this change equals in magnitude and opposite in sign to the former change, the same starting state vector is obtained see Fig.4.6.

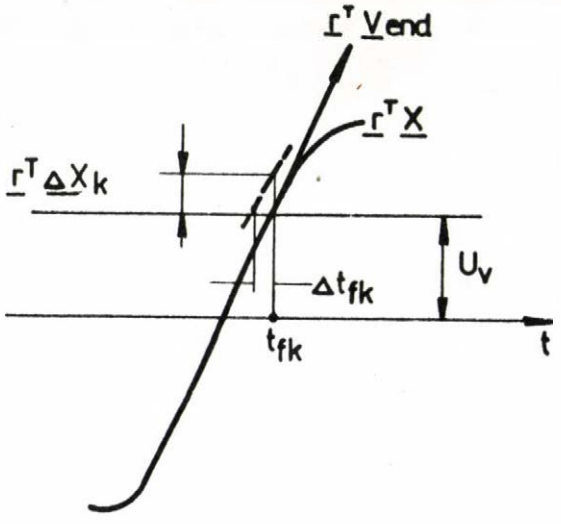

Fig.4.6

In mathematical form the above condition may be written as follows:

$$\underline{r}^T\ (\underline{\Delta X}_o + \underline{V}'_{end}\ \Delta t_o) = 0 \qquad (4.21)$$

From equation (4.21) and(4.14):

$$\underline{\Delta X}_1 = \left(\underline{A} - \frac{\underline{b}\ \underline{r}^T}{\underline{r}^T\ \underline{V}'_{end}}\right) \underline{\Delta X}_o \qquad (4.22)$$

Equation (4.22) gives the relation between the small variation vectors at the end and the beginning of the stroke, therefore a modified transfer matrix is obtained. Denoting that matrix by $\underline{A}_m$, then:

$$\underline{A}_m = \underline{A} - \frac{\underline{b}\ \underline{r}^T}{\underline{r}^T\ \underline{V}'_{end}} \qquad (4.23)$$

The normalized form of that modified transfer matrix is used to get the characteristic equation of the system. The roots of the characteristic equation determine the stability of the drive.

From equations (4.23), (4.17), (4.18) and (4.19):

$$\underline{A}_m\ \underline{V}'_{end} = \underline{V}'_{end} \qquad (4.24)$$

Equation (4.24) shows the property that one of the eigen-values of the modified matrix $\underline{A}_m$ equals unity. The corresponding eigen-vector has the same direction as the velocity $\underline{V}'_{end}$. This result does not mean that the system on the margin of stability.

System Stability

A comparative signal for the firing process of the thyristor can be obtained from a feed-back signal. This signal may be taken from the combination of the rotor and stator fluxes. The combination vector is described by the following expression /see Fig.4.7/:

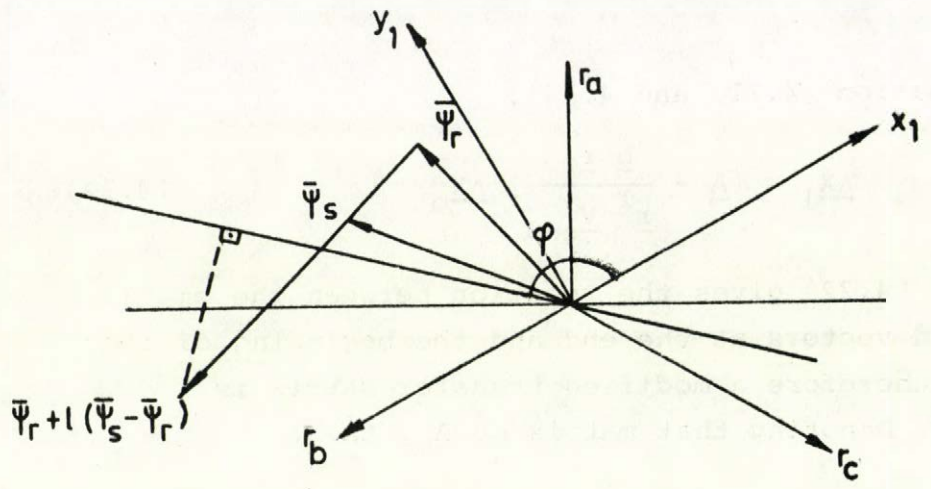

Fig.4.7

$$\bar{\Psi}_r + \ell\ (\bar{\Psi}_s - \bar{\Psi}_r) \qquad (4.25)$$

Since $\bar{\Psi}_r$ and $\bar{\Psi}_s$ are the Park-vector of the rotor and stator fluxes, the required comparative signal is obtained from the projection of the vector expressed in (4.25) on a proper direction. Now the analysis is concerned with the comparative signal for firing the thyristor in phase "r_a". As explained in the previous chapter, after the firing of this thyristor it commutates with the thyristor in phase "r_c" and 3-ph conduction state has occured. The coordinate system x_1-y_1 is used in that case. The angle between the projection axis and the coordinate x_1 in Fig.4.7 is denoted by ϕ. This is the general case since ϕ can take any value. The comparative signal in that case is represented by:

$$\underline{r}^T\underline{X} = R_e\ \{[\bar{\Psi}_r + \ell(\bar{\Psi}_s - \bar{\Psi}_r)]\ \bar{e}^{j\phi}\} \qquad (4.26)$$

Cutting the row vector $\underline{r}^T$ into two row vectors $\underline{r}_1^T$ and $\underline{r}_2^T$ which are independent of ℓ, that is:

$$\underline{r}^T = \underline{r}_1^T + \ell\ \underline{r}_2^T \qquad (4.27)$$

then

$$\underline{r}_1^T = [\,0 \quad 0 \quad \cos\phi \quad \sin\phi \quad 0 \quad 0\,] \qquad (4.28)$$

and

$$\underline{r}_2^T = [\cos\phi \quad \sin\phi \quad -\cos\phi \quad -\sin\phi \quad 0 \quad 0\,] \qquad (4.29)$$

From equation (4.21) the small change in the firing angle can be obtained. That equation is written when k=0. Generally for the $k^{\underline{th}}$ stroke a similar equation is used. Then the small change in the firing angle for the $k^{\underline{th}}$ stroke can be expressed, taking into consideration equation (4.27), as follows

$$\Delta t_{fk} = - \frac{(\underline{r}_1^T + \ell\ \underline{r}_2^T)\ \underline{\Delta X}_k}{(\underline{r}_1^T + \ell\ \underline{r}_2^T)\ \underline{V}'_{end}} \qquad (4.30)$$

where Δt_{fk} is the small change in the firing angle for the $k^{\underline{th}}$ stroke. From equation (4.11) and (4.30)

$$\underline{\Delta X}_{k+1} = \underline{A}\ \underline{\Delta X}_k - \frac{\underline{b}(\underline{r}_1^T + \ell\ \underline{r}_2^T)\ \underline{\Delta X}_k}{(\underline{r}_1^T + \ell\ \underline{r}_2^T)\ \underline{V}'_{end}} \qquad (4.31)$$

The characteristic equation of the system may be obtained using the sampled-data-theorem with the operator $z=e^{pT}$, p is the Laplace transform operator.

For the transfer matrix $\underline{A}$, the corresponding characteristic function is determined from the determinant of the matrix $[z\underline{I} - \underline{A}]$. In equation (4.31) the modified transfer matrix $\underline{A}_m$ equals

$$\left[\underline{A} - \frac{\underline{b}(\underline{r}_1^T + \ell\ \underline{r}_2^T)}{(\underline{r}_1^T + \ell\ \underline{r}_2^T)\underline{V}'_{end}}\right]$$

Denoting the characteristic functions in both cases by ch(z) and chm(z) respectively, then

$$chm(z) = \det. \left[z\underline{I} - \underline{A} + \frac{\underline{b}(\underline{r}_1^T + \ell\, \underline{r}_2^T)}{(\underline{r}_1^T + \ell\, \underline{r}_2^T)\underline{V}'_{end}} \right] \qquad (4.32)$$

Since, for example, the determinant of $[\underline{A} + \underline{U}\,\underline{V}^T]$ equals $\det.[\underline{A}](1+\underline{V}^T\,\underline{A}^{-1}\,\underline{U})$ where $\underline{A}^{-1}$ is the inverse of the matrix $\underline{A}$, then equation (4.32) can be written in the following form:

$$chm(z) = ch(z)(1 + \underline{p}^T(z\underline{I}-\underline{A})^{-1}\,\underline{b}) \qquad (4.33)$$

where

$$\underline{p}^T = \frac{\underline{r}_1^T + \ell\, \underline{r}_2^T}{c_1 + \ell\, c_2} \qquad (4.34)$$

and $c_1=\underline{r}_1^T\,\underline{V}'_{end}$; $c_2=\underline{r}_2^T\,\underline{V}'_{end}$.

To study the system stability, it is convenient to get the normalized form for the modified matrix, as stated before, and the stability is determined from the eigen-values of the modified matrix.

A simple method is introduced to solve this problem without the need to the very much calculations of the normalized matrix for the different values of ℓ and ϕ. It is obvious that these calculations of different ℓ and ϕ correspond to one operating point only. Therefore it is beneficial to obtain a method which reduce these repeated calculations and save the computation time in the digital computers. This method needs to normalize the matrix only two times for two different values of ℓ for example ℓ=0 and ℓ=1. Therefore the characteristic function of the system at any value of ℓ can be obtained from the linear combination of the characteristic functions of the system at ℓ=0 and ℓ=1. To get the roots of the characteristic equation, one of the mathematical methods to solve the algebric equations is used. These roots can determine the system stability. The mathematical description of the problem is as follows:

From equations (4.32)-(4.34):

$$(1 + \ell \frac{c_2}{c_1})\ chm(z) = (1 + \ell \frac{c_2}{c_1})\ ch(z) + g_1(z) + g_2(z) \qquad (4.35)$$

If the characteristic function, chm(z), is of $n^{\underline{th}}$ order then the order of both $g_1(z)$ and $g_2(z)$ is n-1.

Equation (4.35) can be written in the following form:

$$(1 + \ell \frac{c_2}{c_1})\ chm(z) = b_1(z) + \ell\ b_2(z) \qquad (4.36)$$

Therefore knowing the functions $b_1(z)$ and $b_2(z)$ the characteristic function of the system for the different ℓ values can be obtained from equation (4.36). The function $b_1(z)$ can be obtained by putting ℓ=0 in equations (4.33) and (4.34), denoting the characteristic function of the system at ℓ=0 by $chm_o(z)$, then:

$$b_2(z) = (1 + \frac{c_2}{c_1})\ chm_1(z) - chm_o(z) \qquad (4.37)$$

$chm_1(z)$ is the characteristic function of the system at ℓ=1. The procedure of the calculations of the roots of the characteristic equations for the different ℓ and ϕ's is implemented into digital computer program. The flow-chart is given in appendix V.

The results for an operating point; $\alpha=75^o$, speed=0.538 p.u. and $R_{d.c.}$=14.17% are shown in figures 4.8 and 4.9.

Four values of ϕ are chosen, namely, $\phi=-30^o$, 0^o, 30^o and 90^o. For each ϕ, ℓ is varied from -2.5 to +5. The roots are determined and drawn as function of ℓ in Fig.4.8.

For each ℓ value there are six roots. In all cases there are one root equals unity, which verifies the pre-mentioned properity, other near to the zero value. Fig.4.9 gives the root locus only for the complex roots for different ℓ and ϕ's.

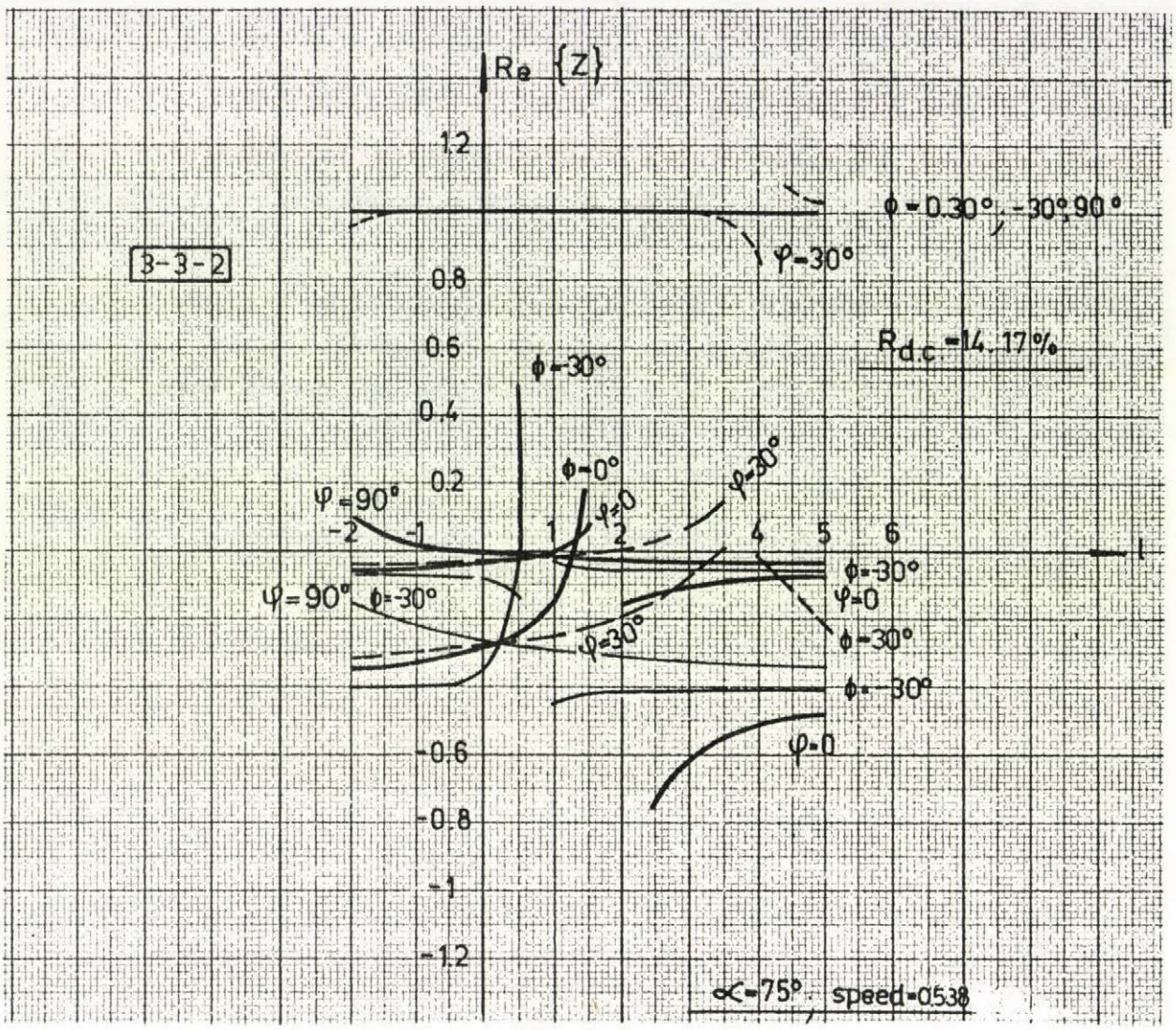
Re {Z}
1.2
0.8
0.6
0.4
0.2
-0.6
-0.8
-1
-1.2
3-3-2
ϕ=0.30°,-30°,90°
φ=30°
Rd.c=14.17%
ϕ=-30°
ϕ=0°
φ=90°
φ=0
φ=30°
-2
-1
1
2
4
5
6
I
ϕ=-30°
φ=0
ϕ=-30°
ϕ=-30°
φ=0
φ=90°
ϕ=-30°
φ=30°
∝=75°, speed=0538

Fig.4.8

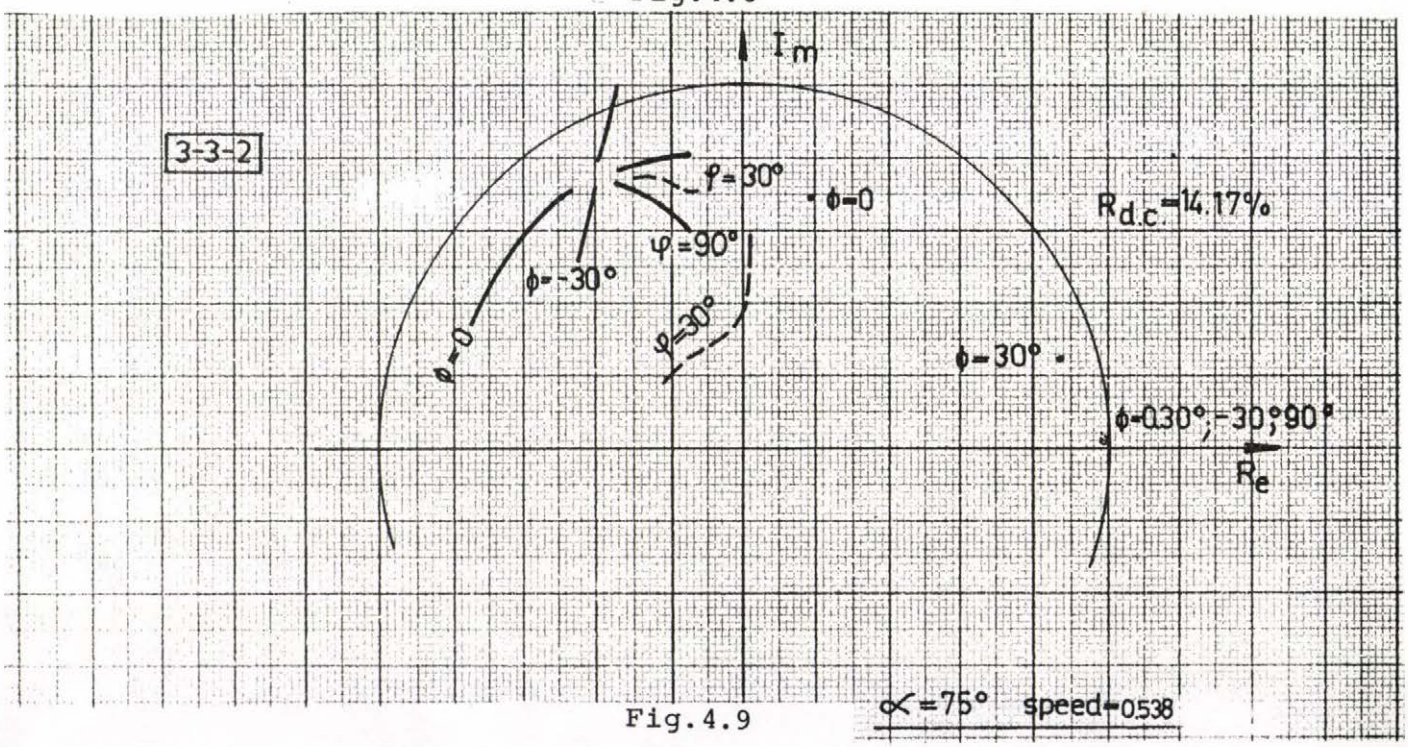
Im
3-3-2
φ=30°
ϕ=0
Rd.c=14.17%
φ=90°
ϕ=-30°
φ=30°
ϕ=0
ϕ=-30°
ϕ=0.30°,-30°,90°
Re
∝=75° speed=0538

Fig.4.9

The figures show, for the case of $\phi=90^{\circ}$, that the drive is stable if $\ell=0$ or $\ell=1$ which means that the comparative signal may be obtained proportional to either the rotor or the stator flux respectively. In that case it has been confirmed that the comparative signal may be simply obtained from the rotor or the stator flux. There is no any need to use a signal which is obtained from a complicated combination of stator and rotor fluxes /other ℓ or ϕ values/. Also at higher values of ℓ, for example, $\ell=4.5$ and $\phi=30^{\circ}$ the system shows lability nature.

Practically it is advised to use the comparative signal proportional to the stator flux because in that case the operation of the drive is accomplished more safely.

In the actual system in the laboratory the comparative signal corresponds to $\ell=1$ and $\phi=90^{\circ}$. The system is stable. Therefore it is demonstrated that the computed solution will favourably predict the performance of the actual system.

The equivalent time constants and oscillation frequences for the mentioned working point can be calculated utilizing equations (4.6)-(4.8). They are presented and tabulated in table 4.1

T_i	1882.6	16.8	1.13	0.31
ω_i	0.00099	0.43	0	0

Table 4.1

$\alpha=75^{\circ}$, speed 53.8% and $R_{d.c.}=14.17\%$

T_i: equivalent time constant

ω_i: oscillation frequency.

These values correspond to $\phi=90^{o}$ and $\ell=1$.

For similar problems if the system is unstable the reference voltage may have the shape of saw-tooth, with frequency of 3sf, f is the supply frequency, instead of constant value. However the stability can be studied in a similar way as before. In that case the deviation of the firing angle has the following expression /see.Fig. 4.10/.

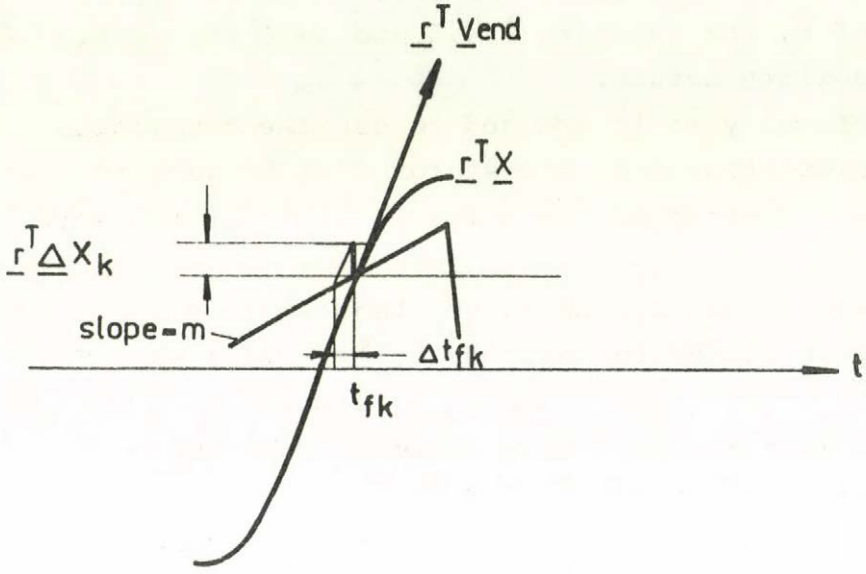

Fig.4.10

$$\Delta t_{fk} = - \frac{(\underline{r}_1^T + \ell\ \underline{r}_2^T)\ \Delta\underline{X}_k}{c_1 + \ell\ c_2 - m} \qquad (4.38)$$

where m is the slope of the reference signal. Denoting the modified characteristic function in that case by chm'(z)

$$chm'(z) = ch(z) + \frac{1}{c'-m} P(z) \qquad (4.39)$$

where

$$c' = c_1 + \ell\ c_2 \quad .$$

Therefore for a certain value of ℓ, c′ is determined and the characteristic function chm(z) can be calculated from equation (4.36) for a given value of ϕ.

The function P(z) is obtained from equation (4.39), if m=0:

$$P(z) = (chm(z) - ch(z))\, c' \qquad (4.40)$$

Using equations (4.40) and (4.39) the modified characteristic functions at certain value of ℓ and for different slopes can be obtained. The stability can be studied. Suitable values of ℓ, ϕ and m can be chosen to stabilize the system.

CHAPTER V

CHARACTERISTICS OF THE CONTROLLED DRIVE

General

It is desirable to make the drive maintain any set speed of the motor at a constant value regardless of load torque changes. In that case the variable speed induction motor exhibits torque/speed characteristics near those of d.c. shunt motor. This can be achieved by the application of a feed-back. For these purposes proper current and speed control circuits are required.

Because that the motor current is very high at starting, it is necessary to make a current feed-back to limit the current at a proper value /about 1.5 of the rated current/ to protect the semi-conductor devices. This current control is also necessary for the protection during the transient and over load cases.

As it is stated previously two values of $R_{d.c.}$ are necessary to have the required performance in the whole region. This can be performed using logic circuits as it will be shown in the next chapter. The control properities were preliminary studied using an approximate method of analysis. Afterwards the periodical steady-state solution was obtained using the exact method with eight-energy-storages. The dynamic behaviour of the controlled drive was studied as well.

5.1 Closed-Loop Transfer Function Using an Approximate Method of Analysis

The shaft speed is fed-back through tachometer and the small value of $R_{d.c.}$ is used to obtain the current feed-back signal. In the approximate analysis only one

time constant is considered for the motor that is the mechanical time constant. The electrical time constants are neglected. The block-diagram for the system with that approximation is given in Fig.5.1. The inner loop in that

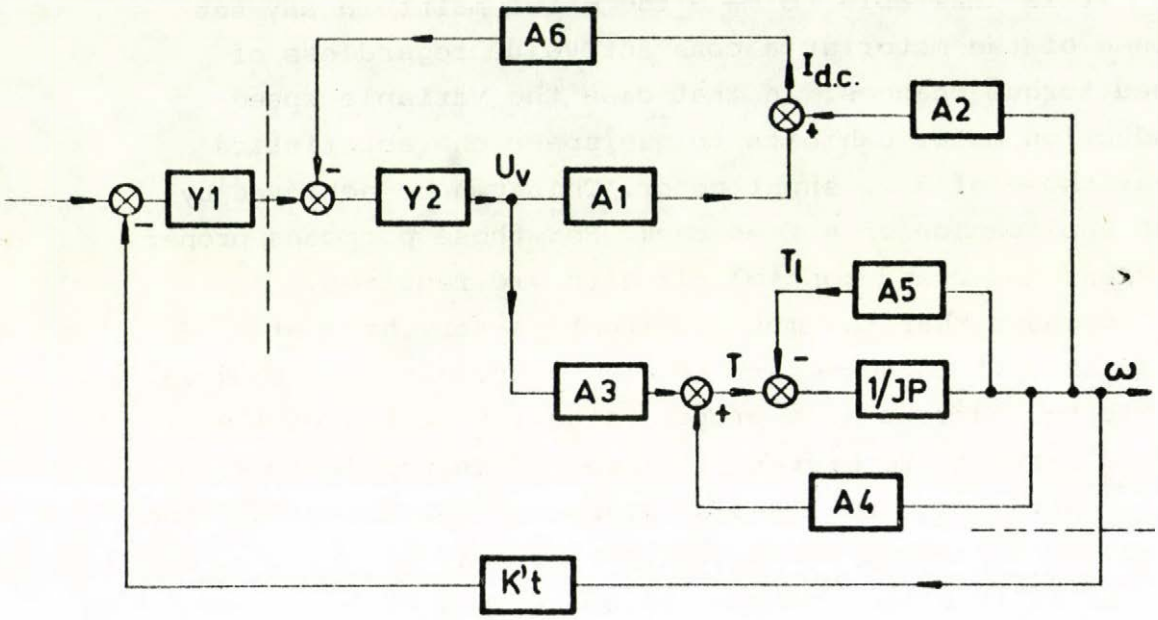

Fig.5.1

block diagram is for the current control and the speed control is represented by the outer loop as it is shown from the dotted lines in Fig.5.1. From the inner loop the following equations hold true:

$$\Delta I_{d.c.} = A_1 \Delta U_v + A_2 \Delta\omega \qquad (5.1)$$

$$\Delta T = A_3 \Delta U_v + A_4 \Delta\omega \qquad (5.2)$$

On the basis of the static characteristics of the system, the above equations are used if a small deviation from the working point has been occured.

From equation (5.1) A_1 is equal to $\frac{\partial I_{d.c.}}{\partial U_v}$ at constant

speed. In that case knowing $I_{d.c.}$ - U_v static characteristic with the speed as parameter, A_1 is the slope of that curve at the required operating point. From the curve shares at different speeds A_2 /equals

$$\frac{\partial I_{d.c.}}{\partial \omega}$$

at constant U_v/ can be calculated. Similarly A_3 and A_4 are obtained knowing the curve shares T-U_v at different speeds. As it is stated in the previous chapter U_v is the control signal which is superimposed on the a.c. comparative signal for firing the thyristors. T is the electromagnetic torque.

It has been shown that the parameters $A_1 \ldots, A_4$ are not constant. They depend on the working point, therefore they have to be calculated for each case. It has been found that the accuracy of the result using this method changes for the different cases.

By refferal to the inner loop in Fig.5.1, the following equations may be written:

$$\Delta T - \Delta T_\ell = J P \Delta\omega \qquad (5.3)$$

$$\Delta T_\ell = A_5 \Delta\omega \qquad (5.4)$$

In equation (5.3) J is the moment of inertia of the drive and P is the Laplace transform operator. A_5 is the slope of the load torque/speed characteristic.

In the current feed-back path a compensated amplifier with the manner shown in Fig.5.2 was used.

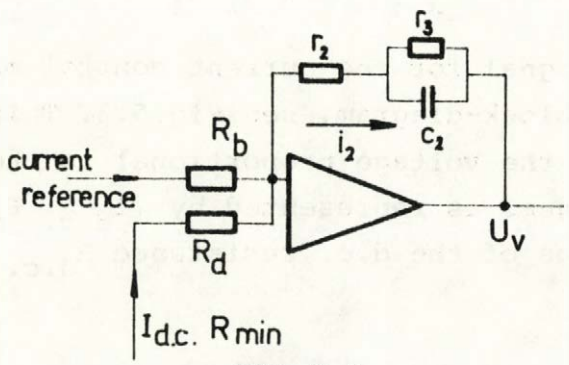

Fig.5.2

It has the following transfer function:

$$Y_2 = K \frac{1 + T_1 p}{1 + T_2 p} \qquad (5.5)$$

where

$$T_1 = \frac{r_2 r_3}{r_2 + r_3} c_2$$

$$T_2 = r_3 c_2$$

$$K = \frac{r_2 + r_3}{R_b}$$

The inner loop of the block diagram in Fig.5.1 for the current control can be simplified to the convential block diagram as it is shown in Fig.5.3.

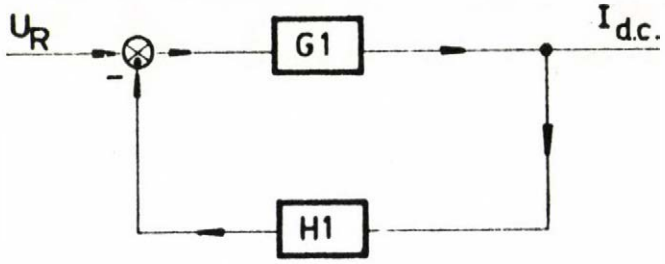

Fig.5.3

The transfer function is:

$$\frac{\Delta I_{d.c.}}{U_R} = \frac{G_1}{1 + G_1 H_1} \qquad (5.6)$$

The desired signal for the current control may be represented by U_R in the block-diagram, see Fig.5.3. This signal is compared with the voltage proportional to the d.c. current. The latter signal is represented by $/I_{d.c.} R_{min}/$, R_{min} is the small value of the d.c. resistance $R_{d.c.}$. This will be

more explained in the next section. In Fig.5.1, A_6 equals to R_{min} multiplied by

$$\frac{R_b}{R_d} ,$$

this is clear from Fig.5.2, since the two input resistances of the amplifier are not equal.

As an example, the method is applied to an operating-point. In equation (5.6) G_1 equals to:

$$G_1 = K \frac{1 + T_1 p}{1 + T_2 p} \left[A_1 + \frac{A_2 A_3 K_1}{1 + T_3 p - K_1 A_4} \right] \qquad (5.7)$$

where

$$K_1 = \frac{1}{A_5} ,$$

$$T_3 = \frac{J}{A_5} .$$

$$H_1 = A_6 \qquad (5.8)$$

The $I_{d.c.} - U_v$, $T - U_v$ and T-n characteristics /n is the motor speed in r.p.m. while ω is the speed in rad./sec./ around the operating point are given in figures 5.4, 5.5 and 5.6 respectively.

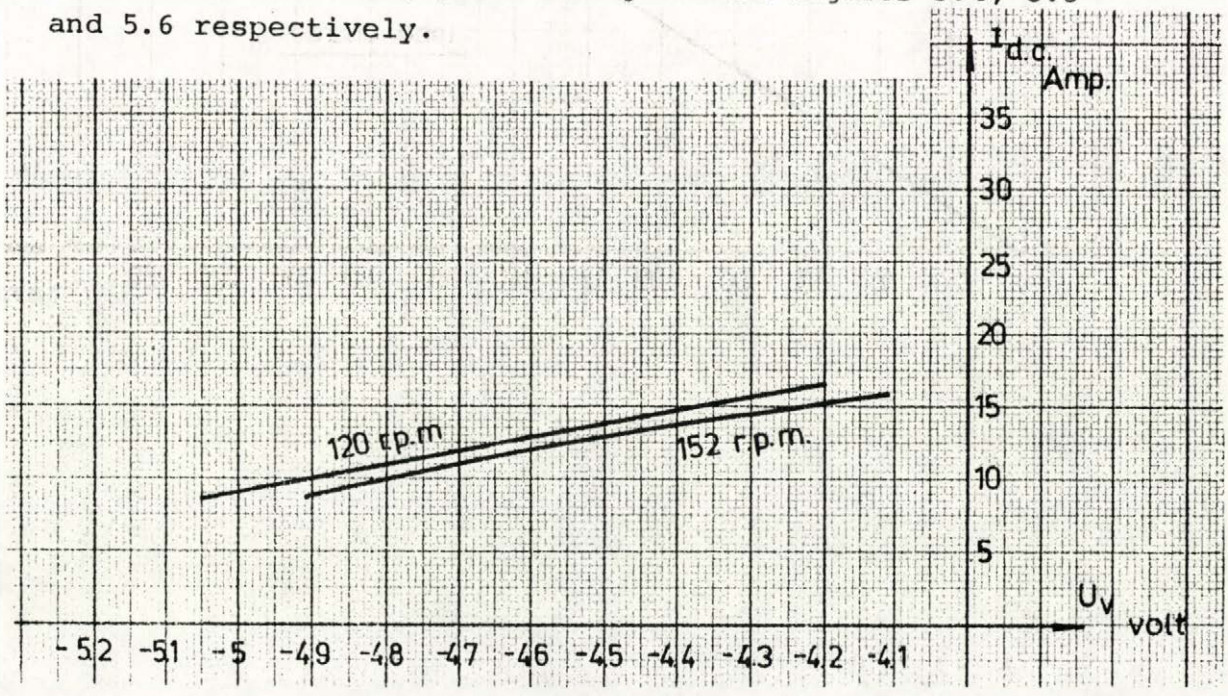

Fig.5.4

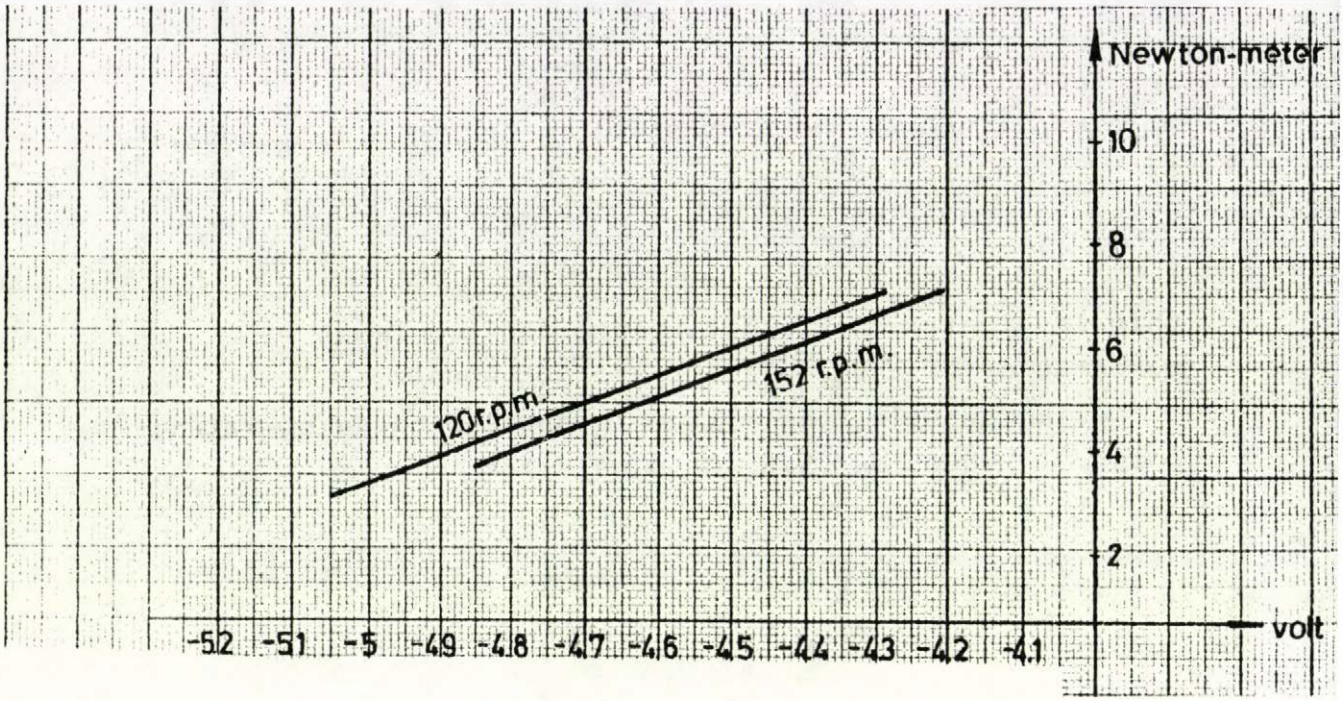
Newton-meter
10
8
6
4
2
120 r.p.m.
152 r.p.m.
-52 -51 -5 -49 -48 -47 -46 -45 -44 -43 -42 -41
volt

Fig.5.5

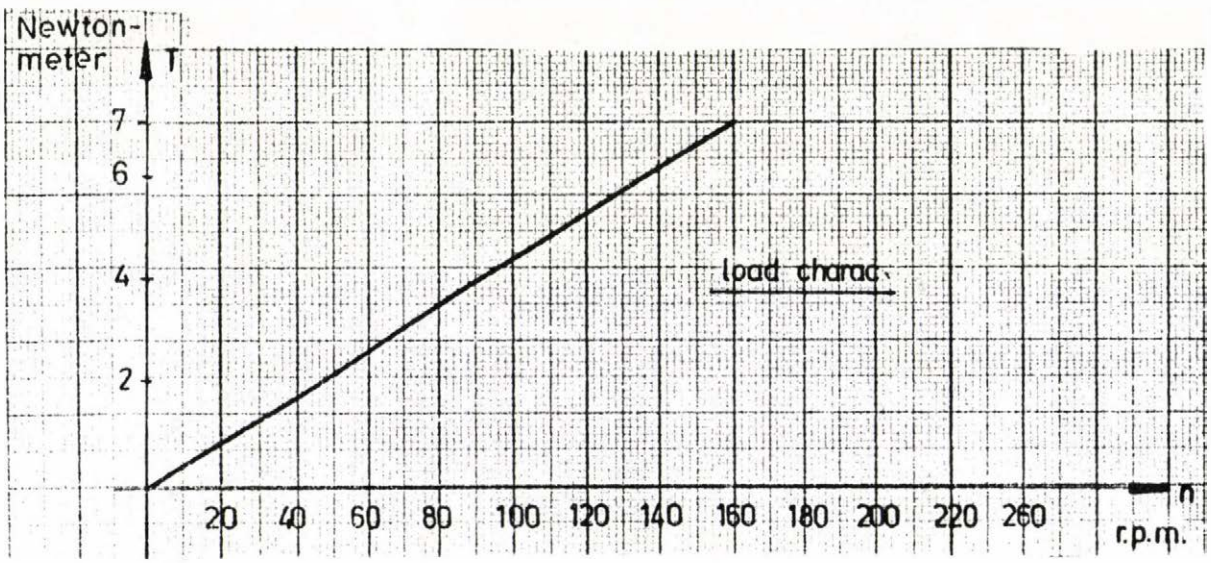
Newton-meter
T
7
6
4
2
load charac.
20 40 60 80 100 120 140 160 180 200 220 260
n
r.p.m.

Fig.5.6

The parameters can be calculated as stated previously

A_1 = 10 A/V
A_2 = -0.22 A/rad/sec.
A_3 = 5.4 Newton-meter/volt
A_4 = -0.127 N-m/rad/sec.
A_5 = 0.413 N-m/rad/sec.
A_6 = 0.275 V/A .

In equation (5.5) K=3.054, T_1=0.0303 sec. and T_2=0.64 sec.

From equation (5.6), (5.7) and (5.8)

$$\frac{\Delta I_{d.c.}}{U_R} = \frac{4.77(1+0.0303p)(10.22+7.2p)}{(p+10.88)(p+1.42)}$$

The output when the input reference signal has a step function of 1.38 volt can be calculated and the time function is shown in Fig.5.7. It is clear that the time function of the current has no over shoot which agrees the actual controlled drive used in test measurements.

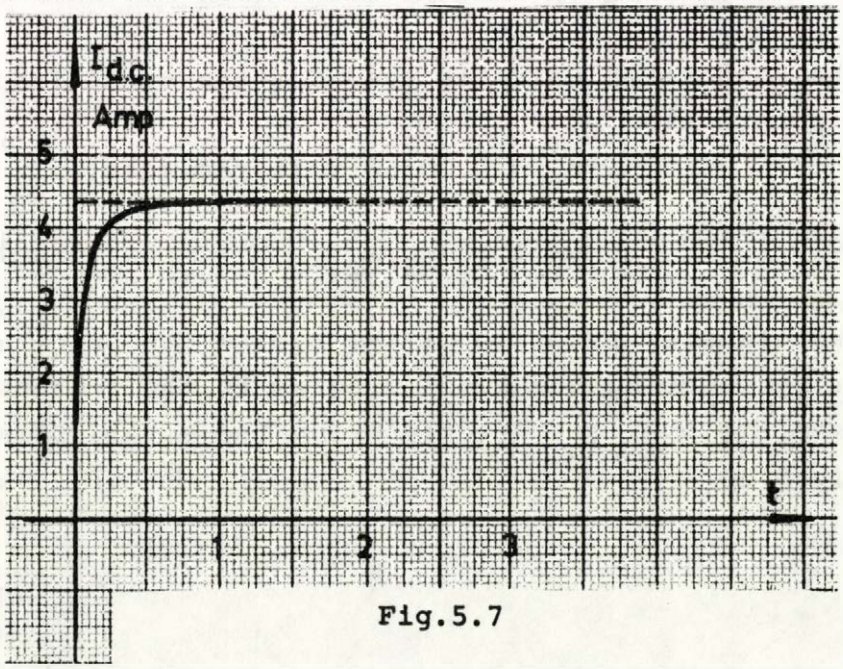

Fig.5.7

Now the outer loop for speed control is considered. It is preferable that the drive has the torque/speed characteristic such that the speed is constant independent of the load torque changes. These requirements can be achieved by using proportional plus integral (p+I) compensating circuit as shown in Fig.5.8.

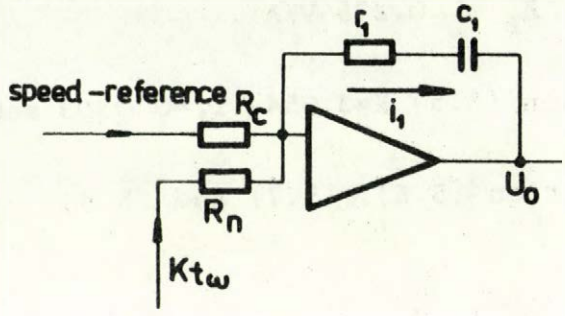

Fig.5.8

It has the following transfer function:

$$Y_1 = K' \frac{1 + T'p}{p} \qquad (5.9)$$

where

$$K' = \frac{1}{R_f\ c_1} \quad \text{and} \quad T' = r_1\ c_1$$

The tachometer which is used for the speed feed-back has a constant:

$$K_t = 0{,}00366 \text{ volt/rad./sec.}$$

In fig.5.1 $K_t' = K_t\ R_f/R_n$

The transfer function of the system can be obtained either by reducing the block diagram to the convential form see Fig.5.9, or directly using the signal flow chart see Fig.5.10.

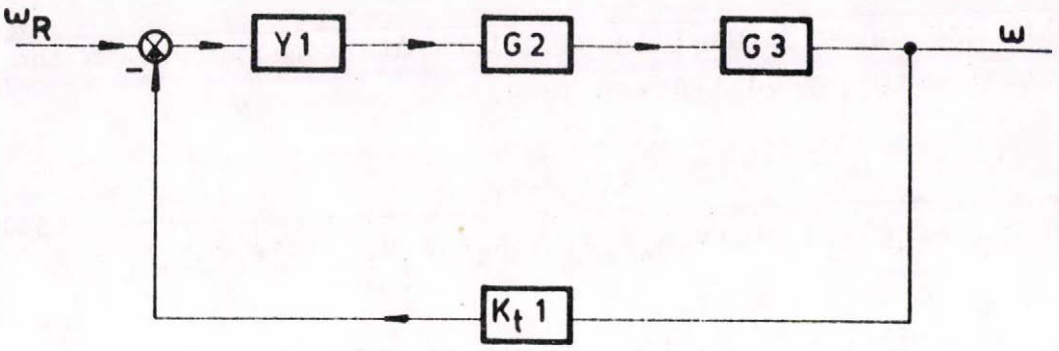

Fig.5.9

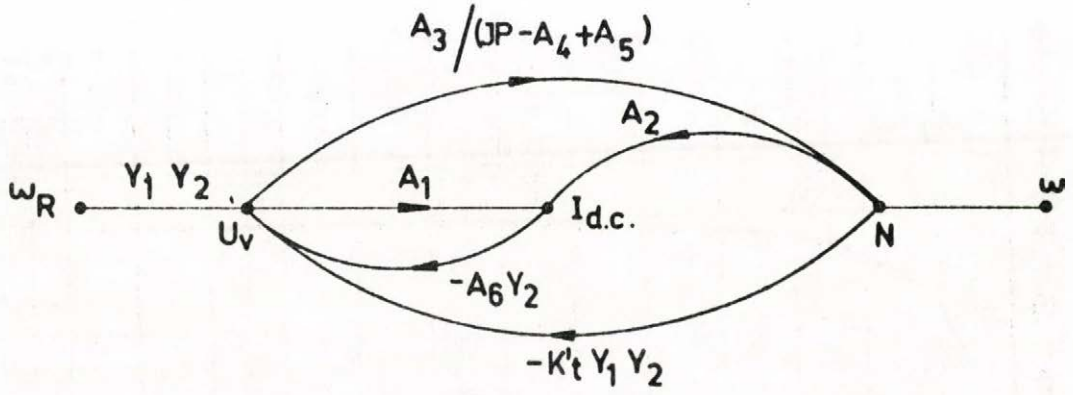

Fig.5.10

$$\frac{\omega}{\omega_R} = \frac{G_2\ G_3\ Y_1}{1 + K'_t\ Y_1\ G_2\ G_3} \qquad (5.10)$$

where

$$G_2 = \frac{Y_2}{1 + Y_2\ A_6 \left(A_1 + \dfrac{A_2\ A_3\ K_1}{1 + T_3\ p - K_1\ A_4}\right)}$$

and

$$G_3 = \frac{A_3\ K_1}{1 + T_3\ p - K_1\ A_4}$$

Similarly as in the current control case, ω_R, in volts, represents the desired speed signal in the block-diagram.

ω is the output signal in the block-diagram represents the actual motor speed /in rad./sec./.

$$\frac{\omega}{\omega_R} = \frac{Y_1 Y_2 A_3 K_1}{(1+T_3 p - K_1 A_4)(1+Y_2 A_6 A_1) + Y_2 A_6 A_2 A_3 K_1 + K'_t Y_1 Y_2 A_3 K_1} \qquad (5.11)$$

In equation (5.9) $T'=1.17$ and $K'=7.04$.

Similarly the time function of the speed due to step function of 0.98 volt in the input is shown in Fig.5.11.

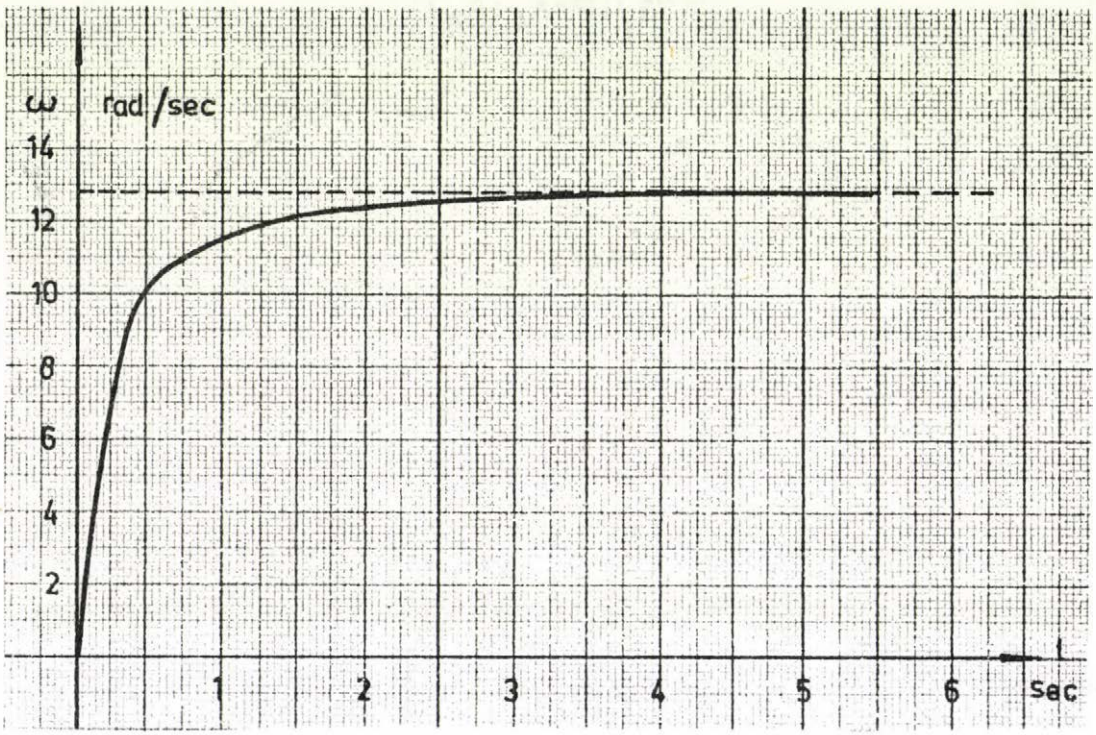

Fig.5.11

The above approximate method may be used in the preliminary study of the control problems and in the design of the compensating circuits.

However the accuracy of the method differs for the different working points.

5.2 Steady-State Periodical Solution of the Controlled Drive

It is required to get the periodical steady-state solution in the case of the controlled drive. The open-loop system without current and speed control is treated exactly using 6-energy storages.

With the addition of the control circuits the exact steady-state solution of the closed-loop system may be obtained using 8-energy storages. Naturally the first six equations are the same as in the case of the uncontrolled system /see chapter III/. Therefore the other two equations have to be obtained. Fig. 5.8 shows the compensating circuit in the speed control channel.

The tachometer output signal ($K_t\omega$), which represents the shaft speed, is compared to the voltage signal proportional to the desired speed W. The error signal

$$\frac{K_t\ \Delta\omega}{R_n}$$

is represented in Fig.5.8 by "i_1". Knowing that x(5) equals (ω-W) and $x(6) = \int x(5)dt$ from chapter III and denoting the output voltage signal of the amplifier by U_o then

$$U_o = \frac{K_t\ T'}{K_2}\ x(5) + \frac{K_t}{K_2}\ x(6) + c' \qquad (5.12)$$

where

$$K_2 = \frac{1}{R_n\ c_1}$$

c' is a constant represents the initial voltage across the capacitor c_1. The compensating circuit in the path of the current control is shown in Fig.5.2. The d.c. current is represented by the signal "$I_{d.c.}\ R_{min}$" which is compared with a signal proportional to the desired value. The latter signal is represented by U_o /see Fig.5.8/.

The out-put voltage signal of the circuit in fig.5.2 is the control voltage signal U_v which is superimposed on the a.c. comparative signal for firing the thyristors. By referral to the mentioned figure:

$$U_v = i_2 \left(r_2 + \frac{r_3}{r_3\, pc_2 + 1} \right) \qquad (5.13)$$

$$i_2 = \frac{U_o}{R_b} + \frac{I_{d.c.}\ R_{min}}{R_d} \qquad (5.14)$$

In equation (5.14) i_2 has two parts. The voltage signal at the output of the amplifier due to the first part may be chosen to represent the seventh state variable x(7), while x(8) is the voltage signal due to the other part

$$\frac{"I_{d.c.}\ R_{min}"}{R_d} \ .$$

By virtue to equation (5.13) and (5.14) it is noticed that in the solution of the problem it may be enough to choose only one more state variable than in the solution of the open-loop system. At this juncture it is possible to take U_v as the required added state variable. The choice of the above state variables x(7) and x(8) is decided only to make the system equations compatible to both steady and transient states analysis, as it will be shown in the next section.

Having called $\frac{d\,x(7)}{dt}$ and $\frac{d\,x(8)}{dt}$ by v(7) and v(8) respectively, then utilizing equations (5.13), (5.14) together with equation (5.12) the following equations can be deduced:

$$v(7) = a_1\, v(5) + a_2\, x(5) + a_3\, x(6) + a_4 - \frac{1}{T_2}\, x(7) \qquad (5.15)$$

$$v(8) = K\, A_6\, \frac{T_1}{T_2}\, \frac{d\, I_{d.c.}}{dt} + K\, A_6\, \frac{1}{T_2}\, I_{d.c.} - \frac{1}{T_2}\, x(8) \qquad (5.16)$$

where:

$$a_1 = \frac{K\ K_t}{K_2}\ \frac{T_1\ T'}{T_2}\ ,\quad a_2 = \frac{T_1+T'}{T_1\ T'}\ a_1\ ,\quad a_3 = \frac{1}{T_1\ T'}\ a_1\ .$$

In equation (5.15) v(5) equals $\frac{d\ x(5)}{dt}$. The d.c. current, $I_{d.c.}$, in equation (5.16) is determined knowing the state variables x(1)...x(4). The constant a_4 in equation (5.15) can be determined from the periodicity condition.

Method of Solution

The nonlinear set of differential equations of the controlled drive containes eight equations, the first six equations are known from chapter III and the other two are v(7) and v(8).

A similar method of solution may be used as stated in chapter III. The routine work is to determine the approximate values of the initial conditions for the eight state variables from an approximate method. The initial conditions of the first six state variables are determined from the open-loop system solution and approximate values are given to the initial conditions for the other two variables. The periodical solution is determined by an iteration method using the transfer matrix as explained in chapter III.

An alternative method is introduced to solve this problem directly and save the computation time of the digital computer. The method is described as follows:

Utilizing the periodical solution of the open-loop system, it is enough to solve the added two differential equations. The initial values for the two added state variables can be calculated and the periodical solution for the controlled drive is obtained. The solution of the differential equation has two parts, the homogenous solution

and the particular integral one. The latter solution may be obtained by setting the initial values of x(7) and x(8) equal zero and using numerical method such as Runge-Kutta. Having called these particular integral solutions by $x(7)_{P.I.}$ and $x(8)_{P.I.}$, the total solutions of the state variables x(7) and x(8) at the end of the stroke have the following form:

$$x(7)_{end} = x(7)_{P.I.} + x(7)_o \bar{e}^{\tau/T_2} \qquad (5.17)$$

$$x(8)_{end} = x(8)_{P.I.} + x(8)_o \bar{e}^{\tau/T_2} \qquad (5.18)$$

where $x(7)_o$ and $x(8)_o$ are the initial values of the state variables at the beginning of the stroke.

In equation (5.15) the constant a_4 is unknown. The particular integral solution $x(7)_{P.I.}$ at the end of the stroke can be written in the form:

$$x(7)_{P.I.} = x'(7) + a_4 T_2(1-\bar{e}^{\tau/T_2}) \qquad (5.19)$$

where x'(7) is the particular integral solution of equation (5.15) without the consideration of the constant a_4.

Utilizing the periodicity condition, the values of the state variables $x(7)_{end}$ and $x(8)_{end}$ are equal to $x(7)_o$ and $x(8)_o$ respectively.

Then:

$$x(7)_o = x(7)_{P.I.} / (1 - \bar{e}^{\tau/T_2}) \qquad (5.20)$$

$$x(8)_o = x(8)_{P.I.} / (1 - \bar{e}^{\tau/T_2}) \qquad (5.21)$$

Having knew $x(8)_{P.I.}$, the initial value $x(8)_o$ is obtained directly using equation (5.21). By virtue to equations (5.19), and (5.20), there are three unknowns, a_4, $x(7)_{P.I.}$

and $x(7)_o$. The value of the control signal U_v for the required working point is known. Therefore the initial value $x(7)_o$ is determined from the equation

$$x(7)_o + x(8)_o = U_v \qquad (5.22)$$

Knowing $x(7)_o$, the constant a_4 is determined using equation (5.20) together with (5.19):

$$a_4 = \frac{U_v - x(8)_o}{T_2} - \frac{x'(7)}{T_2(1-e^{-\tau/T_2})} \qquad (5.23)$$

The periodical solution is obtained without any need to use an iteration method to calculate $x(7)_o$ and $x(8)_o$. The method is applied to a working point /$\alpha=70^o$ and speed=.179/. The time functions of the state variables x(5)...x(8) are shown in figures 5.12 - 5.15.

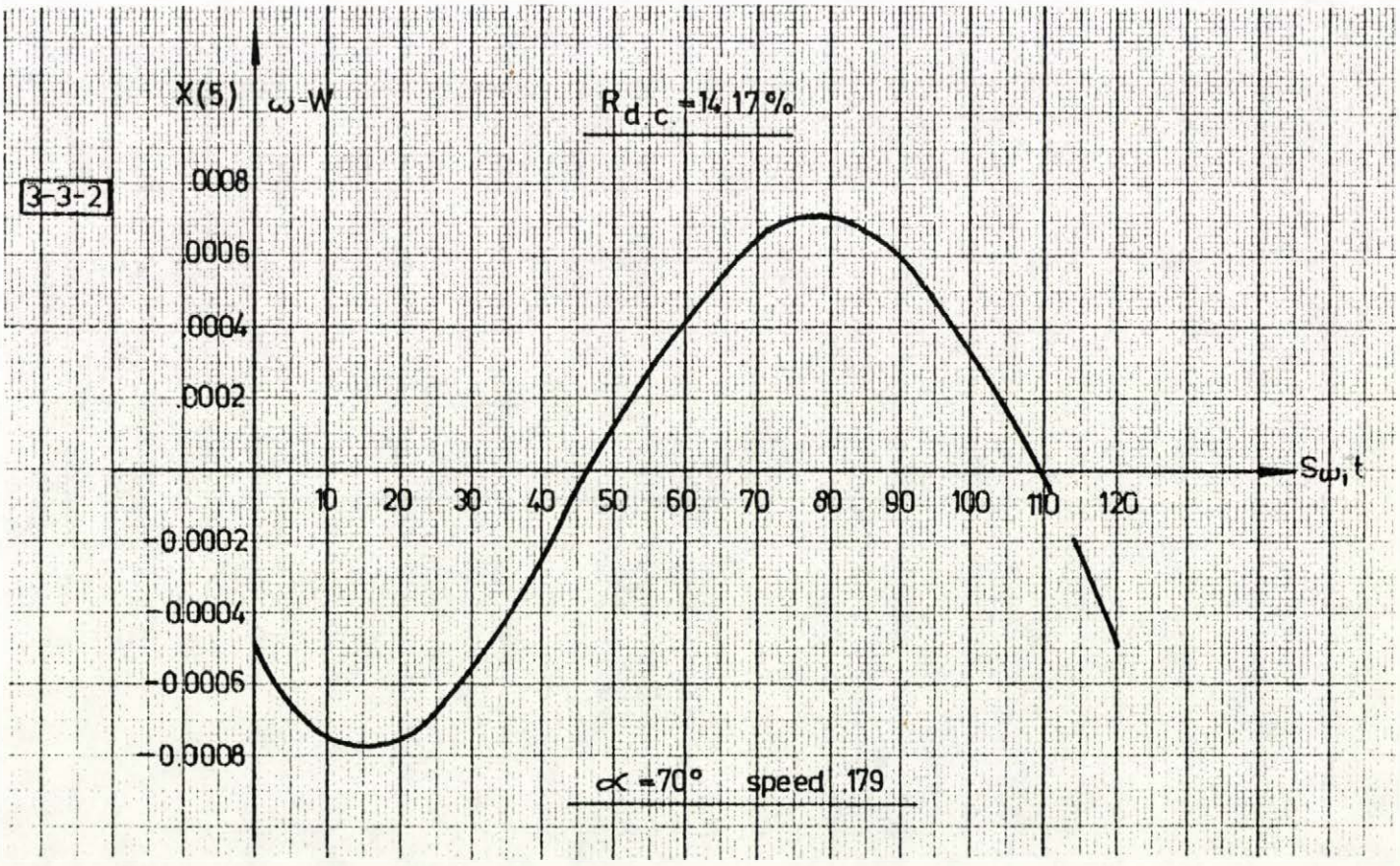

Fig.5.12

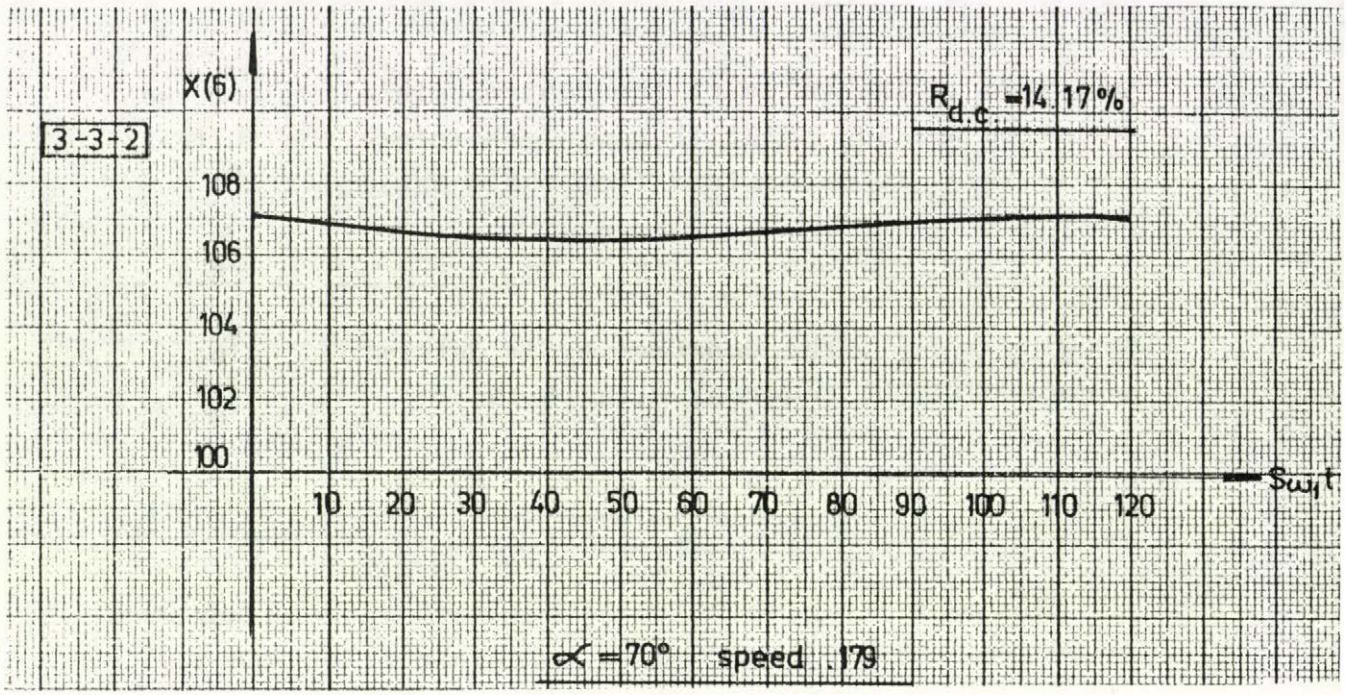

Fig.5.13

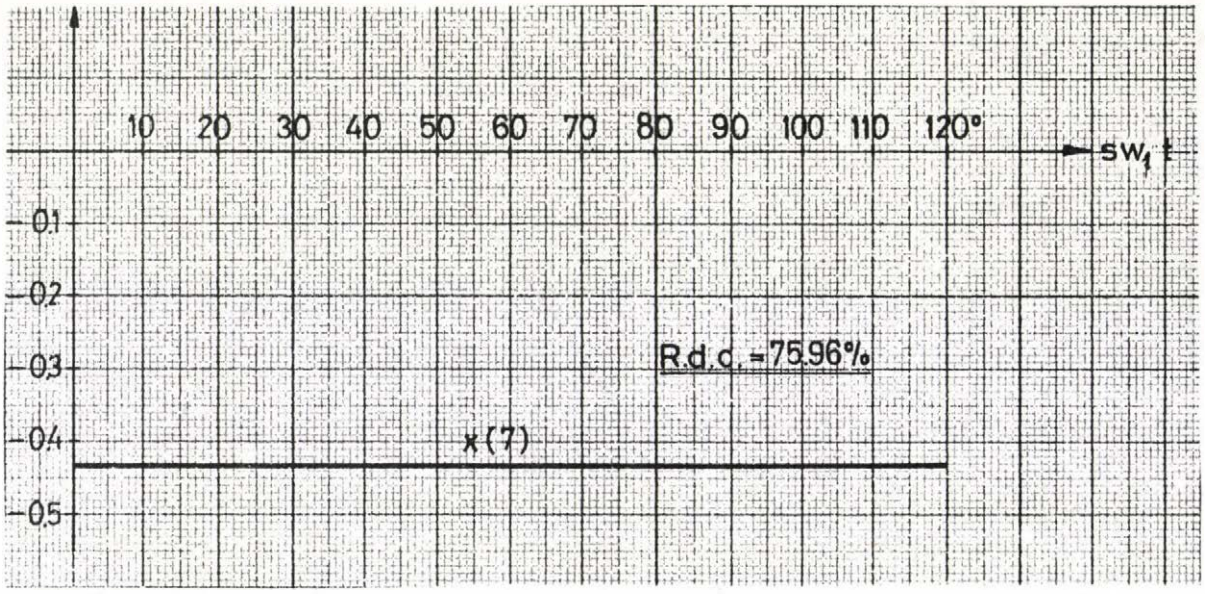

Fig.5.14

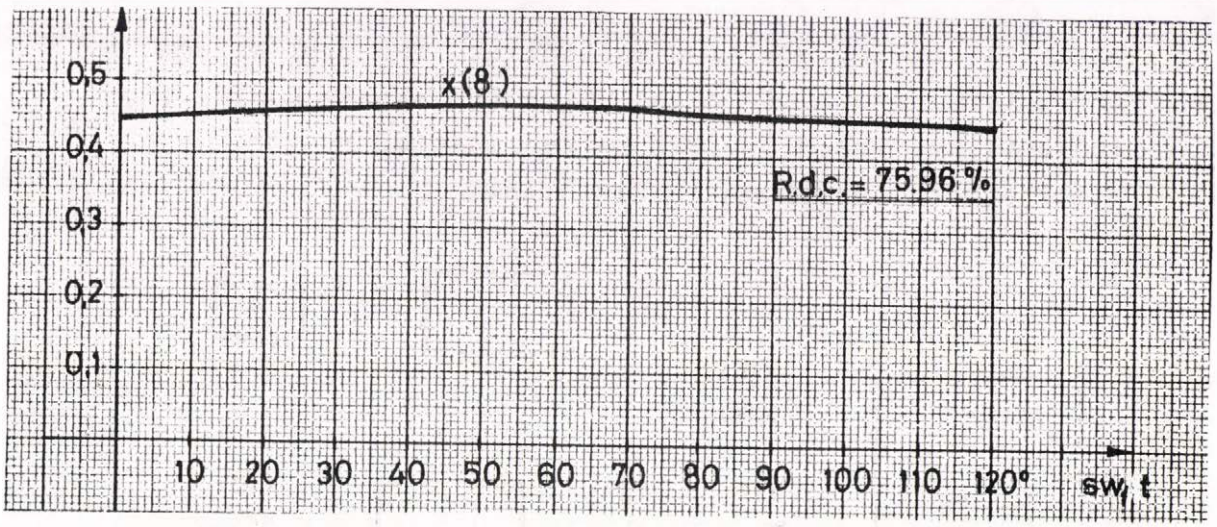

Fig.5.15

5.3 Stability of the Closed-Loop System

Through the studying of the dynamic behaviour of the closed-loop system, it is useful to find out the stability margin of the drive. It has been shown that the most simple and convenient method in that respect is to change one or more of the parameters of the control circuits until the system reach the stability limit.

Among the variety of ways it has been found that the resistance R_b in the path of the reference signal in the current control circuit Fig.5.2 is more suitable parameter for such purposes. Because of choosing that parameter the studying of the system stability both analytically and experimentally may be fulfilled more easily.

In the analytic treatment of the problem, it is necessary to get the characteristic equation of the system in each case. The roots of the characteristic equation determine the system stability.

The new value of the resistance R_b after changing may be denoted by R_b', then:

$$R_b' = \frac{1}{a} R_b \qquad (5.24)$$

where "a" is any positive multiplier. The problem now is the determination of "a" at which the system begins the instability. The drive can be represented by the block-diagram as shown in Fig.5.16.

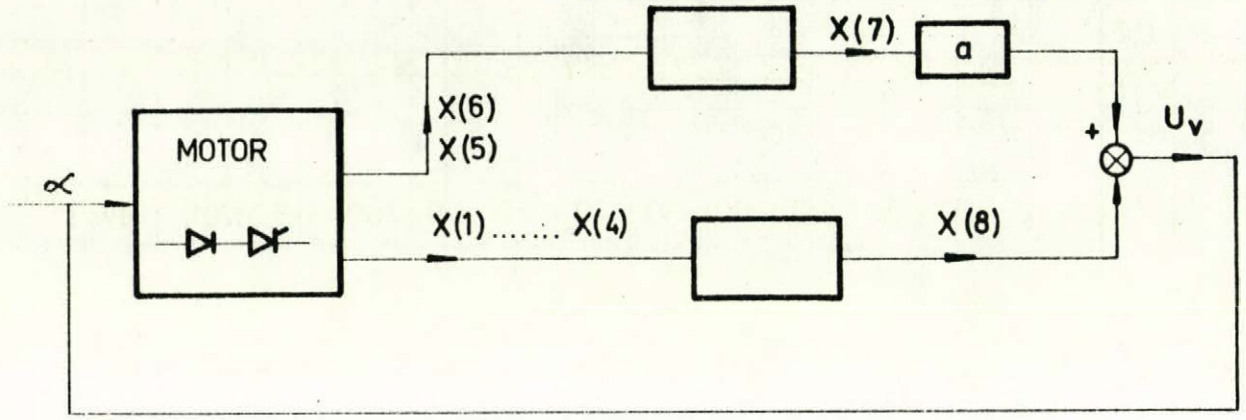

Fig.5.16

Since for all the values of "a" the operating point does not change therefore the instant of the firing of the thyristor is the same, then,

$$a\ x(7) + x(8) = U_v \qquad (5.25)$$

By virtue to equation (5.25), it is clear that the control voltage signal U_v depends on the state variables x(7) and x(8).

As stated in the previous chapter, the stator flux is used as a comparative signal. The state vector $\underline{X}$ now in the case of the controlled drive have eight state variables:

$$\underline{X}^T = [\Psi_{sx}\ \Psi_{sy}\ \Psi_{rx}\ \Psi_{ry}\ \omega\text{-}W\ \Theta\ x(7)\ x(8)] \qquad (5.26)$$

Now if a small variation in the state variables occurs, the comparative and the control signals will change.

Therefore the same starting state vector may be obtained, as explained in the previous chapter, if an incremental change in the firing angle occurs such that

$$\Delta t_{fk} = - \frac{\underline{r}^T \ \underline{\Delta X}_k}{\underline{r}^T \ \underline{V}_{end}} \qquad (5.27)$$

From equation (5.25) and taking into consideration that the comparative signal is proportional to the stator flux the row vector $\underline{r}^T$ has the following expression:

$$\underline{r}^T = [\ 0 \quad 1 \quad 0 \quad 0 \quad 0 \quad 0 \ -a \ -1\ ] \qquad (5.28)$$

By virtue to equations (5.25) and (5.22), the latter is a special case of the former when a=1. The constant "a_4" in equation (5.23) can be written in the general form:

$$a_4 = \frac{U_v - x(8)_o}{aT_2} - \frac{x'(7)}{T_2(1-\bar{e}^{\tau/T_2})} \qquad (5.29)$$

It is shown that "a_4" depends on the multiplier "a" therefore it is convenient to write the constant "a_4" in the following form:

$$a_4 = d_1 + \frac{1}{a} d_2 \qquad (5.30)$$

where

$$d_1 = - \frac{x'(7)}{T_2(1-\bar{e}^{\tau/T_2})} \quad \text{and} \quad d_2 = \frac{U_v - x(8)_o}{T_2}$$

$\underline{V}_{end}$ in equation (5.27) is the velocity of the state vector at the end of the preceding stroke. From equation (5.15), it is shown that the velocity vector is function of the constant "a_4" and in consequence to the multiplier

"a". That vector may be written in the following form:

$$\underline{V}_{end} = \underline{V}_{end_1} + \frac{1}{a}\,\underline{V}_{end_2} \tag{5.31}$$

$$\underline{V}_{end_1} = [v(1)\ v(2)\ldots\ v'(7)+d_1\ \ v(8)]^T \tag{5.32}$$

$$\underline{V}_{end_2} = [\,0\quad 0\ \ldots\quad d_2\quad 0\,]^T$$

In the above equation v'(7) is the value of state variable velocity, v(7), in equation (5.15) at the end of the stroke without considering the constant a_4.

In a similar way as explained in the previous chapter, the row vector $\underline{r}^T$ in equation (5.28) may be cut to two row vectors $\underline{r}_1^T$ and $\underline{r}_2^T$ which are independent of the multiplier "a".

$$\underline{r}^T = \underline{r}_1^T + a\,\underline{r}_2^T \tag{5.33}$$

where

$$\underline{r}_1^T = [\,0\ 1\ 0\ 0\ \ldots\ -1\,] \tag{5.34}$$

$$\underline{r}_2^T = [\,0\ 0\ \ldots\ -1\ \ 0\,] \tag{5.35}$$

Regarding equations (5.27), (5.31), (5.32) together with equation (5.33), the small change in the firing angle at the $k^{\underline{th}}$ stroke may be expressed as follows:

$$t_{fk} = -\frac{(\underline{r}_1^T + a\,\underline{r}_2^T)}{h_1 + a\,h_2} \tag{5.36}$$

where $h_1 = \underline{r}_1^T\,\underline{V}_{end_1} + \underline{r}_2^T\,\underline{V}_{end_2}$, $h_2 = \underline{r}_2^T\,\underline{V}_{end_1}$.

Utilizing the recursion equation of the small variation at the (k+1) stroke /as known from the previous chapter/:

$$\underline{\Delta X}_{k+1} = \underline{A}\,\underline{\Delta X}_k + \underline{b}\,\Delta t_{fk} \tag{5.37}$$

the characteristic function of the system in that case is:

$$\text{chm}(z) = \det.\left[z\underline{I} - \underline{A} + \underline{b}\,\frac{\underline{r}_1^T + a\,\underline{r}_2^T}{h_1 + a\,h_2}\right] \qquad (5.38)$$

The roots of the characteristic equation in each case can be computed used the same theory explained in the previous chapter. The roots determine the system stability.

CHAPTER VI

EXPERIMENTAL WORK

6.1 General

The experimental work was done on connection I(ΔTT) and the half controlled bridge connection. The latter connection was treated in more details than the former one as it is stated in the analytical work. For connection I(ΔTT), the experimental results are given in Fig.6.1.

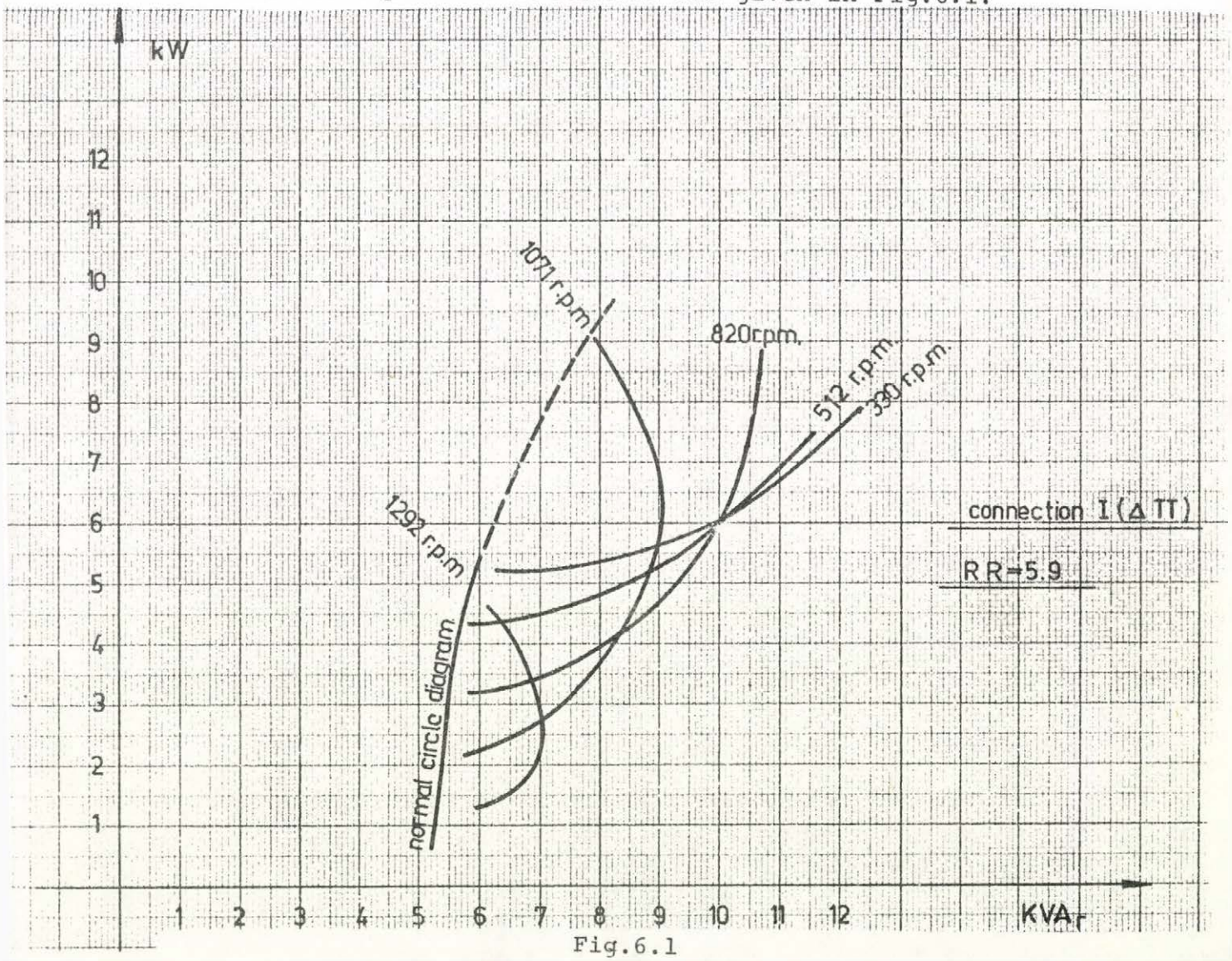

Fig.6.1

The fig. shows the characteristics of the drive when the firing angle of the thyristors is varying while the speed is constant. It is shown from the fig. that the torque cannot be reduced to zero value as it is known analytically.

The following sections will deal with the half controlled bridge connection. The steady-state characteristics of the drive with that connection were studied. The performance curves of the system were obtained and a comparison was made between the measured and computed quantities at some operating-points. Also some oscillograms were obtained from the actual system to compare them with those of the digital computer solutions. The experimental work contains also the study of the closed-loop system with current and speed control. The performance curves were measured. The system-stability was studied. The dynamic behaviour of the controlled drive due to sudden change in the speed reference signal was obtained.

6.2 Connection Diagram

6.2.1 Open-Loop System

The comparative signal for firing the thyristor may be taken proportional to the stator flux. This signal can be obtained from the integration of the slip-ring voltages and some correction signals according to the following equation:

$$\bar{\Psi}_s = \int (\bar{u}_r + R_r \bar{i}_r)dt + L'_r \bar{i}_r \qquad (6.1)$$

The connection diagram for the firing purposes in that case can be represented by Fig.6.2 but without the controller /feed-back from the speed and current/.

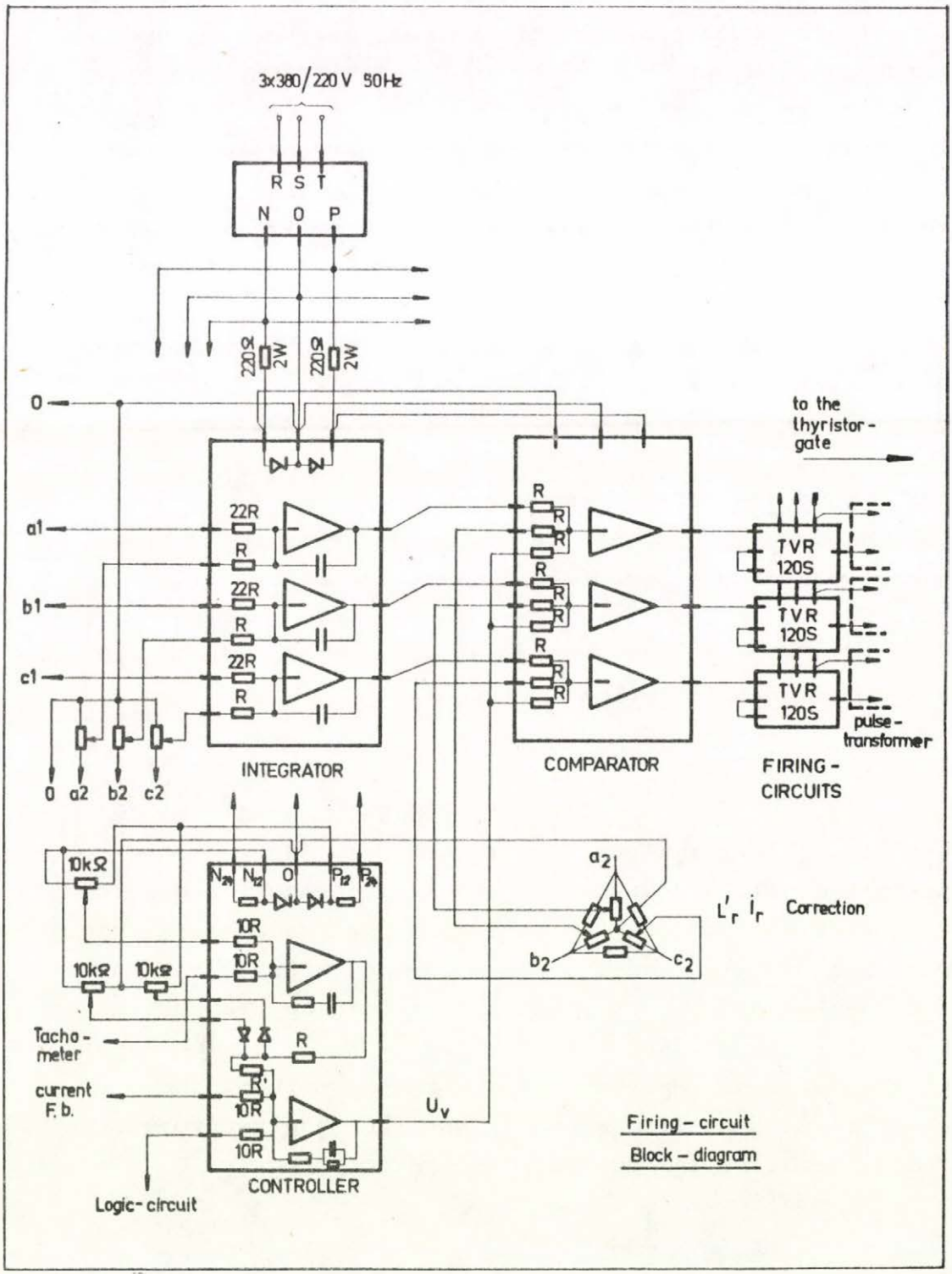
3x380/220 V 50Hz
R S T
N O P
220Ω 2W
220Ω 2W
0
a1
b1
c1
22R
R
INTEGRATOR
0 a2 b2 c2
to the thyristor-gate
COMPARATOR
TVR 120S
TVR 120S
TVR 120S
pulse-transformer
FIRING-CIRCUITS
10kΩ
10kΩ 10kΩ
10R
Tacho-meter
current F.b.
CONTROLLER
Logic-circuit
U_v
a_2
b_2
c_2
L'_r i_r Correction
Firing – circuit
Block – diagram

Fig.6.2

The slip-ring voltages are transformed by a 3-phase Δ/Y potential transformer which has a phase turns ratio of 2:1. The output of the transformer secondaries are represented by a_1, b_1 and c_1 in Fig.6.2. The rotor flux signals are obtained from the integration of $\bar{u}_r + R_r \bar{i}_r$. The signals $R_r \bar{i}_r$ are achieved from the flowing of the transformed values of the rotor currents /a_2, b_2 and c_2 in the figure/ through designed valued resistances. The output of the integrators represent the rotor fluxes. The stator flux signals are obtained from the addition of $L'_r \bar{i}_r$ to that rotor flux signals. The proper addition of $L'_r \bar{i}_r$ to the rotor fluxes is performed as shown in Fig.6.2. In that case the comparator will compare the stator flux signals with the d.c. reference voltage U_v for firing the thyristors.

The open-loop system is stable and the steady-state measurements were performed for that case.

6.2.2 Closed-Loop System

As it is stated analytically two values of $R_{d.c.}$ are required. The chosen values were 75.96% and 14.17%. In the closed-loop system, current and speed control are performed. Fig.6.2 gives the required connection diagram for the firing of the thyristors in that case. A tachometer was used for the feed-back from the motor speed and the small value of $R_{d.c.}$ was used for obtaining the current feed-back signal. Since two values of $R_{d.c.}$ are necessary, therefore it is important to switch out part of the resistance at certain speed to get the required torque/speed characteristics and the required performance.

This process can be obtained automatically using one thyristor parallel to one part of the d.c. resistance. For starting purposes it is necessary to have the total resistance inserted in the rotor circuit. This is achieved if the parallel thyristor is in the blocking state in that case. At the required speed the thyristor is fired, it short-circuits one part of the resistance and the small value of $R_{d.c.}$ remains in the rotor circuit. The turning on and off of the thyristor at the required speeds may be performed by the help of a logic-circuit. Fig.6.3 gives the connection diagram. The required speed at which the thyristor is turned on is adjusted by the potentiometer remarked by n_2 in the diagram. Similarly the adjustment of the potentiometer denoted by n_1 decides the speed at which the thyristor turns off. The operation of the logic circuit can be summarized as depicted in Fig.6.4.

1. The logic circuit was designed such that the firing of the thyristor is achieved when the motor speed becomes n_2, where n_2=0.65.
2. If the voltage of point B is minimum the firing circuit gives pulses to fire the thyristor. The logic elements will verify that condition at the required speed of n_2 as it is shown in Fig.6.4. The figure gives the successive steps of operation of the different parts of the logic circuit.
3. Since the thyristor is fired, it short-circuits part of $R_{d.c.}$ and only the small value of the d.c. resistance, $R_{d.c.}$=14.17%, is inserted in the rotor circuit.
4. In the turnning-off of the thyristor, it is not enough to remove the pulses, since the thyristor current is not zero. In that case it is necessary; by the help of the logic-circuit; that the original firing-circuits for the three thyristors of the half controlled bridge delay the firing angle at that moment such that zero-phase condition is obtained. The thyristor current is zero and the thyristor becomes in the blocking state.

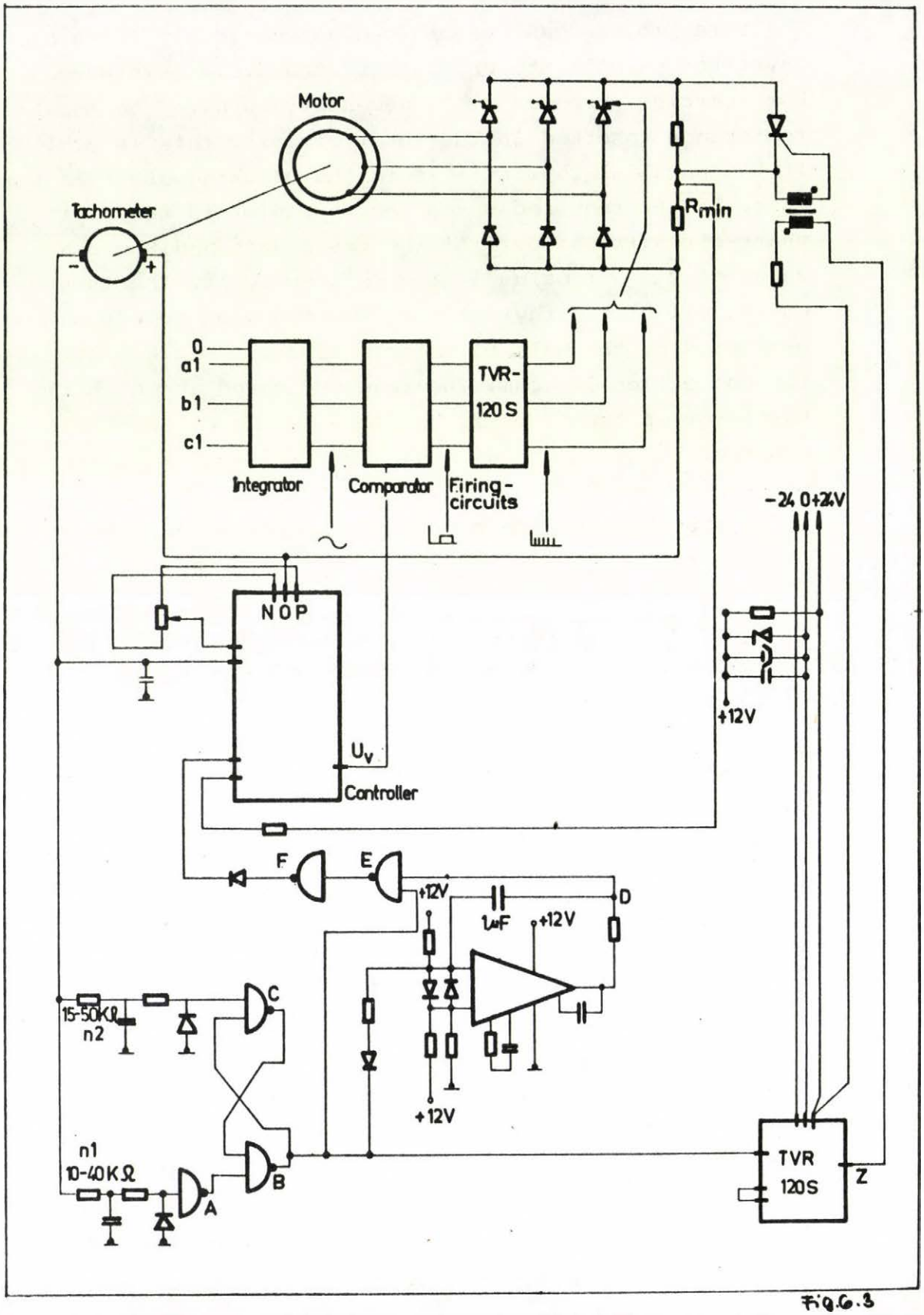
Motor
Tachometer
-
+
Rmin
0
a1
b1
c1
TVR-
120 S
Integrator
Comparator
Firing-
circuits
-24 0+24V
N O P
+12V
Uv
Controller
F
E
+12V
D
1µF
+12V
C
15-50KΩ
n2
+12V
n1
10-40KΩ
B
A
TVR
120S
Z
Fig.6.3

Fig.6.3

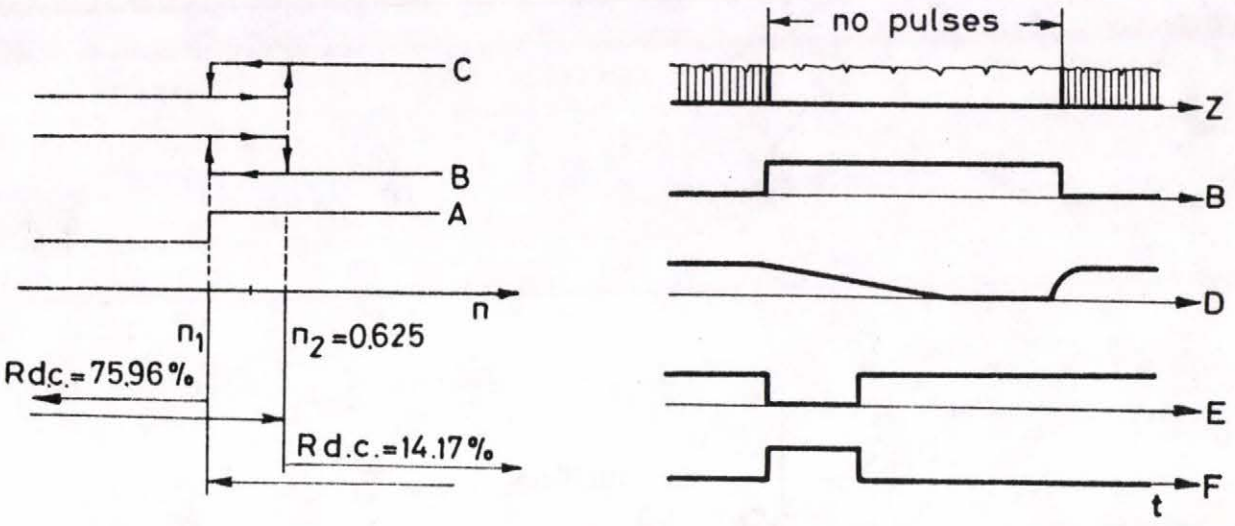

Fig.6.4

5. The control circuits will adjust the firing angle of the main thyristors corresponding to the speed reference signal and the load torque. The total resistance, $R_{d.c.}$=75.96%, is now inserted in the rotor circuit.

It must be noted that the ideal case for the operation of the logic-circuit is that the thyristor turns on and off at the same designed speed. Practically the process is achieved in a small band n_1-n_2 as shown in Fig.6.4. This band depends on the operation of the whole system.

6.3.1 Measurement of the Firing Angle (α)

Normally in the half controlled bridge and bridge connections, the firing angle of the thyristors is measured from the instant at which the voltage in two phases are equal see Fig.6.5. Since the half controlled bridge is inserted in the rotor circuit, then the measurement of the firing angle needs an auxiliary machine. The auxiliary

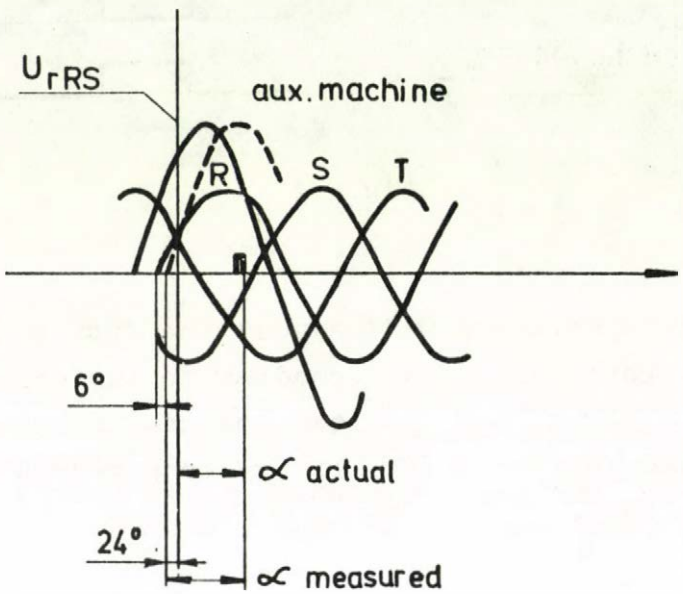

Fig.6.5

induction motor is connected to the same supply as the drive and the two rotors are mechanically coupled, the rotor of the auxiliary motor is left open see Fig.6.6.

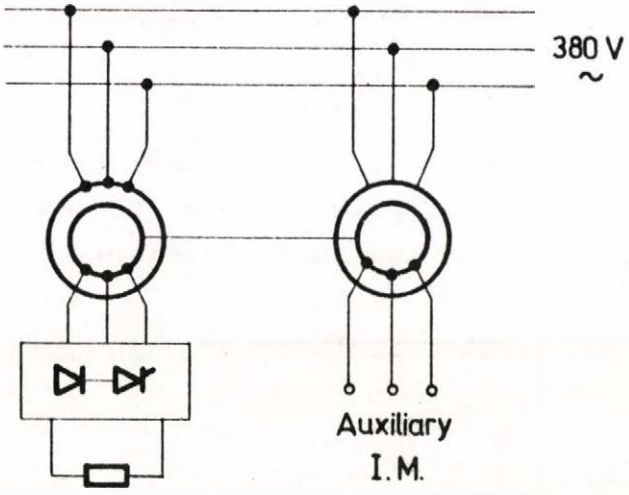

Fig.6.6

Firstly the two machines are switched on and their rotors are open-circuited and the phase shift between the two slip-ring voltages is measured. In our case this phase shift is 36^{o}. At normal running of the drive the angle between the pulse and the open-circuit slip-ring voltage of the auxiliary machine is measured. This angle is denoted by $\alpha_{measured}$. There is a fixed relation between the actual value of α and that measured value, see Fig.6.5

$$\alpha_{actual} = \alpha_{measured} - 24^{o}$$

6.3.2 Measurement of the Nominal Starting Time of the Drive

The nominal starting time "T_{sn}" represents the moment of inertia of the drive in per-unit system

$$T - T_{\ell} = \frac{J}{P} \frac{dw}{dt} \qquad (6.2)$$

where: J is the moment of inertia of the drive,
P is the number of pole pairs of the machine,
ω is the speed of the shaft in electric radians.

In per-unit system if the base value for the torque is denoted by T_b then:

$$\frac{T-T_{\ell}}{T_b} = \frac{J\omega_o}{T_b} \omega_1 \frac{d\ \omega/\omega_1}{d\ \omega_1 t} \qquad (6.3)$$

$\omega_o=\omega_1/P$ is the mechanical angular synchronous speeds.

The nominal starting time of the drive is represented by:

$$\frac{J\omega_o}{T_b} \omega_1$$

Therefore the determination of T_{sn} needs the measurement of the moment of inertia. The well known method described in Fig.6.7 is used for such measurement. In the figure only one induction motor is drawn but the real system has also the another induction motor for measuring the firing angle. The moment of inertia can be calculated from the oscillograms shown in Fig.6.8 J=0,298 Newton-meter sec^2.

Having known, J, the nominal starting time can be calculated.

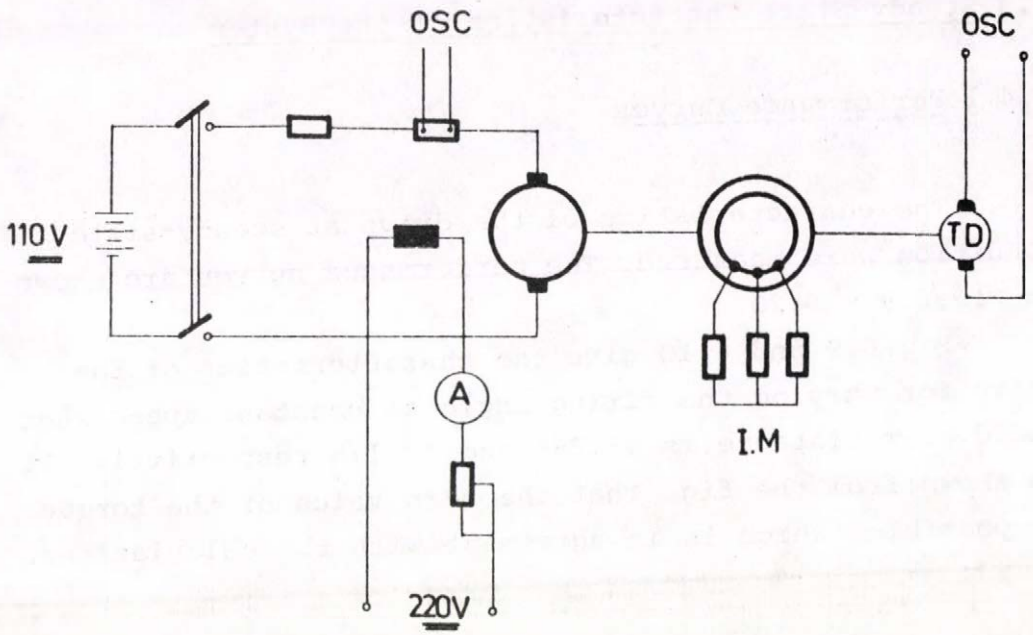
OSC
OSC
110 V
TD
A
I.M
220V

Fig.6.7

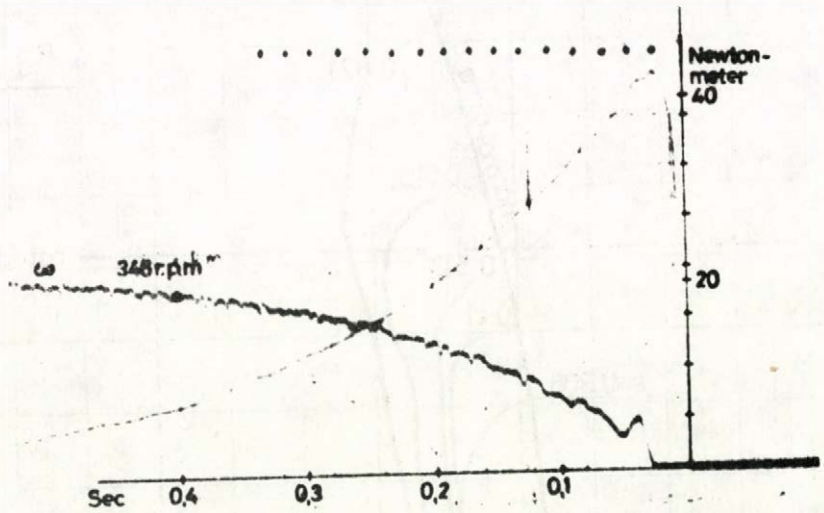
Newton-
meter
40
20
ω 348r.p.m
Sec
0,4
0,3
0,2
0,1

Fig.6.8

6.4 Steady-State Characteristics of the System

6.4.1 Performance Curves

The characteristics of the drive at steady-state condition were measured. The performance curves are shown in Fig.6.9 - 6.20.

Fig.6.9 and 6.10 give the characteristics of the drive for varying the firing angle at constant speed when the d.c. resistance is 75.96% and 14.17% respectively. It is shown from the fig. that the zero value of the torque is possible, which is in agreement with the calculations.

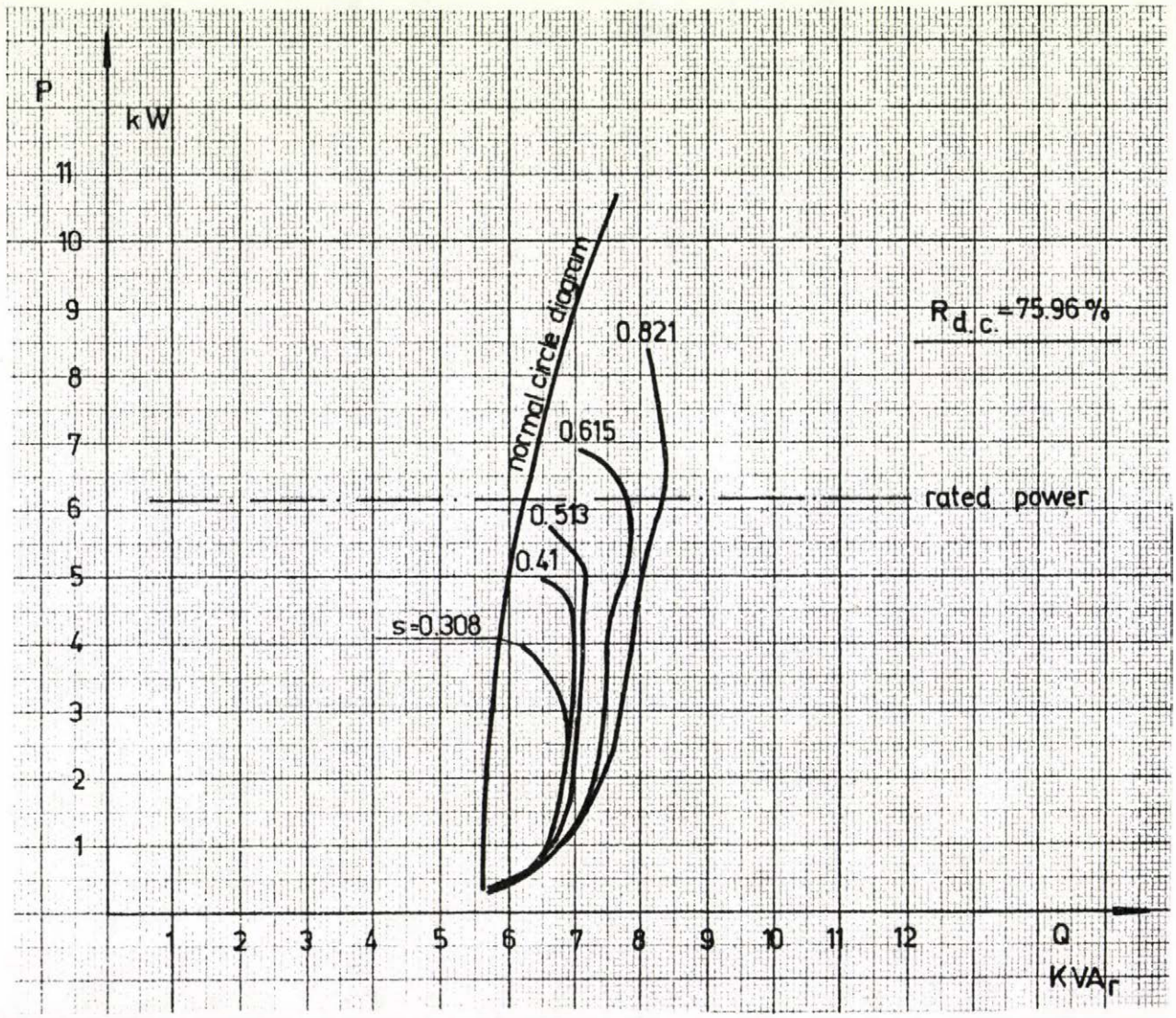

Fig.6.9

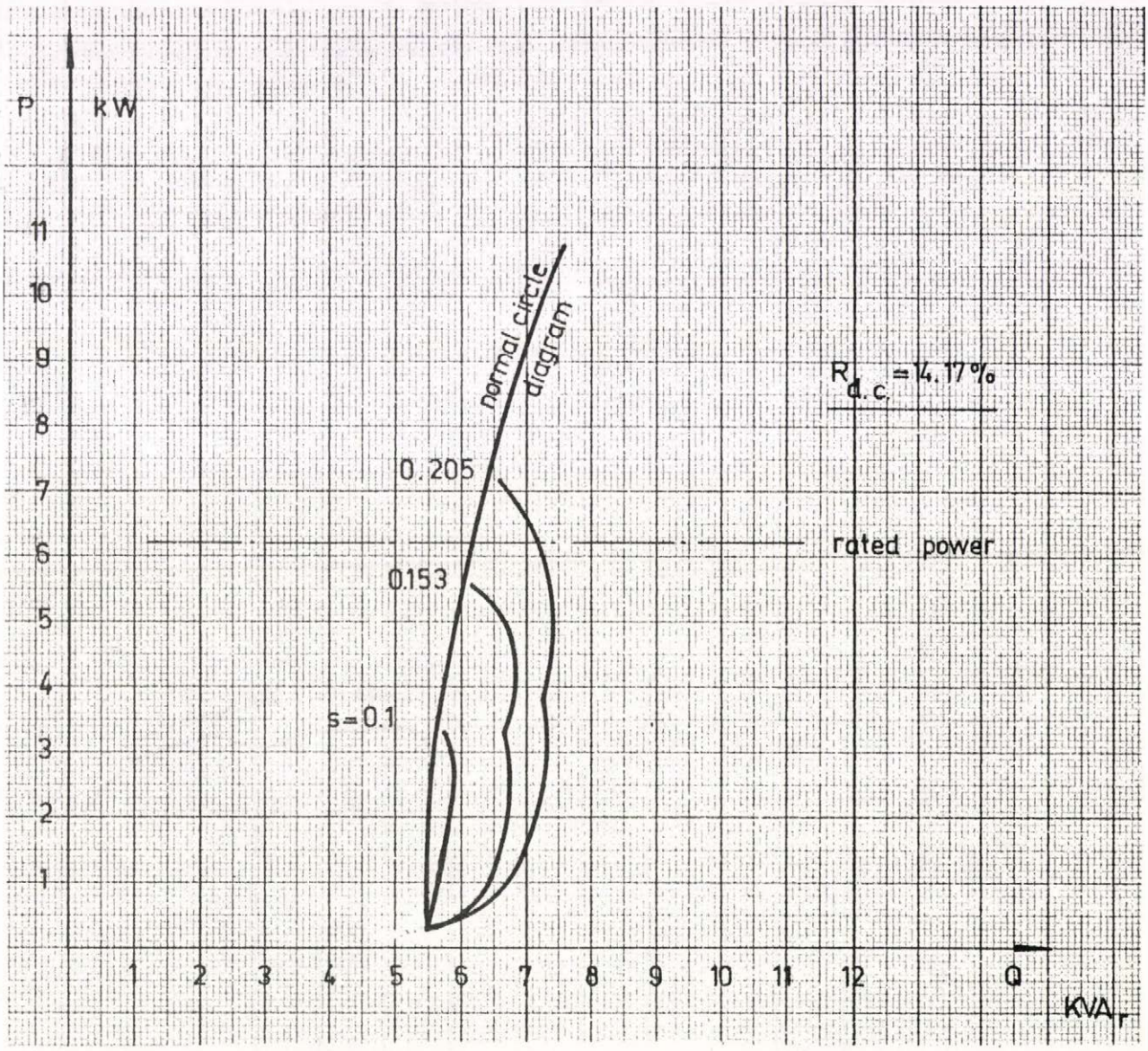

Fig.6.10

The possible working conditions are shown in Fig.6.11. The drive works in 3-2-3-2 ph when the firing angle of the thyristors is small and for further delaying, 3-3-2 ph and 2-0 ph conditions are obtained. The results are conformable with the analytical treatment of the problem. Fig.6.12 gives the relation between the d.c. reference signal U_v and the firing angle α.

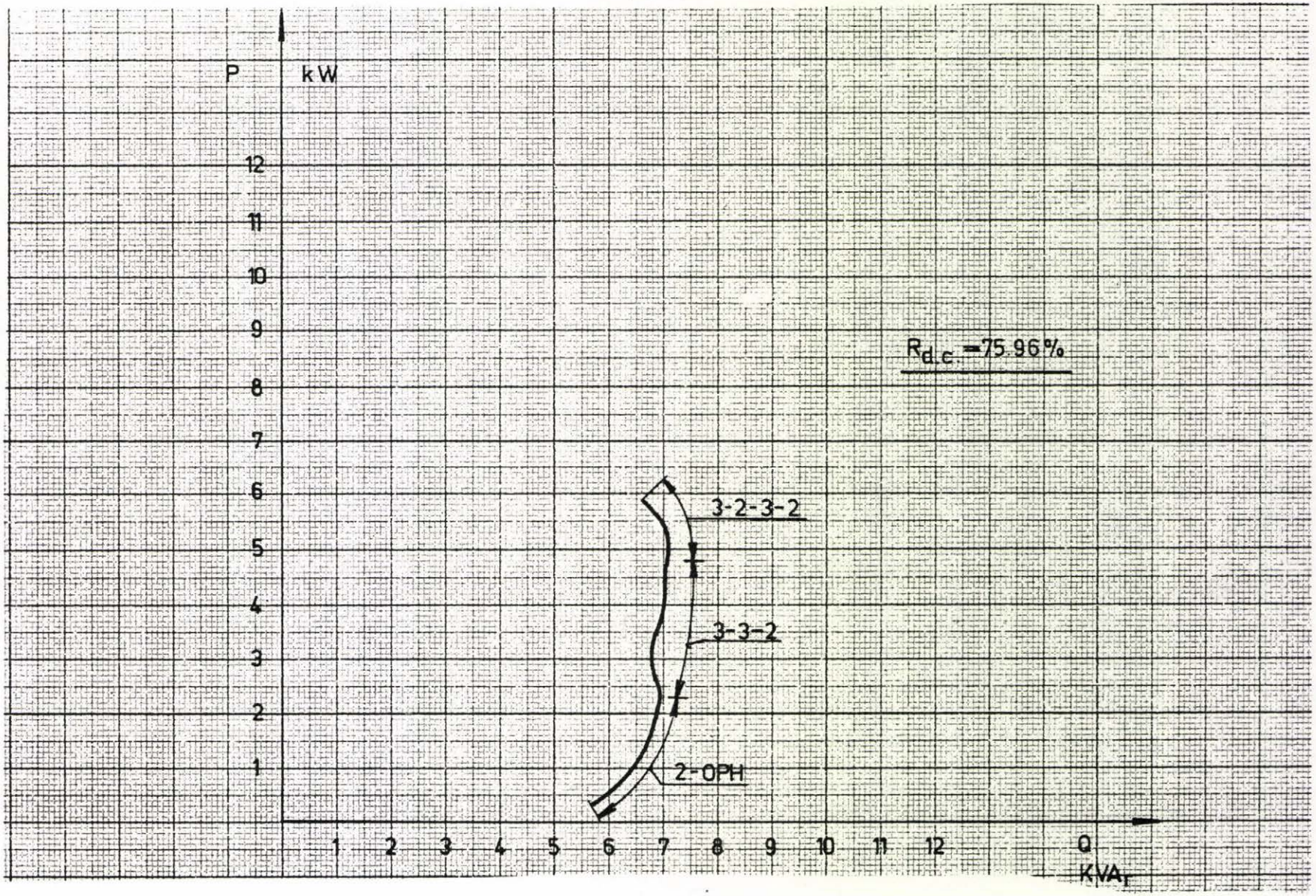
P
kW
12
11
10
9
8
7
6
5
4
3
2
1
$R_{d.c.}$ = 75.96%
3-2-3-2
3-3-2
2-0PH
1
2
3
4
5
6
7
8
9
10
11
12
Q
KVA_r

Fig.6.11

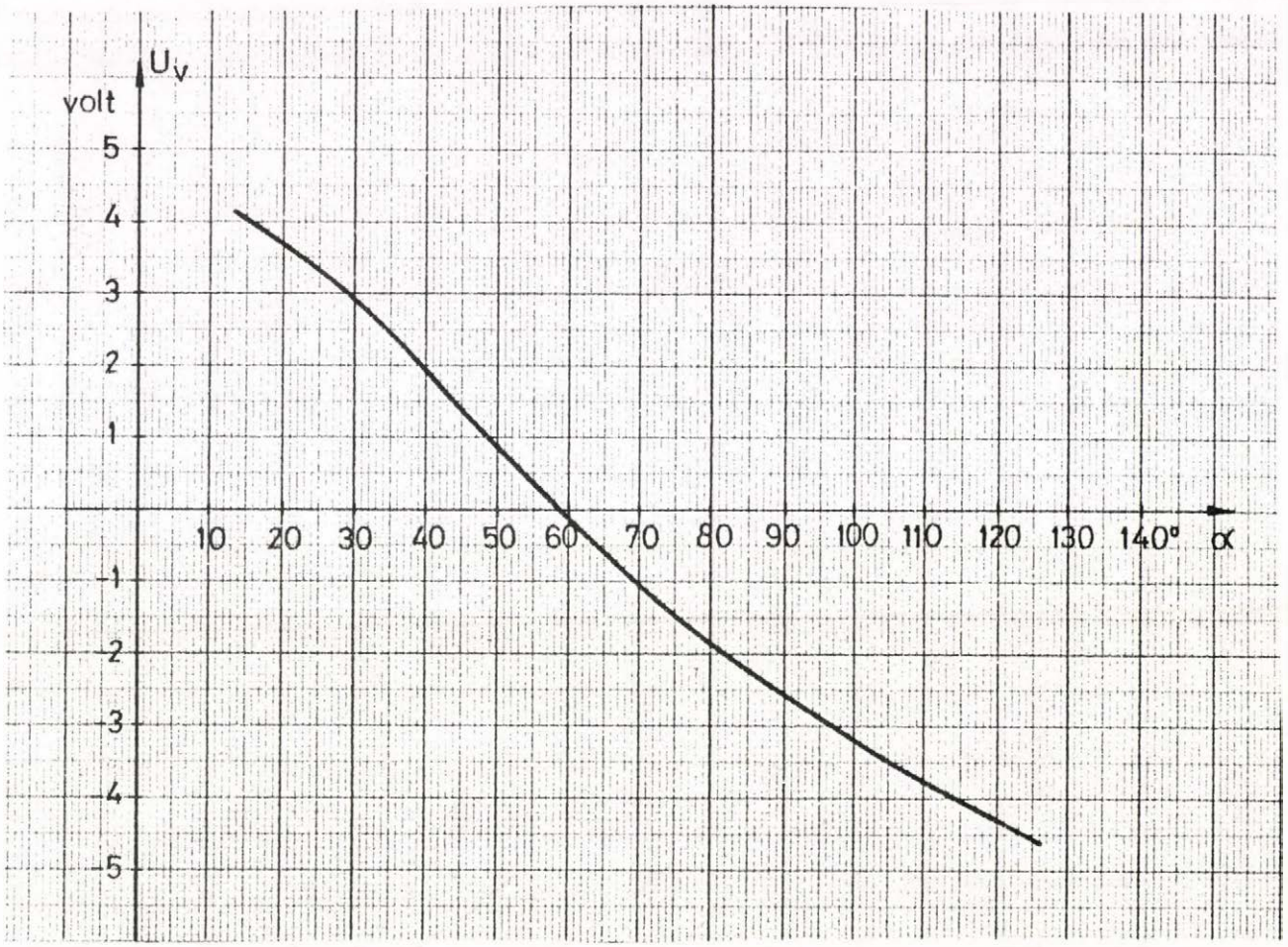

Fig.6.12

In Fig.6.13 the constant d.c. reference voltage curve shares are given. It is obvious that these curve shares represent the constant firing angle curves at different speeds. Figures 6.14 and 6.15 give the mean and the R.M.S. values of the thyristor current respectively at different speeds of the motor and for different firing angles of the thyristors. It is clear that the thyristor current decreases as the speed increases and for constant speed it decreases as the firing angle increases.

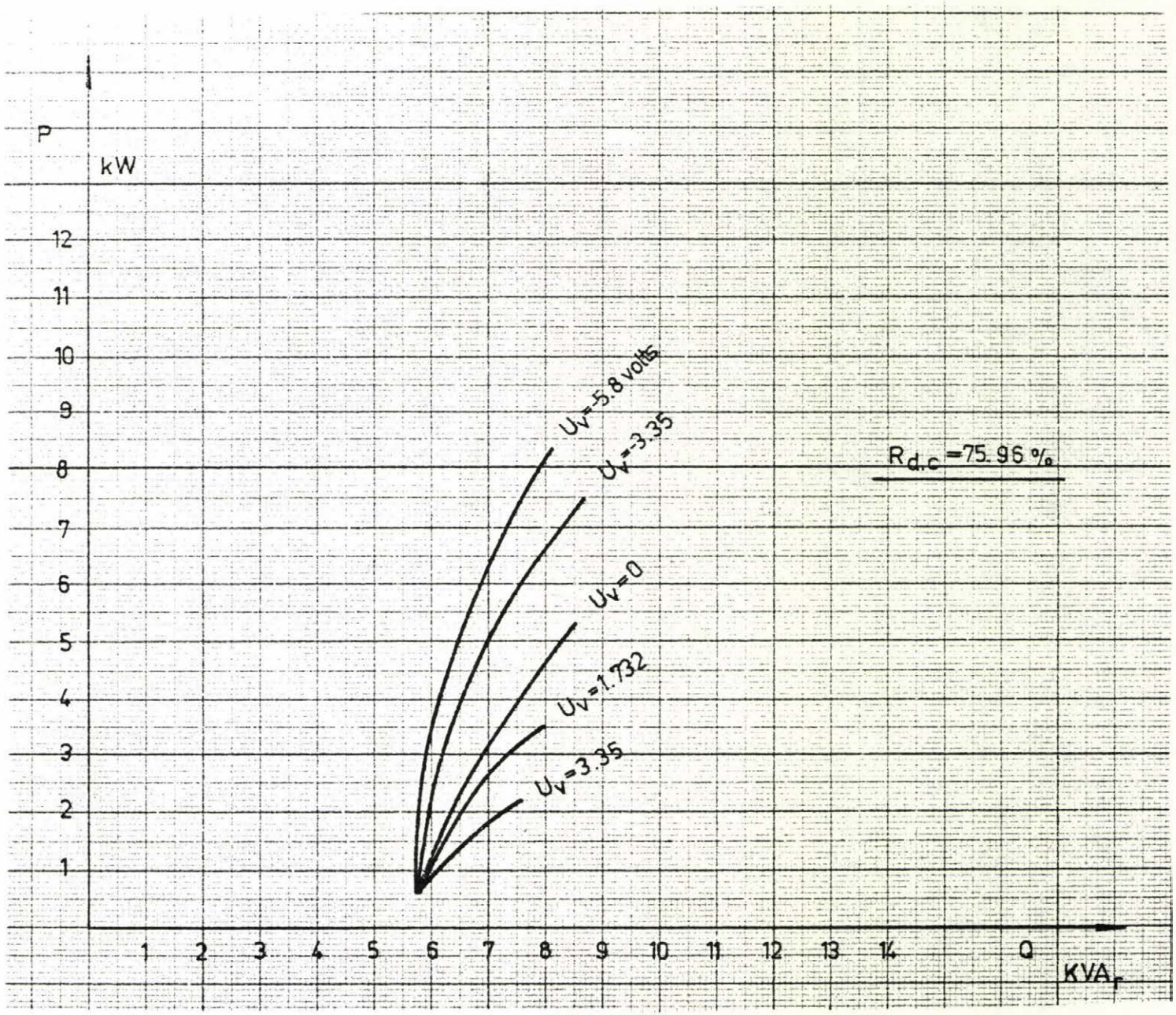
P
kW
12
11
10
9
8
7
6
5
4
3
2
1
1 2 3 4 5 6 7 8 9 10 11 12 13 14 Q
KVAr
Uv=5.8 volts
Uv=3.35
Uv=0
Uv=1.732
Uv=3.35
Rd.c=75.96 %

Fig.6.13

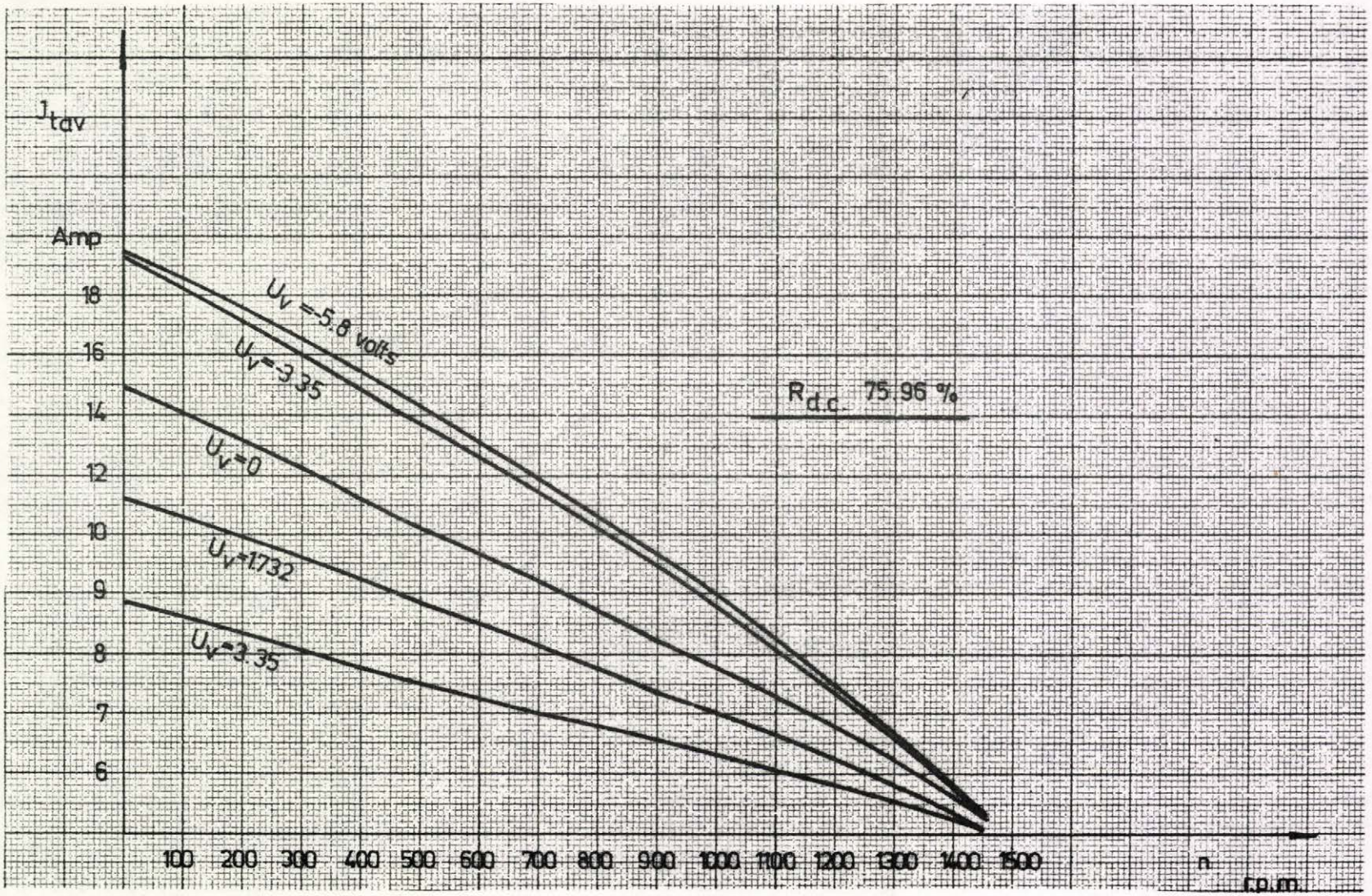
I_{tav}
Amp
18
16
14
12
10
9
8
7
6
U_v = 5.8 volts
U_v = 3.35
U_v = 0
U_v = 1.732
U_v = 3.35
$R_{d.c.}$ 75.96 %
100 200 300 400 500 600 700 800 900 1000 1100 1200 1300 1400 1500
n
r.p.m.

Fig.6.14

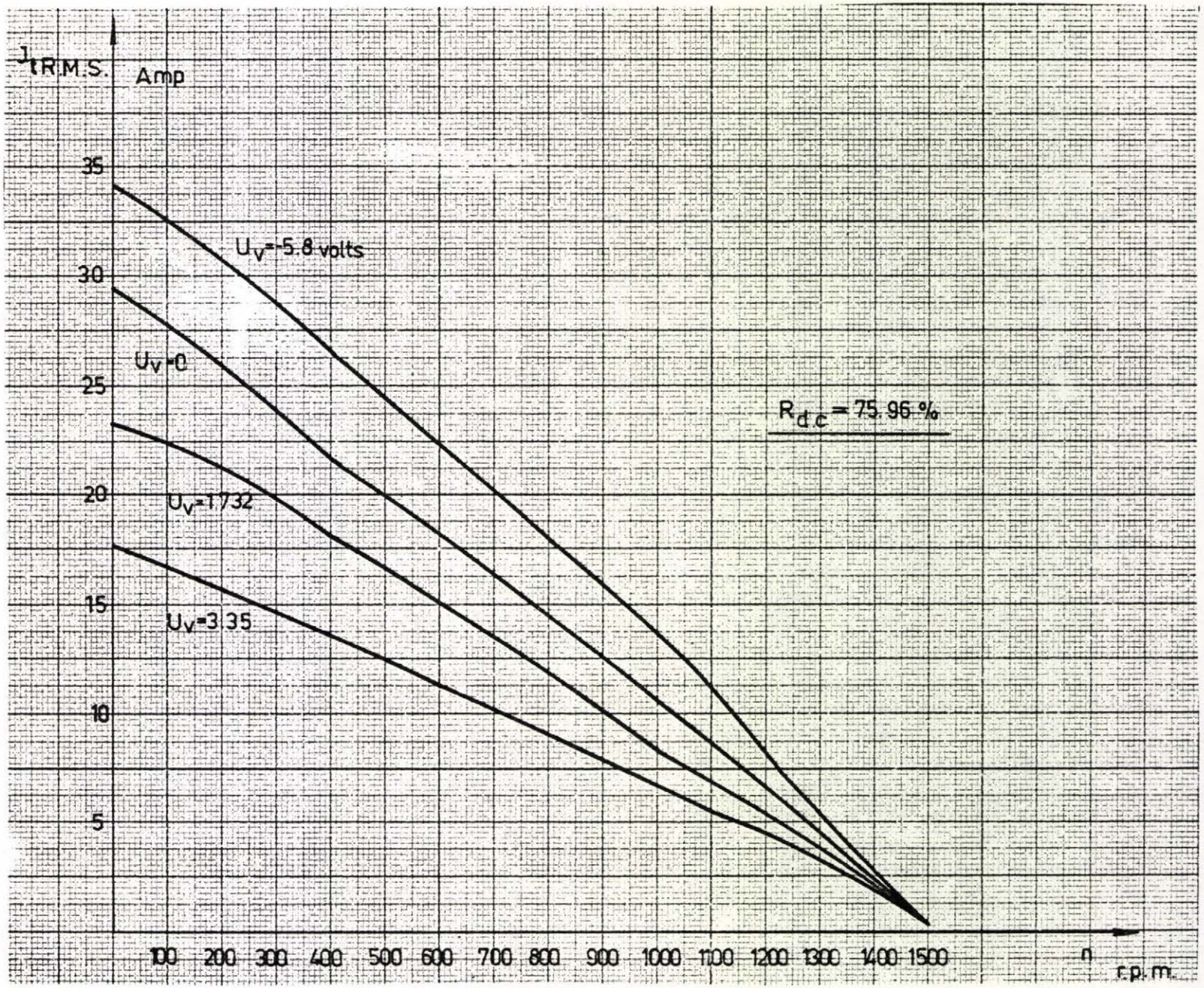
$I_{t\,R.M.S.}$ Amp
35
30
25
20
15
10
5
U_V=5.8 volts
U_V=0
U_V=1.732
U_V=3.35
$R_{d.c}$ = 75.96 %
100 200 300 400 500 600 700 800 900 1000 1100 1200 1300 1400 1500
n
r.p.m.

Fig. 6.15

The curves in Fig.6.14 and 6.15 are necessary in the determination of the thyristors ratings. The figures show that the mean value of the thyristor current at locked rotor condition and minimum firing angle is 20A. and the corresponding R.M.S. value is 35A. With the induction motor used for test measurements,the used thyristors have current rating of 50 A.

Fig.6.16 shows the slip-ring line voltage at different speeds and different firing angles. In that case the slip-ring voltage decreases as the speed increases and it decreases as the firing angle decreases. Fig. 6.17 gives the R.M.S. value of the rotor current at different speeds and firing angles. It is stated in the analytical work that with this connection the possible harmonic components are ..... -5, -2, 4, 7, ... The most predominant harmonic components are -2 and 4. Fig.6.18 gives the fundamental component of the rotor current and its -2 and $4^{\underline{th}}$. harmonic components at different speeds and different firing angles of the thyristors. In Fig. 6.19 the speed/torque curve shares at different firing angles are given for $R_{d.c.}$ = 75.96% and 14.17%. This fig. confirms the requirment of both values of $R_{d.c.}$ to cover the whole region. The fig. also gives the speed/torque characteristics if the R.M.S. value of the rotor current is constant.

Fig.6.20 gives the speed/torque characteristic when the R.M.S. value of the current through the d.c. resistance is constant. The figure shows the case when $R_{d.c.}$=75.96% was used. While fig.6.21 gives the characteristic if the mean value of the current is constant and $R_{d.c.}$=14.17% was used. It is clear from figures 6.20 and 6.21 that the shape of the curves is not regular and the irregularity happens at speed of $\frac{2}{3}$ p.u. It may be occurred due to the effect of upper harmonics. It must be noted that these irregularities in the shape of the curves have to be occurred also in the case of constant rotor current in Fig. 6.19 if the measurements are completed for speeds up to and higher than $\frac{2}{3}$.

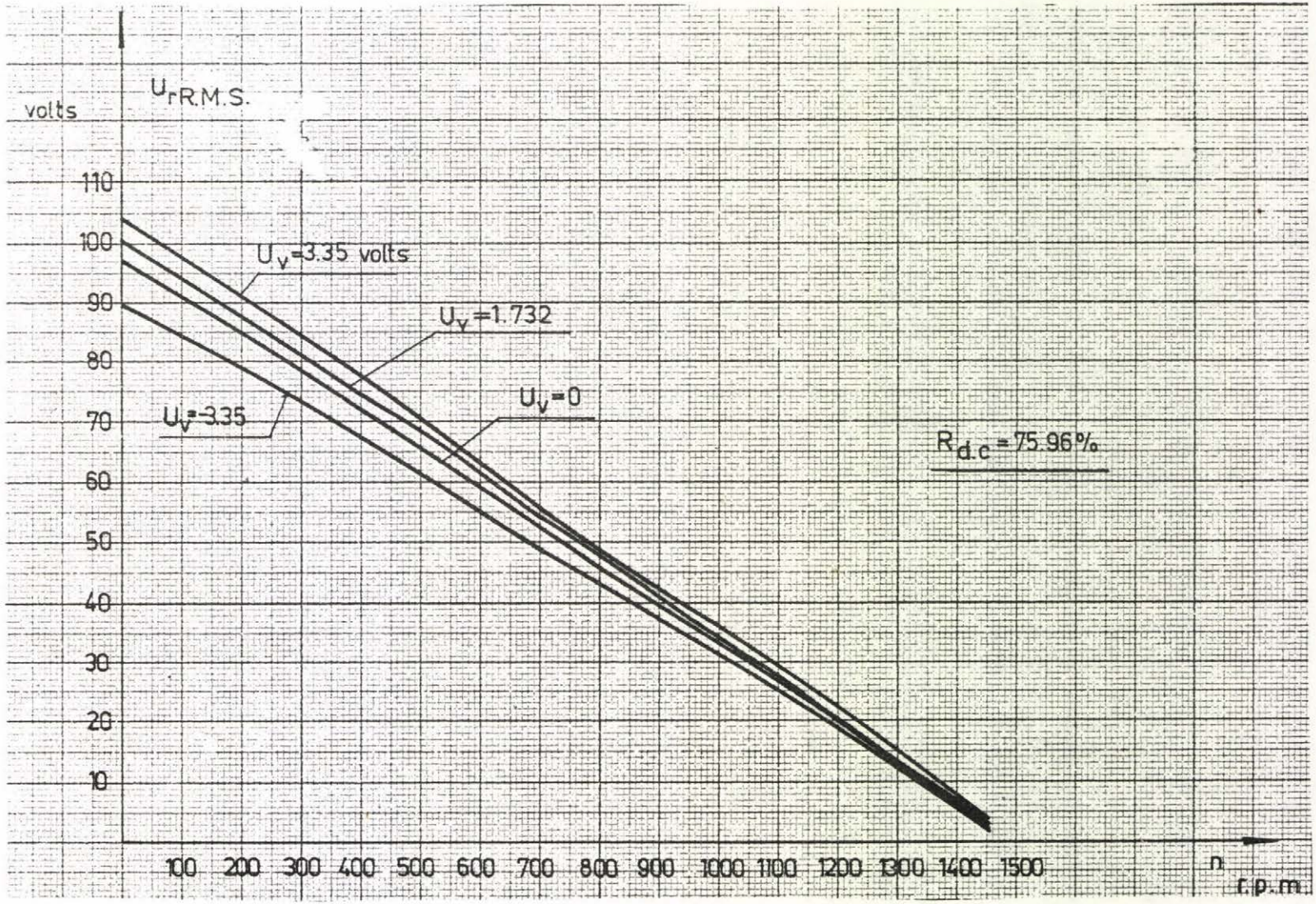
volts
U_r R.M.S.
110
100
90
80
70
60
50
40
30
20
10
U_v=3.35 volts
U_v=1.732
U_v=0
U_v=3.35
$R_{d.c}$=75.96%
100 200 300 400 500 600 700 800 900 1000 1100 1200 1300 1400 1500
n
r.p.m.

Fig.6.16

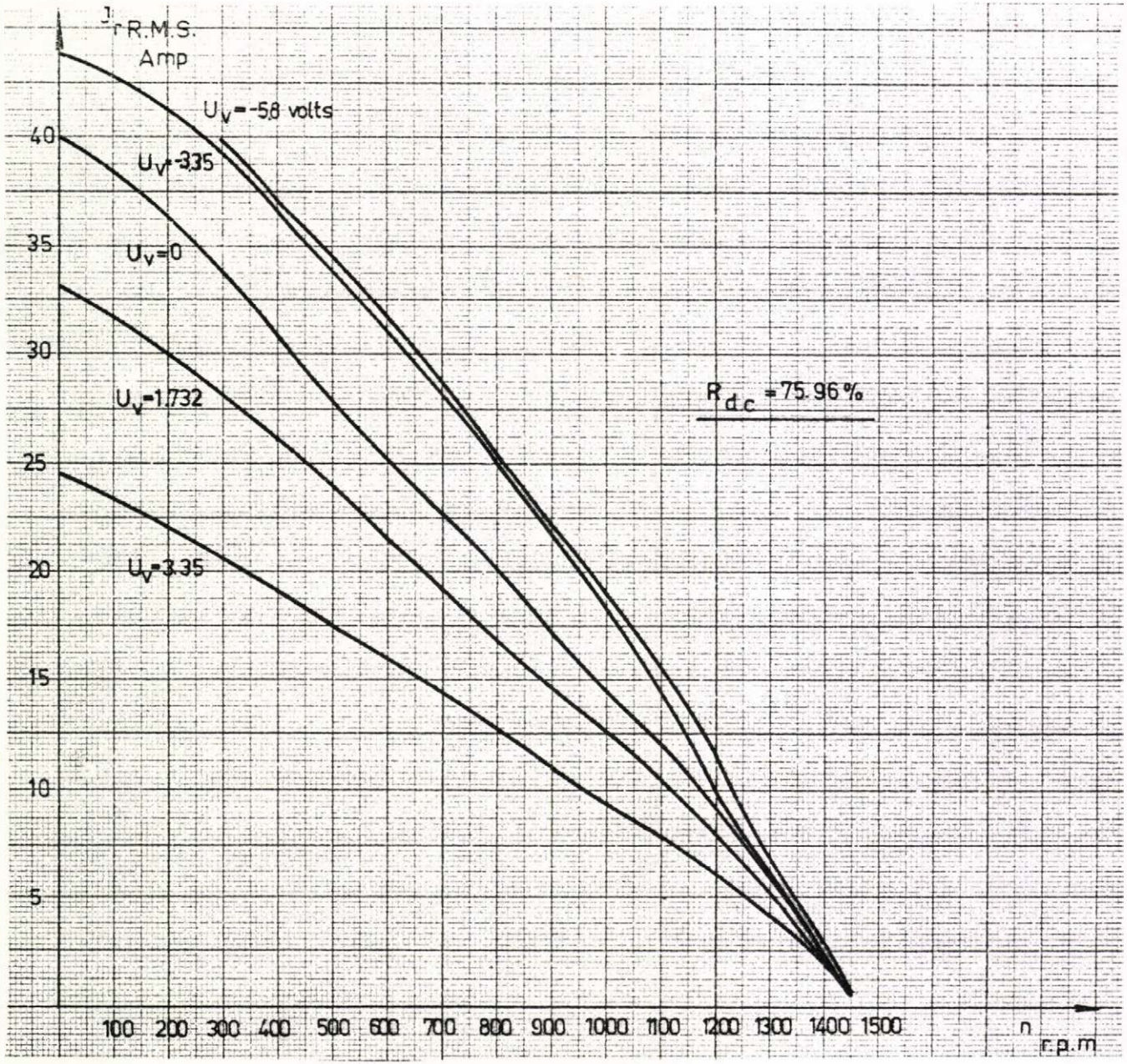
I_r R.M.S. Amp
U_V = -5.8 volts
U_V = -3.35
U_V = 0
U_V = 1.732
U_V = 3.35
$R_{d.c}$ = 75.96 %
40
35
30
25
20
15
10
5
100 200 300 400 500 600 700 800 900 1000 1100 1200 1300 1400 1500
n r.p.m

Fig.6.17

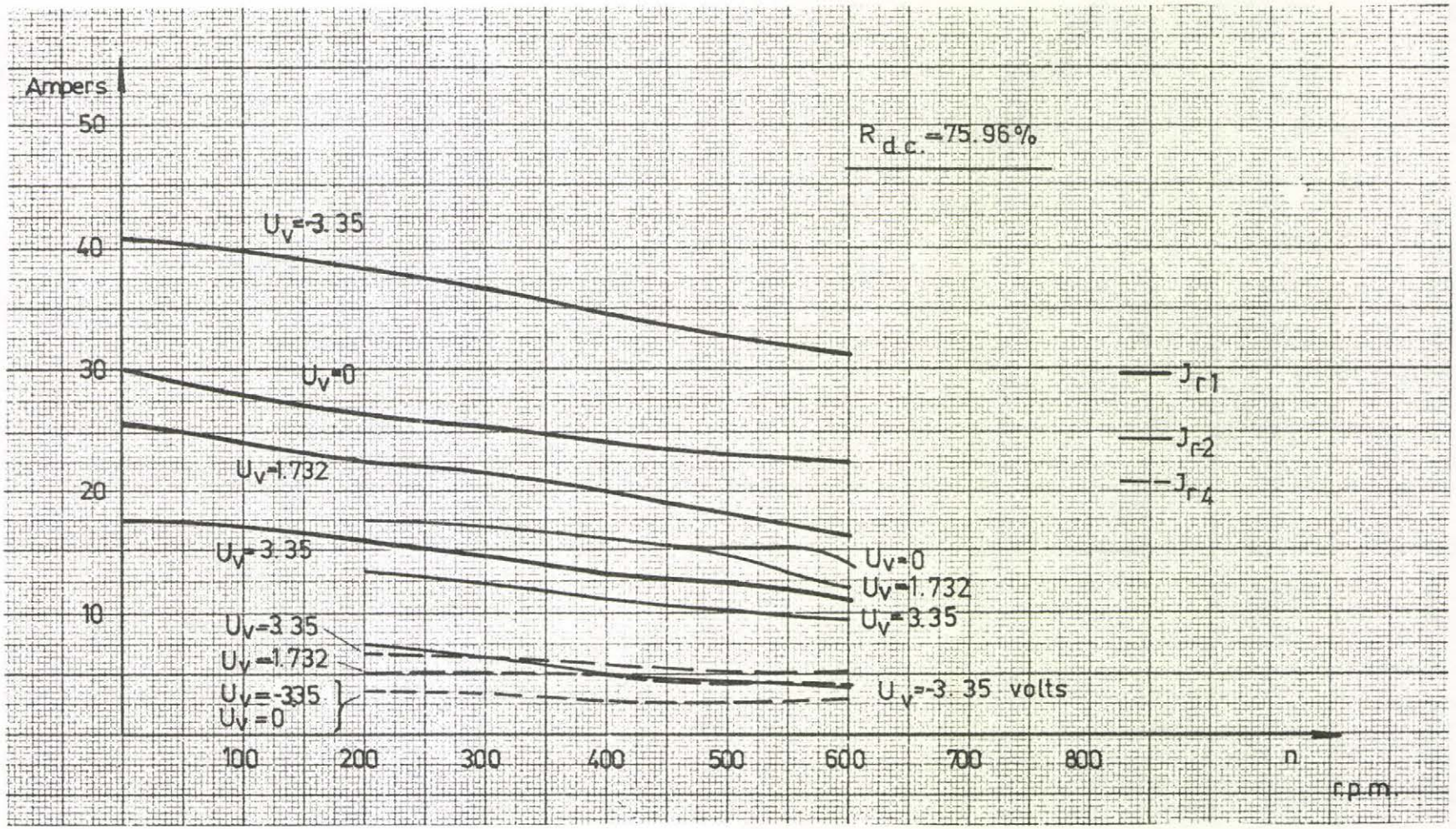
Ampers
50
40
30
20
10
$R_{d.c.}$=75.96%
U_V=-3.35
U_V=0
U_V=1.732
U_V=-3.35
U_V=-3.35
U_V=-1.732
U_V=-3.35
U_V=0
J_{r1}
J_{r2}
J_{r4}
U_V=0
U_V=1.732
U_V=3.35
U_V=-3.35 volts
100
200
300
400
500
600
700
800
n
r.p.m.

Fig.6.18

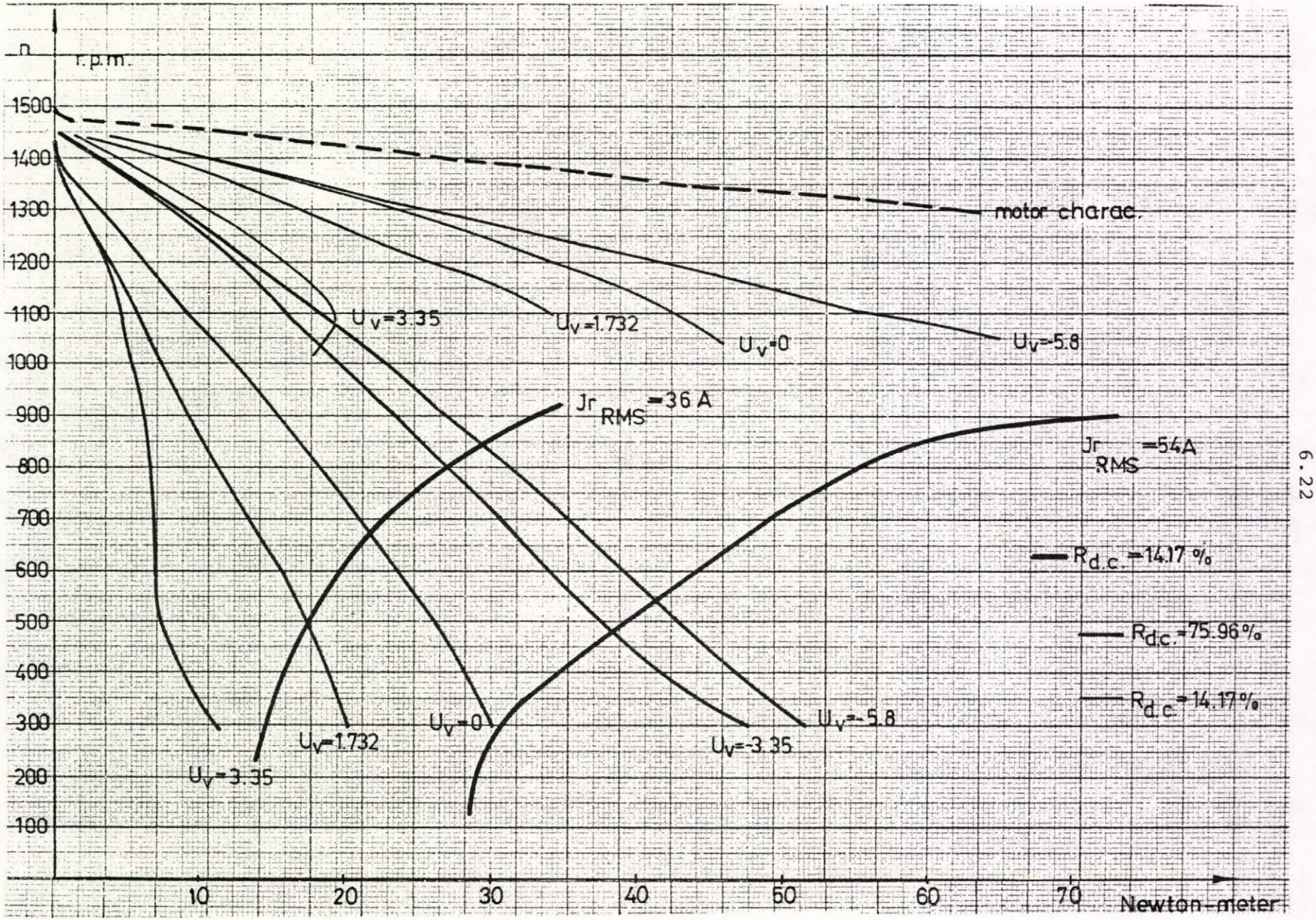
n
r.p.m.
1500
1400
1300
1200
1100
1000
900
800
700
600
500
400
300
200
100
motor charac.
U_v=3.35
U_v=1.732
U_v=0
U_v=-5.8
Jr_{RMS}=36 A
Jr_{RMS}=54A
$R_{d.c.}$=14.17 %
$R_{d.c.}$=75.96%
$R_{d.c.}$=14.17%
U_v=3.35
U_v=1.732
U_v=0
U_v=-3.35
U_v=-5.8
10
20
30
40
50
60
70
Newton-meter

Fig.6.19

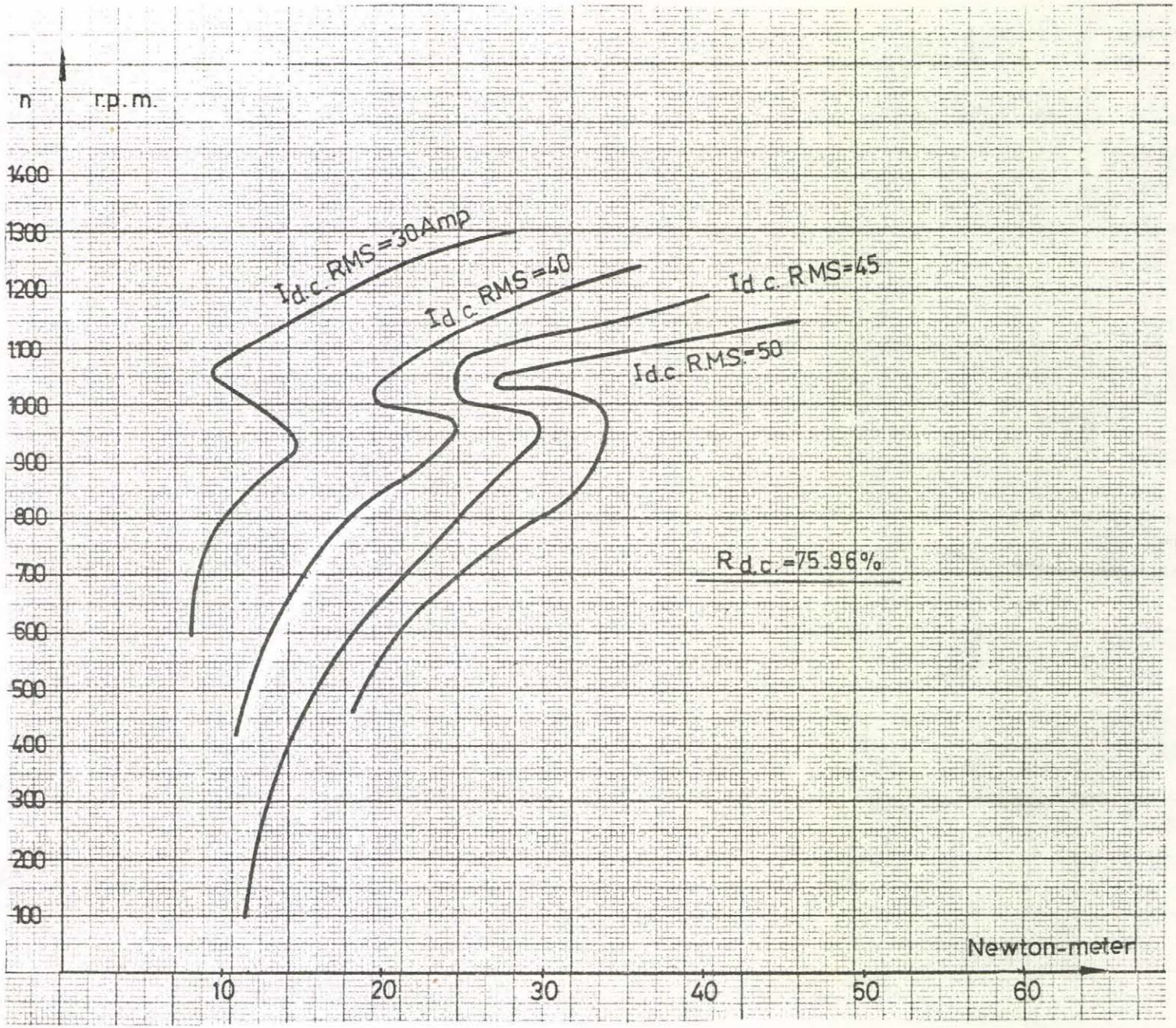
n r.p.m.
1400
1300
1200
1100
1000
900
800
700
600
500
400
300
200
100
Id.c. RMS=30Amp
Id.c. RMS=40
Id.c. RMS=45
Id.c. RMS=50
R d.c. =75.96%
Newton-meter
10
20
30
40
50
60

Fig.6.20

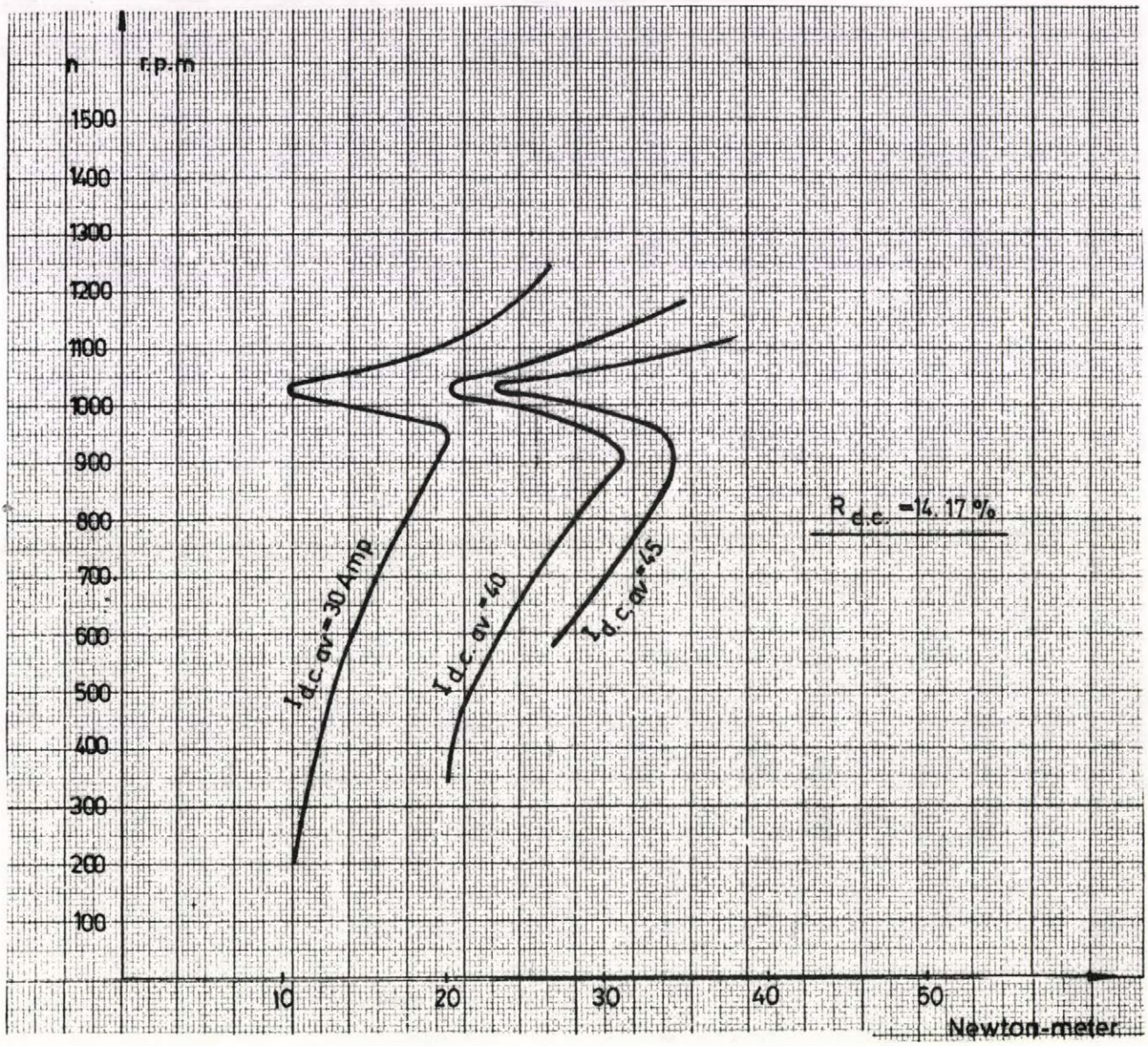
n r.p.m
1500
1400
1300
1200
1100
1000
900
800
700
600
500
400
300
200
100
10
20
30
40
50
Newton-meter
$I_{d.c.\,av}$ = 30 Amp
$I_{d.c.\,av}$ = 40
$I_{d.c.\,av}$ = 45
$R_{e.e.}$ = 14.17 %

Fig.6.21

6.4.2 Comparison Between Measured and Computed Quantities

Computed values such as R.M.S. values of the rotor current and the thyristor current, mean value of the thyristor current .... etc. were compared with the measured values at some working points. Oscillograms for the mentioned working points were made and compared with the analytical graphs.

The working points which were chosen for the comparison are:

1. $\alpha = 5^{o}$, speed=0.486 and the working condition is 3-2-3-2 ph
2. $\alpha = 55^{o}$, speed=0.386 and the working condition is 3-3-2 ph

$R_{d.c.}$=75.96% in both cases.

The comparison is given in tables 6.1 and 6.2.

	i_{r} R.M.S.	i_{rl}	i_{t} R.M.S.	i_{tav}	$i_{sR.M.S.}$	$I_{d.c.av}$	$I_{d.c._{R.M.S.}}$
Computed values	0.942	0.927	0.473	0.283	1.44	0.85	0.851
Measured values	0.868	0.838	0.434	0.254	1.405	0.761	0.841

Table 6.1 $\alpha=5^{o}$, speed 0.486

	i_{r} R.M.S.	i_{rl}	i_{t} R.M.S.	i_{tav}	$i_{sR.M.S.}$	$I_{d.c.av}$	$I_{d.c.R.M.S.}$
Computed values	0.932	0.833	0.477	0.267	1.5	0.801	0.827
Measured values	0.876	0.822	0.455	0.250	1.45	0.749	0.804

Table 6.2 $\alpha=55^{o}$, speed 0.386

Tables 6.1 and 6.2 give the comparison between the computed and measured values of the R.M.S. values of the rotor current, the fundamental component of the rotor current and the thyristor current; the mean value of the thyristor current; the R.M.S. value of the stator current and the mean and the R.M.S. values of the current through the d.c. resistance.

The tables show that the computed and experimentally obtained values are very close to each other. The differences between the measured and the computed values may happen due to the inaccuracy of the measuring instruments at low frequencies.

Fig.6.22 shows the pulses and the slip-ring voltage of the auxiliary machine from which the firing angle can be measured. The fig. represents the case of $\alpha=5^{o}$ and speed of .486 /3-2-3-2 ph/. The computed and the recorded Park-vector path of the rotor current are shown in Fig.6.23 and 6.24 respectively. Similarly the Park-vector pathes of the rotor flux and voltage, computed and recorded quantities, are given in Fig.6.25 and 6.26 and 6.27-6.28 respectively. The computed and the measured values of the phase current, flux and voltage wave forms of the rotor are shown in Fig. 6.29-6.30, 6.31-6.32 and 6.33-6.34 respectively. The computed wave form of the current through the d.c. resistance is shown in Fig. 6.35 while fig.6.36 shows the corresponding measured value. In figures 6.37 and 6.38 the computed and measured wave forms of the electro-magnetic torque are given. The thyristor current and voltage wave forms, computed and measured values are shown in Fig.6.39-6.40 and 6.41-6.42 respectively.

The oscillograms confirm that the computed quantities are favourably conformable with the measured one.

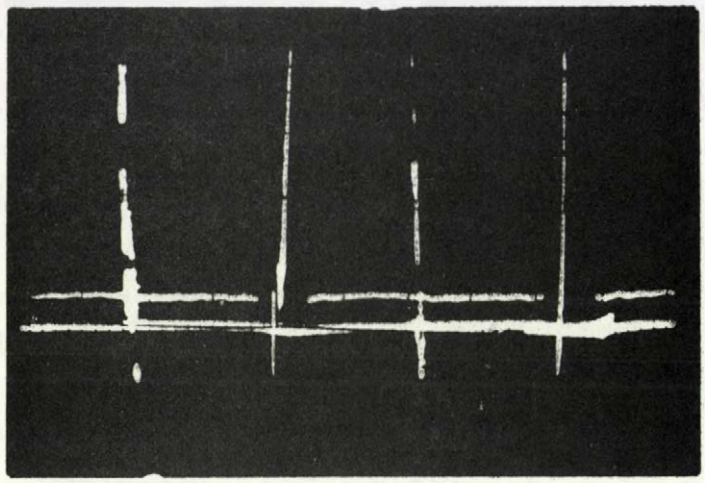

Fig.6.22

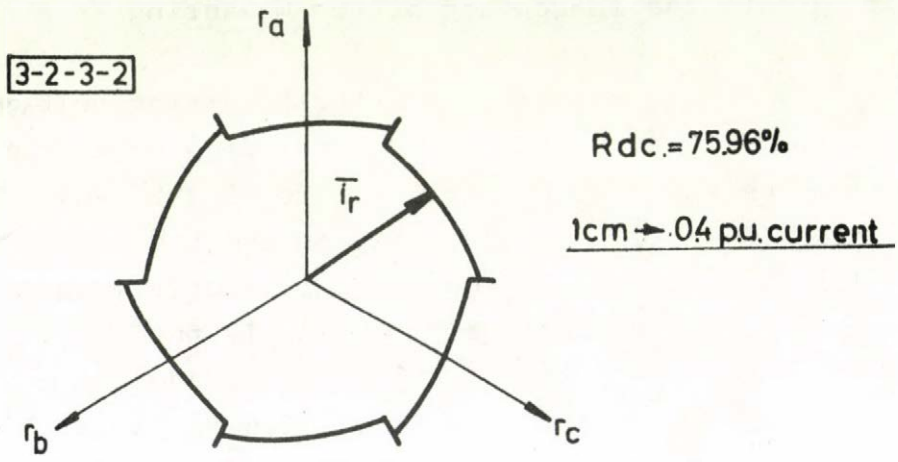

Fig.6.23

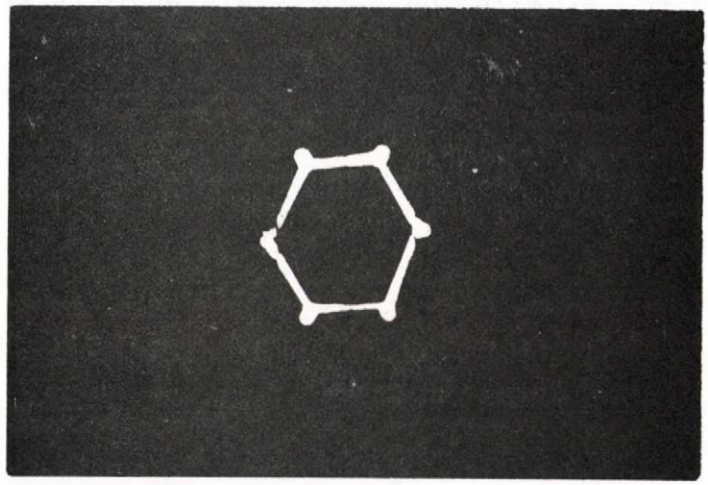

Fig.6.24

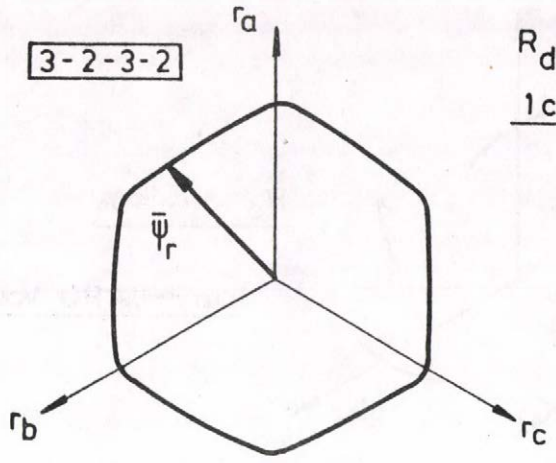

Fig.6.25

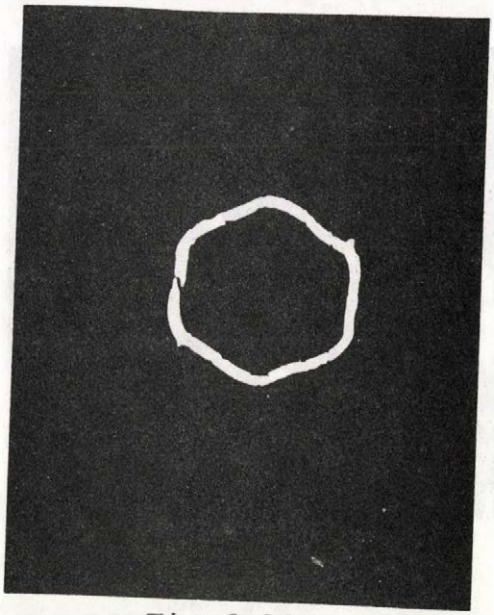

Fig.6.26

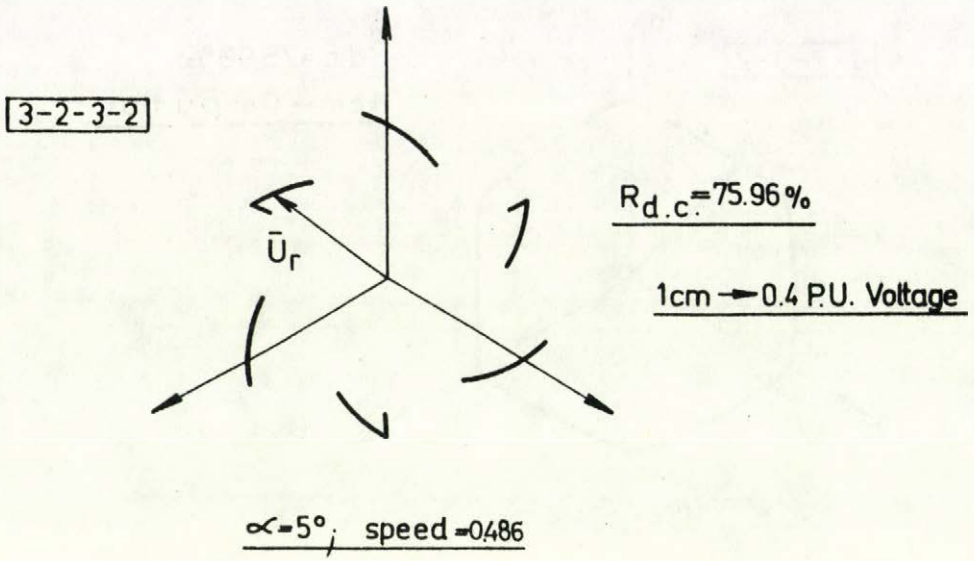

Fig.6.27

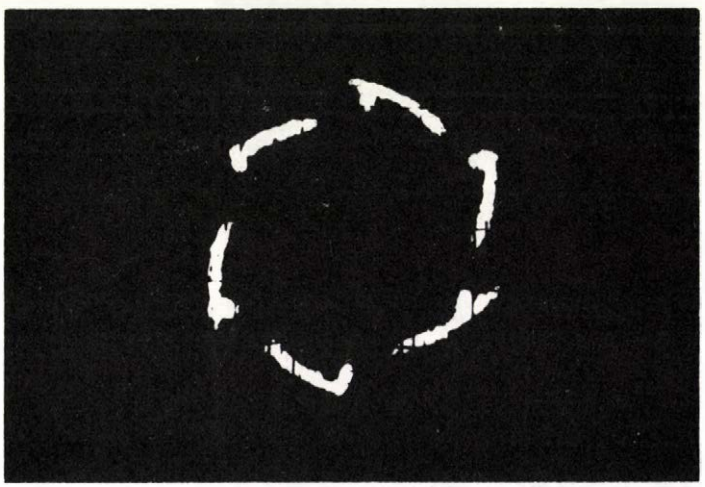

Fig.6.28

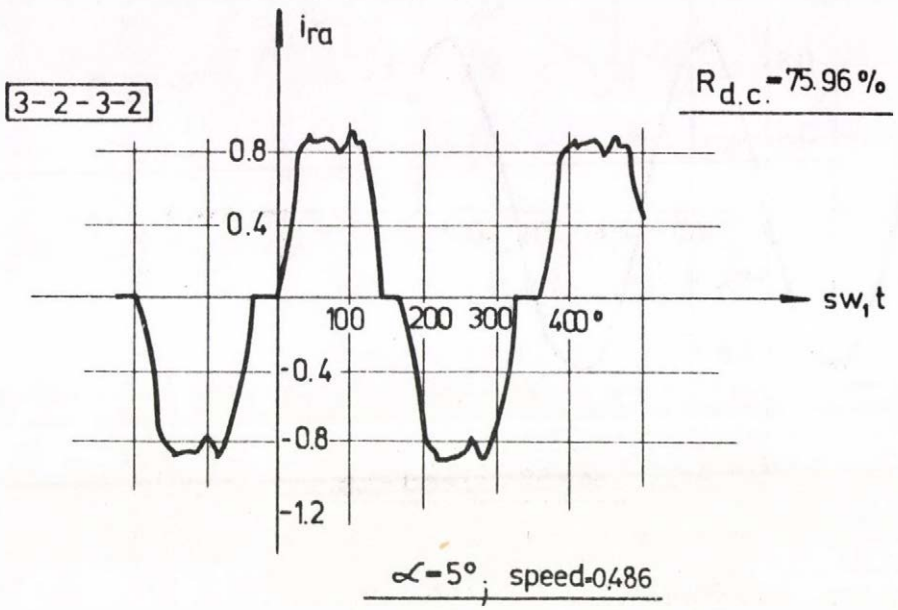

Fig.6.29

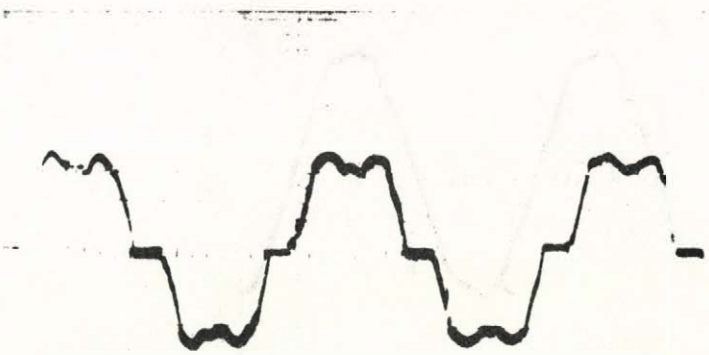

Fig.6.30

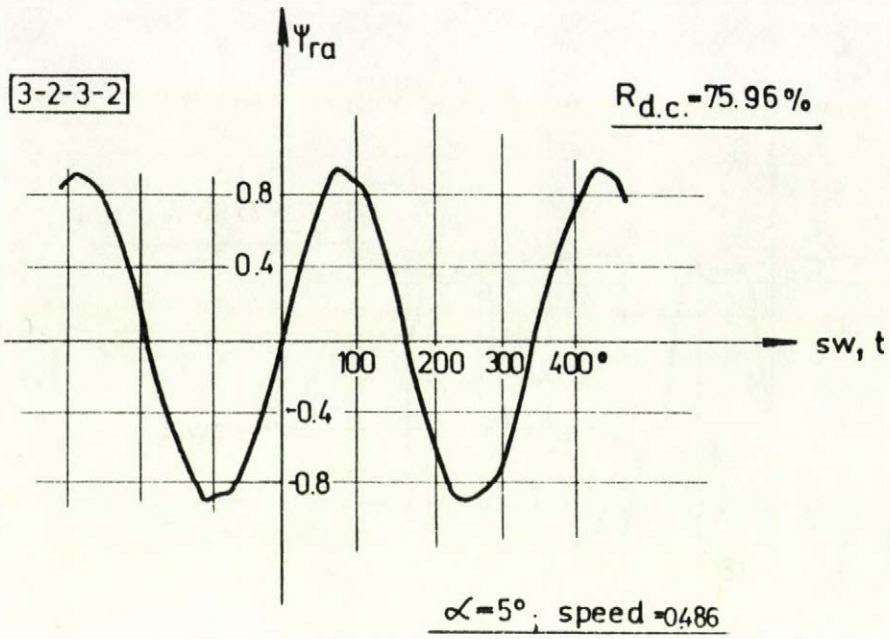

Fig.6.31

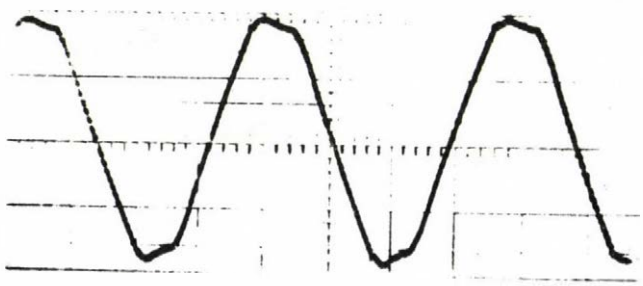

Fig.6.32

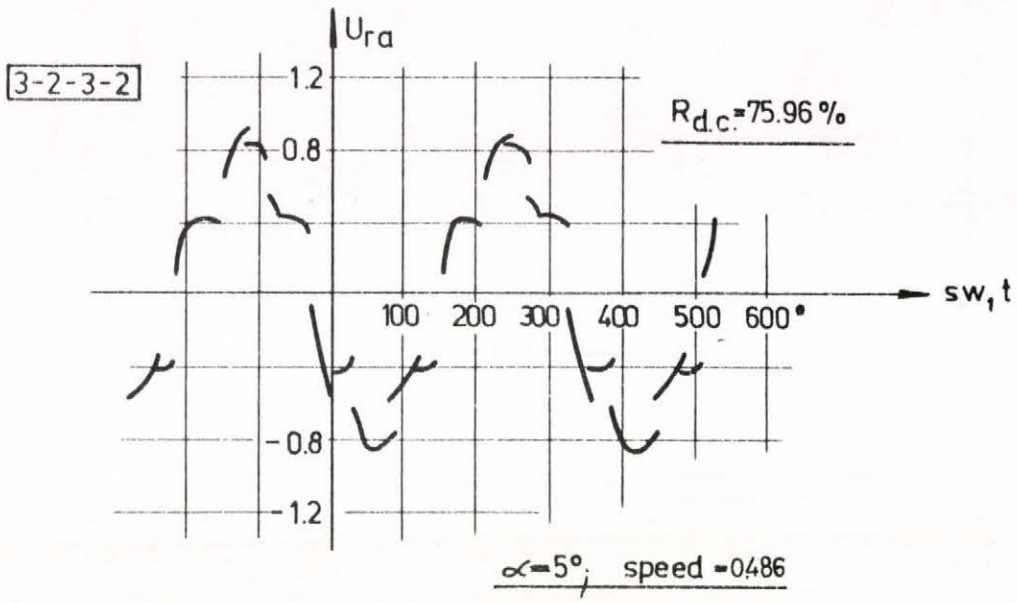

Fig.6.33

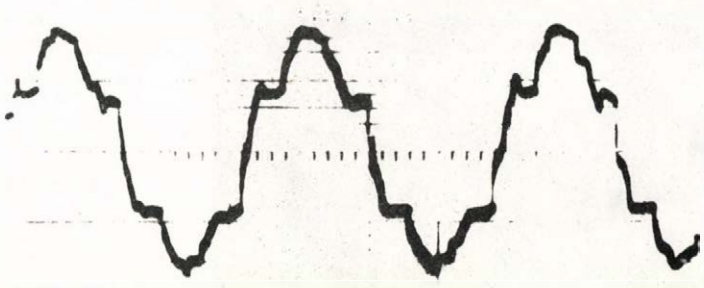

Fig.6.34

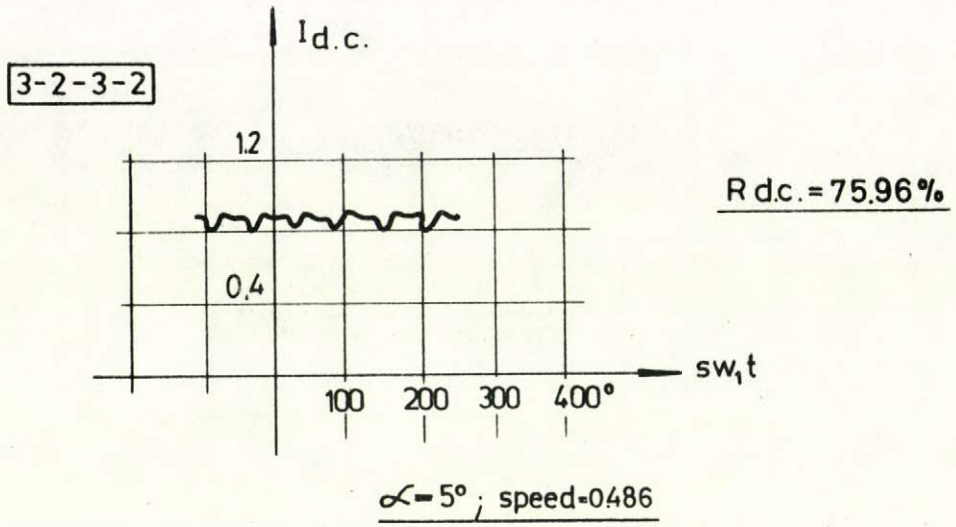

Fig.6.35

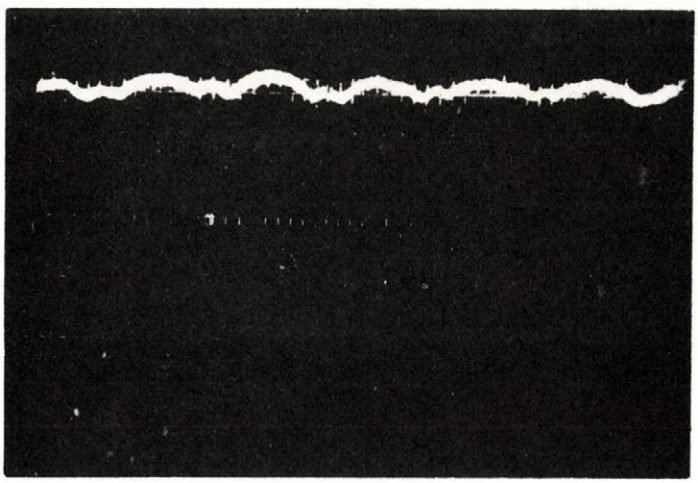

Fig.6.36

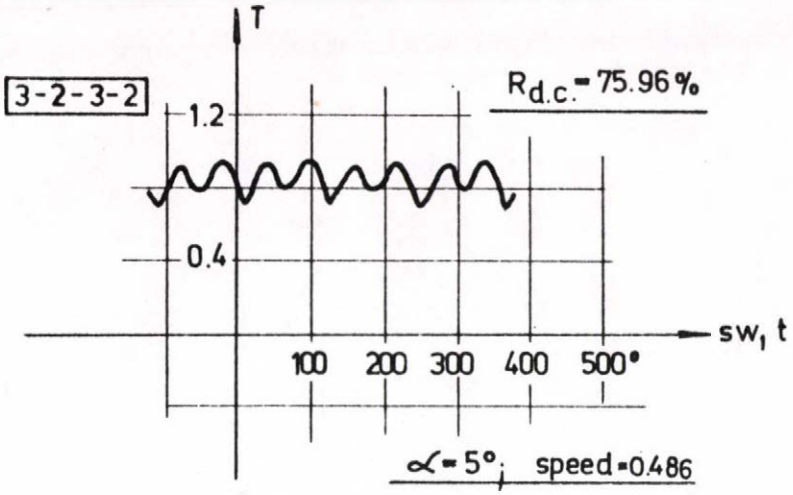

Fig.6.37

Fig.6.38

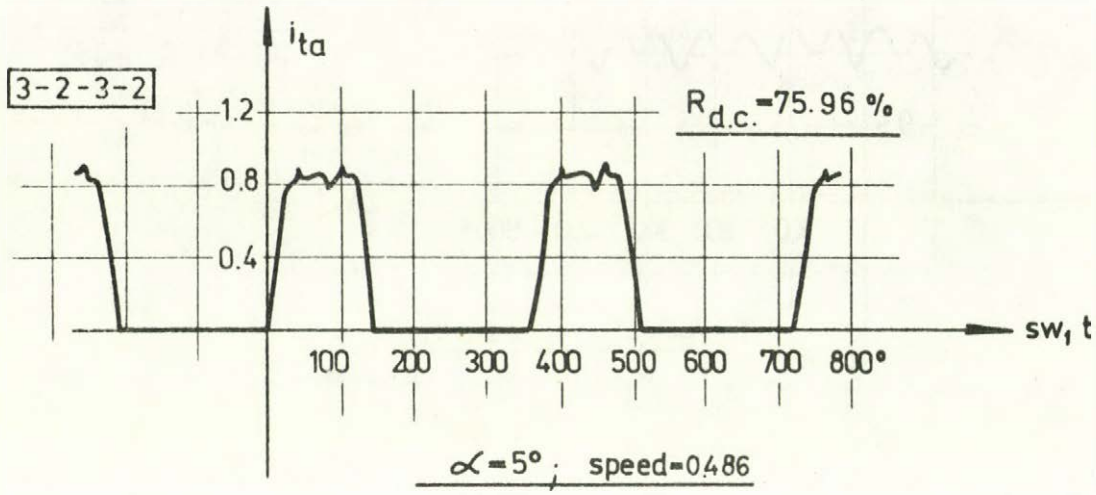

Fig.6.39

Fig.6.40

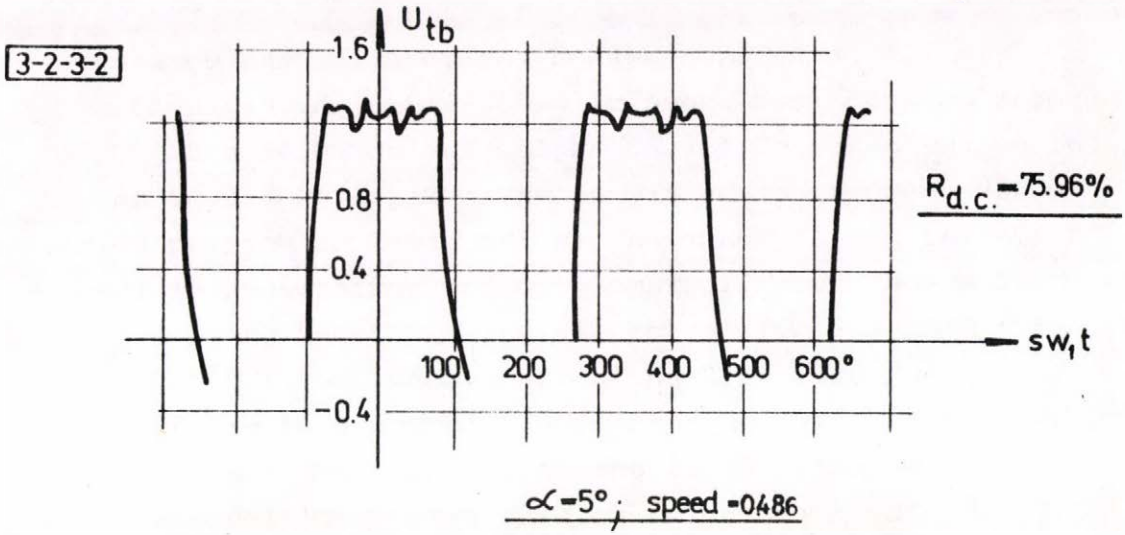

Fig.6.41

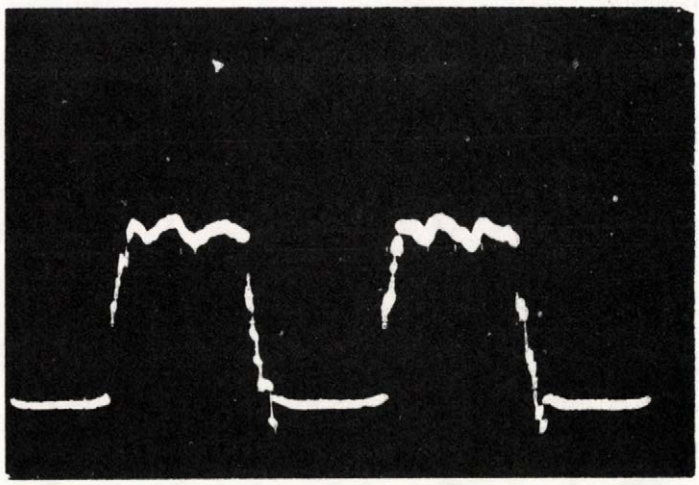

Fig.6.42

Similar comparison method was made for the working point of $\alpha=55^{o}$ and speed of 0.386 3-3-2 ph. Fig.6.43 gives the measured firing angle. The computed and measured oscillograms are shown in Fig.6.44 - 6.63 in a similar way as described in the previous working point.

The above oscillograms give the performance of the drive when the working condition is 3-2-3-2 ph in the first point and 3-3-2 ph in the second one. The drive also works in 2-0 ph condition. Figures 6.64 - 6.74 give the measured oscillograms for the same quantities like the above operating points. These oscillograms correspond to the working point $\alpha=105^{o}$ and speed of 0.179 /2-0 ph/.

It has been shown from the above results that the computed and measured quantities are favourably compliant to each other.

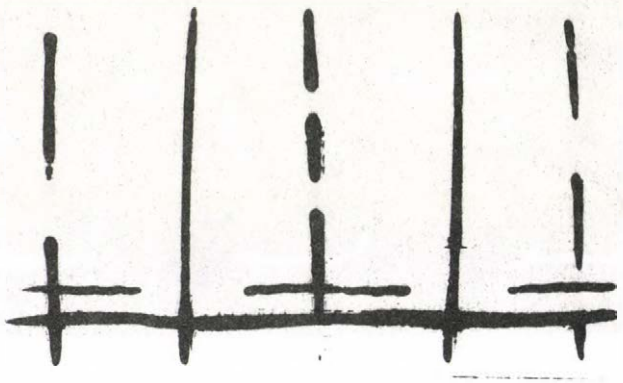

Fig.6.43

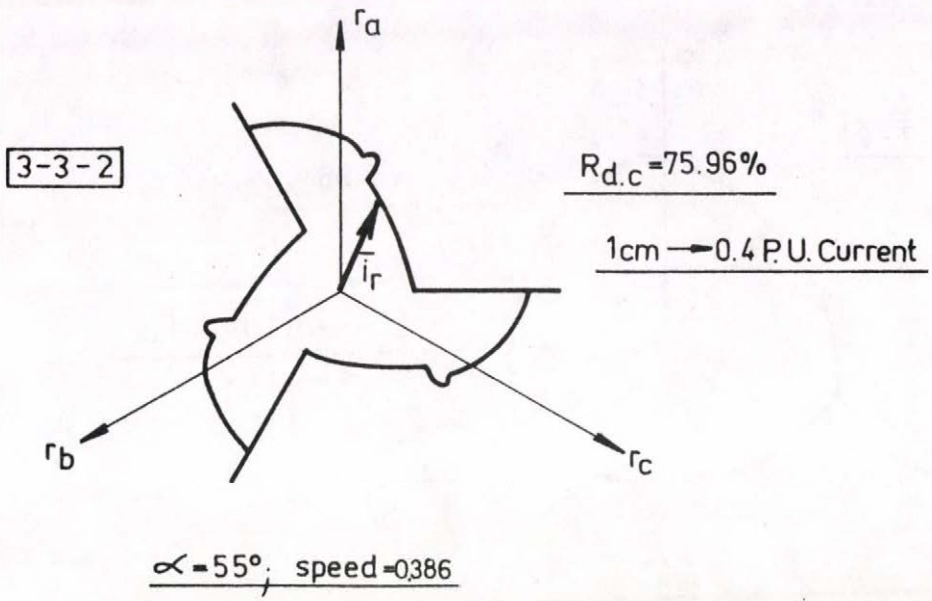

Fig.6.44

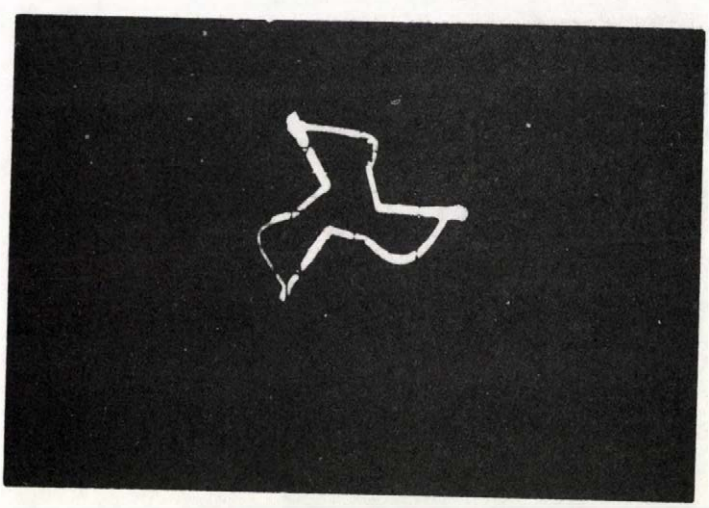

Fig.6.45

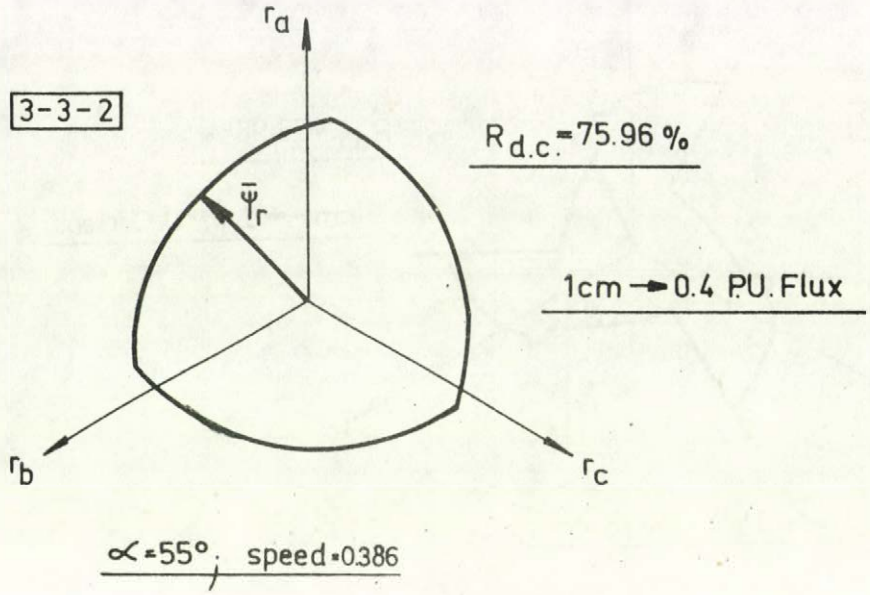

Fig.6.46

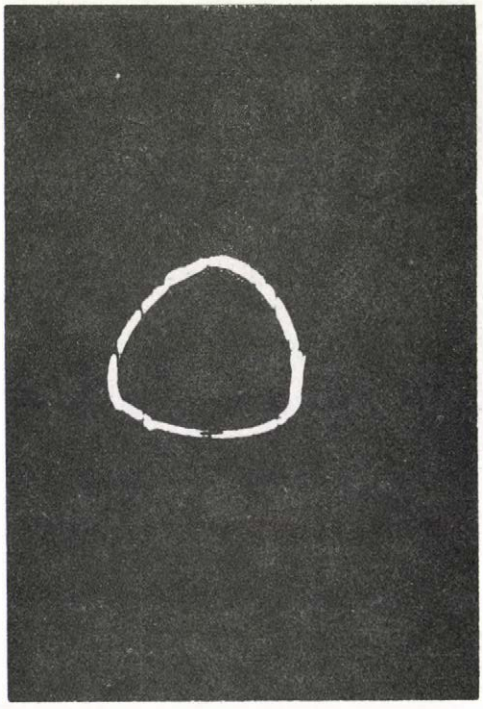

Fig.6.47

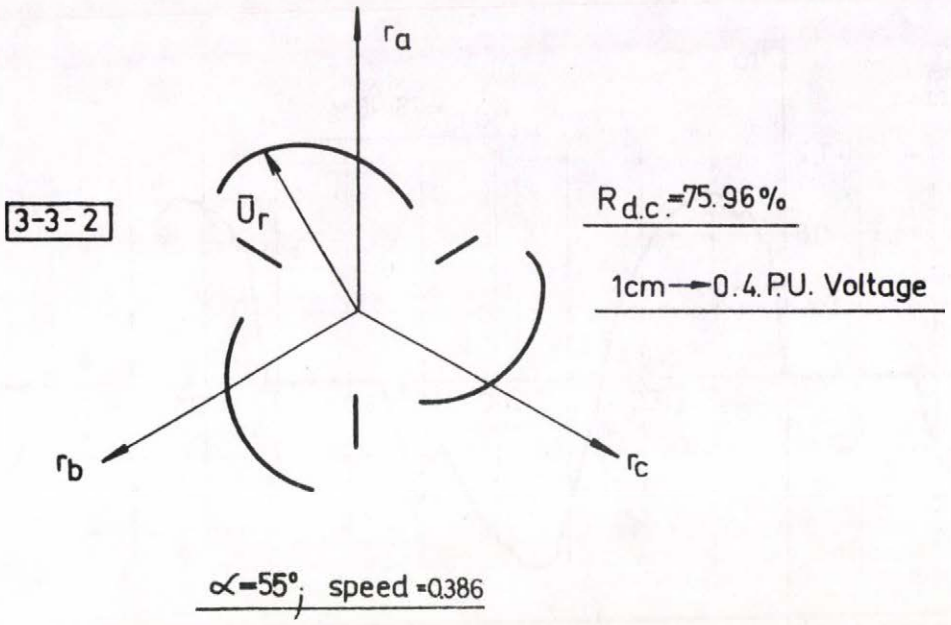

Fig.6.48

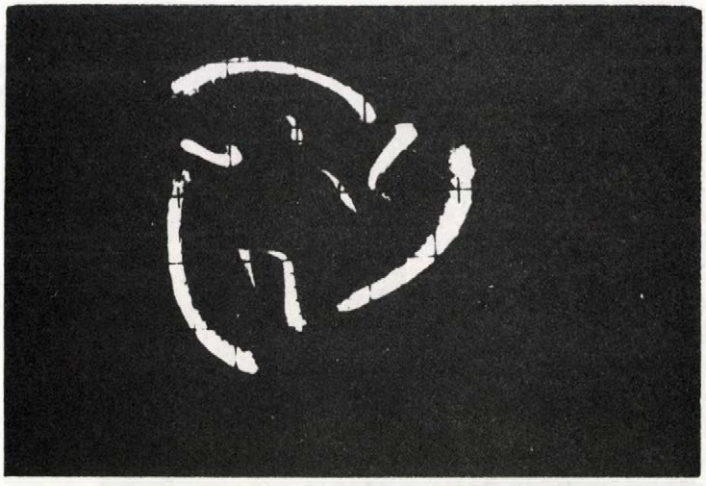

Fig.6.49

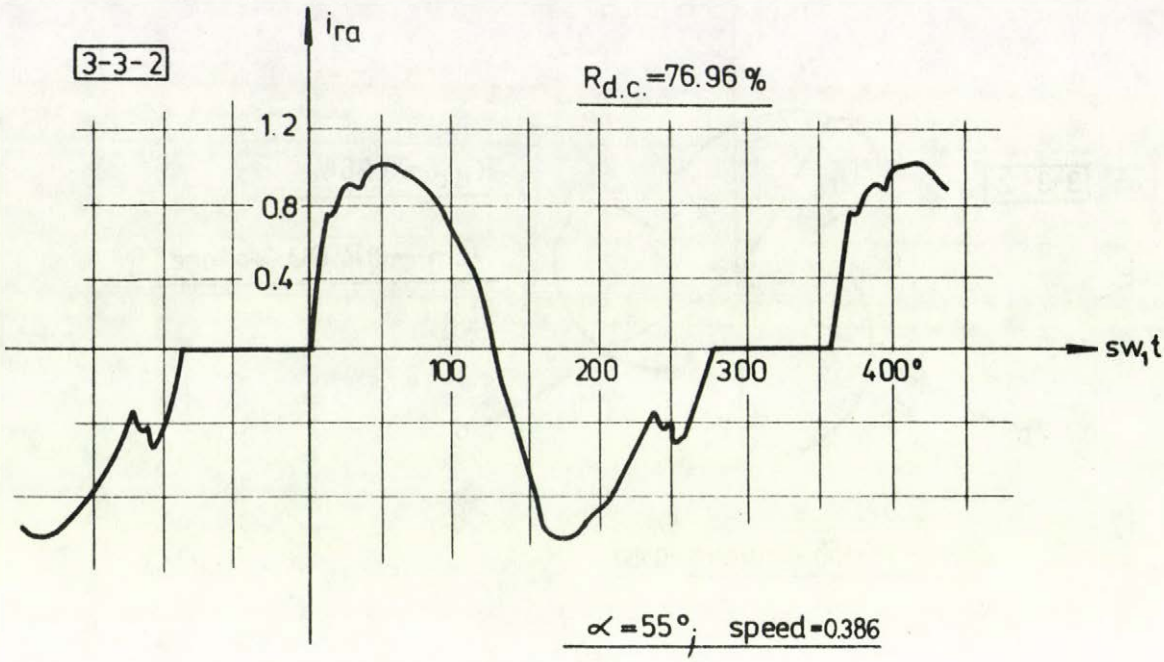

Fig.6.50

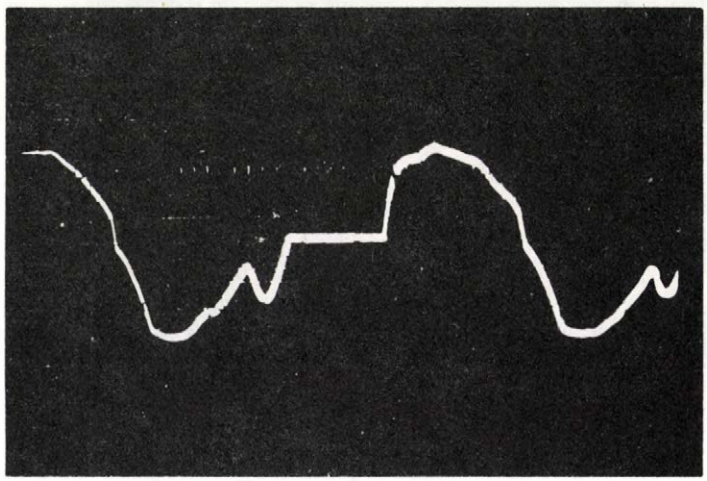

Fig.6.51

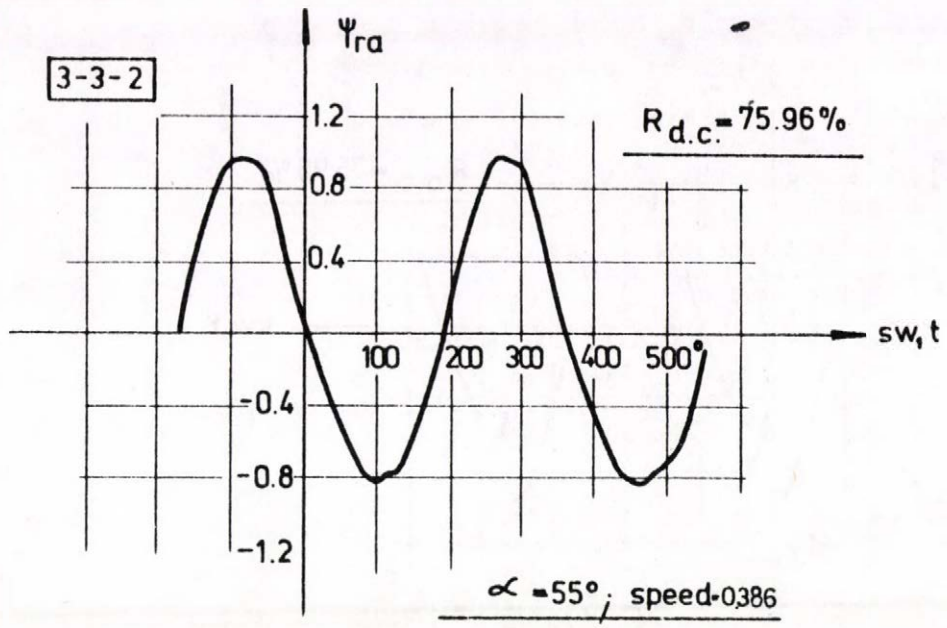

Fig.6.52

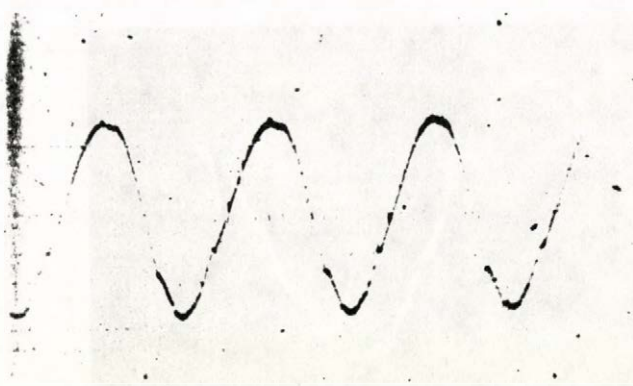

Fig.6.53

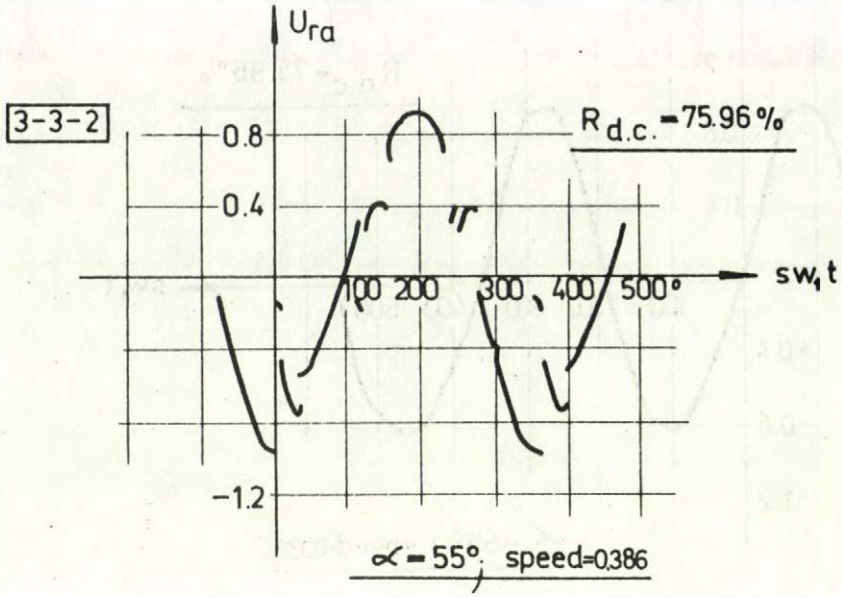

Fig.6.54

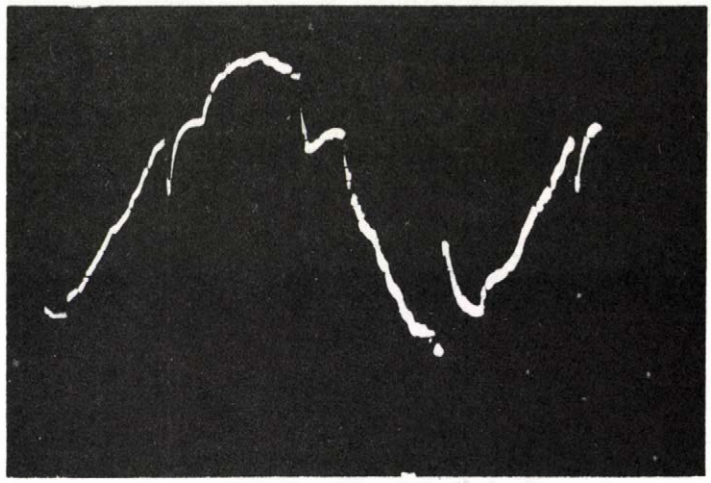

Fig.6.55

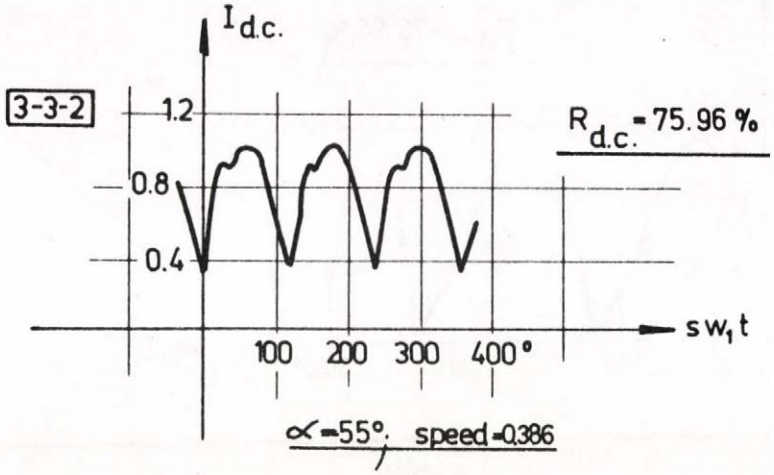

Fig.6.56

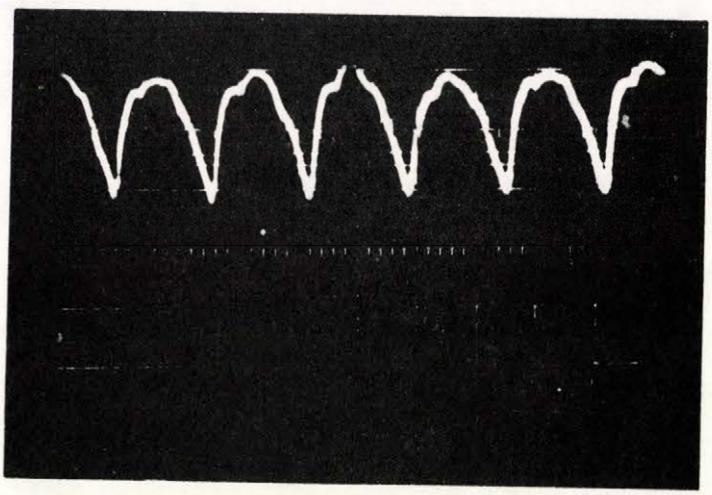

Fig.6.57

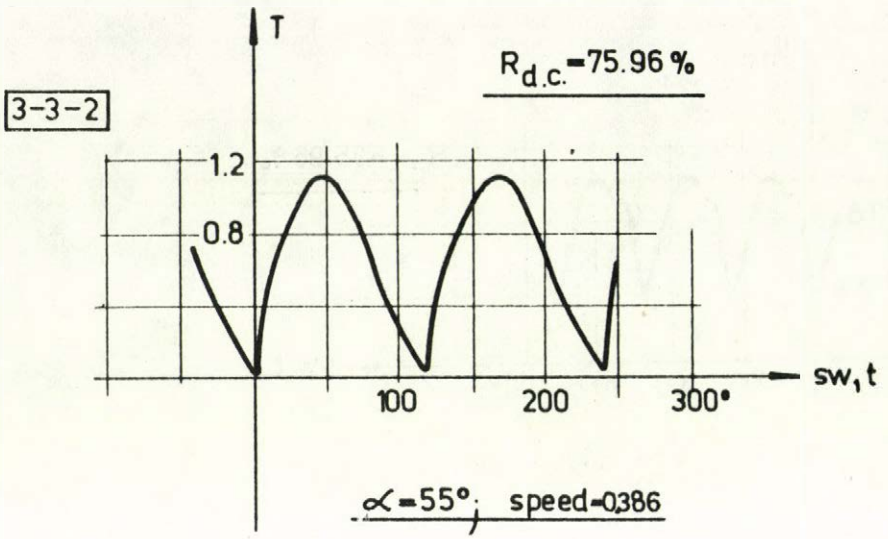

Fig.6.58

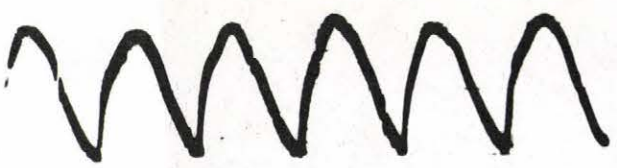

Fig.6.59

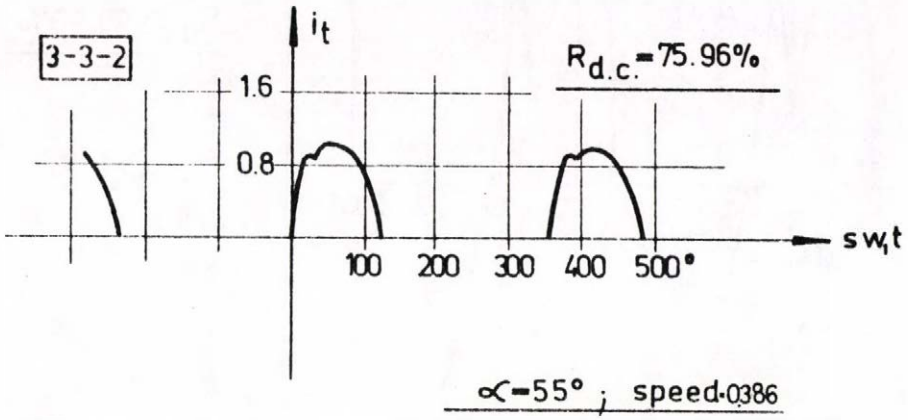

Fig.6.60

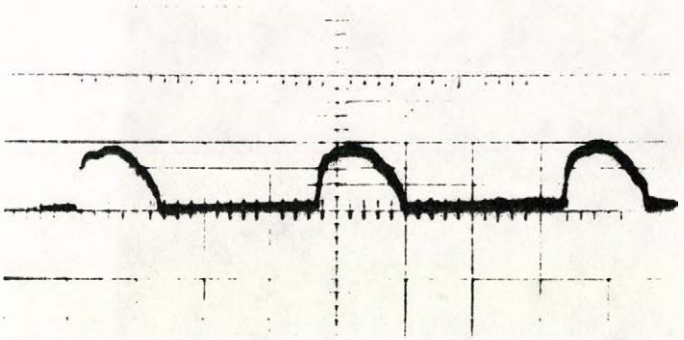

Fig.6.61

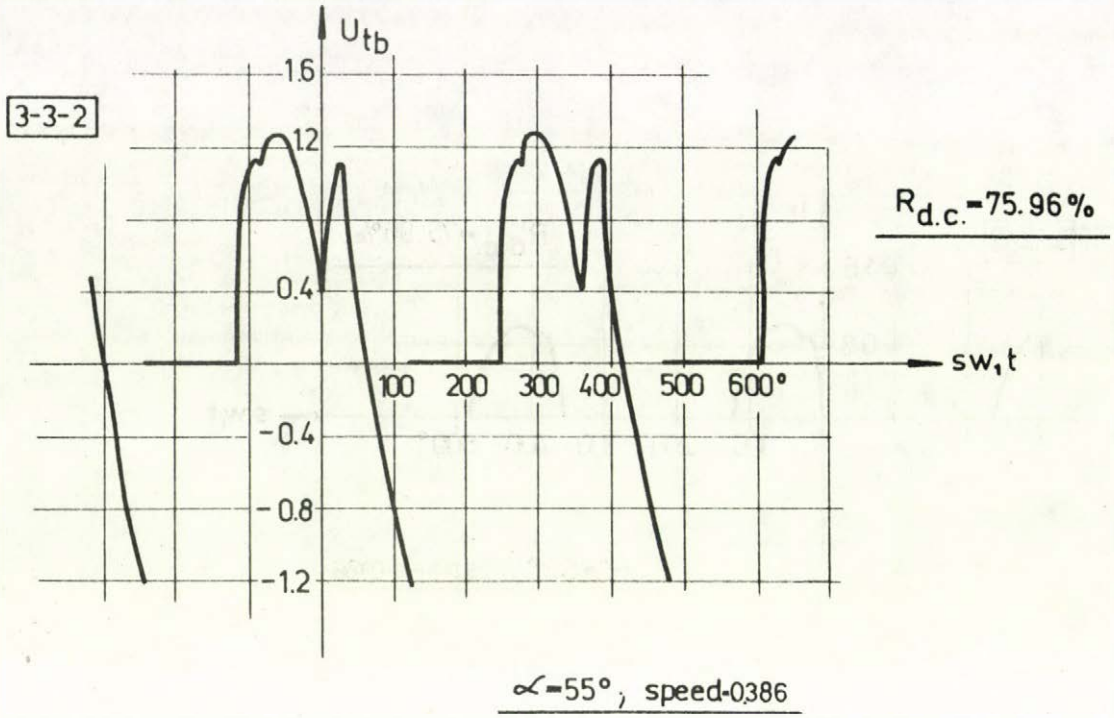

Fig.6.62

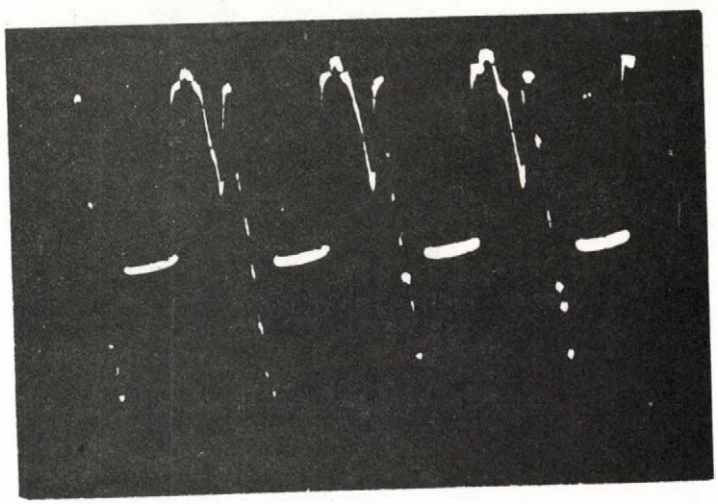

Fig.6.63

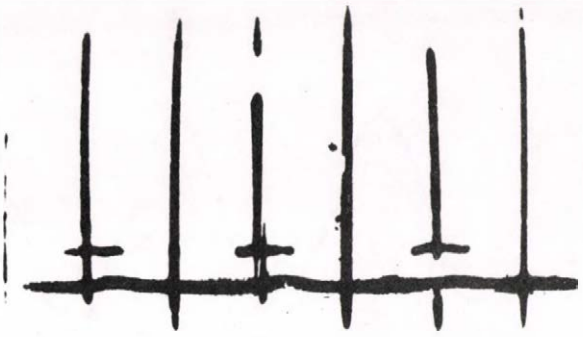

Fig.6.64

Fig.6.65

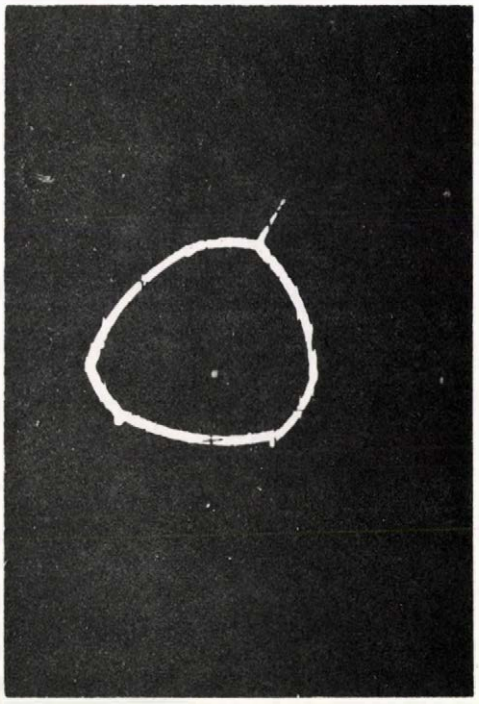

Fig.6.66

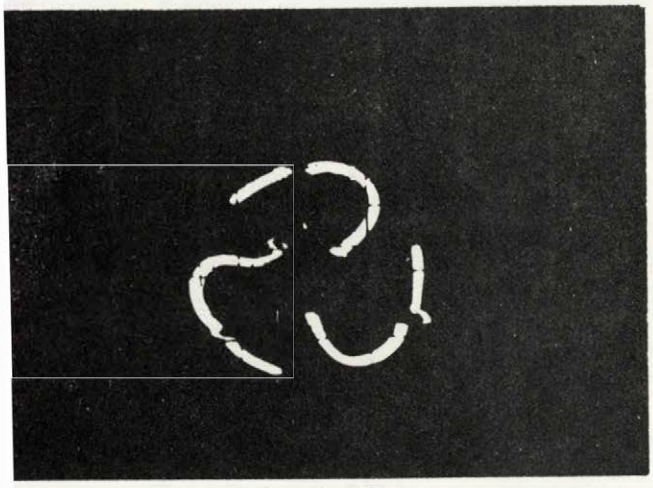

Fig.6.67

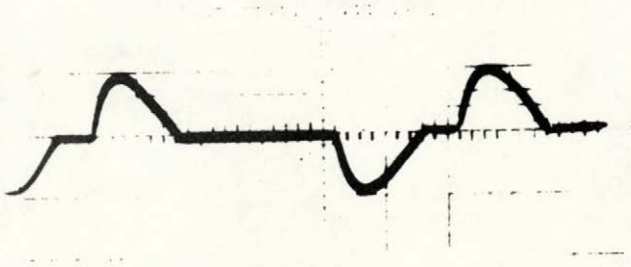

Fig.6.68

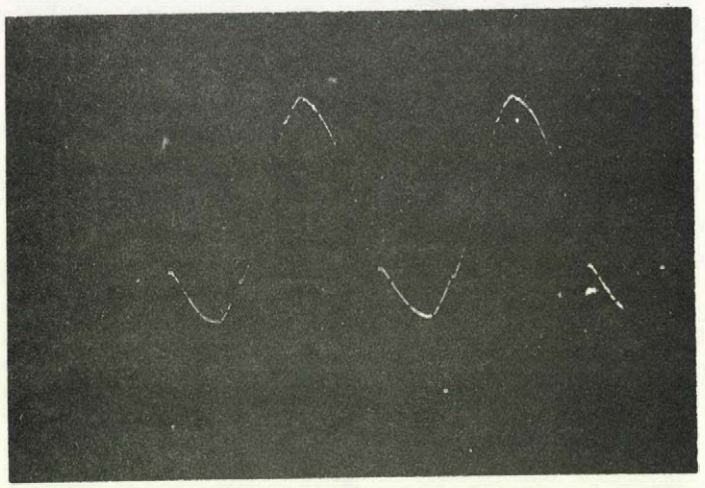

Fig.6.69

Fig.6.70

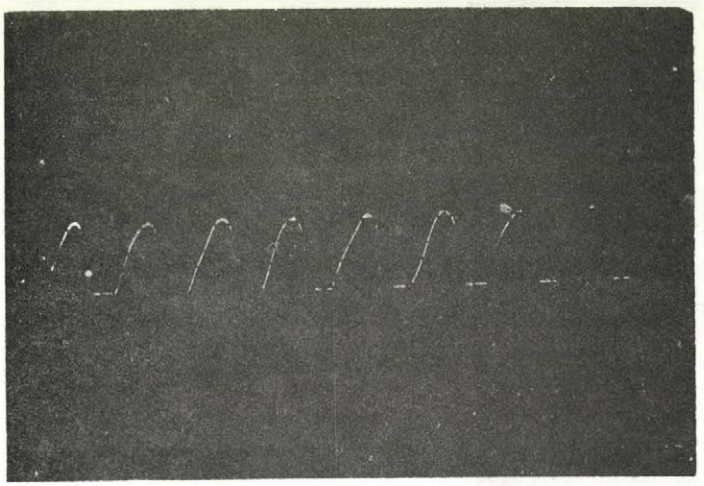

Fig.6.71

Fig.6.72

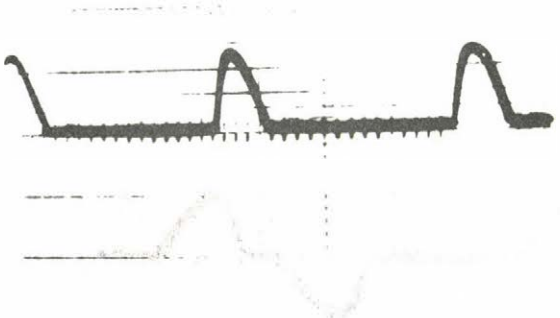

Fig.6.73

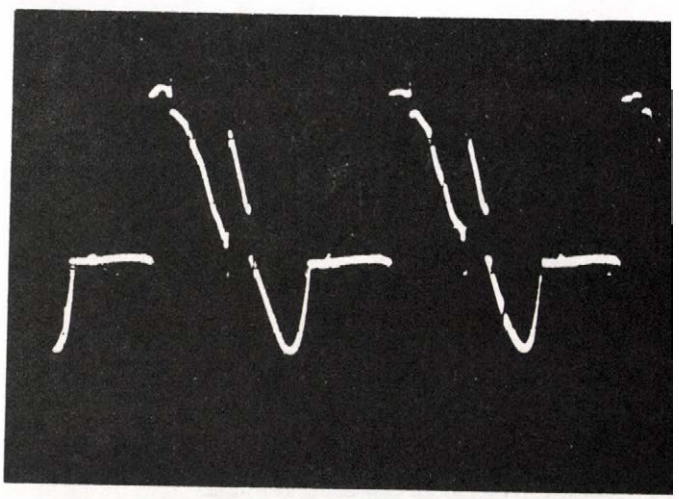

Fig.6.74

6.5 Closed-Loop System Characteristics

The performance of the controlled machine was obtained and the system stability was studied.

Oscillograms for the motor speed and the d.c. current signals were made when sudden changes occur in the speed reference signal. These oscillograms are important for the study of the dynamic behaviour and starting process of the drive.

6.5.1 Characteristics of the Controlled Drive

As it is shown in Fig.6.2 a compensating circuit of integration plus proportional type /P+I/ was used for the speed control. In that case the speed is practically constant for the different load torques. The shunt speed/torque characteristic is shown in Fig.6.75. The following observations can be made on these characteristics:

1. All the speed/torque curves lie within the envelope of the static speed/torque curve for the normal sinusoidal operation.

2. Due to the current-control the load torque has a limit value, in that case the speed is changing while the torque is practically constant.

The relation-ship between the current through the d.c. resistance and the torque is given also in Fig.6.75 for two set speeds.

6.5.2 System Stability

The stability test of the system may be performed in the following manner, by changing the value of one or more of the parameters of the compensating circuits in the current and/or the speed control pathes. The values of the parameters at which the system reaches the limit of the stability are obtained. It has been shown that the most convenient parameter to be chosen for such test is the resistance remarked by R′ in Fig.6.2 in the path of reference signal for the current control.

The original value of that resistance was 110 kΩ. It was found that when the value of that resistance was reduced to 10 kΩ the system begins to be unstable.

6.5.3 Transient Response of the Controlled System

The dynamic behaviour of the controlled drive was studied. The transient test was made as shown in Fig. 6.76, by opening or closing the switch a sudden change in the speed reference signal is obtained. The transient behaviour and the starting processes were investigated. Different sudden changes in the speed reference signals were performed. One test was made such that the high value of $R_{d.c.}$ was inserted in the rotor circuit. Other was made for the case of the small value of $R_{d.c.}$. In the third test the drive was switched from about 20% to 100% of the rated speed and the reverse. In the previous test the high value of the resistance was found in the rotor circuit from the instant of switching up to 67% of the rated speed, afterwards the parallel thyristor was turned on automatically and only the small value of $R_{d.c.}$ was used. In the last test the total switching process was made from stand-still up to the rated speed.

Oscillograms of the speed and the current through the d.c. resistance were made for the previous transient tests as shown in Fig. 6.77 - 6.83.

In Fig.6.77 the drive was switched from zero speed up to 0.54. At that speed the torque is 0.153 and the current is 0.334. Fig.6.78 shows the speed and the current when the motor speed was changed suddenly from 0.54 to 0.135. At the latter speed the torque is 0.04 and the current is 0.224.

In Fig.6.79 and 6.80 the speed was changed from 0.646 /T=0.178, $I_{d.c.}$=.458/ to 0.914 /T=0.243 and $I_{d.c.}$=.418/ and vica-versa. In that case the small value of $R_{d.c.}$ was inserted in the rotor circuit.

Similarly the oscillograms in Fig.6.81 was made when the speed was changed suddenly from 0.21 to 0.914 and the reverse process is shown in Fig.6.82. At speed of 0.21 the torque is .065 and the current is 0.269.

The switching from zero speed up to 0.914 is shown in Fig.6.83. In that fig. it is clear that at speed of 0.625 one part of $R_{d.c.}$ was inserted in the rotor circuit. That was performed automatically with the help of the logic-circuit.

The above oscillograms give both the starting and transient behaviour of the drive.

It has been shown from these oscillograms that the drive operates well during the transient conditions.

The test results both in the steady and transient states confirm that with the half controlled bridge inserted in the secondary circuit of the induction motor a precise and cheap method of converting a normal poly-phase slip ring induction motor into a variable speed motor is feasible. The test results also show the satisfied degree of accuracy of the computations in the analytical treatment of the problem.

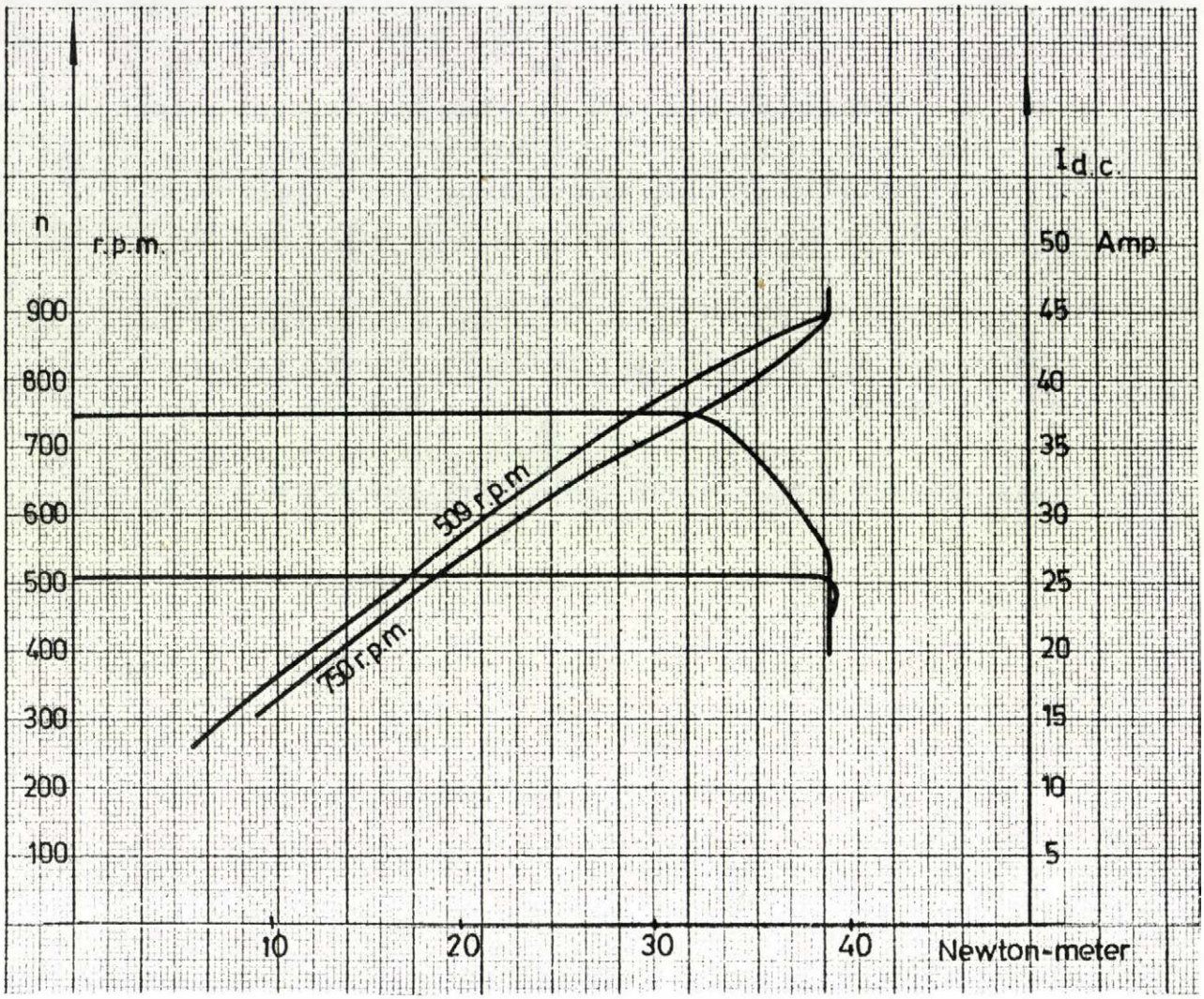

Fig.6.75

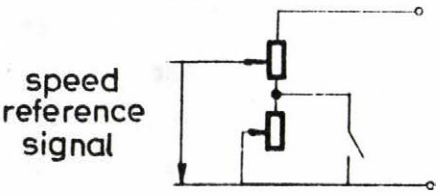

Fig.6.76

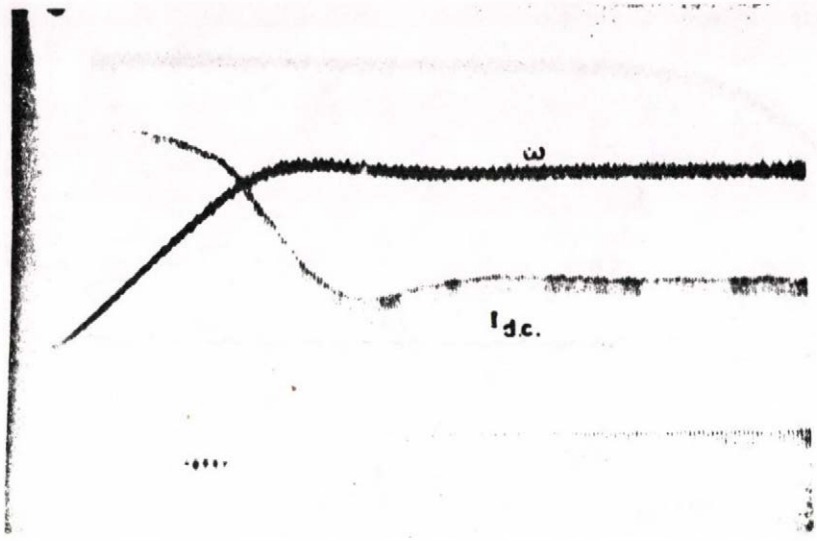

Fig.6.77

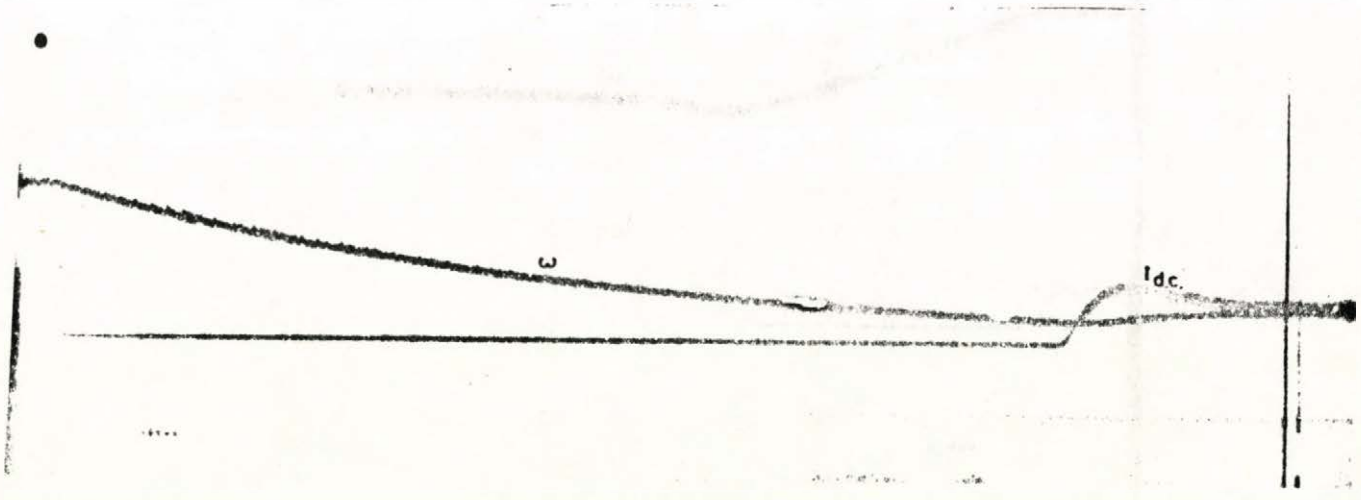

Fig.6.78

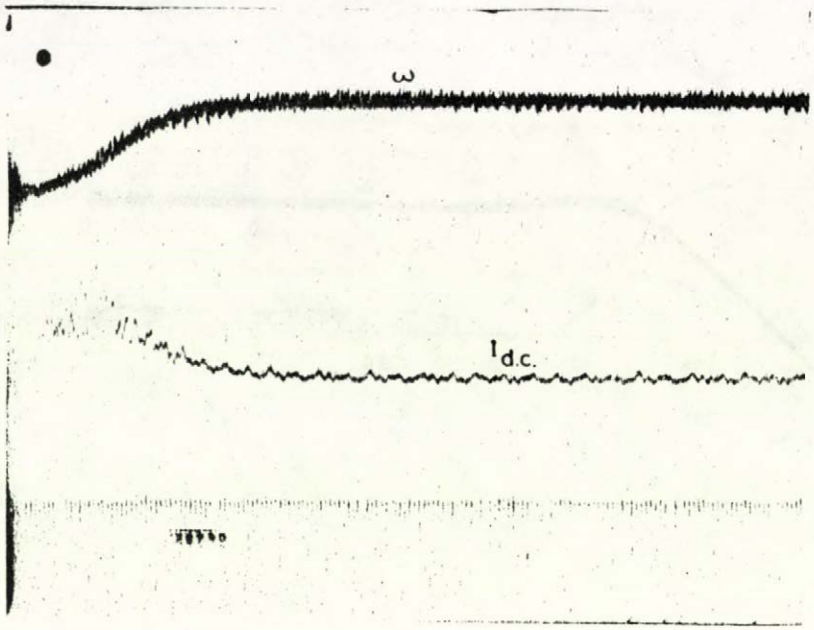

Fig.6.79

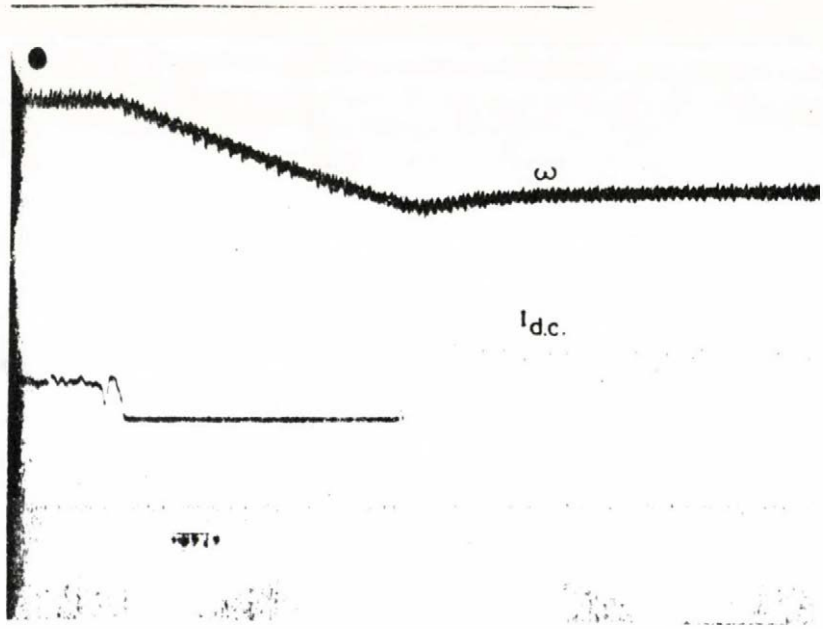

Fig.6.80

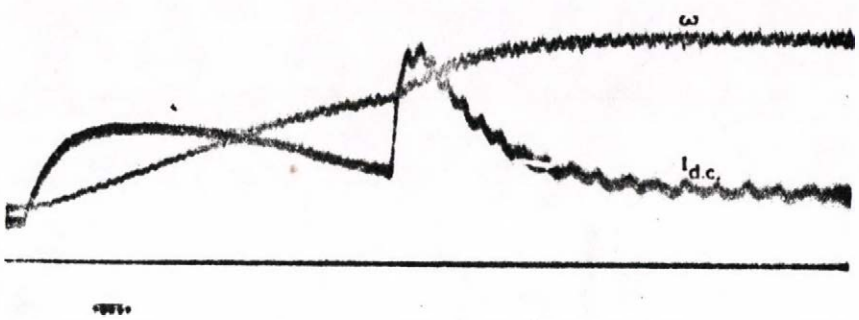

Fig.6.81

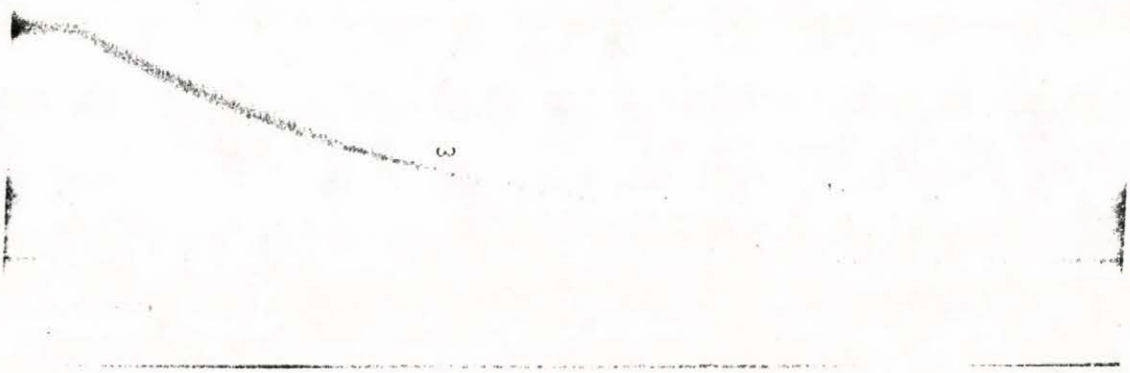

Fig.6.82

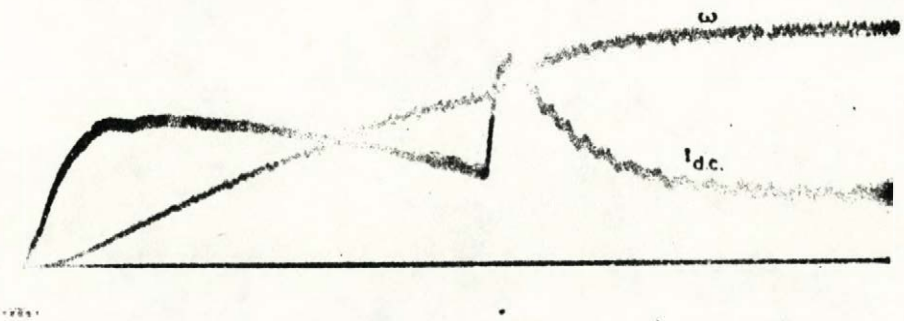

Fig.6.83

CHAPTER VII

CONCLUSION

This dissertation has studied different connections of thyristors in the secondary circuit of the wound rotor induction motors. It has developed methods for predicting the steady-state and dynamic behaviour of both the open-loop system and the controlled drive. The methods used provide a new and powerful tool for studying that case and the similar problems.

Through the studying of the problem the following conclusions have been confirmed:

1. For the control of low horse-power induction motors, using solid-state devices, there are variety of schemes. These methods are simple, inexpensive but lossy. In that respect, it is an advantage to connect the thyristors in the rotor circuit. By this method, the thyristor ratings are favourable. At fault conditions, the excess voltages and short-circuit currents are low. A precise open-loop speed control is possible. This appears to be a feasible method of converting a normal poly-phase slip-ring induction motor into a variable speed motor.
2. The long term permissible torque at big slips will be enough only if the secondary losses are increased, therefore it is necessary to use external resistances parallel to the thyristors circuit. The published work which use similar scheme had not exploited this advantage.
3. With the three phase resistance control connections, it is convenient to add resistances to the slip-rings, before the thyristors circuit. This increases the value of the inner rotor resistances and decreases the dip in the shape of the torque/speed characteristic. Therefore better load limit is achieved.

4. For the realization of the necessary torque/speed control range, two values of the external resistances are generally used. With the small resistances, the requirements are fulfilled at higher speeds with good efficiency. The big resistances are required to have a wide control range.
5. Among the studied connections of the 3-phase resistance control, connection I(ΔTT) needs lower rating thyristors, but the number of the thyristors needed in connection II(ΔT) is only three. However, connection II(ΔT) may give economical solution, this depends on the price of the firing circuits. The performance of the drive with that mentioned connection is favourable, because the power factor, as measured from the voltage and the first harmonic component of the rotor current is high.
6. An another way of controlling the slip-ring induction motor may be carried out by using a half controlled bridge connected to the slip-rings. The half bridge circuit is closed through d.c. resistance "$R_{d.c.}$" without any use of choke coils. Having used this connection, it is possible to attain zero value of the torque. Therefore this connection is the superior if small values of the torque are required. Besides this merits in applications, the control power requirements for this scheme of control are very small since the scheme uses the least number of thyristors and firing circuits. With that connection the semi-conductors circuit is connected directly to the slip-rings without any requirements to add resistances to the inner rotor resistances. This method of control is a new one and its analysis is presented for the first time in that dissertation.

7. Having compared the half-controlled bridge connection with the other solution of stator voltage control, the former is eminent solution throughout the motoring quadrant. The latter may be used economically for braking quadrant.
8. By comparing the half controlled bridge connection and the forced commutated d.c. chopper, connected in the secondary circuit, the latter is not an economical solution because of the large chokes and capacitance. If the applications need low torque values the half controlled bridge is favourable since at that juncture the d.c. choppers use high rating thyristors.
9. Modern state variable techniques have been utilized throughout the analysis. Since matrix methods are exclusively employed, the analysis is well suited to a digital computer solution. The methods used have studied the problem in all its views, the steady-state and the dynamic behaviour of the open-loop and controlled drive systems. This problem and solution demonstrate that the state variable method provide the analyst method for the study of modern a.c. and d.c. drives. The methods of analysis used through that research work provide new tools for solving these problems, specially the study of the dynamic behaviour.
10. It has proven useful to use a coordinate system fixed to the rotor, for the analysis of the problem. If the motor speed is considered constant and the stator resistance is neglected the analysis of the motor can be reduced to that of static three phase R-L circuit. In that case with 3-phase resistance control connections a direct and straight forward method of calculating the steady-state behaviour may be found. With the half controlled bridge connection, even with that approximate method, an iteration

procedure is necessary since in each stroke there are more than two different modes of operation.

11. The steady-state behaviour of the open-loop system have been studied using approximate methods of 2 or 4 energy-storages. The exact solution, which considers the speed oscillations is also presented using 6 energy-storages. It has been shown from the comparison of the different methods that in the study of the steady-state performance, it is enough to use the approximate methods.
12. Having studied the harmonic analysis, it has been shown that for some order of upper harmonics and at certain speeds, the equivalent stator resistance is very high. Therefore the assumption of neglecting the stator resistance cannot be valid. However for the approximate solution it is advisable to use the 4-energy storages method. For studying the dynamic behaviour and the control properities it is suggested to use the exact method.
13. It is enough to prepare the solution only for one stroke, since the solution for the remaining intervals is immediately obtained by means of recursion relationship.
14. The torque/speed characteristic with the d.c. current as a parameter has an anomalous shape at speed of $\frac{2}{3}$. It may be due to the harmonic effect.
15. It has been shown from the study of the dynamic behaviour of the drive that for the purpose of firing the thyristors the a.c. comparative signal may be taken proportional to the rotor or the stator fluxes. The latter case is preferable. The study confirms that there is no need to use a comparative signal formed from complex combination of the stator and rotor fluxes.

16. The characteristic equation of the open-loop system has one root equals unity. The corresponding eigen vector has the same direction as the end valocity vector.
17. In studying the closed-loop system, an approximate method is presented, it considers only the mechanical time constant of the drive. The accuracy of the method changes from one working point to another. This method may be used only for the preliminary study of the problem and in the design purposes of the control circuits.
18. For the controlled drive, speed and current feed back has carried out, the latter is necessary to protect the thyristors during starting and transient cases. Having applied the speed feed-back, the induction motor exhibits torque/speed characteristic similar to those of a d.c. shunt motor. All the torque/speed characteristics lie within the envelope of the static torque/speed curve for the normal sinusoidal operation.
19. Using a signal which is varying with three times the slip frequency /3sf/ as a comparative signal for firing the thyristors, the required speed/torque characteristic can be obtained despensing the use of tachometers. In that case, the control is achieved using static passive elements.
20. The steady-state periodical solution of the controlled drive has presented using 8-energy storages. The method used provides a direct way to achieve the solution without any iteration method if the periodical solution of the open-loop system is known.
21. The steady-state periodical solution of the controlled drive may be achieved using 7-energy storages. The above choice is required to make the system equations

as they are appeared compatible for the dynamic behaviour study.

22. The good correlation between the results of a digital computer solution and that obtained from an actual system confirms that the analytic method used predict the performance of the system. Both the solutions confirm that the proposed scheme is vividly revailing the other near schemes.

APPENDICES

APPENDIX I

The phase value of the thyristor current in the 2-O ph condition is expressed by the equation:

$$\bar{i}_{tf} = \bar{i}_r - \bar{i}_{ro} \qquad (1)$$

where $\bar{i}_r$ is the rotor current and $\bar{i}_{ro}$ is the current through the external resistance. For the calculation of that thyristor current, let us consider three thyristors connected in delta so that the current of the two thyristors B and C equals zero see Fig.I. The rotor currents i_{ra}, i_{rb} and i_{rc} are obtained from the projection of the Park-vector of the rotor current on the axes r_a, r_b and r_c. Then from the Park vector in Fig.II:

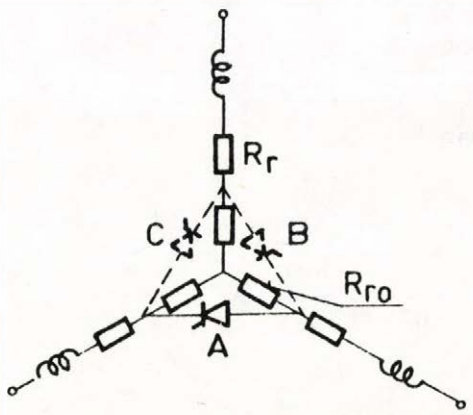

Appendix I

Fig.I

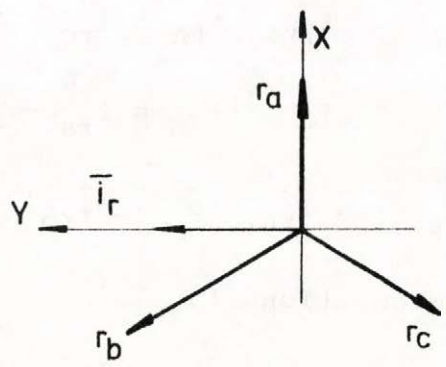

Appendix I

Fig.II

$$i_{ra} = 0$$

$$i_{rb} = \frac{\sqrt{3}}{2} i_{ry}$$

$$i_{rc} = -\frac{\sqrt{3}}{2} i_{ry}$$

The current of thyristor A equals i_{rb}, then:

$$i_{tA} = \frac{\sqrt{3}}{2} i_{ry}$$

$$i_{tB} = 0$$

$$i_{tC} = 0$$

The Park-vector of the thyristor current is:

$$\bar{I}_{t\Delta} = \frac{2}{3} \frac{\sqrt{3}}{2} i_{ry}$$

From Fig.I.:

$$i_{tA} - i_{tC} = i_{rb} - i_{rob}$$

$$i_{tB} - i_{tA} = i_{rc} - i_{roc}$$

$$i_{tC} - i_{tB} = i_{ra} - i_{roa}$$

then: $\bar{i}_{t\Delta} - \bar{a}\, \bar{i}_{t\Delta} = \bar{a}^2(\bar{i}_r - \bar{i}_{ro})$

and from equation (1)

$$\bar{i}_{tf} = \frac{1-\bar{a}}{\bar{a}^2} \bar{i}_{t\Delta}$$

$$\bar{i}_{tf} = j\, i_{ry}$$

APPENDIX II

$$I^2_{t\ R.M.S.} = \frac{1}{6\tau} \int_{\tau_n} \frac{3}{4} i^2_{ry}\, dt + \int_{\tau_c} (i^2_{ra} + i^2_{rc})\, dt$$

to solve the first integral consider the equation:

$$\frac{\sin t}{X'_r} = r\, i_{ry} + \frac{d\, i_{ry}}{dt} \qquad (1)$$

$$\int i^2_{ry}\, dt = \frac{1}{r} \int i_{ry} \left(\frac{\sin t}{X'_r} - \frac{d\, i_{ry}}{dt} \right) dt =$$

$$= \frac{1}{r\, X'_r} \int i_{ry} \sin t\, dt - \frac{1}{2r}\, i^2_{ry}$$

the integral $\int i_{ry} \sin t\, dt$ can be solved also using equation (1). For the solution of the second integral regard Fig.III.

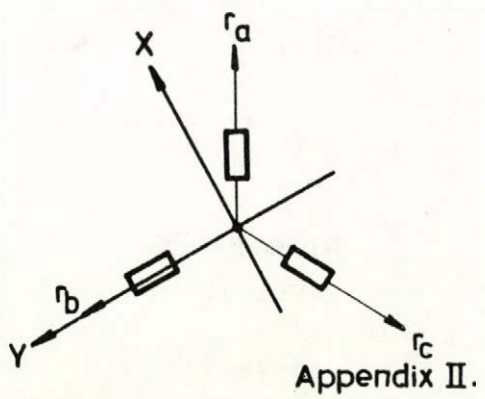

Fig.III

If a coordinate-system is chosen as shown in the figure, then:

$$i_{ra} = \frac{\sqrt{3}}{2}\, i_{rx} - \frac{1}{2}\, i_{ry}$$

$$i_{rc} = -\frac{1}{2}\, i_{rx} - \frac{\sqrt{3}}{2}\, i_{ry}$$

$$\int_{\tau_c} (i_{ra}^2 + i_{rc}^2)\, dt = \int_{\tau_c} (i_{rx}^2 + i_{ry}^2)\, dt$$

The integral in this form can be easily solved as explained above.

APPENDIX III

A reference frame fixed to the rotor is used, in the 3-ph conduction state see Fig.IV.

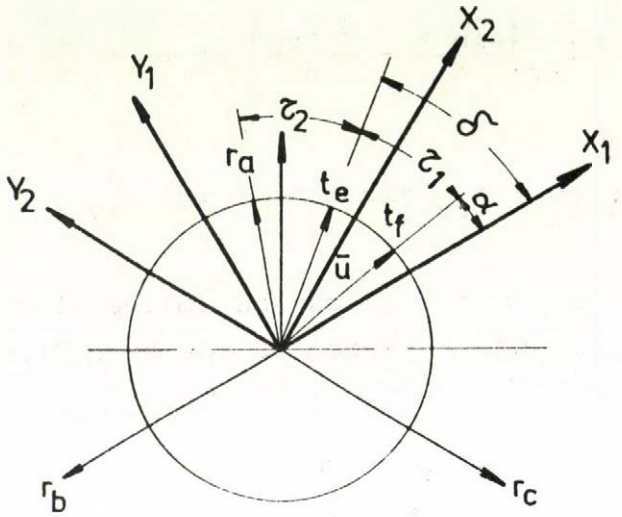

Appendix III

Fig.IV

$$i_{rx} = \frac{U \cos(t+\frac{\Pi}{3})}{R_r+\frac{2}{3} R_{d.c.}}$$

$$i_{ry} = \frac{U \sin(t+\frac{\Pi}{3})}{R_r}$$

$$\bar{i}_r = \frac{U}{R_r(1+RR)} \cos(t+\frac{\Pi}{3}) + j \frac{U}{R_r} \sin(t+\frac{\Pi}{3})$$

The rotor current refered to synchronously rotating coordinate system is

$$\bar{i}_r^{\,*} = \bar{i}_r \, e^{-j(t+\frac{\Pi}{3})}$$

$$\bar{i}_r^{\,*} = \frac{U}{2R_r}\left[\frac{2+RR}{1+RR} - \frac{RR}{1+RR}\, e^{-2j(t+\frac{\Pi}{3})}\right]$$

This is the equation of a circle, the centre is

$$\frac{U}{2R_r}\,\frac{2+RR}{1+RR}$$

and the radius is

$$\frac{U}{2R_r}\,\frac{RR}{1+RR}$$

$$\frac{\bar{i}_r^{\,*}}{U/R_r} = \frac{1}{2}\,\frac{2+RR}{1+RR} - \frac{1}{2}\,\frac{RR}{1+RR}\, e^{-j(2t+\frac{2\Pi}{3})}$$

$\alpha = t_f + \frac{\Pi}{3}$

then at the firing instant

$$\frac{\bar{i}_r^{\,*}}{U/R_r} = \frac{1}{2}\,\frac{2+RR}{1+RR} - \frac{1}{2}\,\frac{RR}{1+RR}\, e^{-j2\alpha}$$

This corresponds to point "a" in Fig.V., point "b" is at the end of the 3-ph conduction interval τ_1. If the are (ab) is considered as a mass then the centre of mass is

$$\frac{1}{2}\,\frac{2+RR}{1+RR} - \frac{1}{2}\,\frac{RR}{1+RR}\,\frac{\sin\tau_1}{\tau_1}\, e^{-j(2\alpha+\tau_1)}$$

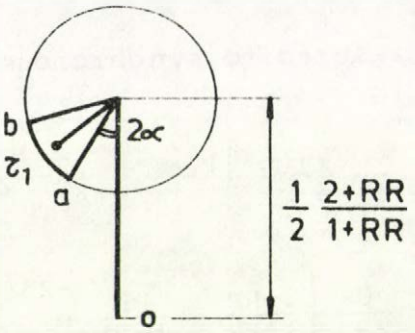

Appendix III

Fig.V

In the 2-ph conduction state a coordinate system x_2-y_2 fixed to the rotor is chosen. Similarly the rotor current refered to synchronously rotating axes is:

$$\bar{I}_r^{\,*} = \frac{U}{2R_r}\left[\frac{1}{1+\frac{3}{4}RR}\left(1+e^{-j(2t+\frac{\Pi}{3})}\right)\right]$$

$$t_e = t_c + \tau_1 = \delta - \frac{\Pi}{3}$$

$$\frac{\bar{i}_r^{\,*}\, t_e}{U/R_r} = \frac{1}{2}\,\frac{1}{1+\frac{3}{4}RR}\left[1+e^{-j(2\delta-\frac{\Pi}{3})}\right]$$

the centre of mass in that case is

$$\frac{1}{2}\,\frac{1}{1+\frac{3}{4}RR}\left[1+\frac{\sin\tau_2}{\tau_2}\,e^{-j(2\delta-\frac{\Pi}{3}+\tau_2)}\right]$$

The equivalent centre of mass gives the value $\frac{\bar{J}_{r1}}{U/R_r}$

$$\frac{\bar{J}_{r1}}{U/R_r} = \frac{1}{2\tau}\left[\tau_1\left(\frac{2+RR}{1+RR} - \frac{RR}{1+RR}\,\frac{\sin\tau_1}{\tau_1}\,e^{-j(2\alpha+\tau_1)}\right) + \right.$$

$$\left. + \frac{\tau_2}{1+\frac{3}{4}RR}\left(1 + \frac{\sin\tau_2}{\tau_2}\,e^{-j\left(2\delta-\frac{\Pi}{3}+\tau_2\right)}\right)\right]$$

$\tau_1 = \delta - \alpha$ and $\tau_2 = \tau - \delta + \alpha$

$$\frac{\bar{J}_{r1}}{U/R_r} = \frac{2+RR}{1+RR}\,\frac{\delta-\alpha}{2\tau} + \frac{1}{1+\frac{3}{4}RR}\,\frac{\tau-\delta+\alpha}{2\tau} + \frac{1}{2\tau}\left[\frac{1}{1+\frac{3}{4}RR}\sin(\tau-\delta-\alpha) - \right.$$

$$\left. - \frac{RR}{1+RR}\sin(\delta-\alpha)\right]\,e^{-j(\delta+\alpha)}$$

APPENDIX IV

The following flow-chart describes the method of the calculation of the steady-state operating point, if the load torque is not constant.

1. The initial conditions of the state-variables for the working point are determined from approximate methods, for example, from the four energy-storages method. The torque value is given. The time at the beginning of the stroke which is determined from the required firing angle is also given.
2. The solution of the differential equations of the system is accomplished using the method of Runge-Kutta /fourth order/. This is referred to in the flow-chart by the subroutine RUNRK. The extinction conditions are regarded when transfering from one mode of operation to the other. Some iterations are made in that case.

3. The subroutine FRACT rotates the end values of the first four state variables /stator and rotor fluxes/ forwardly by $\frac{\Pi}{6}$. This is necessary because in that case the periodicity matrix equals the identity matrix.
4. The deviation between $\underline{X}_{end}$ and $\underline{X}_{st}$ is calculated and correspondingly the error is computed.
5. The transfer matrix is obtained by the perturbation of the starting state variables by an incremental value DEL. For example, if one state variable is perturbated by DEL and the end values are calculated as explained above, one column of the $\underline{A}$ matrix is obtained from the relation

$$\frac{\underline{X}_{end2} - \underline{X}_{end1}}{DEL}$$

where $\underline{X}_{end2}$ and $\underline{X}_{end1}$ are the end values of the perturbated and the original state vector respectively.
6. Similarly if the torque value is perturbated by DEL the vector $\underline{B}_L$ can be calculated.
7. Knowing the transfer matrix $\underline{A}$, the small variation of the starting state vector can be computed (DXST).
8. A new starting values of the state variables are obtained and the total process is repeated.
9. It is unnecessary to calculate for each case a new transfer matrix. For example, after the first three running /it is referred to in the flow-chart by the condition IC ≤ 3/ the same $\underline{A}$ matrix is used to calculate DXST in the sequent running until the deviation or the error is less than the prescribed value.
10. The initial values of the state variables in that case are obtained and the corresponding velocities. The values at the end of each mode (XFR) and the velocities (VFR) are also obtained.
11. The transfer matrix is calculated in that case because it is necessary for the dynamic behaviour study.

12. The data of the working point now is compatible for the computation of the analysis of the system such as the fundamental component of the rotor current, the R.M.S. value of the thyristor current ... and so on.

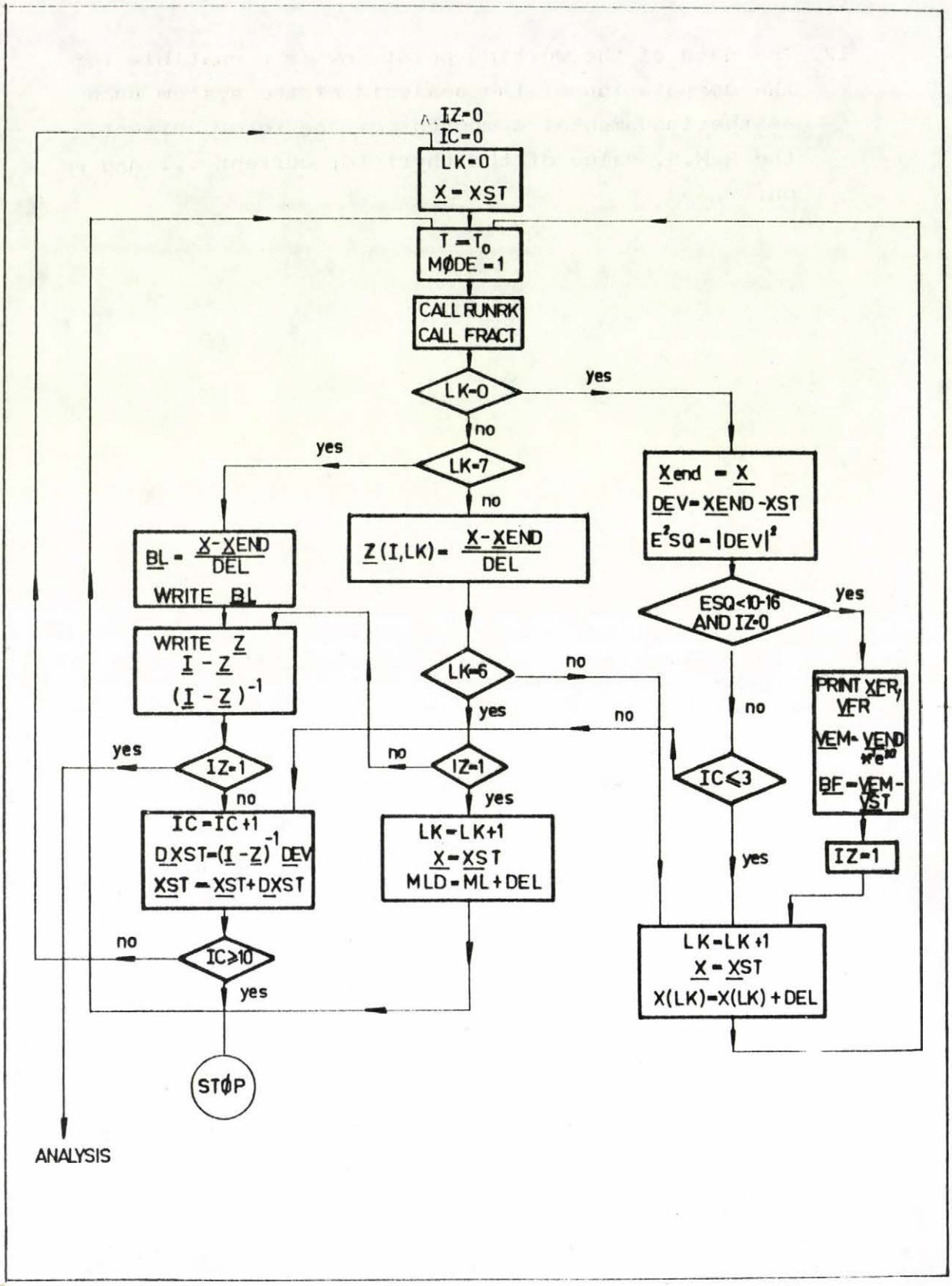
IZ=0
IC=0
LK=0
X = XST
T = T0
MODE = 1
CALL RUNRK
CALL FRACT
LK=0
yes
no
LK=7
yes
no
Xend = X
DEV=XEND-XST
E²SQ = |DEV|²
BL = (X-XEND)/DEL
WRITE BL
Z(I,LK) = (X-XEND)/DEL
ESQ<10-16 AND IZ=0
yes
no
WRITE Z
I - Z
(I - Z)⁻¹
LK=6
no
yes
PRINT XER, VER
VEM=VEND
BF=VEM-VST
IZ=1
yes
no
IZ=1
yes
no
IC≤3
yes
IC = IC+1
DXST=(I-Z)⁻¹ DEV
XST = XST+DXST
LK=LK+1
X=XST
MLD=ML+DEL
LK=LK+1
X=XST
X(LK)=X(LK)+DEL
no
IC≥10
yes
STOP
ANALYSIS

APPENDIX V.

READ $\underline{A}$ matrix and the vectors $\underline{b}_f$ and $\underline{V}end$, READ the nº of Ø i.e. NØ and the required f values

$\underline{b} = \underline{A}\ \underline{b}_f$ the components of the two row vectors $\underline{r}_1^T$, $\underline{r}_2^T$ which equal zero are given here

DØ 1 I = 1,NØ
R1(3) = R2(1) = cos Ø
R1(4) = R2(2) = sin Ø
R2(3) = - cos Ø
R2(4) = - sin Ø

CALL SUBROUTINE ROOTL
CONTINUE

STØP

SUBROUTINE
RØØTL

CALL Subroutine SCALPRØD to calculate $\underline{r}_1^T\ \underline{V}end = c_1$ and $\underline{r}_2^T\ \underline{V}end = c_2$

CALL Subroutine CHPØL to calculate the characteristic function of $(\underline{A} - \underline{b}\underline{R}_0^T) = chm_0(z)$ and $(\underline{A} - \underline{b}\underline{R}_1^T) = chm_1(z)$

$b_1(z) = chm_0(z)$
$b_2(z) = (1 + \frac{c_2}{c_1})\, chm_1(z) - b_1(z)$

$chm(z) = \frac{b_1(z) + f\, b_2(z)}{1 + f\, c_2/c_1}$

CALL Subroutine NPRBM to calculate the roots of the characteristic function using Birstow method

PRINT the Roots and the corresponding f and Ø values

STØP

The above flow-chart describes the explained method to get the roots of the characteristic equations of the system for different ϕ and ℓ's values for a working point.

The description avoids the explanation of the well known mathematical tools which are used during the computations.

These mathematical details can be found, if needed; in any mathematical reference.

1. The program computes the characteristic roots of a working point for different ϕ's. At each ϕ, ℓ is varied.
2. In the main program the required data of the working point are implemented such as the transfer matrix $\underline{A}$ and the vectors $\underline{b}_f$, $\underline{V}'_{end}$, $\underline{r}_1^T$ and $\underline{r}_2^T$. Also the required ℓ and ϕ's are given.
3. The subroutine RØØTL is called after the decision of ϕ and the required ℓ values.
4. The constant c_1 is determined from the scalar-product of $\underline{r}_1^T$ and $\underline{V}'_{end}$. It is made in a separate subroutine SCALPRØD. Similarly c_2 is calculated.
5. For ℓ=0 and ℓ=1 the modified characteristic functions chmo(z) and chml(z) are calculated using another subroutine in which the characteristic function can be computed. It is referred to in the above flow-chart by subroutine CHPØL.
6. $b_1(z)$ and $b_2(z)$ are computed knowing chmo(z) and chml(z).
7. For the different values of ℓ the modified characteristic function is determined.
8. The roots of each characteristic equation are computed using Bairstaw method. This is calculated in a separate subroutine NPRBM.
9. After returning to the main program another ϕ is decided and the whole procedure is repeated.

BIBLIOGRAPHY

[1] P.A.Harwood, " Control of electric motors". New York: Wiley, 1944

[2] P.L.Alger and Y.H.Ku, "Speed control of induction motors using saturable reactors", AIEE Trans. /Power Apparatus and Systems/, Vol.75, pp.1335-1341, 1956 /February 1957 sec./

[3] J.F.Szablya, "Torque and speed control of induction motor using saturable reactors", AIEE Trans., PAS. Vol.77, pp.1676-1682, 1958 /February 1959 sec./

[4] W.Shepherd and G.R.Slemon, "Rotor impedance control of the wound-rotor induction motor", AIEE Trans., PAS, Vol.78, pp.807-814, October 1959.

[5] G.W.Heumann, "Magnetic control of industrial motors" New York: Wiley 1961.

[6] P.L.Alger, Jalaluddin, "Stepless starting of wound rotor induction motors", AIEE Trans. Pt.II. /Applications and Industry/, Vol.81., pp.262-271, Nov.1962.

[7] P.L.Alger, G.Angst, W.M.Schweder, "Saturistors and low starting current induction motors", IEEE Tran., PAS, Vol.84, pp.291-297, June 1963

[8] Charles E.Gunn, "Improved starting performance of wound rotor motors using saturistors", IEEE Tran., PAS, Vol.84. pp.298-302, June 1963.

[9] M.S.Erlicki, J.Ben Uri and Y.Wallah, "Switching drive of induction motors", PROC. I.E.E., Vol.110, No.8. pp.1441, August 1963.

[10] K.Heumann, "Pulse control of d.c. and a.c. motors by silicon-controlled rectifiers", IEEE Trans., /Communication and Electronics/, Vol. pp.390, July 1964.

[11] E.Gerecke, "A survey paper", New methods of power control with thyristors, IFAC, third congress, London 1966.

[12] I.Rácz, "Die Theorie der Asynchronmotoren mit antiparallelen Thyristoren, XIII.Internat.Koll. TU Ilmenau, 1968.

[13] I.Rácz, J.Borka, K.Lupán, Mrs D.Miklós, "Quasi-periodic dynamic behaviour of piecewise linear multi-parameter systems", Periodica Polytechnica, Electrical Engineering, Vol.13, No.3. 1969.

[14] Luke Y.M.Yu, "Constant starting torque control of wound rotor induction motors", IEEE Trans, PAS, Vol.89, No.4. April 1970.

[15] Hunyár M., "Aszinkron motorok vezérlése primer oldali antiparallel kapcsolásu tirisztorpárokkal" Elektrotechnika, 5-6 sz. 1970.

[16] A.Bellini, T.Raimondi, "Sul controlle di velocitá di un motore asincrono trifase mediante parzieliszazions rotorica" Rapp d'Ist. di Aut., Univ. di Roma, No.2. Englio, 1970.

[17] I.Rácz, "Matrix calculation of thyristor-electrical machine schemes", 1.CONFERENCE ON POWER ELECTRONICS, Budapest, 1970.

[18] S.Halász, "Pulsgesteuerter wiederstand im Läuferkreis von asynchronmotoren", 1. CONFERENCE ON POWER ELECTRONICS, Budapest, 1970.

[19] Csörgits, F., "Die Kennlinien der untersynchronen stromrichterkaskade", Periodica Polytechnica, Budapest, Vol. Band 14., No.4. 1970.

[20] T.A.Lipo, "The analysis of induction motors with voltage control by symmetrically triggered thyristors", IEEE Trans., PAS, Vol. 90., No.2. March/april 1971.

[21] P.R.Basu, "A variable speed induction motor using thyristors in the secondary circuit", IEEE Trans., PAS, Vol.90.No.2. March/April 1971.

[22] A.De Carli - M.La Cava, "Steady state behaviour of phase controlled induction motors", Univ.di Roma, Instituto di Automatica, R.2-27, Novembre 1972.

[23] A.Bellini - A.De Carli, "Simulation of phase-controlled induction motors", Univ. di Roma, Instituto di Automatica, R.2-26, Novembre 1972.

[24] B.I.Doyle, R.J.Wooddall, "Adjustable speed drives using a.c. wound rotor motors", Control Engineering, pp. 48-50, June 1973.

[25] I.Rácz, "Control theory of thyristor connections", 2nd CONFERENCE ON POWER ELECTRONICS, Budapest, 1973.

[26] I.Rácz, "Alternating current drives", General Report, 2nd CONFERENCE ON POWER ELECTRONICS, Budapest, 1973.

[27] J.Strycharz, "Einige probleme über den betrieb einer durch analoggeregelten frequenzumwandler gespeisten asynchronmaschine", 2nd CONFERENCE ON POWER ELECTRONICS, Budapest, 1973.

[28] A.A.El-Sattar, "Control of induction motor fed by back-to-back thyristor pairs connected to the rotor circuit", 2nd CONFERENCE ON POWER ELECTRONICS, Budapest, 1973.

[29] J.Borka, A.Varga, "Computer analysis of voltage controlled induction machines", Control in Power Electronics and Electrical Drives, IFAC Symposium, Düsseldorf, 1974.

[30] A.Abd El-Sattar, "Speed control of induction motors by three-phase thyristors in the rotor circuit", Control in Power Electronics and Electrical Drives, IFAC Symposium, Düsseldorf, 1974.